THE ROLE OF SODIUM CHANNEL α AND β SUBUNITS IN MYELINATING GLIA AND DEMYELINATING DISORDERS

by

Heather A. O'Malley

A dissertation submitted in partial fulfillment
of the requirements for the degree of
Doctor of Philosophy
(Cellular and Molecular Biology)
in The University of Michigan
2009

Doctoral Committee:

Professor Lori L. Isom, Chair
Professor Gary B. Huffnagle
Professor Miriam H. Meisler
Professor Kathy Sue O'Shea
Professor Audrey F. Seasholtz

Nothing in life is to be feared, it is only to be understood. Now is the time to understand more, so that we may fear less.

— Marie Curie

ACKNOWLEDGEMENTS

My sincere and deep thanks to all of the many people who have given me support, encouragement and guidance through my graduate studies.

I am forever thankful to my husband Patrick for his love and support. None of this would have been possible without you.

Dyke, Tigwa and Amanda, my predecessors: You each helped to show me what it means to be a scientist and a graduate student, and offered many opportunities for fun and companionship along the way. I'm grateful to each of you.

Chunling: I've said more than once that everything I know about how to do science I learned from you. Thank you for everything I've learned working with you, and for eight years of friendship.

My current fellows in the Isom lab, Luis, Will, Gustavo and Jeff: Thank you for all of your help, companionship and encouragement as well as the invaluable advice and feedback. I'm fortunate to have been able to work with so many great people and great scientists.

I am also grateful to many past Isom lab members. Audrey and Laurence, you have been missed. Thank you for your friendship. Thanks also to Travis and Diana. I wish you both the best of luck as you work your way through your own graduate studies.

Lastly, to Lori: I can't possibly thank you enough. You've been a constant encouragement, advocate and support. You've truly defined for me what it means to have a mentor, not just an advisor. I've always been able to turn to you for help, whether it's been about science or issues affecting me personally. I would not have made it to the end of this long road without you.

Chapter 2 was previously published in Molecular and Cellular Neuroscience in collaboration with the laboratory of Dr. Gary Huffnagle. (O'Malley HA, Shreiner AB, Chen GH, Huffnagle GB, Isom LL. Loss of Na^+ channel β2 subunits is neuroprotective in a mouse model of multiple sclerosis. Mol Cell Neurosci 2009: 40:143-155.)

TABLE OF CONTENTS

LIST OF FIGURES

LIST OF TABLES

CHAPTER ONE

INTRODUCTION

I: VOLTAGE-GATED SODIUM CHANNELS

Voltage-gated sodium channels are key molecular players in cellular electrical excitability, and as such are integral components of the rapid and efficient generation and conduction of the action potential in excitable cells. Sodium channels are specifically responsible for the rising phase of the action potential in nerve, muscle, and other excitable cells. These complex proteins are components of numerous processes involved in excitability, excitotoxicity and disease pathology, cell adhesion and development, among many others, and as such represent a dynamic, ever-growing, and fascinating field of research.

Sodium channel topology

Early studies by Hodgkin and Huxley identified the classical sodium conductance using electrophysiological methods in studies of giant axons from the squid *Loligo* (Hodgkin and Huxley, 1952). At this time, they were unaware of the

presence of specific ion channels in the membrane of excitable cells. They determined that the conductance they observed was reliant on changes in membrane potential but not membrane current. This conductance required both sodium ions for the generation of a rapid and transient inward current and potassium ions for the generation of a slower and sustained outward current (Hodgkin and Huxley, 1952).

Sodium channels are polytopic, multi-subunit intrinsic membrane proteins composed of a single pore-forming α subunit which is capable of conducting sodium ions, and one or more auxiliary β subunits that do not form the pore but which modulate channel function (Catterall, 2000; Yu et al., 2003). Sodium channels purified to theoretical homogeneity from mammalian brain are heterotrimers, composed of one α subunit, one non-covalently linked β subunit (β1 or β3) and one disulfide-linked β subunit (β2 or β4) (Hartshorne and Catterall, 1984; Catterall, 2000; Yu et al., 2003). Sodium channels activate in response to local membrane depolarization, allowing sodium ions to flow down their concentration gradient, which is physiologically from the extracellular space into the interior of the cell. Sodium channel α subunits alone are capable of ion conduction when expressed in heterologous systems, but their activation and inactivation kinetics and voltage-dependence are dissimilar to native channels unless co-expressed with a β subunit (Isom et al., 1994; Isom, 2001). This is especially evident when channels are expressed in oocytes from the frog *Xenopus laevis*. Early experiments co-expressed low molecular weight rat brain

mRNA with cloned α subunit cDNAs in *Xenopus* oocytes, resulting in the restoration of normal channel kinetics, similar to that observed in neurons (Krafte et al., 1988). The components in the low molecular weight mRNA fraction responsible for this restoration of rapid ion conductance were later determined to be the sodium channel β subunits, in particular, β1 (Isom et al., 1992).

The mammalian sodium channel α subunit gene family is composed of at least 10 members, *SCN1A* through *SCN11A* (with corresponding mouse orthologs *Scn1a* through *Scn11a)*, encoding the channel proteins $Na_v1.1$ - $Na_v1.9$ and Na_x (Catterall et al., 2003, 2005). Each α subunit comprises a single polypeptide chain with a molecular weight after post-translational modification of approximately 260 kDa (Catterall et al., 2005). Each polypeptide contains four homologous domains, entitled domains I-IV, that come together in pseudo-tetrafold symmetry to form the ion conducting pore. Each domain consists of six transmembrane segments entitled S1-S6 (**Figure 1.1A**). Segments S5 and S6 from each domain are found lining the interior of the pore, with a short extracellular loop residing at the opening of the pore region, forming the sodium ion signature sequence which determines the ion specificity for conduction (Catterall, 2000)

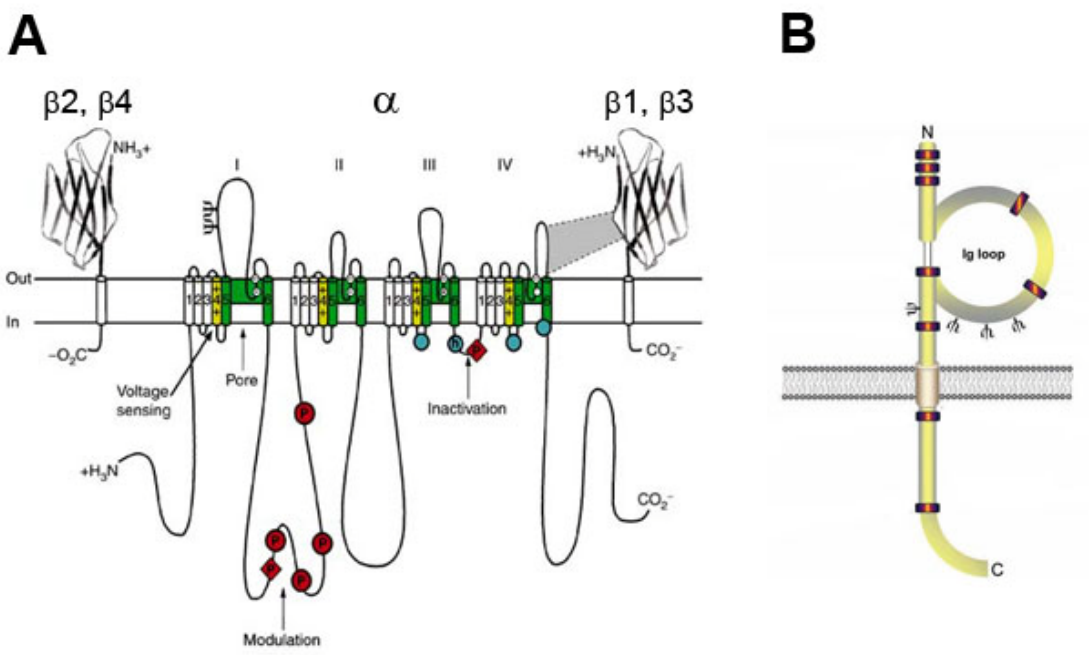

<u>Figure 1.1</u>: Topology of the voltage-gated sodium channel.

A: Representation of the α and β subunits of the voltage-gated sodium channel. The pore-forming α subunit contains four homologous domains designated I – IV with the transmembrane-spanning segments designated S1-S6 in each domain. The intracellular loop forming the inactivation gate is found between domains III and IV. The β1 and β3 subunits associate non-covalently with the α subunit, and the β2 and β4 subunits associate covalently with the α subunit.

B: Representation of the β subunits of the voltage-gated sodium channel. Each β subunit contains an extracellular N-terminus, an extracellular V-type immunoglobulin (Ig) loop, a single transmembrane-spanning domain and an intracellular C-terminus

(Adapted from (Yu and Catterall, 2003) and (Brackenbury et al., 2008a))

The process of channel gating follows a set sequence of events beginning with activation, then inactivation, then channel closing (process reviewed in (Catterall, 2000) and in (Grant, 2001)). Regularly-spaced positively charged residues along the S4 segment of each domain serve as voltage sensors and move within the membrane according to either a sliding-helix (Guy and Seetharamulu, 1986; Catterall, 1992) or a paddle model (Jiang et al., 2003b; Jiang et al., 2003a) in response to membrane depolarization to activate or open the channel pore. This shifts a total of 12 charged residues within the membrane to the extracellular face of the membrane during the process of channel activation. Once the channel has opened, sodium ions are able to flow down the concentration gradient through the pore into the interior of the cell.

The inactivation gate, formed from a short intracellular sequence located between domains III and IV, is postulated to swing in a hinged-lid fashion (reviewed in (Ulbricht, 2005)) to physically occlude, or inactivate, the channel. This occurs spontaneously, within milliseconds of channel opening, in spite of an on-going depolarizing stimulus (Catterall et al., 2005). The specific characteristics of inactivation and the extent to which the occlusion of the pore by the inactivation loop prevents further ion transmission are characteristic of the α subunit (Yu et al., 2003). Inactivation is also coupled to channel activation due to the physical movement of the voltage sensor within the membrane.

After inactivation, the channel closes and becomes fully impermeant to further ions. At this point, the channel is in a refractory state and is unavailable to engage in further cycles of activation until the membrane has returned to its normal resting potential. Once repolarization has occurred, the channel returns to a resting state and is available to engage in another round of activation. This refractory period confers certain physiological advantages such as directional conduction of action potentials.

Persistent sodium current describes sodium current which remains after inactivation when the majority of the transient current has inactivated (reviewed in (Crill, 1996)). Resurgent current describes additional current which can be evoked with a further, usually milder, repolarizing pulse that dislodges a putative inactivating particle from the ion-conduction pore. This current was first described in studies of cerebellar Purkinje neurons (Raman and Bean, 1997). The molecular identity of this particle is not yet known but has been postulated to involve the sodium channel β4 subunit (Grieco et al., 2005b). Both of these current types increase firing rates by promoting channel availability or amount of current present.

Measurements of sodium current by electrophysiological methods are frequently performed in heterologous systems. These can include oocytes obtained from the frog *Xenopus laevis*, and a variety of mammalian cell lines including HEK293

cells, tsA-201 cells and Chinese hamster-derived cell lines. The specific properties of individual sodium channel gene products are often dependent on the cell line in which they are being investigated. For example, co-expression of β1 with $Na_v1.2$ α subunits in HEK vs. Chinese hamster lung cell lines results in shifts in channel voltage-dependence in opposite directions (Isom et al., 1995a). Further, the study of a sodium channel mutation observed in the human neuropathic disease erythermalgia, when performed in two different spinal cord ganglion cell types, produced both neuronal hyperexcitability and hypoexcitability (Rush et al., 2006). Thus, the intracellular microdomain in which a particular sodium channel gene is expressed is critical to its functional phenotype.

Other important tools in characterization and study of sodium channels are the neurotoxins saxitoxin (STX) and tetrodotoxin (TTX). These compounds are heterocyclic guanidines and their application serves to entirely occlude the ion-conducting pore from the extracellular side, preventing ion conduction (Cestele and Catterall, 2000). Both compounds compete for binding to the same site on the channel and bind reversibly with high (sub-nanomolar) affinity. Tetrodotoxin is isolated from the puffer fish ('fugu') (Cestele and Catterall, 2000). Saxitoxin is obtained from blooming dinoflagellates and was once known as paralytic shellfish poison (Schantz, 1986). It engages in binding with the channel at a 1:1 stoichiometric ratio. This allows ^{3}H-saxitoxin to be used to measure the number of channels present in a given sample. In addition, because ^{3}H-saxitoxin is membrane impermeant, it can be used to reliably measure the level of cell

surface sodium channels when used in intact cell binding assays (Henderson et al., 1973; Cestele and Catterall, 2000).

Sodium channel α subunits form a gene family

Voltage-gated sodium channels were first purified from eel electroplax in 1978 by virtue of their ability to bind both tetrodotoxin and saxitoxin (Agnew et al., 1978). This channel was subsequently cloned from eel electroplax by a separate group (Noda et al., 1984). Further studies led to the purification (Hartshorne and Catterall, 1984) and molecular cloning (Noda et al., 1986) of sodium channels from rat brain (Hartshorne and Catterall, 1984) and other tissue types (Catterall et al., 2005).

Each of the channel subtypes composing the sodium channel family exhibit slightly different properties and have unique tissue and subcellular localizations. Channels can also be classified into subfamilies based on their sensitivity to blockade by tetrodotoxin. Channels designated TTX-resistant require micromolar concentrations of tetrodotoxin for effective blockade, while channels designated TTX-sensitive require only nanomolar concentrations for blockade. Early publications proposed some channels to be ‘brain type’ channels. It was later demonstrated, for example, that channels found in neuronal tissue are also expressed in other tissue types such as cardiac muscle (Maier et al., 2002; Malhotra et al., 2004), and 'cardiac' sodium channels are also expressed in brain

(Hartmann et al., 1999), suggesting that channel function and diversity are more complex than originally believed.

The sodium channel gene family is postulated to have originated from a number of early gene duplication events and chromosomal rearrangements. Genes encoding the TTX-sensitive channels (*SCN1A*/$Na_v1.1$, *SCN2A*/$Na_v1.2$, *SCN3A*/$Na_v1.3$, *SCN9A*/$Na_v1.7$) are found in a cluster on human chromosome 2q23-24 or mouse chromosome 2 (Catterall et al., 2005), while the TTX-resistant channels (*SCN5A*/$Na_v1.5$, *SCN10A*/$Na_v1.8$, *SCN11A*/$Na_v1.9$) are clustered separately on human chromosome 3p21-24 or mouse chromosome 9 (Catterall et al., 2005). $Na_v1.4$ and $Na_v1.6$ are encoded independently, with *SCN4A* on human chromosome 17q23-25 or mouse chromosome 11 and *SCN8A* on human chromosome 12q13 or mouse chromosome 15 (Catterall et al., 2005). The primary amino acid sequences of all channels are highly conserved and show a high degree of similarity. $Na_v1.1$, $Na_v1.2$ and $Na_v1.3$, for example, show over 85% sequence similarity. All nine subtypes share at least 50% sequence identity (Catterall et al., 2005).

Sodium channel biosynthesis

Sodium channel α subunits are synthesized in a highly regulated, multi-step process. The early, unmodified channel polypeptide with a molecular weight of approximately 200 kDa is nonfunctional and unable to bind saxitoxin. The

channel then undergoes extensive N-linked glycosylation, after which a pool of “free” α subunits, defined as α subunits not covalently linked to β2, remains in intracellular stores (Schmidt and Catterall, 1986b). In order to reach the plasma membrane where the channel can be functionally active in ion conduction, these "free" α subunits must associate with the β2 subunit. It is postulated that the final step in sodium channel biosynthesis in neurons is association with β2, and that this is concomitant with plasma membrane insertion (Schmidt and Catterall, 1986b). In agreement with this, *Scn2b* null mice show a 50-60% reduction in cell surface sodium channels in neurons (Chen et al., 2002; Lopez-Santiago et al., 2006a). The proportion of the free pool of α subunits found disulfide linked to β2 gradually increases during neuronal development, concomitant with the steady increase in expression of channel protein, as axon outgrowth proceeds and synapses form. Prior to the third postnatal week in rats, ~50% of channels have not associated with a β subunit; by the fourth postnatal week, however, the majority of these pooled channels are found in association with β2 (Schmidt et al., 1985; Scheinman et al., 1989; Gong et al., 1999). The primary channel subtype found in this pool of free α subunits is $Na_v1.2$. $Na_v1.1$, in contrast, associates with β2 upon its first expression between P16 and P19 in rat brain (Gong et al., 1999). This association step of α with β2 before insertion into the plasma membrane serves as the rate-limiting step in channel synthesis (Schmidt and Catterall, 1986b). Insertion of channels into the plasma membrane also decreases their rate of turnover, with the half-life of the pool of free α subunits

estimated at 30 hours, while the half-life of β2-associated channels in the plasma membrane is estimated to be 50 hours (Schmidt and Catterall, 1986b).

Voltage-gated sodium channels are targets for a wide variety of pharmacological agents, each of which have specific binding sites on the α subunit. Seven distinct binding sites have been identified (Cestele and Catterall, 2000; Catterall et al., 2007). Of particular interest is neurotoxin-binding site 1, which binds the neurotoxins saxitoxin and tetrodotoxin at the extracellular side of the pore region (Cestele and Catterall, 2000). The local anaesthetic binding site is found in the inner cavity of the intracellular side of the pore region. This is a three-dimensional site requiring a sequence on the S6 segment from all four domains. Anaesthetic binding to channels is state-dependent, wherein channels which are in the open conformation are more amenable to drug binding (Li et al., 1999). These two sites as well as the other neurotoxin binding sites are summarized in Table I.

Structural components of myelinated axons

When examining patterns of localization of sodium channel protein in the central nervous system (CNS), two elements must be considered. Protein expression can be described in terms of broader localization within different tissues, such as specific brain regions or in particular cell types. Neurons also contain several

cellular subdomains in which proteins can be differentially localized. What are these specialized regions, and what is their function?

The myelin sheath

One of the primary developmental challenges facing higher organisms is the acquisition of the ability to respond rapidly to stimuli, whether this be in terms of rapid movement or of rapid cognition. This has resulted in the development of the myelin sheath. The structure and properties of myelinated axons provide an elegant means by which action potentials can be conducted over long distances in a rapid and effective manner while minimizing loss of electrical signal.

Nearly all vertebrates display some form of compact myelin, a structure which is observed as far back as the ancestors to the modern-day bony fish (teleosts) (Hartline and Colman, 2007). During evolution, the presence of compact myelin appears to have developed in parallel with the evolution of the hinged jaw. This suggests that the development of myelin and the need for rapid saltatory conduction may have been due in part to evolutionary pressure resulting from the predator-prey relationship (Zalc, 2006).

The myelin sheath itself is a multilamellar, lipid-rich structure which ensheathes axons of sufficiently large caliber (reviewed in (Sherman and Brophy, 2005)).

Typically, myelination requires a minimum axonal caliber of 1 μm in order to proceed, with smaller caliber axons in the CNS more permissive for myelination than PNS axons (Salzer, 2003). The relationship between myelin sheath and axon then takes on a characteristic ratio, known as the g-ratio, which is the ratio of axonal diameter to the diameter of the axon + myelin sheath. Most g-ratios lie between 0.6 and 0.7 (Raval-Fernandes and Rome, 1998; Sherman and Brophy, 2005).

Myelin is formed when the myelinating glia make contact with the axon and then extend ramified processes to wind around the axon in a jelly-roll like manner, such that the myelin membranes wrap around the axon multiple times (Baumann and Pham-Dinh, 2001). After several wraps, the cytoplasm is gradually extruded and the plasma membranes come into close apposition, forming compact myelin. The cytoplasmic surfaces of the membrane fuse and the external leaflets come into close contact (McLaurin and Yong, 1995). The extracellular space in compact myelin is only 2 nm thick (Kursula, 2008) and has a periodicity of 12 nm (Baumann and Pham-Dinh, 2001).

Myelination in the CNS is precisely controlled both in terms of which regions and fiber tracts become myelinated, as well as the timing at which myelination proceeds (Baumann and Pham-Dinh, 2001). Myelination in vertebrates begins after birth. Most myelination is complete within the first year in humans but can

continue past the 20th year in some associative regions of the brain (Baumann and Pham-Dinh, 2001). In rodents, myelin formation peaks between days P14 and P28 (McLaurin and Yong, 1995).

In the CNS, axon ensheathment is performed by oligodendrocytes. An individual oligodendrocyte can ensheathe multiple axons, as many as 40 (McLaurin and Yong, 1995; Arroyo et al., 2002; Sherman and Brophy, 2005). Peripheral nervous system (PNS) myelination is performed by Schwann cells which generate a single segment of myelin to ensheath a portion of a single axon (Arroyo et al., 2002; Sherman and Brophy, 2005; Simons and Trotter, 2007). The processes of myelination have been more extensively studied in the PNS due to easy access to large myelinated peripheral nerves such as the sciatic nerve, as well as more permissive *in vitro* systems for the study of PNS myelination.

Axonal subdomains

The myelinated axon can be considered to possess alternating structural elements along its length: the axon initial segment at which the action potential is initiated, followed by the myelin-wrapped axon which is punctated at regular intervals with small gaps in the myelin sheath which form the nodes of Ranvier (reviewed in (Peles and Salzer, 2000; Arroyo et al., 2002)). The axon initial segment and the node of Ranvier share a number of common features but also

have distinct molecular compositions which make them unique from one another (Salzer, 2003). Both of these regions possess an elegant and precise molecular architecture which underlies their normal function.

The node of Ranvier, paranode and juxtaparanode

Axons have two means by which they can increase the rate of signal propagation: increasing the diameter of the axons, leading to giant axons such as those seen in squid, or by the production of an electrical insulator such as myelin which will increase resistance while reducing capacitance along the axon (Hartline and Colman, 2007). Nodes of Ranvier are small, regularly spaced gaps in the myelin sheath which then serve to sustain the transmission of the axon potential as it traverses the length of the axon. It is estimated that consecutive nodes are spaced apart in a manner proportional to axon caliber, an intervening length of approximately 100 times the diameter of the axon (Salzer, 2003). It is at the node that the action potential can be regenerated in totality and then rapidly jump forward to the next node in a unidirectional, saltatory manner along the axon without loss of signal (Salzer, 2003).

The region of myelinated axon between nodes of Ranvier is termed the internode (Arroyo et al., 2002; Quarles, 2002). This area of axonal membrane is not normally electrically active, and is believed to contain low numbers of sodium channels under the myelin sheath, on the order of 25 channels/μm^2 or less

(Waxman, 2002). The myelin sheath itself has low capacitance and high resistance, helping to drive unidirectional current flow and prevent backward leakage of current (Baumann and Pham-Dinh, 2001).

The node of Ranvier itself contains a high density of voltage-gated sodium channels, along with some associated β subunits (H.O'Malley, unpublished observations, (Chen et al., 2004)), which appear as tight clusters in immunofluorescent images. It has been estimated that nodal density exceeds 12000 channels/μm^2 (Waxman and Ritchie, 1993; Poliak and Peles, 2003). During early development, nascent nodes contain high concentrations of $Na_v1.2$. In adults, the predominant sodium channel subtype located at nodes along myelinated axons is $Na_v1.6$ (Boiko et al., 2001b). This developmental switch is dependent on the formation of compact myelin (Kaplan et al., 2001b), and takes place in both central and peripheral myelinated axons. In hypomyelinated *shiverer* mice, $Na_v1.6$ does not appropriately replace $Na_v1.2$ at nodes (Boiko et al., 2001b). In $Na_v1.6$-deficient *med*^{J} mice, the transition to $Na_v1.6$ expression at nodes is delayed as late as six weeks of age in both PNS and CNS nodes (Kearney et al., 2002), while in mice expressing the *med*^{tg} null allele, $Na_v1.2$ expression is retained at nodes to compensate for the loss of $Na_v1.6$, and animals die at approximately three weeks of age, when the developmental switch to $Na_v1.6$ would normally be complete (Vega et al., 2008). These results suggest that, although the properties of $Na_v1.6$ may most effectively conduct action

potentials at nodes, compensatory mechanisms exist which promote normal numbers of channels at nodes regardless of subtype.

Multiple other proteins are specifically localized to the node of Ranvier, such that the clustered sodium channels at the node are part of a macromolecular complex (reviewed in (Arroyo et al., 2002; Poliak and Peles, 2003)). The cytoskeletal adaptor protein ankyrin G is recruited to the nodes of Ranvier where it is able to bind to the cytoskeletal protein spectrin βIV as well as associating with sodium channels, thus serving to anchor the channel complex directly to the cytoskeleton. Ankyrin G binds directly to the α subunit via a short conserved 9 amino acid dileucine motif in the domain II-III linker (Lemaillet et al., 2003; McEwen and Isom, 2004) as well as binding to β1 and β2 subunits (Malhotra et al., 2002). Other proteins enriched at nodes are the cell adhesion molecules Nf186, contactin, and NrCAM and the potassium channels KCNQ2 and K_v3.1. Cell adhesive interactions at nodes of Ranvier contribute to proper nodal formation, including the sequence in which nodal components are recruited during development, as well as to the maintenance of nodal structure (Scherer, 1999; Arroyo et al., 2002). The extracellular matrix protein tenascin-R (TN-R) is also present at the node of Ranvier (Poliak and Peles, 2003).

The paranodal region is located directly adjacent to the node of Ranvier. This specialized structure is the site at which the terminal cytoplasmic loops of the

compact myelin sheath come into close apposition with the axonal plasma membrane (reviewed in (Peles and Salzer, 2000; Arroyo et al., 2002; Rosenbluth, 2009)). In order to maintain efficient saltatory conduction and avoid leakage of current underneath the myelin sheath, the paranode must maintain tight contact between axon and glia. Cell adhesion molecules in the paranode create tight septate-like junctions which appear as electron-dense transverse bands (Scherer, 1999; Arroyo et al., 2002; Poliak and Peles, 2003). In this way the paranode can contribute to the maintenance of appropriate electrical conductivity as well as maintaining the structural integrity of the nodal region.

The transverse bands are created by cell adhesive interactions between three proteins: Caspr (contactin-associated protein, formerly known as paranodin), contactin, and the glial isoform of neurofascin, Nf155 (Bhat et al., 2001; Boyle et al., 2001; Poliak and Peles, 2003). Caspr and contactin are both located on the axonal membrane and engage in *cis* heterophilic cell adhesion. Caspr is a transmembrane protein and a member of the neurexin superfamily (Bhat et al., 2001), while contactin is a glycosyl-phosphatidylinositol (GPI)-anchored protein of the immunoglobulin superfamily (Ranscht, 1988; Gennarini et al., 1989; Einheber et al., 1997). These two proteins form a complex that then binds to the glial Nf155 protein in *trans*, with this tripartite complex forming the transverse bands (Boyle et al., 2001). The sodium channel β1 subunit, located in the nodal region, is also able to engage in cell adhesive interactions with contactin, neurofascin 186, NrCAM, and sodium channel β2 (Ratcliffe et al., 2001; McEwen and Isom, 2004). Association of contactin with sodium channels through β1

increases channel expression at the plasma membrane, further promoting effective conduction (Kazarinova-Noyes et al., 2001; McEwen and Isom, 2004). Mice lacking sodium channel β1 subunits have reduced numbers of nodes of Ranvier in the CNS (Chen et al., 2004). This is postulated to be caused by the loss of sodium channel-contactin interactions, resulting in the destabilization of cell surface sodium channel complexes at nodes.

Proper paranodal formation is also important in sequestering proteins to their normal subcellular domains. Loss of paranodal integrity leads to alterations in the structure and protein localization of the nodal, paranodal and juxtaparanodal regions (Rosenbluth, 2009). In the absence of intact paranodes, sodium channel clusters at the node retain their ankyrin-mediated anchoring to the cytoskeleton and remain nodal. The nodal cluster in this case is sometimes broadened, since the paranode can no longer restrict lateral channel mobility within the membrane. Proteins such as voltage-gated potassium channels or Caspr2 which are normally located in the adjacent juxtaparanodal or internodal regions are then also able to diffuse inward toward the paranode and node. This is seen, for example, in mice deficient in contactin or Caspr (Bhat et al., 2001; Boyle et al., 2001).

The final element of the nodal region is the juxtaparanode, which is located directly adjacent to the paranode and is entirely covered by compact myelin.

This region is enriched in the delayed-rectifier voltage-gated potassium channels $K_v1.1$ and $K_v1.2$ as well as the cell adhesion molecules Caspr2 and contactin-2/TAG-1 (Arroyo et al., 2002; Poliak and Peles, 2003; Salzer, 2003). Caspr2 forms a complex with the potassium channels and their auxiliary β subunits, which remains intact during pathological conditions in which the paranode is disrupted and juxtaparanodal proteins migrate in toward the node (Poliak et al., 2001). The potassium channels present in the juxtaparanode contribute to maintenance of the proper resting potential along the membrane between nodes and assist in repolarization of the membrane during conductance (Peles and Salzer, 2000; Poliak and Peles, 2003). The juxtaparanode can be considered to be a specialized region of the internode.

The axon initial segment

The axon initial segment (AIS) is a specialized axonal domain adjacent to the neural cell body at which the action potential is initially generated. It shares a number of common elements with the node of Ranvier and is present in both myelinated and unmyelinated axons (Salzer, 2003). Like the node, the AIS is a nonmyelinated region of the axon containing dense sodium channel clustering which is enriched in ankyrin G, allowing proteins to become anchored to the actin cytoskeleton. Also similarly to the node of Ranvier, the AIS expresses neurofascin and NrCAM (Salzer, 2003).

The AIS contains a high concentration of sodium channels, similar to the clustering of channels observed at the node of Ranvier. It is this high concentration of channels that allows for the initiation of the action potential by lowering the threshold at which action potential firing can occur (Kole et al., 2007). The AIS specifically expresses $Na_v1.6$ at high levels, as well as lower levels of $Na_v1.2$ and $Na_v1.1$ (Boiko et al., 2003; Duflocq et al., 2008). Whereas the adult node of Ranvier expresses only $Na_v1.6$, the AIS is distinct in its ability to concurrently express both $Na_v1.2$ and $Na_v1.6$ (Salzer, 2003). Interestingly, the specific channel complement expressed by the AIS of different neuronal types varies, as does the specific position along the AIS at which each channel is found, suggesting extensive adaptability of neurons in order to meet particular excitability needs (Lorincz and Nusser, 2008). For example, in cerebellar Purkinje neurons which engage in high-frequency firing, the AIS normally expresses only $Na_v1.6$. In GABAergic interneurons, in contrast, $Na_v1.1$ is expressed in proximal regions and $Na_v1.6$ is expressed in the majority of the AIS (Lorincz and Nusser, 2008).

Localization of sodium channels in brain

The expression patterns of both mRNA and protein products of the different sodium channel genes in the CNS have been studied extensively, both during development and in adult tissue. These studies, when considered as a whole, suggest that channel expression is under elegant and careful control, with the variety of channels available in the sodium channel gene family offering a means

by which cells and tissues can regulate excitability based on specific electrical needs at specific times. What sodium channels are commonly expressed in the CNS, and what are their patterns of expression?

Targeting of sodium channels to specific domains can occur by multiple means. Motifs have been discovered in multiple channels which allow for targeting to different locations. For example, a 9 amino acid motif in the C-terminus of $Na_v1.2$ targets the channel to axons (Garrido et al., 2001). Post-translational regulation and association with adapter molecules offer other means for targeting. These can include masking or revealing of degradation motifs, association with papin, ERM proteins, or ubiquitin ligases (reviewed in (Shao et al., 2009)). Channels can also be modified by kinases including PKA, PKC and calmodulin-dependent kinases (Shao et al., 2009).

$Na_v1.1$

$Na_v1.1$, a TTX-sensitive channel, is highly expressed in brain and is a key contributor to the maintenance of normal neuronal excitability. $Na_v1.1$ is frequently found to be expressed at the somatodendritic plasma membrane, which implicates it more specifically in dendritic excitability. Localization of $Na_v1.1$ is widely conserved between species, further suggesting an essential functional role for this subtype (Vacher et al., 2008).

In the developing rat brain, *Scn1a* mRNA levels are low at embryonic day E18, but increase to moderate levels by P5 as measured by blot and *in situ* hybridization (Beckh et al., 1989; Brysch et al., 1991). Expression levels continue to increase through postnatal day P21, reaching maximal expression by P34 before declining to approximately half maximum levels in adulthood (Gordon et al., 1987; Gong et al., 1999). In examination of whole brain, the overall pattern of $Na_v1.1$ expression is homogeneous throughout the brain (Westenbroek et al., 1989). *Scn1a* mRNA in rat brain is found at negligible levels in adult hippocampus, with a gradient of expression in the Purkinje neuron layer and no detectable expression in granule neurons. *Scn1a* mRNA is also seen in cells of spinal cord grey matter, especially the large motor neurons, primarily in the cell body and major proximal processes (Black et al., 1994a). $Na_v1.1$ is found to be expressed at nodes of Ranvier and axon initial segments in spinal cord and brain (Duflocq et al., 2008; O'Malley et al., 2009) as well as in cell bodies of Purkinje neurons (Kalume et al., 2007).

Mutations in $Na_v1.1$ have been linked to human disease. These mutations are frequently seen in patients with epilepsy, including severe myoclonic epilepsy of infancy (SMEI)/Dravet's Syndrome and GEFS+ (Gambardella and Marini, 2009). Deletion of $Na_v1.1$ in mice results in a lethal epilepsy. Heterozygotes also seize, but are viable. Interestingly, survival of heterozygotes is significantly improved when bred on to the 129Sv genetic background, but heterozygotes begin to display lethality in 85% of animals by the thirteenth postnatal week when bred on

the C57BL/6 genetic background, suggesting the presence of important modifier genes (Yu et al., 2006). These $Na_v1.1$-deficient mice are ataxic, consistent with observation of ataxia and motor control in SMEI patients (Kalume et al., 2007). Reduction in $Na_v1.1$ levels leads to a decrease in both resurgent and persistent current in Purkinje neurons, reducing the extent of fast repetitive firing. $Na_v1.1$ deletion also leads to an increase in expression of $Na_v1.3$ in hippocampal interneurons, which is likely a compensatory change to counter the reduction in excitability (Kalume et al., 2007). It has been proposed that differing functions of $Na_v1.1$ in inhibitory versus excitatory neurons leads to the complex phenotype observed. In $Na_v1.1$ heterozygote or null mice, sodium current is altered in inhibitory interneurons including Purkinje neurons, but excitatory pyramidal neurons do not display alterations in current (Catterall et al., 2008). These data support the theory that specific cellular localization of sodium channels can play a role in their specific functional properties.

$Na_v1.2$

In mature rat brain, the TTX-sensitive channel $Na_v1.2$ shows a rostral-caudal distribution pattern, with high rostral expression that decreases in caudal regions, and high expression in all gray matter. This is in contrast to the more homogeneous distribution and lower levels of protein expression observed for $Na_v1.1$ (Westenbroek et al., 1989). These two channel subtypes have a complementary expression pattern in specific cell types. In cerebellum, $Na_v1.1$ is seen in neuronal cell bodies while $Na_v1.2$ is found primarily in fibers, particularly

unmyelinated fibers (Westenbroek et al., 1989). Interestingly, the ratio of *Scn1a*:*Scn2a* mRNA in whole brain is 3:1, while the protein ratio between these subunits is 2:1, suggesting careful control of protein translation (Black et al., 1994a).

$Na_v1.2$ expression is highest in adulthood, reaching maximal levels by the end of the first postnatal month (Gong et al., 1999). $Na_v1.2$ expression is detectable by E10 and steadily increases through the first postnatal week, with expression thereafter variable depending on brain region (Beckh et al., 1989). *Scn2a* mRNA is found at high levels in the hippocampal granule and pyramidal cells, cerebellar Purkinje neurons, and motor neurons of the spinal cord grey matter as well as other grey matter cells (Black et al., 1994a; Garrido et al., 2001).

$Na_v1.6$

$Na_v1.6$ is not expressed with a rostral-caudal gradient like $Na_v1.2$ but instead displays broad CNS expression (Schaller and Caldwell, 2000). $Na_v1.6$ expression increases during development, with little detectable protein in embryonic stages and increasing amounts by the third postnatal week. $Na_v1.6$ is highly expressed in brain, particularly cerebellum, occipital lobe and frontal lobe (Burbidge et al., 2002), with strong expression seen in cerebellar Purkinje cells (Schaller and Caldwell, 2000). $Na_v1.6$ can also be found in spinal cord motor neurons, and glial expression is detectable by P21 (Schaller and Caldwell, 2000).

Nav1.6 is specifically localized to both nodes of Ranvier (Boiko et al., 2001b) and axon initial segments in myelinated axons (Boiko et al., 2003).

$Na_v1.6$ is a TTX-sensitive channel which displays rapid gating and a significant persistent current. It activates at more hyperpolarized potentials and has a slower rate of recovery from inactivation compared to $Na_v1.2$. Expression of $Na_v1.6$ in retinal ganglion cells appears at the same time as these cells gain the ability to engage in repetitive firing. Mice deficient in $Na_v1.6$ retain this rapid firing capacity, but at a reduced rate as compared to wild type animals (Van Wart and Matthews, 2006). $Na_v1.6$ does not elicit resurgent current in HEK293 cells (Burbidge et al., 2002), but has been shown to produce large resurgent current in cerebellar Purkinje neurons (Raman and Bean, 1997) and DRG neurons in spinal cord (Cummins et al., 2005).

Complete loss of $Na_v1.6$ in mice is lethal, while $Na_v1.6$ heterozygotes are viable. Studies involving crosses between various $Na_v1.6$ mutant mice show that the minimum amount of $Na_v1.6$ required for survival is between 6% and 12% of normal levels (Kearney et al., 2002). Numerous mutant or alternative forms of $Na_v1.6$ have been discovered. Most of these mice display variable amounts of muscle atrophy and disorders of movement (Meisler et al., 2004). The motor endplate disease (*med*, Scn8a ^{med}) mutation was identified first, followed later by other allelic mutations of $Na_v1.6$. *Med*^{J} mice(Scn8a^{medJ}), which express an

aberrantly spliced version of $Na_v1.6$ and only contain approximately 10% of normal levels of $Na_v1.6$, display reductions in muscle mass, dystonia, ataxia, progressive paralysis and decreased conduction velocity (Kearney et al., 2002) Interestingly, the effect of these channel mutations generate different phenotypes depending on genetic background, suggesting the presence of modifier genes and other factors which contribute to proper channel function.

$Na_v1.3$

Scn3a mRNA is expressed weakly or not at all in mature rat brain and is primarily found at embryonic and early perinatal time points (Black et al., 1994a). Some *Scn3a* mRNA is detectable in cortex and other brain regions at E18 via blot hybridization, but this is the only time in rodent development at which any significant expression is observed (Beckh et al., 1989). By P5, there is some $Na_v1.3$ expression remaining in grey matter, but this decreases as well by adulthood (Brysch et al., 1991).

Studies examining sodium channel α and β subunit expression in human brain tissue demonstrate that patterns of expression are largely similar between human and rodent (Whitaker et al., 2001). A notable exception to this in the expression of $Na_v1.3$. $Na_v1.3$ is nearly absent in mature rodent CNS, yet is found at detectable levels in human CNS, reaching comparable expression to $Na_v1.1$ at multiple sites within the human brain (Whitaker et al., 2000).

Sodium channel β subunits

Four genes encoding sodium channel β subunits have been identified to date. Each β subunit is a type I integral membrane protein with an extracellular N-terminus, an extracellular V-type immunoglobulin (Ig) loop which identifies it as a member of the immunoglobulin superfamily of cell adhesion molecules, a single transmembrane-spanning domain and an intracellular C-terminus (**Figure 1.1B**) (reviewed in (Isom, 2001, 2002), also (Isom et al., 1992; Isom et al., 1995c; Morgan et al., 2000; Yu et al., 2003). β1 and β3 associate non-covalently with the α subunit, while β2 and β4 are covalently associated with the α subunit via disulfide linkages. In sodium channels purified to homogeneity from brain, α and β subunits exist in a 1:1:1 stoichiometric ratio, with one non-covalently linked (β1 or β3) and one disulfide-linked (β2 or β4) β subunit for each α subunit (Hartshorne and Catterall, 1984).

The sodium channel β1 subunit

The β1 subunit is encoded by the *SCN1B* gene in humans and the *Scn1b* gene in rodents (Isom et al., 1992; Makita et al., 1994). β1 is a 218 amino acid polypeptide with a molecular weight of approximately 23kDa before post-translational modification and 36kDa after N-linked glycosylation (Isom et al., 1992). β1 has one known splice variant designated β1A in mouse and β1B in human (Kazen-Gillespie et al., 2000; Qin et al., 2003). A splice variant entitled

β1.2 was discovered in astrocytes cultured from rat optic nerve and Schwann cells cultured from rat sciatic nerve (Oh and Waxman, 1994). This was later determined, however, to be an incompletely spliced product including an intron within the 3' untranslated region (Dib-Hajj and Waxman, 1995) . Co-expression of β1 with an α subunit in heterologous systems results in a hyperpolarizing shift of inactivation, increased rates of activation and inactivation, and a significant increase in the peak current amplitude due to promotion of cell surface channel expression (Isom et al., 1992; Patton et al., 1994; Isom et al., 1995a). Binding of β1 to the α subunit is via a weak non-covalent interaction, which can be easily disrupted with mild ionic treatment (Messner et al., 1986).

β1 possesses a number of structural elements which are important for its function, beyond the importance of the Ig loop in cell adhesion. The interactions between β1 and ankyrin G are mediated by the phosphorylation state of the tyrosine residue Y181 in the intracellular C-terminus (Malhotra et al., 2002). Residues in the A/A' face of the β1 Ig loop are required for its interaction with the α subunit (McCormick et al., 1999). The intracellular domain of β1 is specifically required for its interaction with the receptor protein tyrosine phosphatase β (RPTPβ), an interaction that does not take place between RPTPβ and β2 (Ratcliffe et al., 2000).

Loss of the β1 subunit in mice is lethal. The phenotype of *Scn1b* null mice includes retardation of normal growth, multiple seizure types, ataxia, a prolonged cardiac QT interval, and death by the third postnatal week. These mice also display axonal degeneration, disruption of normal nodal architecture, decreases in the number of nodes of Ranvier, and disruptions in neuronal pathfinding and fasciculation (Chen et al., 2004; Lopez-Santiago et al., 2007; Brackenbury et al., 2008b).

The β1B splice variant of β1 contains the same N-terminal domain and Ig loop, but the splicing event results in a novel transmembrane domain and C-terminus. This alternative splicing involves a retained intron, and the human and rat splice variants consequently have significantly different sequences in this region (Kazen-Gillespie et al., 2000; Qin et al., 2003). Co-expression of human β1B with $Na_v1.2$ in oocytes results in an increase in sodium current density but does not significantly modulate channel gating (Qin et al., 2003). Co-expression of rat β1A with $Na_v1.2$ in mammalian cells, however, leads to a shift in the voltage-dependence of inactivation as well as increasing sodium current density (Kazen-Gillespie et al., 2000). Recent work has implicated mutations in β1B in severe myoclonic epilepsy of infancy (SMEI), opening up new lines of investigation to determine the role of this novel β subunit.

The sodium channel β2 subunit

The β2 subunit is a 186 amino acid protein encoded by the *Scn2b* gene located on mouse chromosome 9 and rat chromosome 8 (Isom et al., 1995c; Jones et al., 1996) and the *SCN2B* gene located on human chromosome 11q22. This is the same chromosomal region which encodes N-CAM, also a cell adhesion molecule of the immunoglobulin superfamily (Eubanks et al., 1997). The human and rat orthologs share 89% sequence identity and 93% sequence similarity, with similar predicted structures and retention of four potential N-linked glycosylation sites (Eubanks et al., 1997). β2 migrates at a molecular weight of approximately 32kDa on SDS-PAGE gels. Expression of β2 begins in embryonic development, with *Scn2b* mRNA first detectable at day E9, the same time at which CNS neurogenesis begins and just before the appearance of sodium channel α mRNA. β2 is highly expressed in cerebral cortex and cerebellum as detected by Northern blot (Isom et al., 1995c).

The role of β2 can be further studied using the *Scn2b* global null mouse (Chen et al., 2002; Lopez-Santiago et al., 2006a). *Scn2b* null mice exhibit normal lifespans, unlike *Scn1b* null mice. Deletion of β2 leads to a 50-60% decrease in the number of sodium channels localized at the plasma membrane, as detected by saxitoxin binding assays and confirmed by measurements of peak sodium currents, while not altering the total number of sodium channels present in all cellular membranes (Chen et al., 2002; Lopez-Santiago et al., 2006a). This confirms *in vivo* the role of β2 as a chaperone protein in transduction of the α

subunit to the cell surface which was observed in earlier *in vitro* experiments (Schmidt and Catterall, 1986b). Previous *in vitro* experiments in *Xenopus* oocytes showed that co-expression of β2 with $Na_v1.2$ led to a promotion of fast channel gating and a hyperpolarizing shift in inactivation (Isom et al., 1995c). Electrophysiological studies in β2 null mice demonstrate that the normal function of β2 in excitability is to produce a positive shift in the voltage dependence of inactivation. Deletion of β2 does not lead to a change in conduction velocity in optic nerve, and does not alter axon size or proper formation of nodes of Ranvier in sciatic nerve (Chen et al., 2002). Loss of β2 also does not alter normal nodal structure or clustering of sodium channels at nodes of Ranvier in central myelinated axons (H. O'Malley, unpublished observations). Finally, deletion of β2 results in an increased susceptibility to induced seizures, potentially due to decreases in sodium channel function in inhibitory interneurons (Chen et al., 2002). Interestingly, the effect of co-expression of β2 with different α subunits may differ, suggesting the presence of mechanisms which can finely tailor excitability to cellular needs (Johnson and Bennett, 2006). Deletion of β2 in brain does not lead to compensation by β1, which supports the non-overlapping roles that can be inferred by their distinct mechanisms of binding to the α subunit (Chen et al., 2002). β2 also plays a role in pain pathways via the modulation of TTX-resistant sodium channels in sensory neurons. Loss of β2 in dorsal root ganglion neurons results in decreased sensitivity to noxious thermal stimuli as well as an attenuated response to inflammatory pain. This is proposed to result from the loss of β2-mediated channel plasma membrane insertion as well as β2-

mediated effects on current inactivation properties, with consequent alterations in neuronal excitability (Lopez-Santiago et al., 2006a).

The sodium channel β3 subunit

The sodium channel β3 subunit is encoded by the gene *SCN3B* on human chromosome 11q23 (Morgan et al., 2000) and the Scn3b gene on mouse chromosome 9 (Qu et al., 2001b), sharing 57% sequence identity with β1 but only 40% identity with β2 (Morgan et al., 2000). Similarly to β1, β3 associates in a non-covalent manner with the α subunit. β3 is expressed broadly within CNS tissue and is found at high levels in hippocampus, striatum and the superior cervical ganglion (Qu et al., 2001b), where it has a pattern of expression which is primarily complementary to that of β1 (Morgan et al., 2000). Co-expression of β3 with α results in a hyperpolarizing shift in the voltage-dependence of inactivation, similar to β1, which leads to the presence of more channels able to engage in fast gating (Morgan et al., 2000). Additionally, interaction with β3 promotes cell surface expression of $Na_v1.8$ in a heterologous system (Zhang et al., 2008). Interestingly, despite its homology with β1, β3 does not engage in *trans*-homophilic cell adhesion nor does it bind directly to ankyrin G or contactin (McEwen et al., 2009).

Mice lacking β3 show defects in cardiac ventricular function which resemble abnormalities seen in $Nav1.5^{+/-}$ mice. $\beta3^{-/-}$ hearts display increases in *Scn1b* and

Scn5a mRNA levels. They do not display other overt behavioural phenotypes (Hakim et al., 2008).

The sodium channel β4 subunit

The β4 subunit, a protein 228 amino acids in length, is encoded by the *SCN4B* gene located on human chromosome 11q23 and the *Scn4b* gene on mouse chromosome 9 (Yu et al., 2003). After N-linked glycosylation, β4 has a molecular weight of 38kDa. It shares 35% sequence identity with β2 and 20-22% identity with β1 and β3, retaining the same conserved cysteine residues as β2 and forming disulfide bonds with the α subunit. β4 is primarily found within excitable tissues, with high levels of protein in DRG neurons as well as cortex, Purkinje neurons, spinal cord, skeletal muscle and heart. It shares partial colocalization with β2, but the two subunits have complementary expression patterns in many tissue types (Yu et al., 2003).

Co-expression of β4 with α in tsA-201 cells causes a negative shift in the voltage-dependence of current activation which exceeds that of β2, with no effect on inactivation (Aman et al., 2009). β4 does not promote resurgent current, but does increase persistent current, an effect which is moderated by the presence of β1 (Aman et al., 2009). When co-expressed with $Na_v1.2$ in tsA-201 cells, the effects of β4 on channel kinetics will over-ride those of either β1 or β3 (Yu et al., 2003). In either transfected hippocampal neurons or HEK cells, however, β1

exerts a dominant influence over β4 (Aman et al., 2009). In transfected hippocampal neurons or cultured Neuro2A cells, β4 can also induce neurite outgrowth (Oyama et al., 2006). It is likely that in some neurons, the two β subunits associated with the sodium channel α subunit are β1 and β4. In this situation, the functions of the two auxiliary subunits serve to balance one another, with β1 promoting inactivation and stabilizing the closed state at hyperpolarizing potentials, and β4 promoting channel opening and increased current amplitudes (Aman et al., 2009). *Scn4b* null mice have not been generated to date.

β subunits are cell adhesion molecules

Sodium channel β subunits are unique in their ability to function independently of the α subunit as cell adhesion molecules, making them multifunctional proteins which have distinct properties compared with auxiliary subunits of other voltage-gated ion channels. These cell adhesive properties were postulated when the structure of the β subunits was found to contain a type-V Ig loop, which places the β subunits as members of the immunoglobulin superfamily of cell adhesion molecules (Isom et al., 1995c; Isom and Catterall, 1996).

The β1 subunit engages in a variety of cell adhesive functions and has been proposed to be a component of multiple structural and developmental processes as a result. β1 engages in homophilic cell adhesion during which it is able to

recruit ankyrin to the location of cell-cell contact (Malhotra et al., 2000a). This interaction with ankyrin is mediated by a tyrosine residue in the intracellular tail of β1, residue Y181, and binding is dependent on the phosphorylation state of this residue, allowing for careful control of ankyrin recruitment (Malhotra et al., 2002). The phosphorylation state of this tyrosine residue may be influenced by the ability of β1 to interact during development with RPTPβ, which is able to reduce levels of tyrosine phosphorylation and can modulate channel function (Ratcliffe et al., 2000).

β1 is capable of engaging in *trans*-heterophilic cell adhesion with multiple protein partners including NrCAM, Nf185, contactin and Nf155. Additionally, β1 and β2 can engage in heterophilic cell adhesion via their extracellular domains in an interaction that requires the intracellular domain of β2. β1 and β3 do not engage in cell adhesion (McEwen and Isom, 2004). Both β1 and β2 are capable of interacting with the extracellular matrix protein tenascin-R (Srinivasan et al., 1998; Xiao et al., 1999) which is present at nodes of Ranvier.

β1 is able to play a functional role in neurite outgrowth by virtue of its properties as a cell adhesion molecule. β1-mediated neurite outgrowth requires *trans*-homophilic cell adhesion as well as signaling via the *fyn* kinase signaling pathway (Davis et al., 2004; Brackenbury et al., 2008b). β1 is also involved in

neuronal pathfinding and axon fasciculation during development (Brackenbury et al., 2008b).

The β subunits, and mutations in the β subunits, have been linked to disease. The C121W mutation in β1, which mutates a key cysteine residue within the Ig loop, is a cause of generalized epilepsy with febrile seizures plus (GEFS+) (Wallace et al., 1998; Meadows et al., 2002). Other mutations in β1 not within the Ig loop which lead to a failure to correctly modulate channel kinetics have also been linked to GEFS+ (Xu et al., 2007). Expression of the β4 subunit is reduced by as much as 90% in a mouse model of Huntington's disease, as assayed by microarray data and Northern blotting, and may be involved in neurite degeneration in that model (Oyama et al., 2006). A recently-identified homozygous recessive mutation in the human β1 subunit creating a functional null mutation was linked to Dravet Syndrome, a form of epilepsy (Patino et al., 2009).

Interestingly, roles for β subunits in non-excitable cells have also been discovered. *Scn1b* mRNA can be found in certain cancer cell lines, and β1 protein expression is higher in weakly metastatic cells than in highly metastatic cells (Chioni et al., 2009). The function of β1 in metastasis appears to be as a result of its function as a cell adhesion molecule. The α subunit has also been implicated in cancer. In a non-small-cell lung cancer cell line, sodium channel

function increases metastatic activity, and this metastasis can be blocked by the application of tetrodotoxin (Roger et al., 2007).

Evidence has begun to accumulate to implicate sodium channel β subunits as substrates for proteolytic cleavage by β- and γ-secretases. Secretase proteolysis occurs as a sequential multi-site cleavage event which first sheds the ectodomain of the cleaved protein followed by variable intracellular domains (ICD). Many cleaved proteins are type I membrane proteins involved in cell adhesion and/or migration (Kim et al., 2005). β-site APP-cleaving enzyme 1 (BACE1), the primary β-secretase involved in cleavage in brain, is a type I membrane protein which functions as an aspartyl protease (Huth et al., 2009; Willem et al., 2009). It is expressed at high levels in brain. BACE1 function occurs within acidic endosomes, and in neurons it is transported to the axonal plasma membrane and potentially to pre-synaptic terminals. BACE1 expression can be increased in conditions of cellular stress (Willem et al., 2009).

The β2 subunit is a substrate for both BACE1 and γ-secretase cleavage (Kim et al., 2005; Huth et al., 2009). BACE1 can regulate sodium channel activity via cleavage of β2 subunits, thus promoting channel turnover. The released ICD fragment then contributes to a feedback mechanism which functions to keep channels at lower levels at the plasma membrane (Willem et al., 2009). β2 cleavage by γ-secretase results in a C-terminal fragment which is further cleaved

to generate a short intracellular domain (Kim et al., 2005). These cleaved fragments may play a role in β2-mediated cell adhesion and migration. For example, cleavage of β4 by BACE1 may release an ICD which enhances neurite outgrowth (Miyazaki et al., 2007).

II: DEVELOPMENT OF CNS MYELINATING GLIA AND RELATIONSHIP TO SODIUM CHANNELS

Oligodendrocytes and glial development

Glial cells are diverse and populous cells found throughout the nervous system, serving as important players in both normal nervous system function and development as well as in pathology (Barres, 2008). The primary glial cell types in the CNS are astrocytes, oligodendrocytes and microglia. Glia can be distributed heterogeneously throughout the brain or restricted to a specific region (Wang and He, 2009). During pathology, glial cells can undergo morphological changes including hypertrophy and increased numbers of processes, as well as display increases in proliferation (Wang and He, 2009)

Astrocytes, identifiable by expression of glial fibrillary acidic protein (GFAP), make up a large percentage of CNS glial cells and exhibit a heterogeneous distribution. They associate closely with neurons, including neuronal synapses (Hansson and Ronnback, 2003). Astrocytes are able to form gap junctions and

come into contact with the vasculature, implicating them in maintenance or communication with the blood-brain barrier (BBB) (Wang and He, 2009). They have been proposed to play a role in CNS metabolism via the transport of various soluble factors and nutrients (Hansson and Ronnback, 2003; Wang and He, 2009). Astrocytes also contribute to the maintenance of extracellular ionic balance, particularly during neuronal activity, and are able to aid in the recycling of neurotransmitters at the synapse (Wang and He, 2009).

Oligodendrocytes are the glial cells responsible for myelination of axons in the CNS. Myelinating oligodendrocytes can be smaller cells which generate thinner, shorter segments of myelin on many axons, or larger cells which generate longer, thicker segments of myelin on fewer axons (Baumann and Pham-Dinh, 2001). Mature oligodendrocytes are multipolar cells with numerous processes, a small cell body and dense cytoplasm (McLaurin and Yong, 1995). They are derived from neuroepithelial cells (Fok-Seang and Miller, 1994). The pools of progenitors which give rise to the earliest oligodendrocyte precursor cells (OPCs) are located in regions such as the subventricular zone of the brain and the ventral region of the neural tube (McLaurin and Yong, 1995; Baumann and Pham-Dinh, 2001; Miller, 2002). The exact zone that specifies OPCs is determined by local sonic hedgehog (*Shh*) signaling (Gao and Miller, 2006). Other factors such as bone morphogenetic protein (BMP) may also play a role in proper migration (McTigue and Tripathi, 2008). OPCs retain their mitotic character and are highly migratory, being able to travel long distances to their

destination (Fok-Seang and Miller, 1994). As differentiation proceeds, the cells gradually become less motile. Ultimately, the mature oligodendrocyte is non-migratory and post-mitotic (Baumann and Pham-Dinh, 2001).

Differentiation of oligodendrocytes progresses in a linear fashion through a series of intermediate cell types which can be identified and observed using antibodies against different cell surface antigens (**Figure 1.2**). Development of glial cells parallels neuronal development, with commitment to the oligodendrocyte lineage occurring as early as embryonic days E10-E12.5 in rodents (Zhang, 2001). It is likely that commitment to the neuronal lineage precedes determination of oligodendrocyte fate by a time up to several days (Gao and Miller, 2006).

The first OPCs are bipolar progenitor cells positive for the markers A2B5, platelet-derived growth factor receptor α (PDGFRα) and the chondroitin sulfate proteoglycan NG2 (Baumann and Pham-Dinh, 2001; Zhang, 2001; Miller, 2002). The A2B5 antibody recognizes epitopes on as yet unidentified gangliosides (Baumann and Pham-Dinh, 2001). In rat spinal cord, these A2B5-positive cells are visible by day E14, but are restricted to the ventral spinal cord and only migrate into the dorsal column over time before undergoing further lateral migration (Fok-Seang and Miller, 1994).

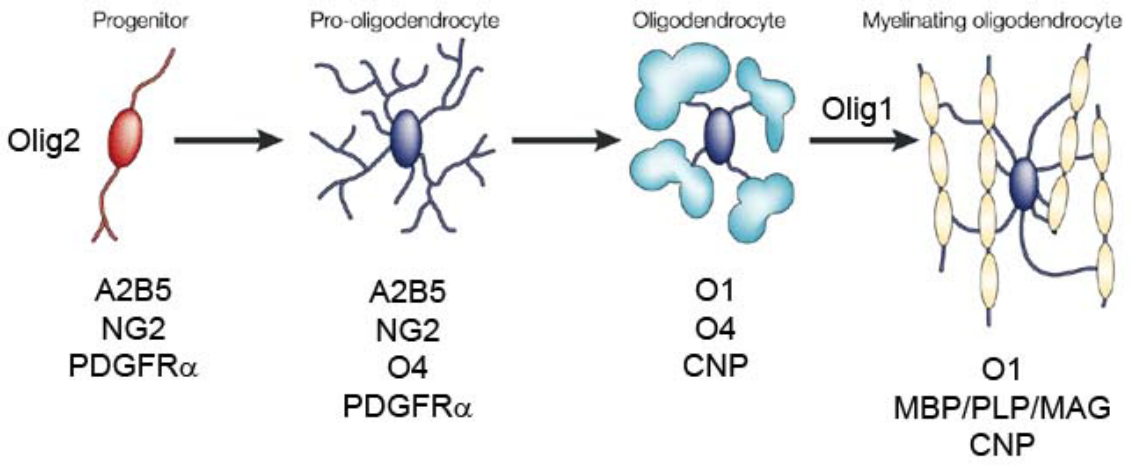

<u>Figure 1.2</u>: Differentiation of oligodendrocytes.

Oligodendrocyte development follows a linear path in which progenitor cells differentiate into pro-oligodendrocytes, followed by oligodendrocytes, which are then able to differentiate into myelinating oligodendrocytes upon contact with an axon. PDGFRα: platelet-derived growth factor receptor; CNP: 2',3'-cyclic nucleotide 3'-phosphodiesterase; MBP: myelin basic protein; PLP: proteolipid protein; MAG: myelin-associate glycoprotein.

These OPCs next differentiate into pre-oligodendrocytes which display a multipolar morphology, acquiring the O4 marker, retaining expression of NG2, and downregulating expression of the A2B5 and PDGFRα epitopes (Zhang, 2001). Interestingly, a number of NG2-positive cells do not continue to differentiate but remain within the CNS in small but significant numbers, representing 5-8% of all adult CNS cells (Fields, 2008). They are distributed throughout the parenchyma, suggesting that they have a role beyond their function as precursor cells. O4-positive pro-oligodendrocytes can be detected in rat spinal cord by day E16 (Fok-Seang and Miller, 1994). It has also been shown that processes of these multipolar NG2-positive cells are able to come into contact with the axolemma at nodes of Ranvier (Butt et al., 1999).

Oligodendrocyte numbers within the CNS are highly regulated. In the presence of axonal support, pro-oligodendrocytes are able to differentiate into myelinating proteolipid (PLP)-positive cells. In the absence of axonal connection, however, these cells will undergo programmed cell death. This is a stage-specific means by which oligodendrocyte cell numbers can be controlled and is not observed in either progenitor cells or terminally differentiated PLP-positive cells (Trapp et al., 1997). Axonal contact is specifically required, as shown by *in vitro* experiments using neural-conditioned media without neuronal cells in which programmed cell death cannot be averted (Trapp et al., 1997). In normal circumstances, approximately 50% of oligodendrocytes die within 2 to 3 days if they do not make contact with an axon (Barres and Raff, 1999). In this way, the nervous system

can ensure that the correct proportion of axon number to oligodendrocyte number is preserved. The presence of fewer axons leads to fewer oligodendrocytes whereas the presence of more axons leads to more oligodendrocytes (Gao and Miller, 2006). Local survival factors such as PDGF and neuregulin also contribute to the final numbers of oligodendrocytes present (Miller, 2002; Simons and Trajkovic, 2006). This is again stage-specific, since post-mitotic oligodendrocytes downregulate expression of PDGF-R and can no longer respond to the presence of PDGF as a survival signal (Barres and Raff, 1999).

NG2-positive pre-oligodendrocytes continue to differentiate into multi-process pro-oligodendrocytes lacking NG2 expression. These cells halt migration along fiber tracts before losing their ability to divide (Baumann and Pham-Dinh, 2001). Finally, pre-oligodendrocytes can differentiate into mature myelinating oligodendrocytes which acquire the O1 marker and lastly begin to express myelin-specific proteins (Zhang, 2001). At this point, oligodendrocytes coming into contact with an axon can begin the process of ensheathment. This is not a sequential process, but occurs simultaneously at all axons with which the oligodendrocyte has established contact, within a time span of 12-18 hours (Barres, 2008).

Myelin composition

The myelin sheath itself contains a large amount of protein, making up approximately 30% of the total myelin composition with the majority of the remaining 70% consisting of lipid (Baumann and Pham-Dinh, 2001). Certain of these proteins are expressed specifically in the CNS or PNS, while others are found in both nervous systems. The majority are strongly hydrophobic and most contain at least one transmembrane domain (Kursula, 2008).

Proteolipid protein (PLP) is found in both PNS and CNS, and is the predominant protein component of CNS myelin (Arroyo et al., 2002; Tzakos et al., 2005). PLP is an integral membrane protein containing four transmembrane domains, and has a molecular weight of approximately 30 kDa. It interacts in the cytoplasm with myelin basic protein (MBP) in order to maintain correct myelin structure (Baumann and Pham-Dinh, 2001; Tzakos et al., 2005).

MBP is also expressed in both PNS and CNS. It comprises over 25% of total CNS protein, but represents only 5 – 15% of PNS protein. MBP is highly basic and is found at the cytoplasmic surface of the myelin membrane (Baumann and Pham-Dinh, 2001; Tzakos et al., 2005). MBP has been proposed to function in clustering myelin components during the process of myelin membrane assembly and compaction (Simons and Trotter, 2007)

The proteins PMP22 and myelin P0 are both found specifically expressed in the PNS. Myelin P0 is the major protein found in PNS myelin, accounting for over 50% of total PNS protein (Tzakos et al., 2005). Myelin P0 is responsible for maintaining appropriate membrane spacing, engaging in homophilic cell adhesion. This interaction may occur both in *trans* and in *cis* (Quarles, 2002). PMP22 may also play a role in adhesion during early stages of myelination. Mutations in PMP22 have been implicated in Charcot-Marie-Tooth disease type 1A (CMT1A) (Tzakos et al., 2005).

2', 3'-cyclic nucleotide phosphodiesterase (CNP) is also found in the cytoplasm in both CNS and PNS and comprises approximately 4% of total myelin protein. It is expressed in glial cells during differentiation. CNP is responsible for the hydrolysis of 2', 3'-cyclic nucleotides into the 2' forms, but the importance of this function has not yet been determined (Baumann and Pham-Dinh, 2001). CNP has been shown to be essential for the maintenance of proper axo-glial contactin CNS nodes of Ranvier (Rasband et al., 2005).

Myelin-associated glycoprotein (MAG) is found in non-compact myelin membranes in both the PNS and CNS. It contains multiple Ig loops and can thereby function in cell adhesion, potentially with a role in axo-glial interactions (Quarles, 2002; Tzakos et al., 2005). MAG represents only 0.1-1% of total myelin protein (Kursula, 2008). MAG is not essential for myelination, but may be

important in the proper formation and maintenance of the myelin sheath (Quarles, 2002). MAG may also be able to inhibit neurite outgrowth (Baumann and Pham-Dinh, 2001).

Finally, myelin oligodendrocyte glycoprotein (MOG), a type I integral membrane protein, is found in the CNS and is a relatively small component of myelin, making up approximately 0.05% of total myelin protein (Baumann and Pham-Dinh, 2001; Tzakos et al., 2005). Its sequence is highly conserved. MOG is specifically localized to the outer lamellae of the myelin sheath, the oligodendrocyte cell body and processes, placing it in an ideal location to interact with the extracellular environment (Baumann and Pham-Dinh, 2001; Quarles, 2002). It is expressed late in development and is likely to be involved in compaction or maintenance of the myelin sheath (Tzakos et al., 2005).

Ionic current in glial cells

Oligodendrocytes and OPCs have long been considered to be non-excitable cells, ultimately serving only as electrical insulators for the excitable neuronal cell they ensheathe. Evidence has shown that OPCs express multiple voltage-gated ion channels, challenging established beliefs and opening the possibility of new and previously uninvestigated roles for glial cells in the nervous system.

Most studies have approached the question of glial excitability through the electrophysiological observation of ionic current in glial cells. Multiple groups have examined the progenitor cell termed the O-2A cell, which has been proposed to be a precursor of both oligodendrocytes and type 2 astrocytes (Barres et al., 1990b; Williamson et al., 1997). It remains unclear, however, if the O-2A cell exists *in vivo*. O-2A cells have been derived from multiple tissue locations, including neonatal rat optic nerve (Barres et al., 1990b), adult rat optic nerve (Borges et al., 1995), neonatal mouse cortex (Sontheimer et al., 1989) and neonatal rat mixed brain (Williamson et al., 1997). O-2A cells in culture display both inward and outward current which can be shown to arise from voltage-gated sodium and potassium channels (Barres et al., 1990b) as well as multiple voltage-gated calcium channels (Williamson et al., 1997). In most cases, however, these currents do not generate action potentials (Fields, 2008).

The ability of glial cells to generate current appears to be downregulated during differentiation and maturation of the progenitor cell (Paez et al., 2008). An early developmental study looked at current expressed in two stages of OPCs as well as two stages of more mature oligodendrocytes. Bipolar A2B5-positive cells showed a TTX-sensitive transient inward sodium current, which decreased as cells acquired the O4 marker. Mature oligodendrocytes did not display any sodium current (Sontheimer et al., 1989). Other studies involving mouse brain slices displayed sodium current at days P3-P8 but not at P10-P18 (reviewed in (Paez et al., 2008)).

The focus of many of studies of ionic current in glia has been the multipolar NG2-positive precursor cell. These cells are found within the hindbrain and forebrain by embryonic day E16-E17 and show large increases in numbers just prior to birth (Wang and He, 2009). NG2 cells in culture generate ionic current, a low density current which is TTX-sensitive and displays fast activation and inactivation as well as a persistent component (Xie et al., 2007). NG2 cells also express both glutamate and γ-aminobutyric acid (GABA) receptors and can synapse with both glutaminergic and GABA-ergic neurons (Wang and He, 2009). Current in NG2 cells has been proposed to play a major role in the establishment of the glial resting membrane potential (Xie et al., 2007).

Interestingly, a recent study has shown the presence of dual populations of NG2-positive cells which share a common morphology and capacity to proliferate (Karadottir et al., 2008). One population has the ability to generate multiple TTX-sensitive action potentials upon depolarization, while the other population does not fire any action potentials. These two cell populations can also be distinguished by several other related characteristics. Cells able to fire action potentials displayed immunostaining with the pan-sodium channel antibody which recognizes all voltage-gated sodium channel subtypes while non-spiking cells did not display sodium channel immunofluorescence (Karadottir et al., 2008). Consistent with previous studies showing decreases in current during

differentiation (Sontheimer et al., 1989), the ratio of firing to non-firing NG2 cells at day P7 was approximately 50:50, while by day P12 this had changed to a ratio of 70:30. The two cell populations also displayed different sensitivities to ischemia. Cells capable of firing action potentials were more susceptible to glutamate-mediated excitotoxicity as compared to non-spiking cells (Karadottir et al., 2008). The presence of the spiking current seen in this study is supported by an earlier examination of NG2 cells in cortex, which were seen to occasionally fire a single action potential in response to depolarizing current (Chittajallu et al., 2004). The role of these newly discovered spiking NG2 cells remains unknown, and opens new avenues of investigation into ion channel function in glia.

What is the function of ion channels in glia? This question is still the subject of active investigation. It is possible that channels contribute to the transduction of signals during development (Barres et al., 1990b). Voltage-gated ion channels have also been proposed to play a role in cell proliferation (Pardo, 2004; Wu et al., 2006) and migration (Paez et al., 2008). Channels may also contribute to the initiation of myelination (Karadottir et al., 2008). Current in glial cells may be able to promote not just early nervous system development but also plasticity in later development, with excitable glia offering a means of dynamic communication with the neuron (Fields, 2008).

III: MULTIPLE SCLEROSIS AND THE ROLE OF SODIUM CHANNELS IN DEMYELINATING DISEASE

What is multiple sclerosis?

Multiple sclerosis (MS) is an inflammatory demyelinating disease of the central nervous system which results in progressive neurological dehabilitation. It is a prominent cause of neurological disability in young adults, with patients often first diagnosed between the ages of 20-40 (Waxman, 2006a; Courtney et al., 2009). MS consists of regions of inflammation, demyelination, axonal damage and axonal loss which form lesions within central nervous tissue.

The cause of MS remains unknown, but is likely to be a result of multiple factors including environmental and genetic factors. Two environmental influences which have been been frequently proposed include vitamin D deficiency, suggested by demographic differences in disease prevalence between regions of the world at different latitudes, and exposure to the Epstein-Barr virus (Courtney et al., 2009; Goodin, 2009). The presence of environmental factors in the etiology of MS is evident from data obtained from patients who moved between areas of differing disease prevalence at different ages. Children under the age of 15 who move acquire the risk level of the area into which they subsequently reside, while individuals who move after the age of 15 retain the risk level of the area from which they moved (Courtney et al., 2009; Goodin, 2009). This suggests the presence of some element in the environment which can have a

lasting impact that contributes to later disease development. The prevalence of MS in populations in the northern hemisphere is estimated to be 1 in 1000 (Courtney et al., 2009; Goodin, 2009). Two- to three-fold more women than men are afflicted with MS; males, however, show higher incidence of more severe progressive disease forms (Courtney et al., 2009).

Many patients first present clinically with episodes of optic neuritis which reveal the presence of demyelinating lesions (Bjartmar et al., 1999). During the course of the disease, visual deficits are a common clinical presentation (Balcer, 2001). Early stages of MS often include a sequence of relapses with intervening periods of clinical remission. During reversible disease stages, including relapses, patients experience acute inflammation which is receptive to treatment with anti-inflammatory and immunomodulatory agents. After an average period of 8-15 years following the onset of disease, however, most patients begin to display irreversible symptoms, and the disease transitions from a relapsing-remitting form to a chronic, progressive form (Bjartmar et al., 1999; Courtney et al., 2009). In these chronic stages, inflammation is minimal or absent and non-reversible damage to axons and axonal loss begins to accumulate. This is consistent with other neurodegenerative diseases such as amyotrophic lateral sclerosis (ALS) or Parkinson's disease which present with early stages of clinically silent neuronal loss followed by later neuronal loss that leads to clear disability. The point at which disability becomes inevitable is not currently able to be predicted but likely occurs at a point at which compensatory and repair mechanisms within the

nervous system can no longer overcome the amount of damage present (reviewed in (Bjartmar et al., 2003)).

MS patients can experience both positive and negative symptoms. Negative symptoms are a result of conduction block and include manifestations such as paresis and ataxia (Smith, 2007). Positive symptoms are a result of aberrant neuronal firing generated at the lesion, often including electrical hyperexcitability, and can involve both paroxysmal (such as painful seizures and intermittent pain) and persistent (chronic pain) components (Sakurai and Kanazawa, 1999). Symptoms also include variable impairments in cognition, including deficits of both memory and learning. Patients frequently experience clinically significant levels of pain which vary depending on disease subtype, with 50-80% of patients reporting having suffered from pain (Olechowski et al., 2009).

A characteristic MS lesion is a focal site of demyelination, astrogliosis, loss of oligodendrocytes, axonal loss and axonal damage. Foamy macrophages filled with membranous debris are often found at lesion peripheries (Ludwin, 2006). Lesions and damage can occur throughout central nervous tissue. Active lesions are typically considered to be acute foci of injury with active inflammation and demyelination, whereas chronic lesions no longer involve ongoing inflammation. Chronic spinal cord lesions exhibit an average of 68% axonal loss (reviewed in (Bjartmar et al., 2003; Ludwin, 2006). Many lesions, particularly those exhibiting

active inflammation, display significant infiltration of microglia and macrophages, with the numbers of macrophages present correlating with the extent of injury (Ferguson et al., 1997). Damage to the optic nerve can lead to loss of 40% of axons or more, with concomitant reductions in nerve cross-sectional area. Even after resolution of the inflammation which precipitates an attack of optic neuritis, nerve pathology can persist for years, with reductions in action potential conduction and nerve atrophy (Kolbe et al., 2009). Patients often show thinning of the retinal nerve fiber layer, which is linked to deficits in vision (Shindler et al., 2008).

MS is often described as an autoimmune disease, and numerous studies have examined specific immunologic components of the pathological process. Many current clinical treatments focus on immune modulation or immune suppression. However, these treatments are incompletely effective and do not reliably address the underlying elements of neurodegeneration and axonal loss. In order to discover therapies which will protect patients from the development of irreversible neurological damage and progressive symptoms, it is essential to understand the molecular mechanisms which contribute to disease development and progression. This includes axonal pathology and the timing of axonal loss.

What pathological elements form the basis of MS clinical symptoms?

The MS lesion is a focal site including multiple pathological changes, but does this lead with certainty to the often-proposed perspective of MS as a lesion-centric disease? Damage to nervous system tissue in MS extends through both grey and white matter tracts, and although some sites are more prone to lesion development, no region of the nervous system is entirely resistant to damage or pathological changes (Chard and Miller, 2009). Additionally, normal-appearing tissue not containing an active or chronic lesion may not in fact be 'normal tissue' when subjected to other means of diagnosis (Bjartmar et al., 2003; Zeis et al., 2008a). It becomes more difficult to distinguish the relative importance of lesion versus non-lesion tissue when considering that the total amount of CNS tissue containing a lesion at any given point in time does not represent the total amount which has contained a lesion at any point in the disease course (Trapp et al., 1998; Bjartmar et al., 2001). Lesions can be resolved and recovered from, and some elements of pathology are more transient than others (Chard and Miller, 2009).

It has been observed that some patients display clinical symptoms which are more severe than would be predicted from the amount of detectable nervous system pathology they exhibit. One of the most common diagnostic methods used to evaluate MS patients is magnetic resonance imaging (MRI) which allows for the visualization of lesions. Lesion load, the total number of lesions throughout the central nervous system at a given point in time, can be a

challenging and potentially misleading tool in diagnosis (Vellinga et al., 2009). It has been theorized that a higher number of lesions leads to more severe neurological disease. However, MRI techniques do not consistently detect lesions which are clinically silent, and are unable to detect regions of pathology which are located outside of countable lesions. Additionally, adaptive changes in the nervous system which lead to functional recovery may make calculation of the number of discrete lesions more difficult (Vellinga et al., 2009). This makes correlations between lesion load and clinical outcome unreliable, and more accurate predictors of disease severity and potential for recovery are required which do not rely on this means of measurement.

A more significant metric when attempting to correlate lesions and clinical course may be the overall distribution and location of lesions. The corticospinal tract is one of the first tissue sites to display progressive damage, and damage in this region is a major contributor to disability (DeLuca et al., 2004). The most prevalent location for lesions is in periventricular regions, and this does accurately correlate with disease scores (Vellinga et al., 2009). In further support of this perspective, progressive versus remitting forms of the disease do not share a consistent lesion distribution. Primary and secondary progressive forms do, however, share a similar pattern of lesion location (Tallantyre et al., 2009).

Myelin damage

Loss of myelin is a significant element of MS pathology. Axons which have lost their insulating myelin sheath also lose their ability to engage in rapid and effective saltatory conduction. Chronic lesions display a larger number of demyelinated axons and numerous astrocytic processes compared to progressive lesions, but with little remaining immune involvement (Black et al., 2007a). Demyelinated regions also contain a mixture of intact and some degenerating axons as the process of degeneration proceeds. Demyelination may begin with delamination of the myelin sheath, along with other alterations in axonal components including increases in filamentous structures and changes in neurofilaments (Zapryanova et al., 2004). Loss of myelin can be a result of apoptosis or necrosis of oligodendrocytes as well as direct attack on the myelin sheath (Ludwin, 2006). Damage to oligodendrocytes can also occur via a "dying-back" mechanism which seems to be a result of metabolic damage not directly involving the cell body, only the more distal processes (Lassmann et al., 1997). Direct and indirect damage to myelin can occur via mechanisms such as immune cell attack, excitotoxicity, or damage via reactive oxygen species or other enzymatic processes (Ludwin, 2006).

Normal-appearing white matter

Nervous system tissue is classified into two primary types: white matter and grey matter (Kandel et al., 2000). White matter consists primarily of long tracts of myelinated axons, deriving its name from the pale colour of the myelin sheath.

Grey matter, on the other hand, contains the neuronal cell bodies and the neuropil, which is made up primarily of dendrites and nonmyelinated axons (Kandel et al., 2000)

Both white and grey matter tracts have been shown to exhibit molecular changes at various stages of MS (Zeis et al., 2008b). Regions of white matter not containing an active or chronic lesion or containing focal regions of demyelination are often referred to as 'normal-appearing white matter' (NAWM). This term is not, however, precisely correct. Degeneration of the axon occurs distal to the location of axon transection, which allows for the retention of myelin in proximal regions even in the absence of a fully intact axon. These empty myelin sheaths can persist after earlier damage. This can result in the misleading appearance of 'normal-appearing' white matter as undamaged tissue, while in fact these regions exhibit significant amounts of damage that are not visible via MRI or with conventional histological myelin stains such as Luxol fast blue (LFB) (Bjartmar et al., 2001; Ludwin, 2006). It is also possible that non-focal damage in regions of NAWM represent nascent lesion sites (Ludwin, 2006). If these regions are developing lesions, it is also possible that the focal inflammation will resolve before the transition to an active lesion, further complicating detection (van der Valk and Amor, 2009).

NAWM may offer a valuable region for the observation of early pathological changes, including axonal loss, alterations in the blood-brain barrier, cell activation and others. These regions may exist in a subtle balance between active inflammation and neuroprotection. Genes related to ischemia and oxidative stress are upregulated in NAWM, with changes seen in levels of transcription factors controlling inflammatory activation as well as anti-inflammatory components (Zeis et al., 2008b). NAWM also displays markers of oligodendrocyte activation and stress including activation of STAT-6 based signaling and increased expression of αB-crystallin, a heat shock protein which can activate microglia after release into the cerebrospinal fluid (van der Valk and Amor, 2009).

Grey matter pathology and observations

MS has long been perceived as a disease primarily affecting white matter, whether this is in terms of the location of injury or of the tissue type which serves as the location in which these injuries are initiated. The examination of white matter lesions has consequently long predominated for both diagnostic and investigative purposes. Recent studies, however, have begun to demonstrate increasingly that grey matter pathology is of critical importance and can play a significant role in patient disability and disease progression. The factors leading specifically to grey matter damage are still not fully understood.

The clinical presentation of MS in grey matter is different than that observed in white matter. For example, grey matter lesions do not contain the extensive inflammatory infiltrates seen in white matter but do exhibit large amounts of demyelination (Geurts and Barkhof, 2008). Damaged grey matter shows increases in activation of astrocytes, microglia and macrophages, similarly to white matter. Demyelination in grey matter is present to lesser extents in acute disease phases, becoming more evident with the onset of chronic disease (Geurts and Barkhof, 2008). As is seen in NAWM, normal-appearing grey matter (NAGM) also displays early molecular changes. Genes involved in mitochondrial energy metabolism are downregulated, as well as genes for multiple glutamate receptors (NMDA, AMPA, kainite and metabotropic) (Zeis et al., 2008b).

Primary progressive MS patients display increasing numbers of cortical lesions as their disease course advances. This increase in cortical lesion load may serve as a contributing factor in grey matter atrophy as well as clinical disability (Calabrese et al., 2009). However, relapsing-remitting patients in early disease stages begin to show grey matter pathology to a higher extent than would be predicted by the minimal lesion load present at that point in time (Inglese et al., 2004), suggesting that factors in addition to lesion number are determinants of the extent of disability. This is consistent with observations in white matter which indicate that lesion load does not always predict clinical outcome. Cortical demyelination is also associated with progressive disease, with lesions in cortex,

hypothalamus and hippocampus correlated with disability levels (Geurts and Barkhof, 2008).

Atrophy

Another element in disease diagnosis and pathology which may provide a useful correlate of clinical outcome is atrophy of central nervous system tissue. Brain atrophy is a more accurate predictor of later neurologic disability than MRI assessment. Additionally, spinal cord atrophy can serve as a predictor of physical disability in patients. These correlations hold true even in patients receiving MS treatments (Zivadinov and Bakshi, 2004). In early stages, grey matter atrophy may occur consequently to white matter atrophy, but this connection does not hold true in later stages where the two can progress independently (Fisher et al., 2008). Measurements in grey versus white matter show that atrophy occurs extensively in both tissue types, and that the rate of atrophy increases throughout the disease course. The extent of grey matter atrophy, however, has frequently been reported to be larger (Zivadinov and Bakshi, 2004; Fisniku et al., 2008). When comparing different disease subtypes, the level of white matter atrophy remains consistent between all types. The extent to which grey matter atrophy occurs over the course of the disease differs between disease type, and correlates well with disease scores (Fisher et al., 2008). For example, secondary progressive patients display more grey matter atrophy than do relapsing-remitting patients (Fisniku et al., 2008). Interestingly, the total volume of brain grey matter shows a correlation with white matter lesion

load, while white matter brain volume does not show this same correlation (Fisniku et al., 2008).

The amount of whole brain atrophy also remains consistent between disease types as well as correlating with disability scores, and is primarily driven by grey matter atrophy as opposed to white matter atrophy (Fisher et al., 2008). In chronic disease, grey matter pathology begins to take on greater overall significance (Geurts and Barkhof, 2008). In relapsing-remitting patients, whole brain atrophy is a predictor of later disease course but can still be ameliorated by treatment with anti-inflammatory agents at early stages (Fisher et al., 2008).

What are the models in use for MS research?

A critical element in the investigation of any human disease or physiological process is the development of a model system in which these occurrences can be researched in a careful, thorough and controlled manner. This also allows for the translation of information obtained through the study of animal models into potential therapies for human patients. What are the models in current use which allow for the study of MS?

The primary animal model of MS is Experimental Allergic Encephalomyelitis (EAE). Several virally-induced models have alternately been used to study MS,

which also lead to an inflammatory demyelinating disease, including Theiler's murine encephalomyelitis virus (TMEV) and mouse hepatitis virus (Baumann and Pham-Dinh, 2001). These models do not replicate MS symptoms as completely as the EAE model and will not be reviewed here. EAE can be induced in rodents and other mammals by the introduction of CNS tissue homogenate or specific peptide antigens. Many of these antigens have been chosen as a result of autoimmune antibodies to these proteins having been found in human disease. EAE is commonly induced by the subcutaneous injection of the desired peptide or tissue homogenate in suspension conjointly with the mineral oil-based Freund's adjuvant. This leads to the rapid development of clinical symptoms in a short time period, often 10 to 14 days, after a single injection (Gold et al., 2006)

EAE is a disease which can present in multiple clinical forms. This variability is linked both to the antigen used for disease induction as well as to the species and/or strain of animal in which induction is performed. In this way, researchers have access to a model system for demyelinating disease and MS which can mimic different pathological aspects or clinical courses of human disease. Interestingly, subtle differences in clinical presentation can be observed with antigens produced by different facilities (Olechowski et al., 2009), further supporting the concept that the EAE model has the potential for broad variability and can reflect the complex etiology and the multiple contributing pathological factors observed in human MS patients.

Animals induced with EAE develop a variety of neurological symptoms, often within the first 10-14 days after disease induction. In rodents, the first sign of disease begins with limpness of the tail, followed by a gradually worsening weakness and then paralysis of the hind limbs. Eventually, the animal will experience paralysis in the front quarters, with severe disease forms resulting in an eventual moribund state or death. Examination of CNS tissue reveals variable numbers and extents of inflammatory and demyelinating lesions, axonal degeneration and loss, and infiltration of immune cells (reviewed in (Pender, 1987; Gold et al., 2006; Emerson et al., 2009)). Mice in the EAE model also experience pain responses, consistent with pain reported by MS patients, with mice experiencing both cold and tactile allodynia. These symptoms occur independently of symptom severity, and are initiated early in the disease course (Olechowski et al., 2009).

Many of the peptide antigens used for the induction of EAE are obtained from the myelin proteins described previously (reviewed in (Kuerten and Angelov, 2008)). EAE induced by the $PLP_{139-151}$ peptide in SJL/J mice leads to a chronic-relapsing disease course. The MOG_{35-55} peptide used to induce EAE in Lewis rats (Adelmann et al., 1995) or C57BL/6 mice leads to a severe and chronic disease (Bernard et al., 1997). In NOD/Lt mice, however, MOG_{35-55} produces a relapsing-remitting disease course (Slavin et al., 1998). The MP4 protein, a fusion protein

with components of MBP and PLP, when used as an antigen in C57BL/6 mice also produces a severe, chronic disease course. A variety of PLP epitopes lead to a mild, transient disease form, with one exception being the severe disease induced by the peptide $PLP_{178-191}$ (Kuerten and Angelov, 2008). Similarly to this widespread resistance to PLP-induced EAE, many strains show resistance to MBP-induced EAE, with strains such as B10.PL and PL/J showing more susceptibility in contrast (Kuerten and Angelov, 2008). Interestingly, EAE can also be induced using axonal antigens. Contactin-2/TAG-1, expressed at the juxtaparanode by axons, was identified as an antigen in human MS and TAG-1-specific T cells can be used to induce a form of EAE that primarily afflicts the cortex and spinal cord grey matter (Derfuss et al., 2009). Immunization with mouse neurofilament light chain (NF-L), a component of the neuronal cytoskeleton, also induces a EAE-like disease with high amounts of axonal pathology and grey matter damage (Huizinga et al., 2008).

A comprehensive evaluation of the different EAE models in use in the current literature will not be undertaken here, but some examples are presented in order to convey the distinct models which are available to researchers. Specific EAE models can reflect a relapsing-remitting course of disease, an acute course of disease to reflect events in the early stages of MS onset, or a chronic course of disease to allow for the investigation of progressive forms of MS.

The C57BL/6 mouse is one of the most common mouse strains used in research, being one of the primary strains onto which 'knockout' or null mice, along with other transgenic modifications, are bred. This makes C57BL/6 mice particularly valuable for use in disease models for the investigation of the effect of precise genetic changes on clinical outcome and other factors. Induction of EAE using the MOG_{35-55} peptide results in a rapid onset, non-remitting disease course which results in extensive disability and inflammation (Bernard et al., 1997; Kuerten and Angelov, 2008). The predominant site of pathological changes in MOG-EAE is in the spinal cord, which exhibits lesions of inflammation and axonal loss with a lesser amount of demyelination. Remyelination is not observed to any significant degree (Bernard et al., 1997; Jones et al., 2008). The optic nerve also displays demyelination and inflammation (Bernard et al., 1997).

In Biozzi mice, induction of EAE with spinal cord homogenate results in a model of secondary progressive MS, which begins as a relapsing-remitting disease and is then followed by progressive chronic disability. These mice display worsening levels of clinical disability, increases in numbers of reactive astrocytes and glial cells, axonal loss, demyelination and remyelination (Hampton et al., 2008). Induction of EAE in SJL/J mice using MBP also produces a relapsing-remitting disease with severe lesions that display extensive Wallerian degeneration but little remyelination(Dal Canto et al., 1995).

Axonal degeneration

Two critical elements in understanding the pathogenesis of MS are the processes of axonal damage and degeneration. Loss of axons is a key factor that underlies the development of non-remitting, long-term disability in patients, but no current therapy is effective in the prevention of axonal damage (Trapp et al., 1998; Black et al., 2007a). How does axonal loss present in patients? What is the relationship between axonal loss, inflammation and demyelination?

Occurrence of axonal loss

Axonal damage begins early in the disease course in the MS lesion, perilesion and NAWM. This may present in a variety of ways such as transection of axons, axon swelling, accumulation of neurofilaments or loss of axons (Trapp et al., 1998; Bjartmar et al., 1999). More axonal loss occurs within the lesion than in other areas (Herrero-Herranz et al., 2008). Axonal loss is most pronounced in patients with higher disability scores as well as in older lesion sites (Silber and Sharief, 1999; Bitsch et al., 2000). However, fiber density does not show a strong correlation with disease duration, suggesting that neuronal loss and atrophy can occur at any time point during the disease course, not only with advanced disease (Ganter et al., 1999).

Early damage becomes evident when patients present with optic neuritis afflicting the optic nerve and, soon after, other myelinated CNS tissues. This is reflected

in the EAE model, in which optic nerve degeneration and concurrent deficits in in visual function begin within the first week following disease induction, suggesting similar time courses of axonal damage and demyelination as compared to human patients (Hobom et al., 2004; Brown and Sawchenko, 2007). MS optic nerve and optic tract both display reductions in total cross sectional area as well as in the total number of axons present (Evangelou et al., 2001).

Aside from the optic nerve, the corticospinal tract is one of the first sites to display progressive damage, and is a major contributor to disability. Degeneration of the corticospinal tract along with degeneration of the sensory tract is observed in multiple degenerative diseases, such as sub-acute combined degeneration of the spinal cord, Strumpell's familial spastic paraplegia and Friedreich's ataxia (DeLuca et al., 2004). In MS, neither tract shows a correlation of axonal loss with lesion load, which is true for both active and chronic lesions (DeLuca et al., 2006).

Mechanisms of injury may also differ in early versus late stages of MS, leading to a need for the investigation of axonal loss in both short and long term animal models. The extent of axonal loss and demyelination also differs between disease subtypes, including between primary and secondary progressive forms (Tallantyre et al., 2009). In secondary progressive MS, spinal cord demyelination is more extensive, while loss of axons in demyelinated regions is more extensive

in primary progressive patients (Tallantyre et al., 2009). Primary progressive MS patients show large amounts of spinal cord pathology, with axonal loss as high as 68% in some regions (Wujek et al., 2002). The most extensive spinal cord damage, observed in both white matter and grey matter equally, is at the cervical level (Bjartmar et al., 2000). Interestingly, reductions in spinal cord area and fibre density differ between genders at different levels of the spinal cord during MS. Both male and female patients have deficits apparent at thoracic levels, while only male patients showed additional pathology at cervical levels (Ganter et al., 1999). This gender difference is consistent with the increased likelihood that males will suffer from a more advanced disease course than females.

Damage to axons is not uniform between all nerves present in a given region of nervous tissue, but can differentially affect fibers of varying sizes, with small caliber myelinated axons typically more vulnerable than large axons. This preferential damage was observed in small axons of the lateral geniculate nucleus, spinal cord, and all regions of the corticospinal tract (Ganter et al., 1999; Evangelou et al., 2001; DeLuca et al., 2006). Small caliber fiber losses begin at early time points in disease (Papadopoulos et al., 2006). These observations require more detailed investigation as well as the mention of some caveats, however. Focal demyelination can lead to localized reductions in axon caliber (Bjartmar et al., 1999). Smaller axons may be more challenging to visualize consistently due to differential staining, and edema and swelling of damaged axons may result in normally small diameter axons appearing to be larger,

skewing the distribution of fibers between groups. It is possible that preferential damage to different axon calibers is based on some property of the large versus small axon. For example, a large axon may have a higher capability for repair due to its size and a larger number of available resources, as well as protection from a thicker myelin sheath (Evangelou et al., 2001; Papadopoulos et al., 2006).

Inflammation, demyelination and axonal degeneration

In normal tissue, there is a reciprocal interaction between axons and myelin, with axons providing factors important for the maintenance of the myelin sheath as well as the proliferation and differentiation of the myelinating glia and the myelin sheath contributing to axonal structure and function. What is the connection between axonal loss and demyelination, and what role does inflammation play in these processes? It had been postulated that axonal loss occurs as a secondary effect consequent to demyelination. This viewpoint was shown to be incomplete after the observation of axonal loss in regions of MS lesions not undergoing demyelination. Some investigators have now begun to propose that axonal assault may precipitate subsequent immune responses leading to the loss of myelinating glia and subsequent demyelination. The interconnection of neurodegeneration, inflammation and demyelination thus offers an interesting subject of investigation.

In MOG-EAE, axonal loss predates the onset of clinical symptoms by several days, at a time when inflammation and demyelination are still low (Papadopoulos et al., 2006). This early loss of axons may amount to only ~10% of normal levels, eventually reaching as high as 50-60% in severely affected regions even after clinical scores recover (Brown and Sawchenko, 2007; Jones et al., 2008). Early infiltration of T cells not sufficient to lead to significant inflammation may be associated with this early damage to axons, as both phenomena continue to increase throughout the course of disease (Wang et al., 2005). Axonal loss also increases noticeably at a time point coincident with the infiltration of OX-42-positive microglia and the development of demyelination (Papadopoulos et al., 2006).

The timing of damage to axons as compared to inflammation may also differ when considering different disease models. In the experimental allergic neuritis model (EAN), inflammation may mediate axonal loss with inflammation occurring first, followed quickly by demyelination and loss of retinal ganglion cells as a late event (Shindler et al., 2008). A study of optic pathology in EAE, in contrast, has found loss occurring independently of inflammation, with retinal ganglion cell damage occurring as a result of apoptosis and at the same time as visual impairment begins (Hobom et al., 2004).

A study of relapsing-remitting EAE in Biozzi mice demonstrated that loss of axons occurs independently of demyelination, appearing before the onset of substantial levels of demyelination, and that this loss of axons persists through relapses (Jackson et al., 2009). Early attacks of active disease do show high correlations between the extent of spinal cord inflammation and clinical score, before significant levels of axonal loss occur. In chronic stages, inflammation is reduced and no longer correlates with clinical score, which now shows a correlation with the extent of axonal loss in the spinal cord (Wujek et al., 2002). Ultimately, animals experiencing a higher total number of relapses and a higher cumulative clinical score also displayed more extensive axonal loss once relapses had ceased and animals had entered a chronic disease stage, reaching up to 66% loss of axons (Wujek et al., 2002; Papadopoulos et al., 2006; Jackson et al., 2009). Additionally, the location of demyelinated areas changed during the course of relapses, with early demyelination observed in lumbar regions of the spinal cord, and later stages showing demyelination increasing in the cervical spinal cord (Jackson et al., 2009).

Different immune effector cells may play a significant role in the processes of axonal damage and loss. Hypertrophy of astrocytes precedes the onset of significant levels of inflammation, and can be seen in regions in addition to those experiencing axonal damage, potentially implicating these cells in early pathological stages (Wang et al., 2005). The numbers of inflammatory cells, such as T cells and microglia, show increases by the first week after induction of

EAE and before visible signs of disease, peaking in number at approximately the same time at which clinical symptoms initiate (Brown and Sawchenko, 2007). At the onset of inflammation, the numbers of infiltrating immune cells correlate with the size of the lesion and the total extent of inflammation (Ayers et al., 2004).

Other factors not directly related to inflammation or demyelination may also play a role in neurodegeneration. Edema can contribute to axonal damage via increases in extracellular pressure which can disrupt blood flow and promote hypoxic/ischemic injury (Bjartmar et al., 1999).

Ultimately, although axonal loss is known to underlie the development of non-remitting clinical deficits, the point at which this irreversible damage occurs is unclear. The amount of axon loss required to result in permanent motor deficits is not known (Jackson et al., 2009). It has been theorized that there is a threshold level of axonal damage after which compensatory mechanisms fail and damage is no longer reversible (Wujek et al., 2002). Interestingly, many more progressive MS patients display spinal cord pathology as compared to patients experiencing clinical remissions, raising the question of whether the spinal cord is less receptive to regenerative processes. Further studies are required to determine the amount of damage sustainable by the central nervous system, as well as specific sites or types of tissue which are more or less susceptible to non-remitting damage.

What molecular markers exhibit altered expression during MS?

A variety of different molecular markers and conditions have been shown to change during the course of MS. Some of these offer valuable tools for the diagnosis of patients or as means by which a prognosis for clinical outcome can be determined.

NAA

N-acetyl aspartate (NAA) has been shown to be useful marker for the measurement of the extent of axonal loss in patients due to its sensitivity as well as by offering a non-invasive means of detecting axonal loss. NAA is the second most abundant amino acid in the CNS, second only to glutamate. It is normally found within neurons and neuronal processes and has a high concentration in the cytoplasm. In spinal cord of chronic MS patients, NAA levels are reduced by approximately one-half, in myelinated and demyelinated axons. This reduction also correlates with the extent of axonal loss (Bjartmar et al., 2000).

APP

Another marker of axonal damage is amyloid precursor protein (APP), which is normally expressed in neurons. Cleavage of APP is responsible for the generation of β-amyloid deposits in Alzheimer's patients. Normally, APP undergoes fast retrograde axonal transport, and it has been proposed that

deposition of APP in regions of pathology is a result of a failure of transportation (Bechtold and Smith, 2005a; Hassen et al., 2008).

Increases in APP expression begin early in the disease course in MOG-EAE, first and most intensely in the lesion and to a lesser extent in other regions (Herrero-Herranz et al., 2008). Periplaque WM from early MS tissue also shows higher APP expression (Bitsch et al., 2000). APP accumulates within active lesions and at the borders of lesions. Chronic-active lesions display decreases in APP staining in central regions of the plaque, while almost no APP is found in chronic lesions potentially due to more extensive loss of axons (Ferguson et al., 1997). In subacute lesions, the APP signal is reduced, with clusters of APP-positive astrocytes observed in clusters at the lesion periphery. Chronic plaques also show dense networks of APP-positive astrocytic processes (Gehrmann et al., 1995).

APP expression is rapidly induced by microglia, astrocytes and oligodendrocytes in response to injury. Its induction correlates with disease signs, and is likely an acute stress reaction, similar to expression of heat shock proteins. In MS tissue, APP is found expressed at increased levels in perivascular regions, including the vascular wall, epithelia, lymphocytes, and resident microglia. In white matter, APP-positive glial cells are oriented in short rows along long fibres (possibly expressed by oligodendrocytess). APP-positive lymphocytes, reactive

astrocytes, foamy macrophages and microglia are also observed in MS lesions (Gehrmann et al., 1995). Finally, APP expression is also observed in perivascular regions (Aboul-Enein et al., 2006).

Neurofilaments

Neurofilaments are intermediate filaments which form an abundant part of the axonal cytoskeleton, composed of heavy, medium and light subunits. The number of neurofilaments as well as their phosphorylation state is a key determining factor in axonal caliber as well as, consequently, conduction velocity. Myelinated axons have a higher proportion of phosphorylated neurofilament, whereas damaged or dysmyelinated axons display a higher complement of non-phosphorylated neurofilaments (reviewed in (Silber and Sharief, 1999)). Normally, phosphorylation of neurofilaments promotes stability of axons and larger axon caliber and increases conduction velocity as well as promoting processes such as axon guidance and regeneration (Silber and Sharief, 1999; Perrot et al., 2008; Shea and Chan, 2008).

Regions of damage show gradual declines in the amount of phosphorylated neurofilaments present with a proportional increase in non-phosphorylated neurofilaments. Axons containing phosphorylated neurofilaments are more likely to retain intact myelin while axons expressing non-phosphorylated neurofilaments display either thin or absent myelin sheaths (Herrero-Herranz et

al., 2008). MS patients also display increased levels of neurofilament light chain (NF-L). This correlates with disability level but not with disease duration, as well as having a higher rate of occurrence in patients who have experienced recent relapses (Norgren et al., 2004).

Nitric oxide and NO synthases

Numerous studies have investigated the potential role of nitric oxide (NO) in MS pathology. Normally, neurons synthesize NO and exist in an environment containing an extracellular NO concentration of approximately 33 nM. Under pathological conditions, however, activated microglia and astrocytes can synthesize micromolar concentrations of NO (Bishop et al., 2009). High levels of NO can be toxic due to its ability to form damaging reactive oxygen species (ROS), including peroxynitrite. MS patients show elevated levels of nitrates and nitrites, downstream products of NO, in the cerebrospinal fluid (Garthwaite et al., 2002). NO metabolites can also be measured at increased levels in hippocampus in EAE (Sajad et al., 2009). NO can function as a vasodilator which is able to increase blood-brain barrier (BBB) permeability (Wu and Tsirka, 2009). Importantly, exposure to NO can lead to conduction block, particularly in electrically active nerves and demyelinated axons (Kapoor et al., 2003; Smith, 2007).

Neurons, astrocytes and oligodendrocytes do not share similar sensitivity to NO release. Neuronal damage occurrs even at low levels of NO. Oligodendrocytes, on the other hand, are more resistant to NO-mediated damage, potentially due to the release of an unidentified secreted factor which can protect neurons in co-culture systems (Garthwaite et al., 2002; Bishop et al., 2009). Addition of NO to an *in vitro* system leads to white matter pathology and axonal damage to an extent which is relative to the rate of NO addition (Garthwaite et al., 2002). These data imply that the mechanism of NO action and damage mediation occur at the axon.

NO is synthesized by NO synthase (NOS), with three major isoforms present in the CNS: endothelial NOS (eNOS), inducible NOS (iNOS), and neuronal NOS (nNOS). Studies of the effects of NOS inhibitors in disease have produced conflicting results. In grey matter ischemia, all three forms of NOS play a role, with eNOS serving as a protective agent and nNOS and iNOS both having deleterious effects (Garthwaite et al., 2002). eNOS can be produced by astrocytes and endothelial cells. eNOS-deficient mice induced with MOG-EAE display delayed symptom onset, but symptoms ultimately become more severe, demyelination is more extensive, and microglial activation and infiltration are increased. In this way, eNOS expression may promote damage in early stages while promoting recovery in late stages (Wu and Tsirka, 2009). iNOS expression in macrophages during EAE correlates with acute axonal injury, with iNOS-expressing macrophages located in close proximity to injured axons. In contrast,

uninjured axons were only in proximity to iNOS-cells. In accordance with these data, perivascular regions of inflamed vessels showed increased levels of nitrotyrosine, a marker for peroxynitrite attack (Aboul-Enein et al., 2006).

GFAP

Glial fibrillary acidic protein (GFAP), an intermediate filament expressed by astrocytes, can be used as a marker for astrogliosis. GFAP-positive astroglia in EAE and MS are reactive astrocytes which are larger than their non-activated, stellar counterparts. In normal spinal cord, GFAP-positive cells have long radial processes, and stellate cells are predominantly seen in grey matter (Bannerman et al., 2007). GFAP levels in MS patients are increased, particularly in those with progressive disease (Norgren et al., 2004). Chronic lesions also show specific increases in GFAP expression (Bjartmar et al., 2000). This change in expression correlates with patient disability, but not with disease duration (Norgren et al., 2004). In the EAE model, regions containing active inflammation at the onset of clinical symptoms contain GFAP-positive astrocytes which are undergoing activation and beginning to re-enter the cell cycle to become multipolar astrocytes (Bannerman et al., 2007).

Activated astroglia are capable of producing pro-inflammatory cytokines to contribute to T cell activation and cytokines to promote survival of oligodendrocytes (Bannerman et al., 2007). Increased activation of astrocytes is

more extensive in grey matter as compared to white matter (Wu et al., 2008). Depletion of reactive astrocytes leads to a reduction in oligodendrocyte survival and decreases in regeneration in CNS injury models. At the same time, reactive astrocytes also produce hyaluronan, which can accumulate and serve as an inhibitor of oligodendrocyte differentiation, suggesting that astrocytes can play a dual role in oligodendrocyte survival and proliferation (Bannerman et al., 2007). Additionally, in normal tissue, oligodendrocyte precursor cells are transported to their final positions along the processes of radial glia, so the loss of radial glia in lesions after activation and transformation into activated multipolar cells may also serve to inhibit accumulation of oligodendroglial cells due to impairments in trafficking (Bannerman et al., 2007).

What evidence implicates voltage-gated sodium channels in MS pathology?

Studies of demyelination provided early indications that sodium channel function may be involved in the pathogenesis of demyelinating disease. It had been observed that, during episodes of myelin loss, remissions and partial recovery of function could occur even before the completion of remyelination, implying that restoration of conduction is not exclusively reliant on the presence of an intact myelin sheath. Additionally, axons which had undergone demyelination were not initially able to overcome conduction block, but were capable of acquiring this ability over time (Black et al., 1991). What property or process formed the molecular basis of this recovery?

Changes in sodium channel distribution – chemical and genetic models

Demyelination induced chemically by injection of lysolecithin, although not a model of MS, will eventually lead to spontaneous remyelination. Studies in rabbit sciatic nerve showed significant increases in the total amount of saxitoxin bound after remyelination had occurred. This was determined to not be exclusively a reorganization of channels already present, but also included synthesis of new channels (Ritchie et al., 1981). Soon after myelin damage occurs subsequent to the injection of lysolecithin, macrophages infiltrate to remove myelin debris and glial cells begin to proliferate. Foci of channels (heminodes) are observed at the edges of the Schwann cells which are initiating remyelination, with these foci eventually fusing to create nascent nodes. This clustering process is inhibited by blocking Schwann cell proliferation (Dugandzija-Novakovic et al., 1995). Similar results were seen in ethidium bromide induced demyelination (another model of demyelination which does not model MS), which damages oligodendrocytes and astrocytes and, when coupled with irradiation, can prevent the return of glial cells to the site of injury. It was observed that, where glial cells associate with the axon, the axolemma develops a dense coating which was proposed to be sodium channels forming nascent nodal regions. When remyelination was initiated, high levels of channels were observed throughout the length of the axonal region, and were gradually excluded from the internodes into clusters at nodes of Ranvier as the myelin sheath reformed (Black et al., 1991).

Genetic models of demyelination and dysmyelination further supported these early observations. Axons in the *shiverer* mouse are hypomyelinated due to a mutation in the gene encoding myelin basic protein (MBP), resulting in many nonmyelinated axons and a tremor/seizure phenotype (Westenbroek et al., 1992a). Saxitoxin binding studies revealed significant increases in channel expression in *shiverer* brain white matter, with less extensive increases seen in grey matter. Importantly, in regions normally lacking myelin, there was little difference observed between *shiverer* mice and their wild type counterparts, suggesting that changes in sodium channel expression are directly related to the process of myelin loss and not simply to the absence of myelin (Noebels et al., 1991). Studies of specific alterations in the expression of $Na_v1.1$, $Na_v1.2$ and $Na_v1.3$ in *shiverer* mice demonstrated preferential increases in $Na_v1.2$ in many hypomyelinated regions without concomitant increases in the other subtypes. These changes were specific to the axon, and not observed in astrocytes or oligodendrocytes (Westenbroek et al., 1992a).

The heterozygotic *Plp*/- mouse is a genetic model of adult-onset demyelination, with normal myelination and sodium channel clustering at nodes of Ranvier observed in early development. Myelin pathology develops by 3 months of age with complete myelin loss after 7 months. Demyelinated axons display diffuse immunostaining for $Na_v1.2$ and loss of normal nodal $Na_v1.6$ clusters, with increases in protein expression levels of $Na_v1.2$ (Rasband et al., 2003). This

demonstrates that loss of myelin can lead not just to changes in sodium channel localization but also to changes in sodium channel protein translation.

Peripheral myelin in the *md* rat forms normally, but these animals lack CNS myelin entirely due to a mutation in the proteolipid protein (*Plp*) gene. Axons are ensheathed by oligodendrocytes but compact myelin does not form correctly. *md* rats experience seizures and die by P24-P28. Studies comparing the relative levels of $Na_v1.1$, $Na_v1.2$ and $Na_v1.3$ in hippocampus, DRG neurons, cerebellum and spinal cord showed high levels of $Na_v1.2$, followed by $Na_v1.1$, but no cell-specific pattern changes were seen and differences from control animals were not significant (Felts et al., 1995). Later studies determined that nodal components including sodium channels, ankyrin G and tenascin-R were retained correctly, but aberrant paranodal formation resulted in mislocalization of the juxtaparanodal proteins $K_v1.1$ and $K_v1.2$ into the paranode. Additionally, the paranodal proteins Caspr/contactin/NF155 were not confined to the normal tight paranodal structure but exhibited diffuse staining patterns instead. Nodes of Ranvier and axon initial segments still correctly expressed predominantly $Na_v1.6$, with some abnormal expression in these subdomains of $Na_v1.2$ and $Na_v1.8$ (Arroyo et al., 2002). In optic nerve and spinal cord, unmyelinated axons conduct action potentials at a slower conduction velocity. Interestingly, in optic nerve from *md* rats, saxitoxin binding experiments did not show changes in total numbers of channels present even in the absence of properly-formed compact myelin (Utzschneider et al., 1993). These studies support the importance of the

correct formation of compact myelin in normal localization of sodium channels as well as node and AIS formation.

Sodium channel function in ion conductance is also important in the process of normal myelination. In an *in vitro* system using dissociated neuronal and glial cells derived from embryonic OF1 mouse pups, inhibition of channel function by application of tetrodotoxin decreased the extent of myelin formation, most significantly when tetrodotoxin was applied before the onset of myelination. Conversely, the application of α-scorpion toxin to force channel opening and slow inactivation led to increases in the amount of myelin formed (Demerens et al., 1996).

Evidence from sodium channel blockade

Another important source of evidence implicating sodium channels in the pathogenesis of demyelinating disease comes from studies involving sodium channel blocking agents in MS and EAE as well as models of hypoxia, ischemia and anoxia. Multiple studies have now approached the question of sodium channel involvement in demyelination and nervous system damage through an examination of the effect of pharmacological sodium channel blocking agents (**Table 1.1**). These include the neurotoxins saxitoxin and tetrodotoxin as well as local anaesthetics, type 1 anti-arrhythmics, and other compounds.

Models of anoxia have offered several intriguing observations regarding sodium channels, energy depletion and white matter damage. Anoxic tissue retains blood supply but is deprived of oxygen. Ischemia, in contrast, is generally a result of disruption of blood flow, such as that observed in stroke (Stys et al., 1992a). White matter and grey matter tissue tracts are both susceptible to damage by anoxia and ischemia, but the mechanisms of damage are different, and white matter is more resistant to insult than grey matter (Stys et al., 1992a).

Studies have been performed in *in vitro* anoxic nerves to assess the effect of sodium channel blockade on injury during anoxia (Stys et al., 1992a). Concentrations of saxitoxin and tetrodotoxin were used which were below that leading to full channel blockade and which did not impair compound action potential (CAP) area in controls. Application of either neurotoxin was protective against anoxia-induced damage, leading to higher CAP areas. Reductions in channel activity can thus have a beneficial effect during anoxic injury.

Hypoxia can lead to neuronal death either via necrosis after the interruption of normal blood flow, or via apoptosis if oxygen levels are altered. After the onset of hypoxia, potassium ions exit the neuron and calcium and sodium ions enter. Sodium channel blockade with tetrodotoxin in a model of hypoxia using cortical neurons reduces the extent of apoptosis, thus improving neuronal survival. This can also be observed via a reduction of the extent of caspase-3 activity visible

after tetrodotoxin application (Banasiak et al., 2004). Activation of sodium channels with veratridine in a model of anoxia to increase sodium permeability led to a reduction in CAP area which was more extensive during anoxia than in non-anoxic conditions (Stys et al., 1992a). Application of veratridine in a separate study also resulted in intra-axonal increases in sodium concentration and cell damage consistent with damage observed in hypoxia (Banasiak et al., 2004). These data implicate sodium channel activity in hypoxia-mediated damage as well.

The sodium channel blocking agent phenytoin is commonly used as an anti-epileptic drug and also possesses additional analgesic effects. It is able to block persistent sodium current and high-frequency firing in axons without interfering with the properties of individual action potentials. The action of phenytoin is not limited to voltage-gated sodium channels, but also blocks voltage-gated calcium and potassium channels at higher doses (Lo et al., 2003). Additionally, phenytoin may increase vascular permeability, decrease toxicity of natural killer cells and suppress immune function (Black et al., 2007b). Treatment with phenytoin protects optic nerve axons from degeneration as well as reducing the severity of clinical symptoms in EAE (Lo et al., 2002). Similar protective effects were subsequently observed with spinal cord axons, with concurrent improvement in clinical outcome and retention of CAP area (Lo et al., 2003). In longer-term studies involving both chronic and relapsing-remitting models of EAE, phenytoin was again shown to have a neuroprotective effect as well as

contributing to a decrease in the amount of inflammatory infiltrate (Black et al., 2006b).

Further support for the theory of neuroprotection conferred by channel blockade comes from studies performed utilizing the anti-arrhythmic drug flecainide in a chronic-relapsing model of EAE. Flecainide is a class Ic anti-arrhythmic which shows state-dependent channel blockade. It binds to the local anaesthetic binding site preferentially during the open state, and drug binding may also be stabilized by the inactivation gate after binding. Flecainide is also able to block persistent late current (Wang et al., 2003). Flecainide administration protected axons from degeneration, reduced demyelination, and increased CAP area. The amount of protection conferred by flecainide treatment was more extensive when administered prior to EAE induction rather than coincident with symptom onset. The effect of flecainide was most evident during relapses or persistent symptom phases, as well as resulting in a decrease in the terminal disability score after the series of relapses had concluded (Bechtold et al., 2004). Flecainide is also protective against conduction block in an *in vitro* system of NO exposure, displaying protection against conduction block even at low concentrations (Kapoor et al., 2003).

Application of sodium channel blockers also offers therapeutic potential in other models of neurological insult or damage, supporting the idea that there is a

common mechanism of injury implicating sodium channels in neuronal damage. Treatment with phenytoin in a model of spinal cord injury effectively protects cellular ultrastructure, reduces edema, and inhibits lipid peroxidation as well as protecting axons and promoting functional recovery (Hains et al., 2004; Kaptanoglu et al., 2005b). In a model of glaucoma, phenytoin was also protective, with treatment leading to a reduction in loss of retinal ganglion cells and protection of optic nerve axons (Hains and Waxman, 2005).

Interestingly, sodium channel blockade may have differing effects in different EAE models, suggesting that the pathway by which channels are involved in pathogenesis may be complex and involve multiple factors beyond ion conductance. In a relapsing-remitting model of MS using the dark agouti rat, treatment with lamotrigine did not have an ameliorative effect on clinical symptoms or disease course. However, a small improvement was observed in the extent of pathology remaining at the end of the disease term (Bechtold et al., 2006).

As a result of the ameliorative effects on clinical symptoms and protection against axonal loss and damage, sodium channel blockers have consequently been proposed as potential therapeutic agents. An important cautionary note comes, however, from a study using either phenytoin or carbamazepine in the EAE model. These compounds were administered as in previous studies,

resulting in the same beneficial effects, and then withdrawn. Almost immediately after treatment was discontinued, animals experienced significant exacerbation of symptoms and rapid death, along with increases in inflammatory infiltrates. These negative effects were more pronounced with administration and withdrawal of phenytoin as opposed to carbamazepine (Black et al., 2007b). This study points to the need for a more complete understanding of the molecular mechanisms underlying MS and EAE, and the role of sodium channels in these processes, in order to develop therapeutics which can be more precisely targeted in order to avoid harmful side effects.

A second important consideration in the use of channel blockers in MS patients is their potential effect in unmasking previously silent negative symptoms. The anti-arrhythmic lidocaine, a short-term state-dependent channel blocker, binds to an intramembrane site which is made accessible upon channel opening. Consequently, lidocaine binding is high when channels are open or inactivated and the membrane is depolarized. This makes lidocaine an effective agent for binding channels which fire at high frequency, such as those found distributed diffusely along demyelinated axons. It is these demyelinated regions and others experiencing conduction block which contribute to the development of negative symptoms in MS patients. Lidocaine is effective in the treatment of positive paroxysmal symptoms, as is its derivative mexiletine (Sakurai and Kanazawa, 1999). Lidocaine is also effective in amelioration of conduction block after spinal cord treatment with NO (Kapoor et al., 2003). However, due to this beneficial

effect in regards to conduction block, treatment with lidocaine can unmask previously silent negative symptoms, and dosages need to be carefully monitored in order to be able to treat positive symptoms with lower doses without provoking negative symptoms at higher doses (Sakurai and Kanazawa, 1999). Lamotrigine and other channel blockers have also been implicated in this uncovering of previously silent lesions (Bechtold et al., 2006).

Changes in nodal structure, channel expression and localization in EAE

Consequent to the previously-described lines of evidence, extensive studies have been undertaken to look specifically at sodium channel expression and involvement in both MS and EAE, as well as changes to the axonal subdomains and structures in which channels are normally located. These studies have begun to elucidate the story of an intricate pathway to nervous system damage and degeneration.

Early saxitoxin binding experiments in MS spinal cord and brain showed retention of channels in neocortex and spinal cord grey matter and no increases in channel numbers in normal-appearing white matter in comparison to control samples. However, in demyelinated lesions, strong increases in saxitoxin binding were seen which correlated roughly with the extent of demyelination in those regions. These experiments did not distinguish between channels expressed in axons versus glia, but regions which also demonstrated extensive axonal loss did not

show significant increases in saxitoxin binding, suggesting these changes in binding capacity to be specific to axons (Moll et al., 1991). These studies in MS tissue thus recapitulate earlier results seen in models of demyelination, in which regions of demyelination exhibit increases in sodium channel numbers.

Multiple domains along the normally myelinated axon need to be considered when investigating the effect of demyelinating disease and the role of sodium channels. The node of Ranvier is a crucial structure in the maintenance of saltatory conduction, but the smaller, compact node is also flanked by the paranodal and juxtaparanodal structures, each of which has an important role in normal conduction. Additionally, multiple tissue sites through the CNS are implicated in disease pathology, each with potential differences in clinical presentation and molecular changes – brain, optic nerve and spinal cord.

Due to the structure and molecular specialization of the node of Ranvier, changes in other proteins of the nodal region, and their impact on the structure of the nodal region, must be also examined when considering a role for sodium channels in demyelination. In normal paranodes, Caspr is present and visible with immunofluorescent staining as small, well-defined structures, numerous in brain white matter and spinal cord grey matter while less numerous in spinal cord white matter. In lesions, however, many demyelinated axons do not express Caspr or other paranodal proteins (Wolswijk and Balesar, 2003). Lesions which do retain expression of paranodal proteins show diffuse distribution of Caspr,

Caspr2 and Kv channels without normally-formed aggregates (Coman et al., 2006). Demyelinated axons adjacent to lesions retain Caspr expression, often in elongated segments and with an increased diameter, and sometimes with a higher intensity of fluorescent signal directly adjacent to the node. This has been suggested to be more common at the periphery of chronic lesions as opposed to active lesions. It is possible that retention of Caspr may persist for a time after the onset of demyelination, with alterations in localization preceding complete loss of myelin. Axons in regions of damage which display aberrant Caspr expression are also more likely to express other markers of injury such as non-phosphorylated NF (Wolswijk and Balesar, 2003). These alterations in paranodal structure are also seen in studies involving partial nerve axotomy, where lesion sites showed disruption of normal Caspr localization (Henry et al., 2006).

During remyelination, patterns observed in normal development of nodes and paranodes are recapitulated. Regions of remyelination, either complete or incomplete, contain clusters of nodal, paranodal and juxtaparanodal proteins which form before the onset of remyelination, but in incompletely remyelinated tissue these clusters are less compact and more elongated (Coman et al., 2006). Once myelin is again detectable, the length of these protein clusters decrease as compared to demyelinated regions, beginning to more closely resemble the small clusters seen in normal tissue (Coman et al., 2006). This suggests that clustering of paranodal and nodal proteins begins at least at a nascent level before remyelination occurs, with sodium channels clustering first before Caspr,

such that re-formation of normal structure in nodes is followed by the paranode and lastly the juxtaparanode (Coman et al., 2006).

Alterations in localization during MS are also observed for both neurofascin isoforms, NF155 and NF186. In NAWM, both proteins are correctly expressed at paranodes and nodes, respectively. In demyelinating lesions, axons retaining myelin display elongated or disrupted NF155 expression, while NF186 expression is elongated in regions devoid of myelin. Increases in NF155-positive regions were more apparent along damaged axons expressing non-phosphorylated NF. Observation of these NF155-positive regions show that normal nodal length is maintained but the paranodes elongate and begin to overlap with the juxtaparanodes and regions of $K_v1.2$ expression. Regions undergoing severe damage displayed continuous NF155 expression extending through the nodal gap. In areas where NF155 expression was absent, expression of sodium channels was also disrupted, suggesting that paranodal alterations precede changes in channel localization (Howell et al., 2006). In EAN, a model of inflammatory neuropathy which displays axonal loss and conduction block, localization of NF186 and gliomedin are also disrupted prior to the onset of clinical symptoms. Nodes with abnormal neurofascin signal also displayed abnormalities in expression of ankyrin G and $Na_v1.6$ (Lonigro and Devaux, 2009). These changes in paranodal proteins thus accompany the changes observed in sodium channels. Proper channel function in the propagation of the action potential cannot be sustained in the absence of proper

nodal formation, and so these paranodal changes may also play a critical role in disease pathogenesis and progression.

What changes are observed in the subcellular localization of sodium channels? In myelinated axons in normal adult tissue, the adult node of Ranvier contains tight clusters of $Na_v1.6$ channels without detectable levels of $Na_v1.2$. Normally nonmyelinated fibers are $Na_v1.2$-positive, while very few nonmyelinated fibers are $Na_v1.6$-positive (Craner et al., 2004b). In MS and EAE lesions, however, immunofluorescent examination of demyelinated axons reveals dramatic changes in channel localization. Normal sodium channel clustering is mostly retained in unaffected and periplaque tissue, but in demyelinated regions channels are either found in broadened aggregates or spread diffusely along axons (Coman et al., 2006). These changes are a result of specific alterations in both $Na_v1.2$ and $Na_v1.6$, which are expressed in extended and diffuse patterns along axons even at early disease stages (Craner et al., 2003a; Herrero-Herranz et al., 2007). The number of $Na_v1.2$-expressing axons increases progressively over time. The number of Caspr-flanked nodes decrease, and the numbers of $Na_v1.6$-positive nodes decrease while numbers of $Na_v1.2$-positive nodes increase (Craner et al., 2003a). Changes in $Na_v1.6$ occur predominantly in axons lacking intact myelin, with myelinated axons showing little or no channel redistribution (Herrero-Herranz et al., 2008). Sodium channel clustering is also disrupted in EAN, with reductions in immunofluorescent signal, widening of nodes, and diffuse localization of channels (Lonigro and Devaux, 2009). These

alterations have the potential to have significant and deleterious effects on neuronal excitability. Proper generation and conduction of the action potential is dependent on the channel composition and channel numbers at the node of Ranvier, and alterations in channel subtype or the shape of the channel cluster can impair normal conduction.

Changes in channel expression also correlate with other markers of injury. Damaged β-APP-positive nerves are predominantly $Na_v1.6$-positive, while only a small population of β-APP+ axons are $Na_v1.2$-positive (Craner et al., 2004b; Herrero-Herranz et al., 2008). Changes in chronic lesions differ from active lesions. Chronic lesions contain a higher number of demyelinated axons without significant β-APP expression, and the β-APP which is present is not uniformly associated with $Na_v1.6$. Approximately 1/3 of axons in chronic lesions express $Na_v1.6$ in non-continuous patches, while the other 2/3 do not express $Na_v1.6$. $Na_v1.2$ is generally not expressed in axons in chronic lesions, but can be expressed at low levels along astrocytic processes (Black et al., 2007a). These differences confirm that studies of MS and EAE must take into account chronic versus active forms of the disease, since the pathology displayed by these differing forms is not always identical.

The sodium-calcium exchanger (NCX) is a transporter involved in ion homeostasis which exchanges intracellular sodium ions for extracellular calcium

ions. Healthy axons do not express high levels of NCX, while damaged nerves display increased levels of NCX expression. Both $Na_v1.2$ and $Na_v1.6$ colocalize with these increases in NCX expression. However, axons positive for both $Na_v1.6$ and NCX also express the damage marker β-APP in the majority of cases, while axons expressing both $Na_v1.2$ and NCX are predominantly β-APP-negative (Craner et al., 2004b). Interestingly, many NCX-positive processes in MS spinal cord are also $GFAP^+$, extending parallel to demyelinated lesions and morphologically resembling reactive astrocytes. Some of these cells also express $Na_v1.2$ (Black et al., 2007a), but $Na_v1.6$ does not display significant colocalization with GFAP (Herrero-Herranz et al., 2008). These data raise the question of whether $Na_v1.2$ and $Na_v1.6$ have similar or differing functions during disease and in damaged axons.

Another line of evidence implicating sodium channels in the broader pathology of MS is found in studies of the cerebellum. MS patients often experience deficits in movement such as ataxia, which characteristically arises from problems in the cerebellum. In normal cerebellum, $Na_v1.8$, a slow TTX-resistant channel with rapid recovery from inactivation, is not detected. During both MS and EAE, however, cerebellar Purkinje neurons display several molecular changes. These cells abnormally express $Na_v1.8$ and its binding partner annexin II/p11 at higher levels in both the soma and proximal dendrites, and Purkinje neurons in EAE displayed aberrant spiking patterns (Black et al., 2000; Craner et al., 2003b; Damarjian et al., 2004; Saab et al., 2004). These changes in channel

complement in the Purkinje neurons will consequently alter the firing properties of these cells, which are critical in the maintenance of normal cerebellar function. This was confirmed in studies involving cultured Purkinje cells, where transfection with Nav1.8 led to altered spiking activity and action potential amplitude (Renganathan et al., 2003).

Aberrant sodium channel expression also underlies changes in PNS conduction in the Trembler-J mouse, a model of the inherited demyelinating neuropathy Charcot-Marie-Tooth disease type IA. These mice, which contain a mutation in the peripheral myelin gene *Pmp22*, display demyelination and consequent remyelination along with axonal atrophy. Sodium channels cluster at heminodes in unmyelinated regions, and appropriate juxtaparanodal protein sequestration is lost. Peripheral nodes express $Na_v1.6$ correctly, but also show increased expression of $Na_v1.8$ (Devaux and Scherer, 2005). These data lend support to the concept that not only do channels need to be clustered correctly for normal function, but that the normal complement of channel subtypes needs to be retained.

The term ‘channelopathy’ has been coined to describe clinical syndromes which are a result of aberrant ion channel function. This can be a result of mutation or of alterations in channel expression (Waxman, 2001; Catterall et al., 2008). In this way, the evidence presented implicating sodium channels in MS leads to the

potential classification of MS as a channelopathy, providing a new perspective on the etiology, development and pathology of this complex disease.

Sodium channel β subunits.

The auxiliary sodium channel β subunits have not been extensively studied in EAE models or in models of demyelination. In Lewis rats induced with EAE by injection of MBP, small decreases in mRNA for β1and β2 can be detected at later stages of disease, but these changes are not visible at early time points (Nicot et al., 2003). In injury to sensory neurons this pattern is reiterated. Both β1 and β2 are downregulated in damaged DRG neurons, as is $Na_v1.9$, implicating β subunits in neuropathic pain (Coward et al., 2001). Additionally, loss of β2 in DRG neurons decreases sensitivity to certain classes of painful stimuli, such as noxious thermal stimuli (Lopez-Santiago et al., 2006a).

Does β2 play a role in abnormal neuronal excitability during injury? In the spared nerve injury (SNI), axon transection, or spinal nerve ligation (SNL) models, there are significant increases in β2 expression in both myelinated and unmyelinated fibers. Inflammation alone does not cause this change in β2 levels. In this way, β2 expression may be an attempt to compensate for damage by promoting the insertion of channels into the plasma membrane (Pertin et al., 2005).

β3 has also been implicated in pathology in pain pathways in the peripheral nervous system, with β3 found to be upregulated in spinal cord and medium diameter sensory neurons in induced painful diabetic neuropathy in rat (Shah et al., 2001). In the chronic constriction injury pain model, β3 expression is increased in small diameter fibers, rather than those of medium diameter (Shah et al., 2000).

Sodium channel expression in microglia may play a role in MS

Microglia, the resident immune cells of the CNS, can function as either regulatory or effector cells, while other immune cells are excluded from the CNS. They bear a strong resemblance to macrophages and also have a functional resemblance to monocytes due to their cytokine and chemokine signaling pathways (Wang and He, 2009). Microglia represent 5-15% of the brain cell population, and are located in key positions for early inflammatory responses (Carson, 2002). Microglia are normally quiescent, but are capable of responding to injury or insult through activation, which may occur via multiple pathways and stimuli, including axonal transection (Newell et al., 2007; van der Valk and Amor, 2009). Upon activation, they proliferate and become capable of migration, adopting a hypertrophic morphology, and later adopt the morphology of an ameboid phagocytic cell (Wang and He, 2009). Microglia express multiple types of ion channels, including voltage-gated sodium channels (Black et al., 2008).

Under normal conditions, microglia express sodium-calcium exchangers in order to accomplish outward flux of calcium ions, but this can reverse in pathology as well as in situations of increased intracellular sodium concentration. Membrane depolarization can also lead to calcium influx via sodium-calcium exchangers. This reverse exchange of ions is a component of the respiratory burst which occurs as a result of phagocytosis, subsequently also leading to microglia-mediated neurotoxicity via the release of ROS (Newell et al., 2007).

In uninjured tissue, microglia remain in a resting state where they do not express significant levels of $Na_v1.6$. After insult or injury, numbers of microglia increase coincident with the time of maximal inflammation and clinical deficit, with corresponding increases in $Na_v1.6$ expression. Upregulation of microglial $Na_v1.6$ expression is particularly noticeable at the edges of MS plaques (Craner et al., 2005). Increases in microglial activation occur more extensively in grey matter as compared to white matter (Wu et al., 2008). Microglia may also be present in regions in which lesions are in the process of forming, before other pathologic or inflammatory elements are visible (van der Valk and Amor, 2009).

Treatment with the sodium channel blocker phenytoin may block activation of microglia and macrophages in addition to its action on axonal sodium channels, which could potentially ameliorate acute phases of disease but not later stages. Alternately, the effect of phenytoin may be distinct in axons as opposed to

microglia and macrophages (Black et al., 2006b). Application of tetrodotoxin to microglia *in vitro* leads to a reduction in phagocytic capacity similar to that observed in microglia in the $Na_v1.6$-deficient *med* mice. Treatment with phenytoin also leads to a decrease in numbers of activated microglia (Craner et al., 2005). Sodium channel blockade also reduces the production of cytokines related to microglial activation as well as decreasing the cell's ability to migrate in response to chemoattractant signals (Black et al., 2008).

IV: HYPOTHESES OF NEURODEGENERATION - ION CONDUCTANCE, EXCITOTOXICITY AND ENERGY DEPLETION

Evidence has accumulated implicating changes in sodium channels and sodium conductance in the pathology of multiple sclerosis, other demyelinating and dysmyelinating diseases, and related neurological injuries. What are the mechanisms proposed to underlie damage to nervous system tissue during these disease and injury processes, and what is the role proposed for voltage-gated sodium channels therein?

One of the predominant and most compelling theories of sodium channel involvement in multiple sclerosis and EAE integrates improper ionic homeostasis, differing properties of channel subtypes and energy failure into an overarching

model of damage. In this model, reorganization of sodium channels along demyelinated regions of axons is a means by which the nervous system attempts to adapt in order to overcome damage, which ultimately serves as both a beneficial and a deleterious occurrence (reviewed in (Bechtold and Smith, 2005a; Waxman, 2006a, b; Smith, 2007)).

As previously discussed, sodium channels in myelinated axons are clustered at high density in gaps in the myelin sheath called nodes of Ranvier (Arroyo et al., 2002; Kazarinova-Noyes and Shrager, 2002). In mature animals, the molecular identity of CNS nodal channels is $Na_v1.6$ (Boiko et al., 2001b). Multiple studies have now shown that demyelinated, dysmyelinated, and myelinated axons that have become injured contain diffusely-localized sodium channels, and that the molecular identity of these channels is primarily $Na_v1.2$ and $Na_v1.6$ (Craner et al., 2003a; Craner et al., 2004a; Craner et al., 2004b; Black et al., 2007a). These are likely to represent a mixture of channels present along the axon before the onset of damage, either those present beneath the intact myelin sheath or channels previously located in the axon initial segment or cell body undergoing changes in localization, as well as newly-synthesized channels or channels from intracellular stores (Smith, 2007). Differences in current characteristics of $Na_v1.2$ versus $Na_v1.6$ studied in heterologous expression systems form the basis for a model (**Figure 3**) in which these channels contribute to recovery from conduction block or axonal damage, respectively (reviewed in (Waxman, 2006b, a; Trapp and Stys, 2009). $Na_v1.2$ and $Na_v1.6$ are both capable of producing rapidly

activating and inactivating currents in heterologous expression systems. $Na_v1.6$ reprimes rapidly and, of the two, is able to better sustain high frequency impulses. Importantly, in this model, $Na_v1.6$ is proposed to generate a larger persistent current than does $Na_v1.2$ (Waxman et al., 2004). Because of their differential current kinetics, $Na_v1.2$ is proposed to be responsible for recovery from conduction block (**Figure 3A**), while $Na_v1.6$ is proposed to be responsible for induction of a signaling cascade leading to axonal damage (**Figure 3C**).

Conduction block along demyelinated axons is responsible for a multitude of symptoms in patients. Without the ability to engage in saltatory conduction, the exposed axon is unlikely to maintain propagation sufficient for the action potential to reach the other side of the demyelinated region. A newly demyelinated axon, containing low numbers of sodium channels along the region which was formerly ensheathed by myelin, has a low capacity for the maintenance of electrical activity (Smith, 2007). As this exposed region begins to accumulate sodium channels, it gains the potential to engage in non-saltatory or continuous conduction, which is significantly less efficient than saltatory conduction. The fragile balance along these denuded axons between damage and recovery remains highly susceptible to imbalance, which is consistent with the increases in negative symptoms observed by many patients after seemingly innocuous activities which provoke repetitive use of the damaged axon. The higher conduction requirements along demyelinated axons stimulated by activity, exertion or temperature can prompt conduction block which manifest as episodes

of disability (Smith, 2007). Positive symptoms can be a result of hyperexcitability or maintained persistent current, resulting in experiences such as tingling or aberrant visual experiences such as flashes of light (Bechtold and Smith, 2005a).

What molecular pathways lead to damage in this model? During MS and EAE $Na_v1.2$, the channel subtype usually expressed along normally non-myelinated axons, is more likely to be expressed along uninjured axons, whereas $Na_v1.6$ is more likely to be expressed along injured axons (Craner et al., 2004a; Black et al., 2007a; Herrero-Herranz et al., 2008). Increases in $Na_v1.2$ levels are postulated to offer the potential for recovery from conduction block by the establishment of non-saltatory conduction (Waxman, 2006a). In contrast, persistent current generated by increased levels of $Na_v1.6$, is proposed to result in an influx of excess sodium ions into the interior of the axon. This has the potential to force the reverse operation of the sodium-calcium exchanger as an attempt to re-establish proper ionic balance, resulting in an accumulation of calcium within the axon (Waxman, 2006b, a). This exchanger normally transports sodium ions via the electrochemical gradient, allowing for the possibility for this reverse operation to occur in situations of ionic imbalance (Bechtold and Smith, 2005a). This dual model of sodium channel involvement is supported by evidence demonstrating both upregulation of the sodium-calcium exchanger and the colocalization of $Na_v1.6$ and the sodium-calcium exchanger in injured nerves.

Once calcium levels within the axon have reached high concentrations, a cascade of injury mechanisms is then proposed to lead to axonal loss. Early studies in models of anoxia, a reproducible white matter injury model, were among the first to implicate calcium in pathways of axonal damage (reviewed in (Stys, 2004). Increases in calcium levels within the damaged axon are proposed to activate calcium-dependent damaging downstream injury pathways, including the activation of proteases, lipases and NOS (Waxman, 2006a, b). Changes observed in lesions are consistent with the activity of calcium-dependent proteases, including damage to neurofilaments, microtubules and intracellular organelles (Dutta et al., 2006). Calpain has been implicated as one protease contributing to axonal damage, and is capable of the degradation of multiple neuronal proteins including spectrins, neurofilaments and myelin. In support of this proposed role in damage, inhibition of calpain has been showed to ameliorate axonal damage in MOG-EAE (Hassen et al., 2008).

Another key element in this model is energy depletion, which can occur either independently or as a consequence of changes in sodium channel expression. Increases in NO levels in MS lesions can contribute to inhibition of mitochondrial function, thereby depleting stores of ATP (Smith, 2007). Various mitochondrial genes related to ATP synthesis have been shown to be downregulated in lesions (Waxman, 2006b; Smith, 2007), further depleting energy stores. Availability of ATP is critical for the maintenance of ionic homeostasis, particularly for the operation of sodium-potassium pumps which are major contributors to the

maintenance of this ionic balance. ATP is also required for voltage-gated sodium channel function (Trapp and Stys, 2009). The co-localized increases of both $Na_v1.6$ and the sodium-calcium exchanger in damaged axons may, for example, lead to localized increases in energy needs. In this way, an electrically active axon has a higher energy requirement than a non-active axon, and increases in sodium channel expression along demyelinated axons consequently have the potential to exacerbate existing conditions of energy deprivation, promoting the likelihood that the axon will be damaged or undergo degeneration even though the presence of these excess channels also allows recovery from conduction block.

NO has been shown to play a role early in the axonal damage cascade (Bechtold and Smith, 2005a). Application of NO to optic nerve leads to energy depletion, which can be ameliorated by the application of tetrodotoxin (Garthwaite et al., 2002). Similar results were obtained using the sodium channel blockers flecainide or lidocaine in NO-treated spinal roots (Kapoor et al., 2003). Indeed, application of tetrodotoxin in NO-treated optic nerve helped to regulate ATP levels, supporting the importance of maintenance of energy stores (Garthwaite et al., 2002). These data suggested that reduced energy requirements from reductions in sodium current may have a beneficial effect in spite of the potential detrimental effect of decreases in conduction.

Interestingly, studies involving blockade of components in this overarching model other than sodium channels have often resulted in incomplete amelioration of disease symptoms and effects. Blockade of the sodium-calcium exchanger in a model of anoxia did not afford full protection against damage, but interestingly, protection was enhanced by co-treatment with TTX (Stys et al., 1992a). Blockers of voltage-gated calcium channels have also been studied, including broad-range channel blockers as well as blockers of specific subfamilies such as the L-type calcium channels. One study demonstrated a less severe clinical score, but also noted that efficacy of blockade decreased over the disease course and did not ameliorate infiltration of immune cells (Brand-Schieber and Werner, 2004).

Sodium channel involvement in demyelinating disease can therefore be seen as a significant contributing factor to pathogenesis and axonal damage. To summarize, differing sodium current properties of $Na_v1.2$ versus $Na_v1.6$ are proposed to result in differential effects, beneficial versus detrimental, in demyelinated lesions. Increases in $Na_v1.2$ are proposed to contribute to recovery from conduction block, while increases in $Na_v1.6$ are proposed to promote excess influx of sodium ions into the intra-axonal compartment, leading to reverse operation of the sodium-calcium exchanger, consequent accumulation of calcium within the axon, and the initiation of damaging downstream injury cascades. These changes are further compounded by energy depletion which also contributes to injury and pathology.

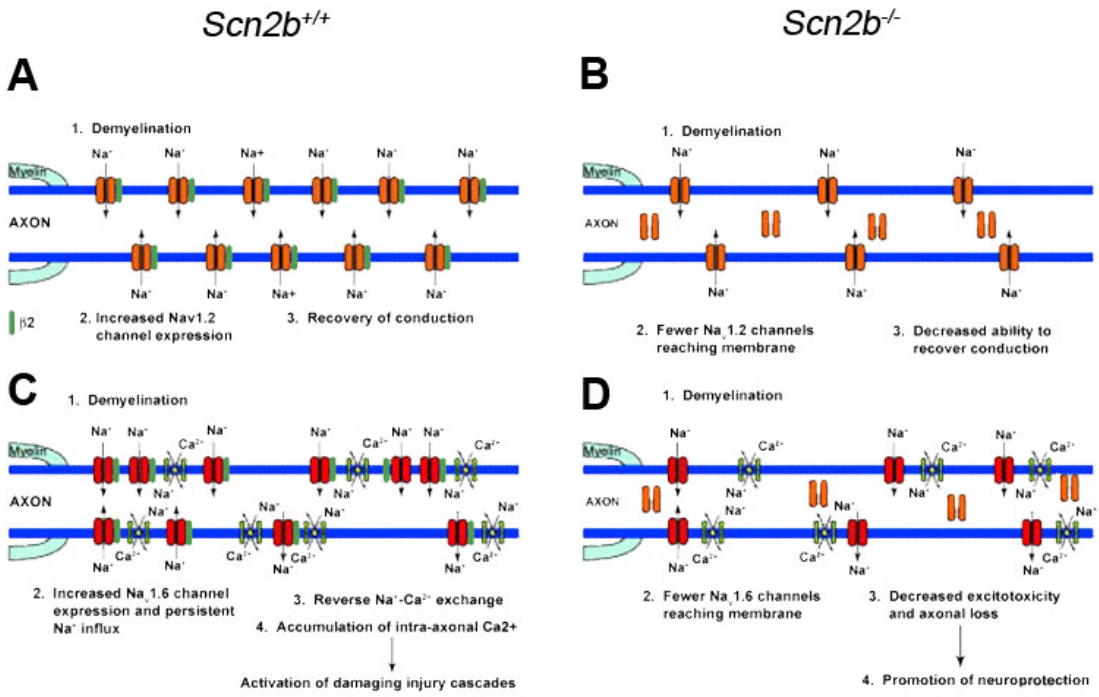

<u>Figure 1.3</u>: Proposed mechanism for the role of β2 in neuroprotection.

A: Alterations of $Na_v1.2$ expression in demyelinated regions allow for the development of non-saltatory conduction and the potential for recovery from conduction block. **C**: Alterations of $Na_v1.6$ expression in demyelinated regions result in a persistent influx of sodium ions into the axon, leading to the reverse operation of the sodium-calcium exchanger. The resultant influx of calcium ions into the axon activates damaging downstream injury cascades and leads to axonal degeneration.

B: Decreases in sodium channel expression at the axonal plasma membrane due to the loss of β2 do not lead to alterations in expression of $Na_v1.2$ through demyelinated regions, inhibiting the development of non-saltatory conduction and the potential for recovery from conduction block. **D**: Decreases in sodium channel expression at the axonal plasma membrane due to the loss of β2 do not lead to alterations of $Na_v1.6$ through demyelinated regions. Persistent influx of sodium ions into the axon is decreased, diminishing the effects of excitotoxicity and sparing the axon.

(Adapted from (Waxman et al., 2004))

V: RATIONALE FOR THESIS RESEARCH

At the onset of this thesis project, little to no information had been published regarding the role of the sodium channel β subunits in demyelinating disease or myelinating glia. Numerous lines of evidence had implicated the pore-forming sodium channel α subunits in the pathogenesis of demyelinating disorders, in particular MS and its animal model EAE. I was interested in the study of the β2 subunit and its role in both normal development as well as disease.

Our laboratory has previously generated a *Scn2b* null mouse (Chen et al., 2002). In our original characterization of these mice, we determined that they expressed 40-50% fewer sodium channels at the neuronal plasma membrane, leading to a comparable decrease in the peak amplitude of the sodium current. Evidence had additionally begun to demonstrate that axons in MS and EAE specifically displayed aberrantly localized sodium channels along demyelinated regions and that blockers of sodium channel function were able to be neuroprotective in models of demyelinating disease.

I hypothesized that sodium channel β2 subunits could play a role in demyelinating disease due to the role of β2 as a molecular chaperone in the insertion of sodium channels into the plasma membrane, thereby regulating the numbers of channels at the cell surface. I hypothesized that loss of β2 may be

neuroprotective during EAE due to the decreased amount of sodium current present in central axons in these mice, which could thus ultimately lead to decreases in calcium-mediated excitotoxicity (**Figure 3B, D**). I therefore used our *Scn2b* null mice in the EAE model in order to assess the effect of loss of β2 during demyelinating disease. I next translated my results in the mouse EAE model into tissue from human patients to determine whether the alterations I observed in mice could also be detected in humans.

Finally, I aimed to investigate the expression of sodium channel α and β subunits in myelinating glia, specifically the oligodendrocytes of the CNS which are critical cell types involved in MS. Information about developmental expression of different sodium channel subunits may contribute to our understanding not only of myelination in normal systems but may offer new means by which remyelination can be promoted during disease.

Channel Blocker	Effect in EAE	Primary Clinical Use
Phenytoin	Neuroprotection, reduction of inflammation, improvement of clinical symptoms. Withdrawal leads to rapid worsening of symptoms and death	Anti-epileptic
Flecainide	Neuroprotection, reduction of inflammation, improvement of clinical symptoms	Anti-arrhythmic
Lamotrigine	Neuroprotection, reduction of inflammation, improvement of clinical symptoms	Anti-epileptic
Carbamazepine	Neuroprotection, reduction of inflammation, improvement of clinical symptoms. Withdrawal leads to rapid worsening of symptoms and death	Anti-epileptic

Table 1.1: Sodium channel blockers tested in the EAE model.

(Adapted from (Waxman, 2008b)).

Table 1.2: Sodium channel binding sites.

(Reviewed in (Cestele and Catterall, 2000), (Catterall et al., 2007), (Catterall et al., 2005))

BINDING SITE	COMPOUND(S) BOUND	GENERAL FUNCTION	LOCATION OF BINDING
Neurotoxin binding site 1	Saxitoxin, tetrodotoxin μ-conotoxins	Pore blockade	S2-S6 of all four domains, extracellular side
Neurotoxin binding site 2	Batrachotoxin, veratridine, aconitine, grayanotoxin	Lipid-soluble channel activators	DI-S6 & DIV-S6
Neurotoxin binding site 3	α-scorpion toxins, sea anemone toxins	Slowing of channel inactivation	Complex site, includes DI-S6 and DIV-S6 as well as DIV-S3/S4 loop
Neurotoxin binding site 4	β-scorpion toxins	Enhancement of activation	DII-S3/S4 loop
Neurotoxin binding site 5	Brevetoxin, ciguatoxin	Enhancement of activation and inhibition of inactivation	DI-S6 & DIV-S5
Neurotoxin binding site 6	δ-conotoxins	Slowing of inactivation, similar to α-conotoxins	DIV-S4
Local anaesthetic binding site	Local anaesthetics, anti-epileptics, anti-arrhythmics	State-dependent channel blockade	Inner pore residues, S6 from multiple domains

CHAPTER TWO

LOSS OF NA^+ CHANNEL β2 SUBUNITS IS NEUROPROTECTIVE IN A MOUSE MODEL OF MULTIPLE SCLEROSIS

SUMMARY

Multiple sclerosis (MS) is a CNS disease that includes demyelination and axonal degeneration. Voltage-gated Na^+ channels are abnormally expressed and distributed in MS and its animal model, Experimental Allergic Encephalomyelitis (EAE). Up-regulation of Na^+ channels along demyelinated axons is proposed to lead to axonal loss in MS/EAE. We hypothesized that Na^+ channel β2 subunits (encoded by *Scn2b*) are involved in MS/EAE pathogenesis, as β2 is responsible for regulating levels of channel cell surface expression in neurons. We induced non-relapsing EAE in *Scn2b*$^{+/+}$ and *Scn2b*$^{-/-}$ mice on the C57BL/6 background. *Scn2b*$^{-/-}$ mice display a dramatic reduction in EAE symptom severity and lethality as compared to wildtype, with significant decreases in axonal degeneration and axonal loss. *Scn2b*$^{-/-}$ mice show normal peripheral immune cell populations, T cell proliferation, cytokine release, and immune cell infiltration into the CNS in response to EAE, suggesting that *Scn2b* inactivation does not compromise

immune function. Our data suggest that loss of β2 is neuroprotective in EAE by prevention of Na^+ channel up-regulation in response to demyelination.

INTRODUCTION

Multiple sclerosis (MS) is an autoimmune, inflammatory CNS disease characterized by demyelination and axonal degeneration (Dutta and Trapp, 2007). Patients experience multiple symptoms including muscle weakness or paralysis, impaired motor coordination, optic neuritis, and cognitive dysfunction. Following demyelination in MS, action potential conduction is significantly impaired or lost. A population of axons then recovers the ability to conduct action potentials in spite of myelin loss, contributing to clinical remission. In contrast, another population of axons degenerates in response to demyelination and this process has been implicated as the primary cause of permanent disability (reviewed in (Bechtold and Smith, 2005b; Waxman, 2006a)). Neuroprotection is a critical goal in the development of MS therapies; if axons are spared, strategies for the promotion of remyelination and restoration of saltatory conduction can then be initiated.

Evidence is accumulating that intra-axonal accumulation of Na^+ leading to Ca^{2+} overload plays a major role in neurodegenerative disease (reviewed in (Bechtold and Smith, 2005b; Coleman, 2005; Frohman et al., 2005; Stys, 2005; Waxman,

2006a; Smith, 2007)). Up-regulation and diffuse distribution of $Na_v1.2$ along demyelinated axons is proposed to have beneficial effects, resulting in recovery from conduction block and clinical remission. However, up-regulation and diffuse distribution of $Na_v1.6$ along demyelinated axons is proposed to lead to Na^+ influx mediated by persistent Na^+ current (Smith et al., 1998; Burbidge et al., 2002; Herzog et al., 2003; Rush et al., 2005), accumulation of intra-axonal Na^+, activation of reverse Na^+-Ca^{2+} exchange, accumulation of intra-axonal Ca^{2+}, and activation of damaging injury cascades (Craner et al., 2004b; Waxman et al., 2004; Waxman, 2008a, b). Consistent with this, reductions in plasma membrane calcium ATPase isoform 2 (*PMCA2*) levels of activity lead to delays in neuronal Ca^{2+} clearance, neuronal damage, and axonal loss in spinal cord neuronal cultures (Kurnellas et al., 2005). In contrast, but also in agreement with this hypothesis, cyclophilin D null mice are neuroprotective in EAE because their mitochondria are able to more effectively handle elevated Ca^{2+} (Forte et al., 2007).

Other observations support the hypothesis that Na^+ influx through voltage-gated Na^+ channels plays a role in neurodegeneration. Nitric oxide, which is increased in MS lesions, increases the probability of Na^+ channel opening and thus increases the amplitude of persistent Na^+ current in neurons (Li et al., 1998; Bielefeldt et al., 1999; Hammarstrom and Gage, 1999; Rush et al., 2005). Low doses of Na^+ channel blocking agents such as phenytoin and flecanide are neuroprotective in EAE and MS (Fern et al., 1993; Dave et al., 2001; Hewitt et

al., 2001; Schwartz and Fehlings, 2001; Lo et al., 2002; Sareen, 2002; Lo et al., 2003; Hains et al., 2004; Hemmings, 2004; Bechtold et al., 2005; Kaptanoglu et al., 2005a; Waxman, 2005; Besancon et al., 2008; Kapoor, 2008; Waxman, 2008b). In addition, pharmacological blockade of Na^+ channels reduces secondary injury and increases recovery from trauma following experimental spinal cord injury (Kaptanoglu et al., 2005a), results in protection of retinal ganglion cells and optic nerve axons in an experimental model of glaucoma (Hains and Waxman, 2005), and provides a neuroprotective effect in an animal model of hypoxic-ischemic encephalopathy (Papazisis et al., 2008), suggesting that blockade of persistent Na^+ current may be a general mechanism of neuroprotection.

Neuronal Na^+ channel up-regulation and/or redistribution following nerve injury or demyelination may have both beneficial and detrimental effects, leading not only to recovery from conduction block, but also to intra-axonal accumulation of Na^+ and the initiation of a cascade of signaling events that ultimately result in axonal degeneration and permanent disability (England et al., 1990; England et al., 1991; Moll et al., 1991; Westenbroek et al., 1992b). These observations demonstrate that the regulation of cell surface expression and function of Na^+ channels in injured or demyelinated neurons is critical to neuronal survival and recovery in disease. A complete understanding of these processes is essential for the development of novel and more effective neuroprotective agents.

We showed previously that deletion of the Na^+ channel β2 subunit (encoded by *Scn2b*) in mice results in reduced Na^+ channel cell surface expression with a corresponding decrease in Na^+ current density in both CNS and PNS neurons (Chen et al., 2002; Lopez-Santiago et al., 2006b). In the present study we sought to test the hypothesis that β2 subunits play a role in axonal degeneration in demyelinating disease via control of Na^+ channel expression. We show that *Scn2b*$^{-/-}$ mice have attenuated symptoms and reduced axonal degeneration in an animal model of MS, Experimental Allergic Encephalomyelitis (EAE). *Scn2b*$^{-/-}$ mice have normal inflammatory and immune responses in EAE, suggesting that the mechanism of neuroprotection in these animals is not immunomodulatory but is a direct effect on axons. Finally, we show that, while $Na_v1.2$ and $Na_v1.6$ are distributed similarly along demyelinated axons in wildtype and null mice, $Na_v1.6$ protein expression, which is normally up-regulated in brain in EAE, is attenuated in *Scn2b*$^{-/-}$ mice, suggesting that the level of $Na_v1.6$ mediated current in the demyelinated regions of axons may be reduced compared to wildtype. We conclude that *Scn2b* plays a critical role in neurodegeneration and propose that Na^+ channel β2 subunits may provide a novel target for future drug development in neuroprotection.

RESULTS

Scn2b$^{-/-}$ mice display attenuated EAE symptom severity and lethality

We induced EAE in *Scn2b*$^{+/+}$ and *Scn2b*$^{-/-}$ mice using myelin oligodendrocyte glycoprotein $(MOG)_{35-55}$ peptide, an induction protocol that produces a chronic, non-remitting disease course in mice bred on the C57BL/6 genetic background (Chabas et al., 2001; McQualter et al., 2001). *Scn2b*$^{+/+}$ mice (Fig. 1A, filled squares) displayed a disease course in which symptoms began to present between days 10 to 15 post-injection and rapidly progressed beyond clinical stage 3 (corresponding to full hind limb paralysis), as assessed by daily scoring of clinical symptoms using a five-point grading system. In contrast, *Scn2b*$^{-/-}$ mice (Fig. 1A, open squares) displayed a significantly less severe disease course, with symptoms also first appearing between days 10 to 15 post-injection, but with the disease course rarely progressing past clinical stage 2 (corresponding to hind limb weakness). Control animals of both genotypes, which received all parts of the EAE induction protocol with the exception of the MOG_{35-55} peptide, did not display clinical symptoms at any time during the experimental time course, up to 70 days post-injection (data not shown).

To account for the possibility that differences in observed clinical symptoms were due to alterations in the timing of symptom onset, rather than to an amelioration of symptom severity, data were also plotted as mean clinical score assessed at each day post-onset of symptoms (Fig. 1B). *Scn2b*$^{-/-}$ mice (open squares)

displayed a consistent and significant reduction in disease severity compared to *Scn2b*$^{+/+}$ mice (filled squares), consistent with observations made post-injection (Fig. 1A). Thus, a significant improvement in clinical symptom severity was observed in the absence of β2, with no observable changes in the time of onset of the disease.

Scn2b$^{-/-}$ mice displayed a significant reduction in EAE-induced lethality. We determined the percentage of mice able to develop at least stage 1 clinical symptoms (corresponding to a limp tail) and used this as an indication of the ability of *Scn2b*$^{-/-}$ mice to develop EAE (Fig. 1C). Both genotypes were equally susceptible to the onset of EAE; nearly every mouse treated with the MOG_{35-55} peptide successfully reached at least clinical stage 1 (96.9% *Scn2b*$^{+/+}$ *vs*. 93.1% *Scn2b*$^{-/-}$). We then determined the percentage of mice reaching end stage during the experimental time course, with end stage defined as a moribund or dead animal. Only 16.7% of *Scn2b*$^{-/-}$ mice reached end stage compared to 53.6% of *Scn2b*$^{+/+}$ mice, representing a 31% decrease in EAE-induced lethality in the absence of β2. This decrease in lethality was also apparent when survival data were plotted (Fig. 1D), showing a marked decrease in survival of *Scn2b*$^{+/+}$ mice compared to *Scn2b*$^{-/-}$ mice over time.

***Scn2b*$^{-/-}$ mice display decreased axonal degeneration in EAE**

Axonal loss is a characteristic component of EAE and underlies the development of clinical symptoms (Stys et al., 1992b; Bjartmar et al., 2003; Waxman, 2006a). We used transmission electron microscopy (TEM) to evaluate the extent of axonal degeneration and axonal loss in *Scn2b*$^{+/+}$ and *Scn2b*$^{-/-}$ mice during EAE. We examined ultrathin cross-sections of optic nerve from all experimental groups (peptide and control) at 19 days post-injection (dpi) of the MOG_{35-55} peptide. At this time point, both genotypes displayed similar clinical symptoms (see Fig. 1A). A representative set of electron micrographs is shown (Fig. 2, A-D). To assess the extent of axonal loss, we quantified the total number of axons per field of view (FOV) in optic nerve cross-sections from each genotype (Fig. 2E). In control tissues of both genotypes, optic nerve sections showed normally myelinated, large, medium, and small axons (Stys et al., 1991). In EAE optic nerve, both genotypes exhibited axonal loss. *Scn2b*$^{+/+}$ optic nerves displayed a 24.0% decrease in total axon number/FOV during EAE (at 19 dpi) compared to control tissue at the same time point ($p < 0.0001$). In contrast, *Scn2b*$^{-/-}$ EAE tissue displayed only a 6.2% decrease in axon number compared to control at this time point ($p = 0.0003$). When total axon numbers/FOV in *Scn2b*$^{+/+}$ and *Scn2b*$^{-/-}$ optic nerves after EAE induction were compared, a significant difference was also observed, with 24.75% fewer axons in *Scn2b*$^{+/+}$ mice than *Scn2b*$^{-/-}$ ($p < 0.0001$). There was a small but significant increase in total axon number/FOV in control tissue for *Scn2b*$^{-/-}$ optic nerves compared to *Scn2b*$^{+/+}$ ($p = 0.0002$), suggesting that absence of $\beta 2$ may decrease normal axonal loss during brain development.

We next quantified the number of axons that were in the process of degeneration for each genotype using the same set of TEM images (Fig. 2G). Control tissue contained few, if any, degenerating axons. In contrast, after EAE induction, nerves displayed axonal degeneration, as well as degeneration of the myelin sheath, characteristic of the disease. As expected, for both genotypes, there was a significant increase in the extent of degeneration in EAE tissue compared to control: a 456% increase in *Scn2b*$^{+/+}$ and a 274% increase in *Scn2b*$^{-/-}$ ($p < 0.0001$ for both). *Scn2b*$^{+/+}$ optic nerve during EAE showed an average of 9.3 degenerating axons/FOV, compared to 5.8 degenerating axons/FOV in *Scn2b*$^{-/-}$ tissue, representing a 1.6-fold difference ($p < 0.0001$). We thus observed a greater extent of pathology in *Scn2b*$^{+/+}$ tissue compared to *Scn2b*$^{-/-}$, in spite of similar symptom severity in these mice at this time point (19 dpi). No differences were observed between groups of control nerves, showing that loss of β2 does not induce axonal degeneration in the absence of disease.

We calculated the extent of axonal degeneration as a percentage of total axon number (Fig. 2H); this value was obtained for each image independently and values were then averaged together for each genotype and condition. This measurement confirmed that observed differences in degeneration between genotypes were not due simply to the changes in total axon numbers in *Scn2b*$^{+/+}$ *vs*. *Scn2b*$^{-/-}$ mice post-EAE induction. Consistent with the results presented in

Fig. 2B, we observed a significant difference in the percentage of axonal degeneration between genotypes at 19 dpi during EAE. 12.15% of *Scn2b*$^{+/+}$ nerves were determined to be undergoing degeneration, compared to 5.34% of *Scn2b*$^{-/-}$ nerves; this represents a 228% difference ($p < 0.0001$). There was also a significant increase in the level of degenerating axons after EAE induction in each genotype as compared to control: 623% for *Scn2b*$^{+/+}$ and 286% for *Scn2b*$^{-/-}$ ($p < 0.0001$ for both). No differences were observed between control groups.

Finally, we calculated the percent of axons that were demyelinated or thinly myelinated (defined by zero, one, or two myelin wraps) in optic nerves of *Scn2b*$^{+/+}$ *vs*. *Scn2b*$^{-/-}$ mice at 19 dpi (Fig. 2F). We observed an increase in the percentage of demyelinated or thinly myelinated axons in both genotypes following EAE induction compared to control conditions ($p < 0.0001$ for both genotypes). Comparing genotypes, we observed a difference in the percentage of demyelinated or thinly myelinated axons in EAE: 5.8% of *Scn2b*$^{+/+}$ vs. 3.9% of *Scn2b*$^{-/-}$ axons ($p < 0.0001$).

***Scn2b*$^{-/-}$ mice exhibit normal inflammatory and immune responses to MOG_{35-55} peptide**

To develop symptoms of EAE, animals must be able to successfully mount an inflammatory immune response to the presence of MOG antigen. Critical mediators of this response include pro-inflammatory cytokines and activated T

cells. A possible explanation for the decreased EAE pathology observed in *Scn2b*$^{-/-}$ animals is that *Scn2b* deletion results in an impaired immune response. To test this possibility, we performed experiments to assess the ability of *Scn2b*$^{-/-}$ animals to mount an inflammatory immune response to the MOG_{35-55} peptide.

Fluorescence-activated cell sorting techniques were used to assess populations of peripheral immune cells in naïve mice and mice induced with the EAE protocol for both genotypes (Fig. 3). Animals were sacrificed at 12 dpi and splenocytes isolated for immediate analysis. In EAE animals, spleens from both wildtype and null animals were significantly enlarged, as assessed by visual observation, compared to spleens from animals not exposed to the MOG_{35-55} peptide (data not shown). We used cell surface markers to quantify populations of dendritic cells (CD11c), B cells (CD19) and T cells (CD4 and CD8a). Cells obtained from naïve animals showed similar population distributions of each of these cell types for both genotypes (Fig. 3A), indicating that resting numbers of peripheral immune cells in the absence of antigen are not altered as a result of *Scn2b* deletion. Importantly, cells obtained after EAE induction also showed similar distributions between wildtype and null mice (Fig. 3B). Finally, we used Western blot analysis to determine whether splenocytes express Na^+ channel α or β2 proteins, either under naïve conditions or after EAE induction. As shown in Fig. 3C and Fig. 3D, no immunoreactive β2 or Na^+ channel bands ($Na_v1.1$, $Na_v1.2$, or $Na_v1.6$), respectively, were detected in splenocyte lysates, in contrast to brain membranes. Thus, loss of β2 does not measurably affect peripheral immune cell

populations, either under control conditions or in the presence of antigen during an inflammatory immune response.

The inflammatory response to MOG *in vivo* may be modulated by cytokine release. We therefore examined the ability of splenocytes from *Scn2b*$^{+/+}$ and *Scn2b*$^{-/-}$ animals induced with EAE to release cytokines *in vitro* in response to the presence of MOG_{35-55} peptide. We used ELISA to quantify levels of cytokine release (Fig. 3E). We monitored IFN-γ to assess levels of pro-inflammatory/Th1-type cytokines, IL-4 to assess levels of anti-inflammatory/Th2-type cytokines, and IL-10 to assess levels of regulatory cytokines. In all cases, we found no significant differences between splenocytes isolated from *Scn2b*$^{+/+}$ and *Scn2b*$^{-/-}$ mice. These data indicate that the *Scn2b* null mutation does not result in impairment of the release of inflammatory mediators in response to antigen.

T cells are critical mediators of the inflammatory process during EAE pathogenesis. EAE is considered to be a T cell-mediated autoimmune disease model (Kuchroo et al., 2002) and there is some evidence suggesting a role for Na^+ channels in T cells (Khan and Poisson, 1999; Lai et al., 2000). Abnormal activation of T cells is thus another possible explanation for the milder symptoms of EAE observed in the null mice. We evaluated the ability of T cells from *Scn2b*$^{+/+}$ and *Scn2b*$^{-/-}$ mice to respond to the presence of the MOG_{35-55} peptide *in vitro* during EAE induction (Fig. 4). We obtained splenocytes from naïve and

EAE-induced *Scn2b*$^{+/+}$ and *Scn2b*$^{-/-}$ mice at 13 dpi and cultured them with increasing concentrations of MOG_{35-55} peptide. After 72 h in culture, proliferation was quantified by [^{3}H]-thymidine incorporation over a 24-hour period. As expected, T cells from naïve animals of either genotype that had not been previously exposed to the peptide did not display any significant proliferative response. In contrast, cells from EAE animals (both *Scn2b*$^{+/+}$ and *Scn2b*$^{-/-}$) exhibited a robust proliferative response at all concentrations of peptide. The magnitudes of these responses were similar for wildtype and null cells. Thus, *Scn2b* deletion does not compromise the ability of T cells to proliferate in response to antigen and does not result in defects in antigen presentation or cytokine production that would influence the induction of MOG-specific T cell recall responses *in vitro*.

Another critical component of the immune response during EAE is the successful invasion of immune effector cells into the CNS. We labeled cross sections of spinal cord to visualize the infiltration of cells into the white matter during EAE (Fig. 5). Microglia are present in the CNS and can function as macrophages in brain. During EAE, activation of microglia occurs in response to injury and/or inflammation and contributes to disease pathogenesis. Na^{+} channels have been shown to contribute to microglial activation in MS and EAE and phenytoin reduces spinal cord infiltrates in mice with EAE by 75% (Craner et al., 2005), thus their diminished activation in *Scn2b*$^{-/-}$ mice is a possible explanation for the attenuated symptoms of EAE. The OX-42 antibody recognizes a shared

CD11b/CD11c epitope, the CR3 (C3bi) complement receptor and thereby labels microglia, macrophages, monocytes and granulocytes. Cells labeled in the CNS are predominantly microglia (Robinson et al., 1986). In naïve tissue, OX-42 labeling was undetectable in both *Scn2b*$^{+/+}$ (Fig. 5A) and *Scn2b*$^{-/-}$ (Fig. 5B) spinal cord. During EAE, OX-42 positive cells invaded the white matter in both wildtype (Fig. 5C) and null (Fig. 5D) tissue. Higher magnification views of individual cells (inset, Fig. 5C and 5D) show OX-42-positive cells with a characteristic activated morphology, having a rounded cell body and few or no processes.

T cells are important mediators during EAE; we have already shown that T cell proliferation *in vitro* in response to the MOG_{35-55} peptide is similar in cells isolated from *Scn2b*$^{+/+}$ and *Scn2b*$^{-/-}$ animals (Fig. 4). Anti-CD3 antibody recognizes the T cell receptor-associated CD3 molecular complex and serves as a marker for T cells (Miescher et al., 1989). Using anti-CD3, we show that activated T cells are not detectable in naïve white matter isolated from either *Scn2b*$^{+/+}$ (Fig. 5E) or *Scn2b*$^{-/-}$ (Fig. 5F) mice. During EAE, activated T cells infiltrate into the spinal cord in both genotypes with similar patterns (Fig. 5G, 5H; higher magnification views of CD3-positive cells, inset, Fig. 5G and 5H).

Coincident with the first appearance of inflammation and clinical deficits in mice with MOG-EAE, glial fibrillary acidic protein (GFAP)-positive adult radial glia in spinal cord white matter undergo mitosis and phenotypic transformation to

hypertrophic, stellate astroglia (Lee et al., 1990; Tani et al., 1996; Holley et al., 2003; Bannerman et al., 2007). These reactive astrocytes accumulate within and at the margins of EAE/MS lesions and function as antigen presenting cells, as well as contribute to the synthesis of pro-inflammatory cytokines (Lee et al., 1990; Tani et al., 1996; Holley et al., 2003; Bannerman et al., 2007). Anti-GFAP staining in *Scn2b*$^{+/+}$ and *Scn2b*$^{-/-}$ spinal cord is similar under control conditions and in EAE. GFAP-positive cells in *Scn2b*$^{+/+}$ (Fig. 5I) and *Scn2b*$^{-/-}$ (Fig. 5J) control mice are elongated with radially oriented processes. In contrast, GFAP-positive cells in *Scn2b*$^{+/+}$ (Fig. 5K) and *Scn2b*$^{-/-}$ (Fig. 5L) mice in EAE display similar patterns, appearing to have lost their radial orientation and taken on an enlarged, stellate morphology.

Taken together, these results demonstrate that immune cell infiltration into the CNS during EAE occurs normally in *Scn2b*$^{-/-}$ mice, and that there are no significant alterations under control conditions. Loss of *Scn2b* does not measurably compromise the ability of the immune system to mount an appropriate inflammatory response to the presence of the MOG_{35-55} peptide. It is interesting that *Scn2b*$^{-/-}$ mice exhibit a lower percentage of demyelinated or thinly myelinated axons in optic nerve under conditions of EAE compared to wildtype mice, in spite of a normal immune response to the MOG_{35-55} peptide. *Scn2b* is expressed in oligodendrocyte precursor cells (OPCs) as well as in neurons (Cahoy et al., 2008). Thus, similar to other cell adhesion molecules expressed by

OPCs or axons (Gallo and Armstrong, 2008), β2 may participate in inhibition of remyelination. This will be the focus of future investigations.

Na^+ channel expression levels are altered in EAE

Previous studies have reported changes in Na^+ channel expression in EAE and MS; however, these results were based on immunofluorescence rather than on biochemical methodologies that measure protein levels and thus may have reflected channel redistribution rather than up-regulation (Craner et al., 2004a; Craner et al., 2004b). To address this issue, we performed a series of experiments to investigate changes in protein levels of Na^+ channel α and β subunits in brain and spinal cord under control conditions and in EAE. Fig. 6, upper panel, shows changes in $Na_v1.1$, $Na_v1.2$, and $Na_v1.6$ expression in *Scn2b*$^{+/+}$ and *Scn2b*$^{-/-}$ whole brain homogenates under control conditions and under conditions of EAE. Western blots were then stripped and reprobed with anti-α-tubulin as a loading control. Our results show that $Na_v1.6$ expression is increased in EAE in *Scn2b*$^{+/+}$ brains and that this up-regulation is attenuated in *Scn2b*$^{-/-}$ brains (Fig. 6C). In contrast to predictions from previous immunofluorescent studies, we did not observe increases in overall $Na_v1.2$ expression in brain in EAE in either genotype (Fig. 6B). We observed that $Na_v1.1$ is increased in EAE in *Scn2b*$^{-/-}$ null brain but is unaffected in *Scn2b*$^{+/+}$ brain (Fig. 6A). This change in $Na_v1.1$ expression in EAE has not been reported previously. In Fig. 6, lower panel, we show that β subunit expression in whole brain is not altered in either genotype under control conditions or in EAE (Fig. 6

D-G). Overall, we did not observe significant changes in any of the β subunits in brain, with the exception of the absence of β2 in the *Scn2b*$^{-/-}$ animals.

We next performed Western blot experiments using spinal cord homogenates to determine whether comparable changes in Na^+ channel expression occurred in EAE as shown above (Fig. 7). In contrast to our results in brain, but in agreement with previous reports (Craner et al., 2004a; Craner et al., 2004b), we observed increased $Na_v1.2$ expression in *Scn2b*$^{+/+}$ spinal cord in EAE (Fig. 7B). Levels of $Na_v1.2$ expression in *Scn2b*$^{-/-}$ spinal cord did not increase in demyelinating disease, consistent with our hypothesis that the absence of β2 attenuates Na^+ channel up-regulation in EAE. Similarly, we observed increased $Na_v1.6$ expression under EAE conditions for *Scn2b*$^{+/+}$ but not for *Scn2b*$^{-/-}$ spinal cord, again consistent with our hypothesis that β2 contributes to this up-regulation in neurons (Fig. 7C). In contrast to the changes in $Na_v1.1$ expression observed in brain, we observed comparable levels of this channel protein in spinal cord when comparing control and EAE conditions for each genotype.

Axonal Na^+ channel localization is altered similarly in EAE in *Scn2b*$^{+/+}$ and *Scn2b*$^{-/-}$ mice

Diffuse $Na_v1.2$ and $Na_v1.6$ localization along demyelinated axons during EAE has been reported previously (Craner et al., 2004a; Craner et al., 2004b). We performed immunofluorescence confocal microscopy using longitudinal frozen

sections of optic nerve (Fig. 8) and spinal cord (Fig. 9) from EAE and control animals to determine whether the *Scn2b* null mutation altered this localization pattern. In all panels of Fig. 8 and Fig. 9, anti-Caspr antibody was used to mark the paranodal regions. In Fig. 8, panels A, E, and I, we show that $Na_v1.1$ and $Na_v1.2$ are absent from optic nerve nodes of Ranvier in adult wildtype animals under control conditions. As expected (Caldwell et al., 2000; Boiko et al., 2001a; Kaplan et al., 2001a), $Na_v1.6$ is the predominant Na^+ channel clustered at the nodal gap. This expression pattern is not altered by the *Scn2b* null mutation under control conditions (panels B, F, and J), as previously demonstrated (Chen et al., 2002). In contrast to a previous report using Biozzi mice (Craner et al., 2003a), we observed the appearance of $Na_v1.1$ at nodes in both genotypes under conditions of EAE (panels C and D). In agreement with previous reports (Craner et al., 2004a; Craner et al., 2004b), we observed $Na_v1.2$ and $Na_v1.6$ immunolocalization at nodes as well as along demyelinated regions of wildtype optic nerve axons and this localization pattern was similar for *Scn2b*$^{-/-}$ mice (panels G, H, K, and L). Thus, while the levels of $Na_v1.1$ and $Na_v1.6$ protein expression are altered in *Scn2b* null brain compared to wildtype under conditions of EAE, we did not observe differences in the localization patterns of these Na^+ channels between genotypes in optic nerve under control or EAE conditions.

Fig. 9 demonstrates immunolocalization of $Na_v1.1$, $Na_v1.2$, and $Na_v1.6$ in *Scn2b* null and wildtype spinal cord under control conditions and in EAE. In both genotypes, under control conditions, we observed nodal clustering of

predominantly $Na_v1.1$ (panels A and B) and $Na_v1.6$ (panels I and J), with $Na_v1.2$ observed in a sub-population of nodes (panels E and F). We observed $Na_v1.1$ (panel C), $Na_v1.2$ (panel G), and $Na_v1.6$ (panel K) immunolocalization at nodes as well as along demyelinated regions in *Scn2b*$^{+/+}$ spinal cord in EAE. A similar pattern was observed for *Scn2b*$^{-/-}$ spinal cord in EAE (panels D, H, and L, respectively). Thus, as observed for optic nerve, the *Scn2b* null mutation does not alter the pattern of Na^+ channel localization under control or EAE conditions. Taken together, our results suggest that the absence of β2 alters Na^+ channel protein expression levels but does not affect channel localization in optic nerve or spinal cord axons under control conditions or in EAE.

DISCUSSION

β2 subunits are critical modulators of neuronal Na^+ channel cell surface expression and thus, of excitability. Insertion of newly synthesized Na^+ channels into the plasma membrane in primary neurons is concomitant with α-β2 association (Schmidt et al., 1985; Schmidt and Catterall, 1986a). *Scn2b* null neurons show a ~50% reduction in the level of functional Na^+ channels (Chen et al., 2002; Lopez-Santiago et al., 2006b). In *Scn2b* null optic nerve, the integral of the compound action potential is reduced and the threshold for action potential generation is increased, consistent with a reduction in the level of functional cell

surface Na^+ channels at nodes of Ranvier (Chen et al., 2002). The present study demonstrates that deletion of *Scn2b* is neuroprotective in EAE *in vivo*. These results are consistent with the idea that axonal sparing in *Scn2b*$^{-/-}$ mice is a result of attenuated $Na_v1.6$ upregulation in response to demyelination. In addition, these results are consistent with the possibility that, in the absence of *Scn2b*, there is a reduction in persistent Na^+ current produced by other Na^+ channel gene products within the lesions. Previous studies in a heterologous system have shown that the combination of $\beta2 + \beta3$ increases the level of persistent Na^+ current mediated by $Na_v1.2$ expressed in tsA-201 cells while the combination of $\beta1 + \beta2$ has no effect on persistent current (Qu et al., 2001a). Thus, the specific combination of Na^+ channel α and β subunits is likely critical to determining the level of persistent Na^+ current in demyelinated axons.

Similar to the mechanism put forth by Waxman and colleagues (Waxman, 2006a), we propose that in *Scn2b* wildtype and null mice $Na_v1.2$ is diffusely expressed along demyelinated axons in EAE where it supports recovery from conduction block. $Na_v1.6$ becomes up-regulated along some demyelinated axons in wildtype mice in EAE and contributes to axonal damage via mediation of persistent Na^+ current followed by accumulation of intra-axonal Na^+, activation of reverse Na^+-Ca^{2+} exchange, and accumulation of intra-axonal Ca^{2+}. We propose that *Scn2b*$^{-/-}$ mice are protected from axonal damage during EAE due to attenuation of $Na_v1.6$ up-regulation along demyelinated axons, thus reducing the harmful effects of the predicted persistent Na^+ current. In addition, the absence of

β2 may attenuate the level of persistent Na^+ current mediated by Na^+ channels in demyelinated lesions. The observed appearance of $Na_v1.1$ at optic nerve nodes of Ranvier in EAE in both genotypes, as well as increased expression of $Na_v1.1$ protein in *Scn2b*$^{-/-}$ brain during EAE, compared to *Scn2b*$^{+/+}$, provide an intriguing avenue of investigation for future work, as the involvement of $Na_v1.1$ in demyelination has not been investigated. The level of persistent current generated by $Na_v1.1$ in native optic nerve axons is not known (Lossin et al., 2003; Spampanato et al., 2004; Vanoye et al., 2006), thus we are unable to predict whether an increase in $Na_v1.1$ expression during demyelination would lead to axonal degeneration similar to that proposed for $Na_v1.6$. The reduction in axonal loss observed in *Scn2b*$^{-/-}$ mice compared to *Scn2b*$^{+/+}$, however, suggests that $Na_v1.1$-mediated Na^+ current in the absence of β2 does not activate injury cascades, and may instead promote recovery from conduction block, as predicted for $Na_v1.2$. Thus, the role of Na^+ channels in demyelinating disease is complex, with relative expression levels of different channel genes predicted to provide critical modulation of the eventual course of the disease and extent of pathology. Importantly, our results demonstrate that *Scn2b*$^{-/-}$ mice have normal inflammatory and immune responses in EAE, supporting our hypothesis that the mechanism of neuroprotection in these mice is due to changes in the expression levels of axonal Na^+ channels rather than to immunomodulation. Intriguingly, it was shown previously that *Scn2b* mRNA levels are down-regulated at advanced stages of monophasic EAE in rats (Nicot et al., 2003). This may represent a compensatory mechanism in neurons to attenuate the damaging effects of

$Na_v1.6$ up-regulation in demyelinating disease and is consistent with the present results in *Scn2b* null mice.

Our results suggest a molecular mechanism for the observed pharmacological effects of Na^+ channel blocking agents in MS/EAE and may open a novel avenue for therapeutic intervention. We propose that administration of drugs targeting Na^+ channels effectively results in a similar situation in neurons as loss of $\beta 2$ – a significant reduction in the level of functional Na^+ channels. Deletion of Na^+ channel α subunits in mice is lethal (reviewed in (Meadows and Isom, 2005)). Administration of Na^+ channel pharmacological agents (e.g. anti-convulsants, anti-arrhythmics, and local anesthetics), while effective in MS, can also result in serious systemic side effects. For example, recent studies have shown that withdrawal of phenytoin can exacerbate symptoms and result in lethality in the EAE model (Black et al., 2007b). Our approach, in contrast, is novel and opens the possibility that through targeting $\beta 2$, the level of cell surface Na^+ channel expression can be incrementally and perhaps specifically modulated, so that in the future safer and more effective therapies for protection against axonal loss following neuronal injury and/or demyelination may be realized.

EXPERIMENTAL METHODS

Mice: *Scn2b*$^{+/+}$ and *Scn2b*$^{-/-}$ mice were generated in our laboratory on the C57BL/6 genetic background (Chen et al., 2002), and have been established as congenic strains through repeated backcrossing to C57BL/6 mice for over 15 generations. All mice used in this study were female *Scn2b*$^{+/+}$ or *Scn2b*$^{-/-}$ mice bred from congenic *Scn2b*$^{+/-}$ littermates, between the ages of 12 and 24 weeks of age. All animal procedures were approved by the University of Michigan Committee on the Use and Care of Animals and mice were housed in the University of Michigan Unit for Laboratory Animal Medicine.

Induction of EAE: MOG_{35-55} peptide was synthesized and purified by the University of Michigan Protein Structure Facility, Ann Arbor, MI or by Auspep, Parkville, Australia. Peptides were tested between both facilities to ensure that disease progression was identical; individual lots from each facility were also tested upon receipt. 150 μg of purified MOG_{35-55} peptide were emulsified in sterile PBS and complete Freund's adjuvant (CFA; Difco, Franklin Lakes, NJ), and supplemented with 4 mg/ml *Mycobacterium tuberculosis* (Difco). 100 μl of emulsion, or emulsion lacking peptide (as a control), were injected subcutaneously into each hind flank of the animal. All animals (peptide and control groups) were immediately injected intravenously with 350 ng of inactivated pertussis toxin (List Biological Laboratories, Campbell, CA) in sterile PBS and again after 48 hours. Animals were monitored daily for the

development of clinical symptoms following induction using a five-point clinical scale as follows: 0: no visible impairment, 1: limp tail, 2: limp tail with hind limb weakness, 3: hind limb paralysis, 4: ascending paralysis with hind limb paralysis, 5: moribund or death. Animals in between two stages were given half scores. Animals reaching stage 5 were assigned a score of 5 for the remainder of the experimental time course. Animals experiencing paralysis were given water *ad libitum*, moist chow was placed on the cage floor twice daily, and animals were hand-fed when necessary.

Transmission Electron Microscopy: Scn2b$^{+/+}$ and *Scn2b*$^{-/-}$ mice (MOG peptide and control groups), at time points post-injection indicated in the figure legends, were anesthetized and perfused intracardially with 0.1M Sorenson's buffer (pH 7.4) followed by 2.5% glutaraldehyde in Sorenson's buffer. Nerves were carefully dissected and placed in fresh fixative for a minimum of 2 h, rinsed, and post-fixed in 1% osmium tetroxide. Samples were washed in several changes of buffer, dehydrated with graded alcohols and embedded in Spurr's epoxy resin. Semi-thin sections were stained with 1% toluidine blue for morphological examination and to establish orientation. Ultrathin (70 nm) transverse sections were then stained in uranyl acetate/lead citrate. For analysis, one ultrathin section from each of three mice under control or EAE conditions was examined using a Phillips CM-100 TEM located in the Microscopy and Image Analysis Laboratory (MIAL), University of Michigan. A minimum of fifty non-overlapping fields of view (160.4 μm^2 per field of view) from each section were obtained at

7900x magnification. From each image, total numbers of myelinated axons were counted manually (including both intact and degenerating axons). In the same images, the number of degenerating axons was counted. The percentage of degenerating axons was calculated per field of view and values for all fields of view in each group of mice were averaged. A myelinated axon was defined as an axon wrapped by two or more layers of myelin. A degenerating axon was defined as a collapsed or delaminated myelinated axon containing membranous debris. Images were digitally recorded using a Kodak 1.6 Megaplus high-resolution digital camera system. All values are reported as mean ± SEM. This assessment was first performed by the investigator who prepared the samples and then was repeated by another investigator who was blind to genotype and experimental condition. Both investigators calculated similar values.

Splenocyte Culture: Spleens were removed from control and peptide groups of *Scn2b*$^{+/+}$ and *Scn2b*$^{-/-}$ mice at 12-14 dpi. The spleens were mechanically separated, triturated, and washed to obtain a single-cell suspension of splenocytes. Red blood cells were lysed and splenocytes washed in HBSS. Cells were counted and cultured in RPMI supplemented with 5% fetal bovine serum (Invitrogen), 1% penicillin/streptomycin (Invitrogen), 200 mM L-glutamine (Invitrogen), 100 mM sodium pyruvate (Invitrogen), 10mM non-essential amino acids (Invitrogen) and 50μM β-mercaptoethanol (Sigma-Aldrich). MOG_{35-55} peptide was added to all culture wells at a concentration of 20 μg/ml, with the

exception of cultures used for T cell proliferation assays, which were cultured with varying concentrations of peptide as indicated in the figure.

Fluorescence-activated cell sorting: For surface staining, spleen cells were washed and resuspended at a concentration of 10^7 cells/ml in FA Buffer (Difco) + 0.1% NaN_3. Fc receptors were blocked by the addition of anti-CD16/32 (Fc block; BD Pharmingen). After Fc receptor blocking, 10^6 cells were stained in a final volume of 120 µl in 12 x 75 polystyrene tubes for 30 min at 4°C. Leukocytes were stained with the following monoclonal antibodies, according to the manufacturer's instructions: CD4 (RM4-5), CD8a (53-6.7), CD3 (17A2), CD19 (ID3), CD11c (HL3) (all BD Pharmingen). Cells were washed twice with FA buffer, resuspended in 100 µl buffer, and 200 µl of 4% formalin was added to fix the cells. Cells were gated for live cells by forward scatter (FSC) and side scatter (SSC) before analysis. A minimum of 20,000 events were acquired on a FACSCalibur flow cytometer (BD Pharmingen) using CellQuest software (BD Pharmingen).

T cell proliferation/ELISA: To assess T cell proliferation, MOG_{35-55}-sensitized spleen cells were isolated from *Scn2b*$^{+/+}$ and *Scn2b*$^{-/-}$ mice as described above and cultured for 72 h in 96-well, round-bottom microculture plates at a concentration of 5 x 10^6 cells/ml in 0.2 ml of RPMI-complete medium in the presence or absence of 5 - 80 µg/ml MOG_{35-55} peptide. For proliferation, [^{3}H]-

thymidine (1 μCi/well, MP Biomedicals, Irvine, CA) was added at 72 h, and mean incorporation into DNA was measured at 96 h by liquid scintillation counting. To measure the levels of Th1 and Th2 cytokines, MOG_{35-55}-immunized spleen cells (5×10^6/ml) were cultured in RPMI-complete medium in 6-well plates in the presence or absence of 20 μg/ml MOG_{35-55} peptide. After 72 h, cells were recultured in the presence of MOG_{35-55} peptide in 24-well plates at 1×10^6/ml. After 24 h, the culture supernatants were collected and assessed for cytokine production. The levels of Th1 (IFN-γ), Th2 (IL-4) and Th2/Treg (IL-10) cytokines in culture supernatants were measured by the ELISA OPTEIA (IL-4 and IL-10; BD Pharmingen) or DuoSet (IFNγ; R&D Systems, Minneapolis, MN) system according to the manufacturer's instructions.

Immunofluorescence Microscopy: Spinal cords or optic nerves were dissected from *Scn2b*$^{+/+}$ and *Scn2b*$^{-/-}$ mice (MOG peptide and control) at the time post-injection indicated in the figure legends. 10 μm cryosections were generated. Sections were fixed with 4% paraformaldehyde, washed 3 times in 0.05 M phosphate buffer (PB), and blocked for a minimum of 1 h in PBTGS (0.1M PB, 0.3% Triton X-100, 10% normal goat serum). Sections were incubated overnight in primary antibody diluted in PBTGS, followed by incubation in goat anti-mouse, anti-rabbit or anti-rat secondary antibody as appropriate, coupled to either Alexa 488 (green) or Alexa 594 (red) (Molecular Probes, Carlsbad, CA) and diluted in PBTGS. Sections were washed three times with 0.1 M PB after each antibody

step. Sections were air-dried and coverslipped using GelMount anti-fade mounting medium (Biomeda, Foster City, CA). Digital images were collected using an Olympus FluoView 500 confocal microscope with FluoView software located in the Department of Pharmacology, University of Michigan, or an Olympus BX51 fluorescent microscope located in the University of Michigan Microscopy and Image Analysis Laboratory.

Western blot: *Scn2b*$^{+/+}$ and *Scn2b*$^{-/-}$ mice were sacrificed and brains and spinal cords were immediately removed and stored in ice-cold homogenization buffer. Membranes were prepared as described previously (Isom et al., 1995b). For splenocyte preparations, cells were isolated as described above and lysed with RIPA buffer. 'Complete' protease inhibitor tablets (Roche Diagnostics, Indianapolis, IN) were included in all solutions at twice the recommended concentration to prevent Na^+ channel degradation. Western blot analysis was then performed as described (Malhotra et al., 2000b; Malhotra et al., 2004) to detect Na^+ channel α and β subunit polypeptides, as described in the figure legends. Briefly, samples were solubilized in SDS-PAGE sample buffer containing 1% SDS and 500 mM β-mercaptoethanol, heated for 5 min at 80°C, and separated on 4-15% acrylamide SDS-PAGE gradient gels for α subunit detection or 10% acrylamide SDS-PAGE gels for β subunit detection. Proteins were transferred to nitrocellulose and probed with specific antibodies followed by secondary antibodies conjugated to horseradish peroxidase and visualized using

the West Dura or West Femto enhanced chemiluminescence detection system (Pierce, Rockford, IL). Blots which were re-incubated with a second primary antibody against α-tubulin (as a loading control) were first stripped with ReBlot Plus Antibody Stripping Solution (Chemicon, Temecula, CA) according to manufacturer's instructions. For quantification of Western blots, densitometric analysis of bands was performed using NIH ImageJ software. Band density was normalized to α-tubulin signal for comparison.

Antibodies: Primary antibodies for Western blotting and immunocytochemistry were used as follows: anti-CD3 (dilution 1:250, BD Pharmingen, San Jose, CA), OX-42 (1:100, BD Pharmingen), anti-GFAP (1:500, Molecular Probes, Carlsbad, CA), anti-$Na_v1.1$ (1:100-1:250, NeuroMab, Davis, CA), anti-$Na_v1.2$ (1:100-1:250, NeuroMab), anti-$Na_v1.6$ (either 1:200 (polyclonal, Western blotting, Sigma-Aldrich) or 1:200 (monoclonal, immunofluorescence, NeuroMab)), anti-Caspr (either 1:1500 (polyclonal, Dr. Elior Peles) or 1:500 (monoclonal, NeuroMab)), anti-β1 (anti-scn1ba1 (Fein et al., 2007)), anti-β2ec (a resynthesis of anti-β2ec antibody previously characterized in (Chen et al., 2002)), anti-β3 (Chen et al., 2004), anti-β4 (a polyclonal antibody to β4 was generated against the peptide sequence KKLITFILKKTREKKKECLV used in (Grieco et al., 2005a)), and anti-α-tubulin (1:5000, Cedarlane Laboratories, Hornby, ON).

Statistical Analysis: Data were calculated as mean +/- SEM , compared using the Student's t-test, and plotted using GraphPad Prism statistical software. Significant differences were defined as $p < 0.05$.

Figure 2.1**: *Scn2b*$^{-/-}$ mice exhibit reduced symptom severity and lethality in EAE.**

Mean EAE clinical score post-injection of MOG_{35-55} peptide (**A**) and post-onset of clinical symptoms (**B**). *Scn2b*$^{+/+}$ (filled squares), *Scn2b*$^{-/-}$ (open squares). For post-onset data, day 0 represents the first day on which an individual animal displayed clinical symptoms. For (**A**) and (**B**), data points represent the average of clinical scores observed on that day for all animals (± standard error). Mice reaching end stage were assigned a score of 5 for the remainder of the experimental time course and included in calculations. (**C**) Percent of mice reaching stage 1 clinical symptoms and end stage EAE (moribund or death). (**D**) Survival curve post-injection. *Scn2b*$^{+/+}$ (dotted line), *Scn2b*$^{-/-}$ (solid line). Data represent combined observations from 5 independent experiments. * : $P < 0.005$, ** : $P < 0.05$. For **A**, **C** (stage 1) : (n = 32 for *Scn2b*$^{+/+}$, n = 29 for *Scn2b*$^{-/-}$). For **B**, **C** (stage 2) : (n = 31 for *Scn2b*$^{+/+}$, n = 27 for *Scn2b*$^{-/-}$).

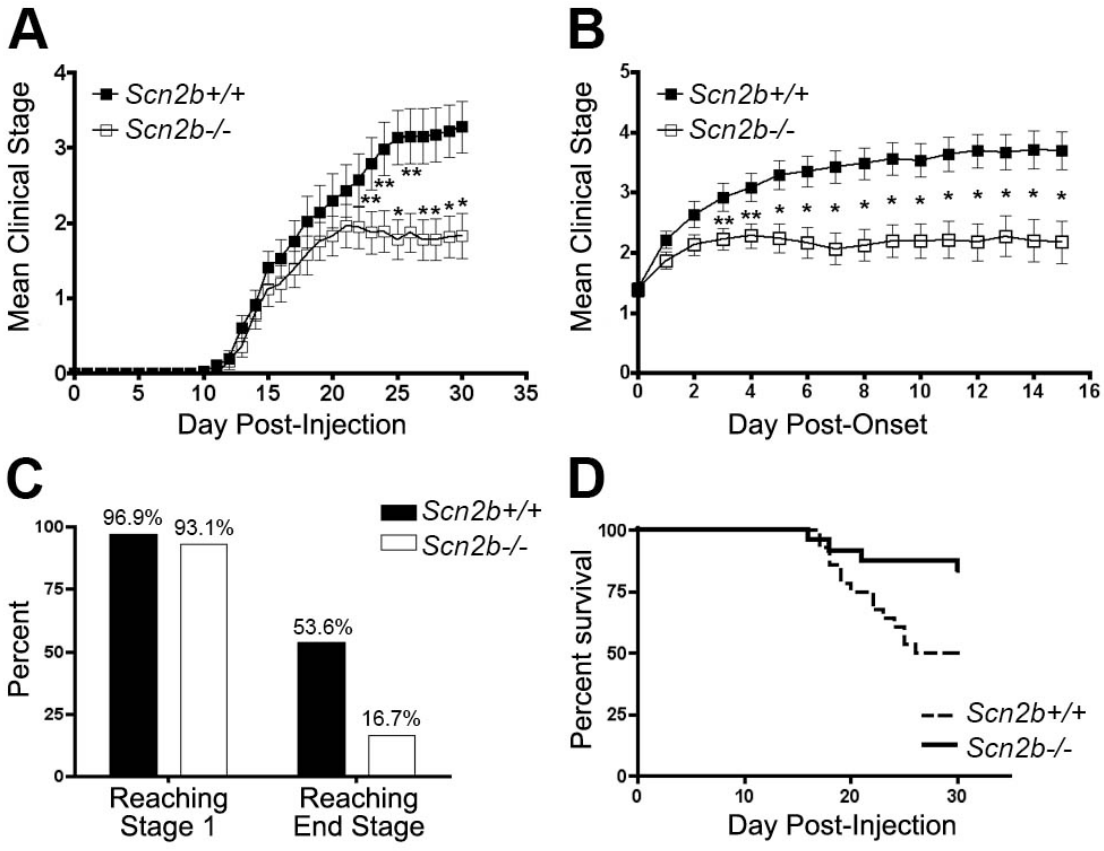
A
Mean Clinical Stage
Scn2b+/+
Scn2b-/-
Day Post-Injection
B
Mean Clinical Stage
Scn2b+/+
Scn2b-/-
Day Post-Onset
C
Percent
96.9%
93.1%
53.6%
16.7%
Scn2b+/+
Scn2b-/-
Reaching Stage 1
Reaching End Stage
D
Percent survival
Scn2b+/+
Scn2b-/-
Day Post-Injection

Figure 2.2: *Scn2b*$^{-/-}$ mice display decreased axonal loss, axonal degeneration, and demyelination in optic nerve in EAE.

EAE was induced in *Scn2b*$^{+/+}$ and *Scn2b*$^{-/-}$ mice and optic nerve axons were isolated at 19 dpi. **(A-D)** Representative transmission electron micrographs of optic nerve cross-sections from control and EAE mice. (**A**) *Scn2b*$^{+/+}$ and (**B**) *Scn2b*$^{-/-}$ control tissue showing numerous, normally myelinated axons. (**C**) *Scn2b*$^{+/+}$ tissue after EAE induction, displaying extensive axonal loss, grossly swollen and degenerating axons (arrows), and myelin debris (arrowhead). Oligodendrocyte (O). (**D**) *Scn2b*$^{-/-}$ tissue after EAE induction, displaying degenerating axon (arrow) and myelin debris (arrowhead) but a lesser extent of axonal loss. Scale bar = 2μM. All micrographs at 7900x magnification. (**E-H**) Quantification of data obtained from micrographs. (**E**) Mean number of axons (intact + degenerating) per FOV. (**F**) Mean percentage of demyelinated axons (relative to total axon number for each image) per FOV. Axons ensheathed by zero, one, or two myelin wraps were counted. (**G**) Mean number of degenerating axons per FOV. (**H**) Mean percentage of degenerating axons (relative to total axon number for each image) per FOV. *: $P<0.0001$. n = 156 FOV *Scn2b*$^{+/+}$ (EAE), n = 158 FOV *Scn2b*$^{+/+}$ (control), n = 162 FOV *Scn2b*$^{-/-}$ (EAE and control).

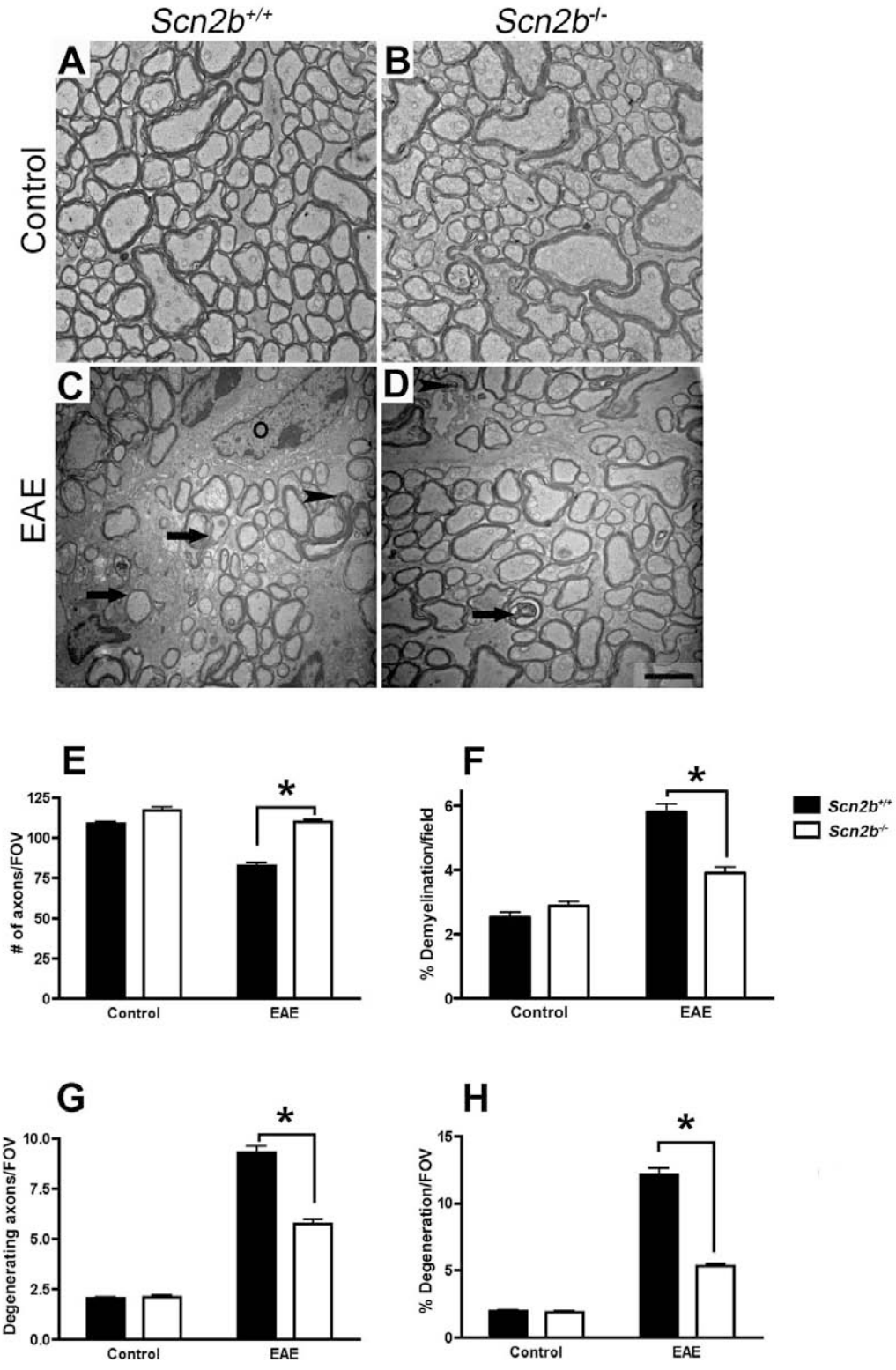
Scn2b+/+
Scn2b-/-
A
B
C
D
Control
EAE
E
# of axons/FOV
125
100
75
50
25
0
Control
EAE
*
F
% Demyelination/field
6
4
2
0
Control
EAE
*
Scn2b+/+
Scn2b-/-
G
Degenerating axons/FOV
10.0
7.5
5.0
2.5
0.0
Control
EAE
*
H
% Degeneration/FOV
15
10
5
0
Control
EAE
*

Figure 2.3: The *Scn2b* null mutation does not alter immune cell profiles or cytokine release under control or EAE conditions.

Scn2b$^{+/+}$ and *Scn2b*$^{-/-}$ mice under control and EAE conditions display similar populations of peripheral immune cells. (**A**) Flow cytometry, naïve animals. Naïve *Scn2b*$^{+/+}$ (top) and *Scn2b*$^{-/-}$ (bottom) mice display similar populations of immune cells. Representative dot plots are shown; quadrants are labeled with mean percentages (n = 3). (**I**) CD11c (dendritic cell) and CD19 (B cell) populations. (**II**) CD8a and CD4 T cell populations. (**B**) Flow cytometry, EAE animals. *Scn2b*$^{+/+}$ (top) and *Scn2b*$^{-/-}$ (bottom) mice display similar populations of immune cells at 12 dpi. Cells were pooled from three spleens before single analysis. (**I**) CD11c (dendritic cell) and CD19 (B cell) populations. (**II**) CD8a T cell populations. (**III**) CD4 T cell populations. (**C,D**) Splenocytes do not express Na^+ channel proteins. Splenocytes from *Scn2b*$^{-/-}$ and *Scn2b*$^{+/+}$ mice under naïve and EAE conditions were isolated. Equal aliquots of splenocyte homogenates or rat brain membranes (as a control) were analyzed using Western blotting. Lane 1: *Scn2b*$^{+/+}$ control splenocytes, Lane 2: *Scn2b*$^{+/+}$ EAE splenocytes, Lane 3: *Scn2b*$^{-/-}$ control splenocytes, Lane 4: *Scn2b*$^{-/-}$ EAE splenocytes. Molecular weight markers are shown in kdal. (C) Probe: anti-β2 antibody. Arrow shows immunoreactive Scn2b band. (D) Probe: anti-Na_v1 antibodies against Pan-Na^+ channel protein, $Na_v1.1$, $Na_v1.2$, or $Na_v1.6$. (**E**) Cytokine release is similar in *Scn2b*$^{+/+}$ and *Scn2b*$^{-/-}$ splenocytes. Splenocytes from *Scn2b*$^{+/+}$ and *Scn2b*$^{-/-}$ mice at 13 days post-induction displayed similar levels of antigen-stimulated cytokine release after 72h *in vitro* following stimulation with MOG_{35-55} peptide. I: IFN-γ. II: IL-4. III: IL-10.

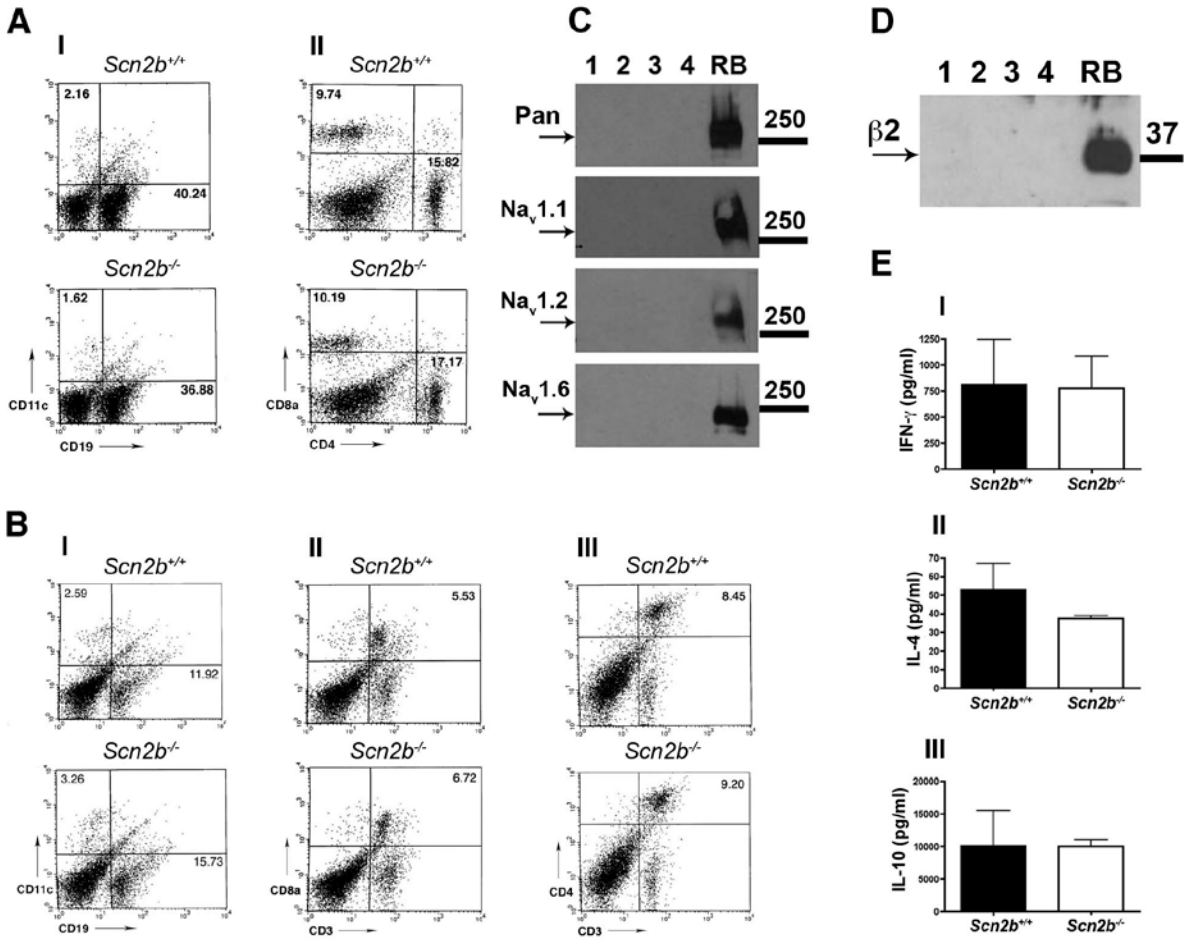
A
I
Scn2b+/+
2.16
40.24
Scn2b-/-
1.62
36.88
CD11c
CD19
II
Scn2b+/+
9.74
15.82
Scn2b-/-
10.19
17.17
CD8a
CD4
C
1 2 3 4 RB
Pan
250
Nav1.1
250
Nav1.2
250
Nav1.6
250
D
1 2 3 4 RB
β2
37
E
I
IFN-γ (pg/ml)
1250
1000
750
500
250
0
Scn2b+/+
Scn2b-/-
II
IL-4 (pg/ml)
70
60
50
40
30
20
10
0
Scn2b+/+
Scn2b-/-
III
IL-10 (pg/ml)
20000
15000
10000
5000
0
Scn2b+/+
Scn2b-/-
B
I
Scn2b+/+
2.59
11.92
Scn2b-/-
3.26
15.73
CD11c
CD19
II
Scn2b+/+
5.53
Scn2b-/-
6.72
CD8a
CD3
III
Scn2b+/+
8.45
Scn2b-/-
9.20
CD4
CD3

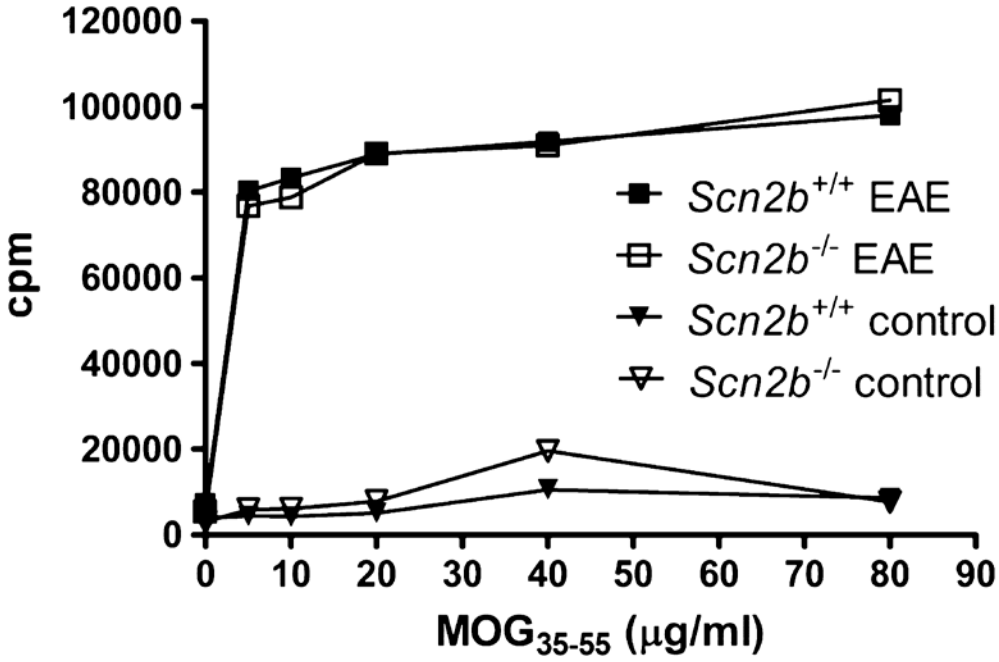

Figure 2.4: T cell proliferation in *Scn2b*$^{+/+}$ and *Scn2b*$^{-/-}$ mice.

T cells from *Scn2b*$^{+/+}$ and *Scn2b*$^{-/-}$ mice at 13 dpi in EAE display similar levels of proliferation *in vitro* in response to the presence of MOG_{35-55} peptide at varying concentrations. T cells from naïve mice do not display significant proliferation in response to the presence of peptide. No proliferation was observed in the absence of peptide in any group. n = 3 for EAE animals, n = 1 for controls.

Figure 2.5: Cellular infiltration into *Scn2b*$^{+/+}$ and *Scn2b*$^{-/-}$ spinal cord at 19 dpi in EAE.

(A-D) *Scn2b*$^{+/+}$ and *Scn2b*$^{-/-}$ mice display similar extents of microglial infiltration after induction of EAE and absence of infiltration in control tissue. **A, B**: *Scn2b*$^{+/+}$ (**A**) and *Scn2b*$^{-/-}$ (**B**) control spinal cord sections, showing an absence of OX-42 immunopositive staining. **C, D**: *Scn2b*$^{+/+}$ (**C**) and *Scn2b*$^{-/-}$ (**D**) spinal cord cross-sections after EAE induction, displaying significant increases in microglial infiltration as observed by increased OX-42 (CD11b/c) immunofluorescence. Inset (in **C**, **D**) shows OX-42-positive cells with an amoeboid, activated morphology. Scale bar, 100μm; inset 20 μm. **(E-H)** *Scn2b*$^{+/+}$ and *Scn2b*$^{-/-}$ mice display similar extents of T cell infiltration after induction of EAE, and absence of infiltration in control tissue. **E, F**: *Scn2b*$^{+/+}$ (**E**) and *Scn2b*$^{-/-}$ (**F**) control spinal cord sections, showing an absence of CD3-positive staining. **G, H**: *Scn2b*$^{+/+}$ (**G**) and *Scn2b*$^{-/-}$ (**H**) spinal cord cross-sections after EAE induction, displaying significant increases in infiltration as observed by increased CD3 immunofluorescence. Inset (in **G**, **H**) shows CD3-positive cells. Scale bar, 200μm; inset 10μm. **(I-L)** Increases in reactive astrocyte numbers in both *Scn2b*$^{+/+}$ and *Scn2b*$^{-/-}$ mice following EAE induction as compared to controls. **I, J**: *Scn2b*$^{+/+}$ (**I**) and *Scn2b*$^{-/-}$ (**J**) control spinal cord sections, showing GFAP-positive astrocytes with radial processes around tissue periphery. **K, L**: *Scn2b*$^{+/+}$ (**K**) and *Scn2b*$^{-/-}$ (**L**) spinal cord cross-sections after EAE induction. Increased numbers of GFAP-positive astrocytes with stellate morphology and astrocyte invasion to white matter is visible. Scale bar, 100μm.

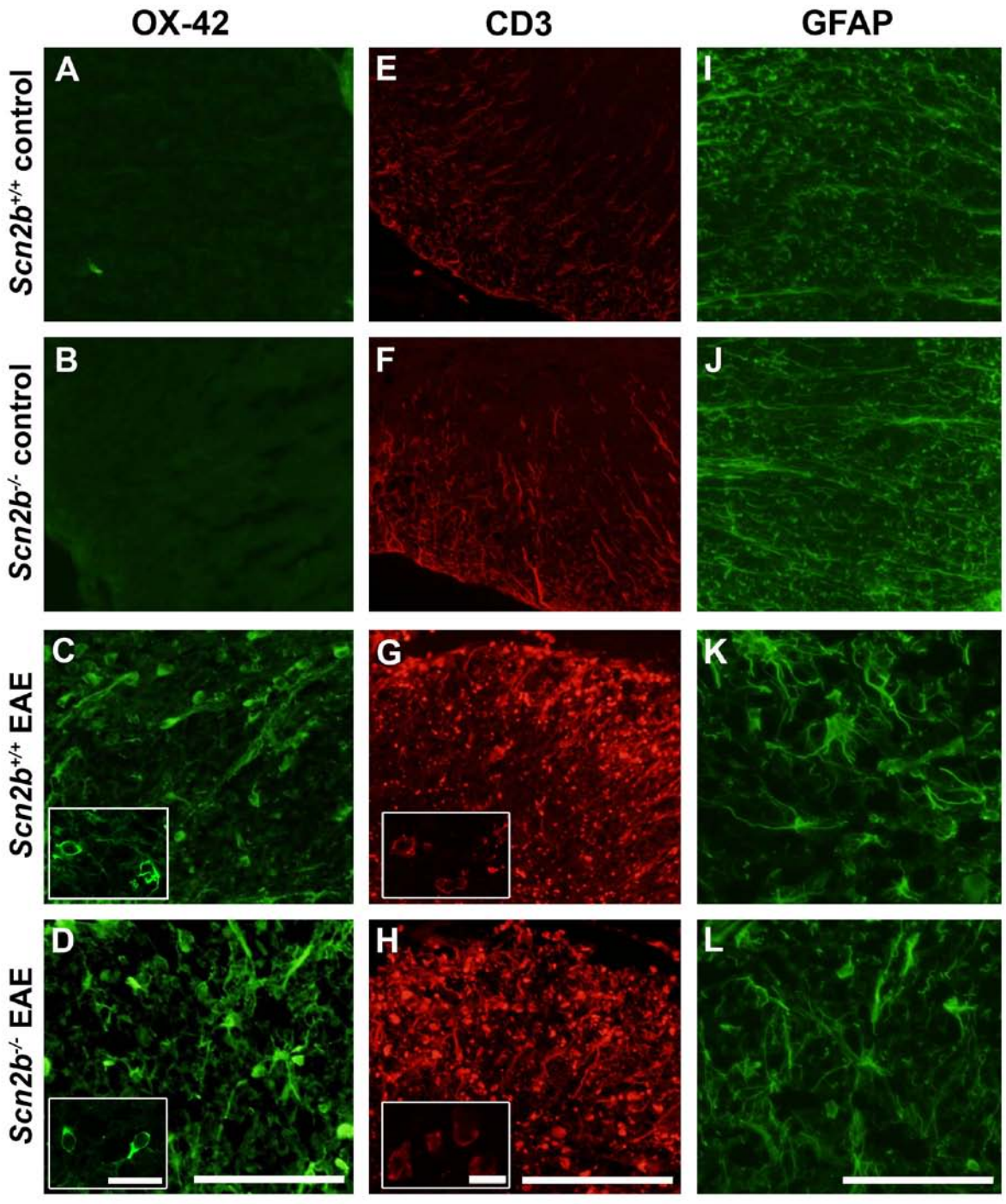
OX-42
CD3
GFAP
A
E
I
B
F
J
C
G
K
D
H
L
Scn2b+/+ control
Scn2b-/- control
Scn2b+/+ EAE
Scn2b-/- EAE

<u>Figure 2.6</u>: Expression levels of Na^+ channel α and β subunits in *Scn2b*$^{+/+}$ and *Scn2b*$^{-/-}$ brain.

Western blots of mouse brain homogenates were probed with antibodies to $Na_v1.1$, $Na_v1.2$ or $Na_v1.6$, or to $\beta1$, $\beta2$, $\beta3$, or $\beta4$. Samples were collected 15 dpi in EAE. Lanes were loaded with equal amounts of protein; blots were stripped and reprobed with anti-α-tubulin as a loading control and this signal is shown at ~50 kDa in the bottom gel section in each panel. **A**: Anti-$Na_v1.1$. **B**: Anti-$Na_v1.2$. **C**: Anti-$Na_v1.6$. (**D-G)** *Scn2b*$^{+/+}$ and *Scn2b*$^{-/-}$ mice display no differences in expression levels of Na^+ channel β subunits under control or EAE conditions. $\beta2$ was absent in *Scn2b*$^{-/-}$ brains. No difference in expression of $\beta2$ was observed in *Scn2b*$^{+/+}$ tissue under control conditions vs. EAE conditions. **D**: Anti-$\beta1$. **E**: Anti-$\beta2$. **F**: Anti-$\beta3$. **G**: Anti-$\beta4$.

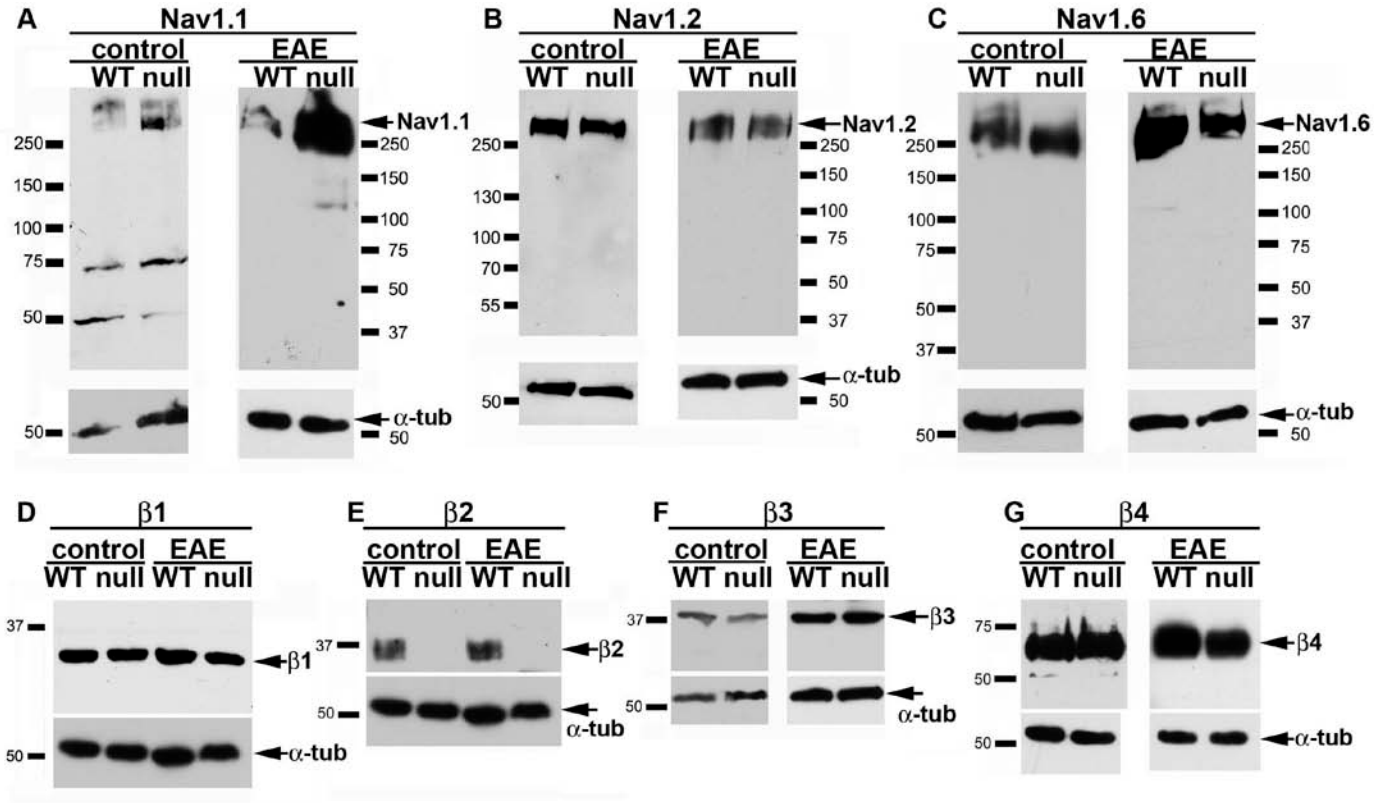
A
Nav1.1
control
EAE
WT null WT null
Nav1.1
α-tub
B
Nav1.2
control
EAE
WT null WT null
Nav1.2
α-tub
C
Nav1.6
control
EAE
WT null WT null
Nav1.6
α-tub
D
β1
control
EAE
WT null WT null
β1
α-tub
E
β2
control
EAE
WT null WT null
β2
α-tub
F
β3
control
EAE
WT null WT null
β3
α-tub
G
β4
control
EAE
WT null WT null
β4
α-tub

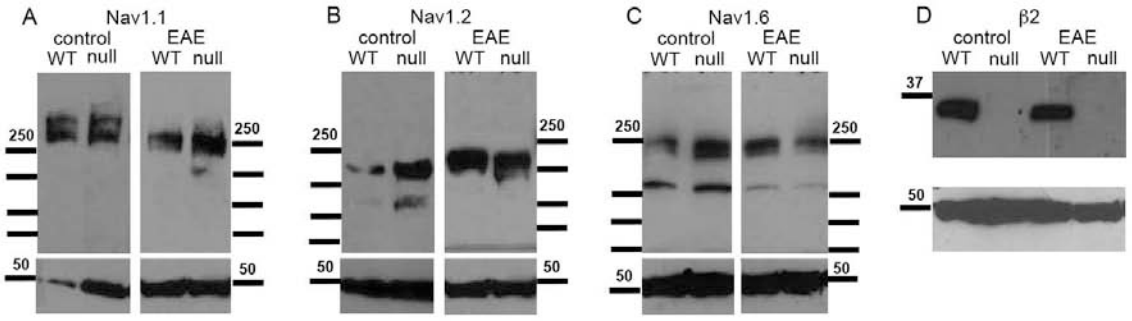

Figure 2.7: Expression levels of Na^+ channel α and β subunits in *Scn2b*$^{+/+}$ and *Scn2b*$^{-/-}$ spinal cord.

Western blots of mouse spinal cord homogenates were probed with antibodies to $Na_v1.1$, $Na_v1.2$, $Na_v1.6$, or $\beta2$. Blots were stripped and reprobed with anti-α-tubulin as a loading control and this signal is shown at ~50 kDa in the bottom gel section in each panel. **A**: Anti-$Na_v1.1$. **B**: Anti-$Na_v1.2$. **C**: Anti-$Na_v1.6$. **D**: $\beta2$ was absent in *Scn2b*$^{-/-}$ tissues. No difference in expression of $\beta2$ was observed in *Scn2b*$^{+/+}$ tissue under control conditions vs. EAE conditions.

Figure 2.8: Localization of Na+ channel α subunits in optic nerve.

Scn2b$^{+/+}$ and *Scn2b*$^{-/-}$ mice display alterations in localization of Na^+ channel α subunits after induction of EAE as compared to controls in longitudinal sections of optic nerve. (**A-D**) $Na_v1.1$ immunolocalization. **A, B**: *Scn2b*$^{+/+}$ (**A**) and *Scn2b*$^{-/-}$ (**B**) control optic nerves show an absence of $Na_v1.1$ at the nodal gap. **C, D**: *Scn2b*$^{+/+}$ (**C**) and *Scn2b*$^{-/-}$ (**D**) nerves after EAE induction display $Na_v1.1$ immunofluorescence along axons as well as at some nodes of Ranvier. Scale bar, 10μm. (**E-H**) $Na_v1.2$ immunolocalization. **E, F**: *Scn2b*$^{+/+}$ (**E**) and *Scn2b*$^{-/-}$ (**F**) control optic nerves do not express $Na_v1.2$. **G, H**: *Scn2b*$^{+/+}$ (**G**) and *Scn2b*$^{-/-}$ (**H**) optic nerves show diffuse immunofluorescence along demyelinated axons and at nodes. Scale bar, 20μm. (**I-L**) $Na_v1.6$ immunolocalization. **I, J**: *Scn2b*$^{+/+}$ (**I**) and *Scn2b*$^{-/-}$ (**J**) control optic nerves contain clustered $Na_v1.6$. **K, L**: *Scn2b*$^{+/+}$ (**K**) and *Scn2b*$^{-/-}$ (**L**) optic nerves after EAE induction display $Na_v1.6$ immunofluorescence at nodes of Ranvier as well as along demyelinated axons. Scale bar, 10μm.

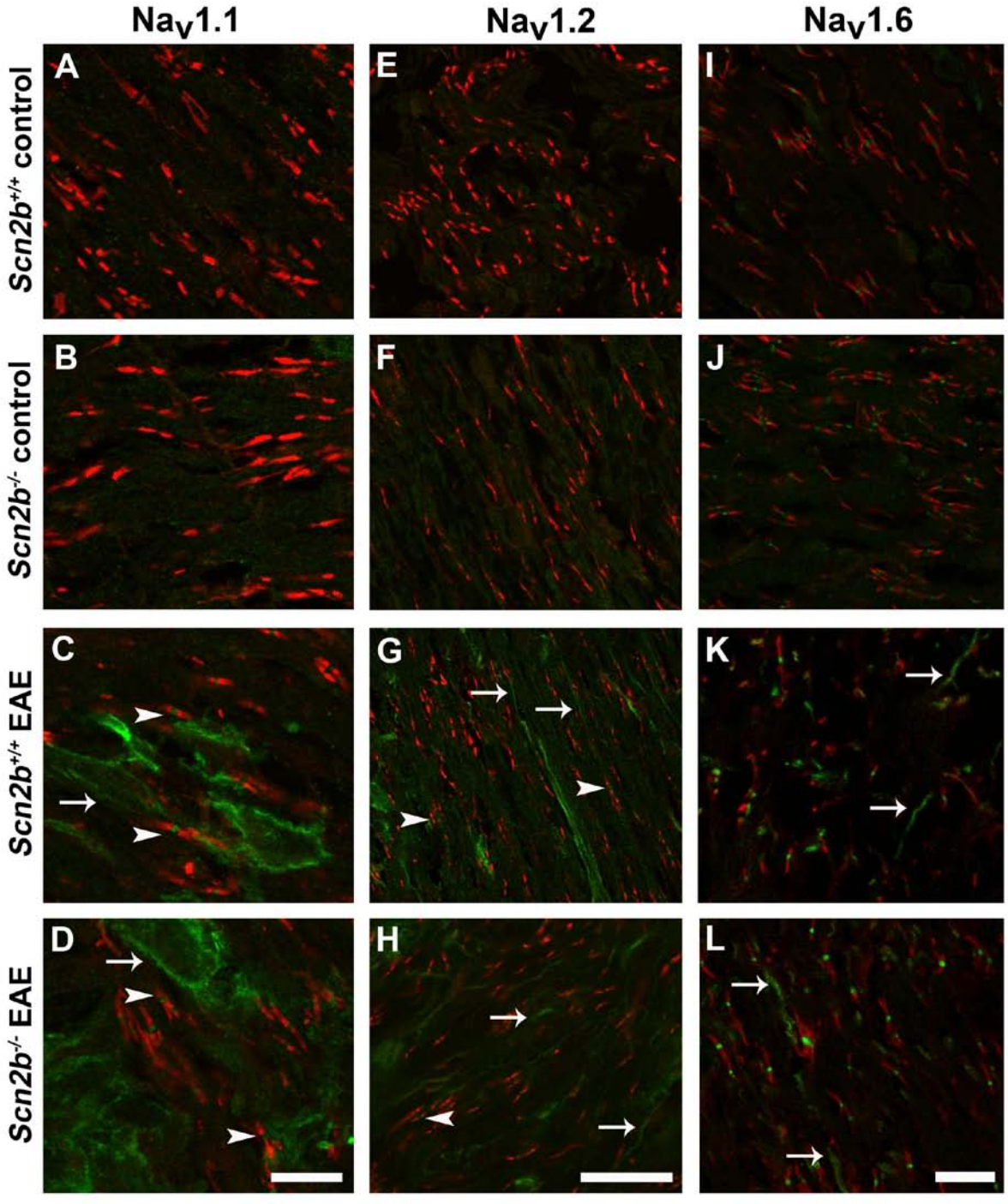
Na$_V$1.1
Na$_V$1.2
Na$_V$1.6
Scn2b$^{+/+}$ control
Scn2b$^{-/-}$ control
Scn2b$^{+/+}$ EAE
Scn2b$^{-/-}$ EAE
A
B
C
D
E
F
G
H
I
J
K
L

Figure 2.9: Localization of Na^+ channel α subunits in spinal cord.

Scn2b$^{+/+}$ and *Scn2b*$^{-/-}$ mice display alterations in localization of Na^+ channel α subunits after induction of EAE as compared to controls in longitudinal sections of spinal cord. (**A-D**) $Na_v1.1$ immunolocalization. **A, B**: *Scn2b*$^{+/+}$ (**A**) and *Scn2b*$^{-/-}$ (**B**) control spinal cords express $Na_v1.1$ at some nodes of Ranvier. **C, D**: *Scn2b*$^{+/+}$ (**C**) and *Scn2b*$^{-/-}$ (**D**) spinal cords after EAE induction display $Na_v1.1$ immunofluorescence along axons as well as at some nodes of Ranvier. Scale bar, 20μm. (**E-H**) $Na_v1.2$ immunolocalization. **E, F**: *Scn2b*$^{+/+}$ (**E**) and *Scn2b*$^{-/-}$ (**F**) control spinal cords express $Na_v1.2$ at some nodes of Ranvier. Scale bar, 10μm. **G, H**: *Scn2b*$^{+/+}$ (**G**) and *Scn2b*$^{-/-}$ (**H**) spinal cords show diffuse immunofluorescence along demyelinated axons and at nodes. Scale bar, 20μm. (**I-L**) $Na_v1.6$ immunolocalization. **I, J**: *Scn2b*$^{+/+}$ (**I**) and *Scn2b*$^{-/-}$ (**J**) control spinal cords contain clustered $Na_v1.6$. Scale bar, 20μm. **K, L**: *Scn2b*$^{+/+}$ (**K**) and *Scn2b*$^{-/-}$ (**L**) spinal cords after EAE induction display $Na_v1.6$ immunofluorescence at nodes of Ranvier as well as along demyelinated axons. Scale bar, 10μm.

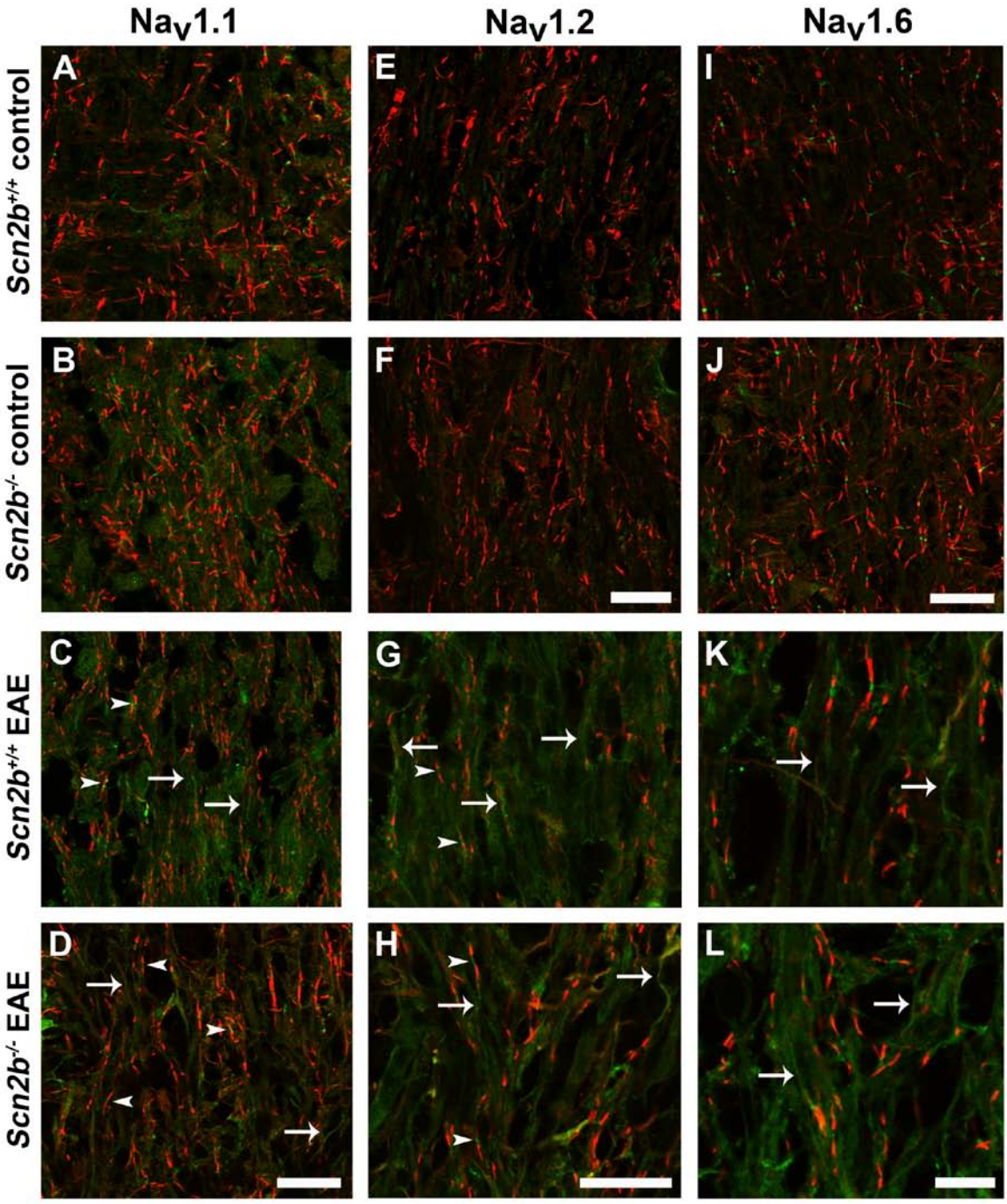
Na$_V$1.1
Na$_V$1.2
Na$_V$1.6
Scn2b$^{+/+}$ control
Scn2b$^{-/-}$ control
Scn2b$^{+/+}$ EAE
Scn2b$^{-/-}$ EAE
A
B
C
D
E
F
G
H
I
J
K
L

CHAPTER THREE

CHANGES IN SODIUM CHANNEL α AND β SUBUNIT SUBCELLULAR LOCALIZATION IN MULTIPLE SCLEROSIS BRAIN

SUMMARY

Multiple sclerosis (MS) is a dehabilitating neurological disease of the central nervous system (CNS) characterized by the presence of multiple lesions which consist of localized inflammation, demyelination, axonal degeneration and neuronal loss. MS is estimated to afflict upwards of 350,000 adults in the United States alone and over a million worldwide, with higher prevalence in residents of northern latitude regions. It is a primary cause of neurological disability in young adults, with diagnoses frequently made between the ages of 20 to 40.

Voltage-gated sodium channels are key mediators of electrical excitability and are responsible for the initiation and propagation of the action potential in excitable cells. Numerous studies have now examined the expression of pore-forming sodium channel α subunits in CNS tissue from MS patients, as well as related proteins such as the sodium-calcium exchanger and protein components

of the nodes of Ranvier such as the cell adhesion molecule Caspr. Demyelinated regions of axons in MS display diffuse localization of channels $Na_v1.2$ and $Na_v1.6$, and alterations in these channels are proposed to be adaptive changes aimed at overcoming conduction block, which have both functionally beneficial and detrimental roles, respectively. Ultimately, sodium influx into damaged axons mediated by these channels represents a critical step in the initiation of damaging injury cascades which lead to neurodegeneration.

In this study, we provide evidence for the localization of voltage-gated sodium β subunits in MS brain, as well as protein expression levels of the sodium channel α subunit $Na_v1.1$, a channel that has not been previously investigated in MS. We demonstrate that protein expression levels of $Na_v1.1$ are altered in MS patients compared with unafflicted patients, as well as between lesion and non-lesion brain regions in MS patients. Further, our results expand on previously published studies of β1 subunit expression in MS brain and provide the first demonstration of β2, β3, and β4 expression in normal and diseased brain tissues.

INTRODUCTION

Multiple sclerosis (MS) is an inflammatory demyelinating disease of the central nervous system (CNS) in which patients experience a variety of neurological

symptoms including optic neuritis, deficits in movement, pain, fatigue and cognitive deficits (Dutta and Trapp, 2007). The disease takes its name from the numerous lesions observed within all regions of the CNS, which consist of focal regions of demyelination, axonal loss and axonal damage, and inflammation (Ferguson et al., 1997; Bjartmar et al., 1999; Ludwin, 2006). Patients typically present with early symptoms between the ages of 20 to 40, and often suffer from a relapsing-remitting disease course in initial stages (Bjartmar et al., 1999). Most patients will, within 10 to 15 years of diagnosis, convert to a chronic, non-remitting disease course in which neurological symptoms no longer respond to therapies and deficits become more severe (Bjartmar et al., 1999; Courtney et al., 2009). It is estimated that two- to three-fold more women than men are afflicted with MS; however, males are more likely to suffer from more severe progressive forms of MS (Courtney et al., 2009; Goodin, 2009). Many current therapies attempt to address the immunological component of the disease, but these do not treat the other elements of disease pathology, namely, neurodegeneration and demyelination. It has been shown that development of non-remitting deficits is a result of axonal damage and degeneration ((Trapp et al., 1998), also reviewed in (Bechtold and Smith, 2005a; Waxman, 2006a)). In early stages of the disease, the nervous system is typically able to compensate for damage via mechanisms such as remyelination. As damage in the CNS accumulates, however, it is theorized that adaptive mechanisms gradually fail or are overwhelmed, and patients experience permanent neuronal loss (reviewed in (Bjartmar et al., 2003)).

Changes in expression and/or localization of voltage-gated sodium channels have been proposed to underlie processes of axonal degeneration in MS. Sodium channels, specifically the channel subtypes $Na_v1.2$ and $Na_v1.6$, both normally expressed in multiple subcellular domains of CNS neurons, have been observed by multiple groups to display diffuse expression along demyelinated regions of axons (Craner et al., 2003a; Craner et al., 2004a; Craner et al., 2004b; Coman et al., 2006; Herrero-Herranz et al., 2007). It has been hypothesized that this diffuse expression of $Na_v1.2$ may contribute to recovery from conduction block and that $Na_v1.6$, which displays a persistent sodium current component when expressed in heterologous systems (Smith et al., 1998; Burbidge et al., 2002), contributes to increases in intra-axonal sodium concentrations (reviewed in (Bechtold et al., 2004; Stys, 2005; Waxman, 2006a, b)). This ionic imbalance drives the sodium-calcium exchanger in reverse, leading to increases in calcium concentration within the axon and the subsequent activation of damaging downstream cascades which lead to degeneration of the axon (Stys et al., 1992a; Craner et al., 2004a; Craner et al., 2004b). We have previously generated a *Scn2b* null mouse in which the auxiliary β2 subunit is deleted, leading to a 40-50% decrease in the number of sodium channels at the neuronal plasma membrane (Chen et al., 2002; Lopez-Santiago et al., 2006a). We proposed that this reduction in cell surface channels in the null mice would result in neuroprotection in demyelinating disease. To test this hypothesis, we induced wildtype and null mice with a model of MS, Experimental Allergic

Encephalomyelitis (EAE) (O'Malley et al., 2009). *Scn2b* null mice displayed significant amelioration of clinical symptoms and decreased lethality, as well as decreases in axonal loss and degeneration and demyelination compared to their wildtype counterparts. In support of our hypothesis, wildtype mice displayed a significant increase in CNS $Na_v1.6$ expression in response to EAE, and this response was reduced in *Scn2b* mice (O'Malley et al., 2009). In contrast to the literature, neither genotype displayed changes in CNS $Na_v1.2$ expression in EAE, suggesting that the increased anti-$Na_v1.2$ immunofluorescence signal along demyelinated axons may have been due to redistribution of existing channels from other subcellular domains (O'Malley et al., 2009). Interestingly, we also found that *Scn2b* null mice showed unexpected increases in expression of $Na_v1.1$ in brain in response to EAE (O'Malley et al., 2009). This novel observation suggested that channels other than $Na_v1.2$ and $Na_v1.6$ may be important in the CNS response to demyelinating disease.

In this study, we investigated the expression of sodium channel α and β subunits in brain tissue from human MS patients and control patients. Extensive studies of the localization of $Na_v1.2$ and $Na_v1.6$ during demyelination in both MS and EAE have been published (Craner et al., 2003a; Craner et al., 2004a; Craner et al., 2004b; Coman et al., 2006; Herrero-Herranz et al., 2007; Herrero-Herranz et al., 2008). In contrast, expression and localization of the sodium channel β subunits in MS have not been addressed. Consequent to our previous mouse studies, we were also interested in investigating the localization and expression

of $Na_v1.1$. Here, we present an examination of sodium channel α and β subunits in MS brain, demonstrating expression of $Na_v1.1$ in grey matter, white matter and plaque regions in both control and MS brain and expression of β subunits in glia and at nodes of Ranvier.

RESULTS

Sodium channel subunit expression in grey matter

Classically, MS has been considered to be predominantly a white matter disease. Evidence has been accumulating to implicate grey matter in MS pathology to a greater extent than was once believed (reviewed in (Geurts and Barkhof, 2008)). Following our previous investigation of the role of *Scn2b* in EAE, we set out to investigate the expression of $Na_v1.1$ and β2 in human brain samples obtained from the UCLA Brain Bank, beginning with the analysis of normal appearing grey matter (NAGM). Our previous studies demonstrated aberrant localization of $Na_v1.1$ in EAE at nodes of Ranvier in sections of spinal cord and optic nerve from *Scn2b* wildtype and null mice, as assessed by immunofluorescence. Increases in $Na_v1.1$ polypeptide expression were also measured in *Scn2b* null brain lysates during EAE compared to wildtype (O'Malley et al., 2009). These previous protein expression experiments in mouse utilized whole brain and did not differentiate between protein expressed in white matter or grey matter. We aimed to

determine whether changes in $Na_v1.1$ expression occurred in white matter or grey matter from human MS brain compared to controls. To this end, we performed Western blot analysis of membrane preparations of NAGM from 3 control brains and 4 MS brains (**Figure 3.1**). In maintaining each brain sample as an individual homogenate, we were able to not only observe differences in expression between control and disease tissue but also to assess the amount of variability between individual brains within each category. We first probed with anti-$Na_v1.1$ in NAGM samples, then stripped and reprobed the membrane with anti-α-tubulin to provide a loading control (**Figure 3.1A**). As expected, in this Western blot as well as the others presented in this study, samples from individual brains displayed variations in protein expression levels. Overall, however, MS NAGM samples displayed strong expression of $Na_v1.1$, with similar expression levels in all samples examined. In comparison, while some variability was observed between samples, in general, we observed lower levels of $Na_v1.1$ expression in control samples of NAGM compared to MS samples (**Figure 3.1D**). A separate SDS-PAGE gel was used to measure levels of β2 expression in MS and control NAGM (**Figure 3.1C**). We observed that the human samples contained β2 immunoreactive peptides of multiple molecular weights, possibly suggesting differential glycosylation, and a subject for future investigation. In contrast to $Na_v1.1$, levels of β2 polypeptides were consistently low in all samples analyzed, with minor variability between brains in both MS and control groups. No overall differences in β2 protein levels were observed between control and MS NAGM. Inclusion of brain membranes in this experiment and subsequent

experiments from *Scn2b* wildtype and null mouse demonstrated specificity of the anti-β2 antibody.

Sodium channel subunit expression in white matter

In a second set of experiments, Western blotting was performed to examine channel protein expression in MS and control brain samples obtained from normal appearing white matter (NAWM) (**Figure 3.2**). **Figure 3.2A** demonstrates $Na_v1.1$ expression. A high amount of variability was observed between individual brain samples in these NAWM samples. Two of three samples obtained from control brains displayed low expression of $Na_v1.1$, while the third showed significantly higher $Na_v1.1$ expression. This sample, (#3406), was the same sample which showed higher expression levels of $Na_v1.1$ in NAGM (see **Figure 3.1A**). In samples from MS brain, two of four samples showed strong $Na_v1.1$ expression, while the other two samples had low levels of $Na_v1.1$, similar to controls. It is important to note that NAWM regions appear unaffected in standard histological tests such as Luxol fast blue staining, but may in fact contain regions of developing or past pathology. The observed differences in $Na_v1.1$ expression may reflect these unknown pathological changes. We also evaluated β2 subunit protein expression levels on the same SDS-PAGE gradient gel (**Figure 3.2B**). Similar to NAGM, anti-β2 immunoreactive polypeptides of multiple molecular weights were found to be expressed in all samples in both MS and control groups with no observed differences in β2 protein levels.

Sodium channel subunit expression in plaque regions in MS brain

We next performed Western blotting experiments to examine expression of $Na_v1.1$ and β2 in protein samples obtained from white matter brain blocks containing an MS lesion. It is important to note that these blocks also contained peri-lesion tissue as well as NAWM and thus were not solely composed of damaged tissue. In addition, the brain samples obtained for use in these experiments were taken from a mixed pool of chronic versus chronic-active lesion types, which may also account for some of the observed variation. A control aliquot of NAWM from one MS brain was included for purposes of comparison. We first analyzed $Na_v1.1$ expression in 5 homogenates from lesioned white matter (**Figure 3.3A**). Variability between individual samples was again observed, with some samples displaying high levels of $Na_v1.1$ expression as compared to low or moderate expression in others. The pattern of variation in these samples did not strictly correspond to relative expression levels of $Na_v1.1$ observed in MS NAWM (see **Figure 3.2A**, MS samples) or MS NAGM (see **Figure 3.1A**, MS samples), suggesting that molecular changes in MS brain are unique to the lesion area as compared to adjacent brain regions. We then probed the same membrane for β2 expression. Similar to observations in NAWM and NAGM, β2 was expressed at low levels in all samples, with no alterations in β2 expression observed between different lesion samples (**Figure 3.3B**). The anti-α-tubulin signals in this experiment (**Figure 3.3C**) demonstrate the difficulty of detecting sodium channel α and β subunits in human brain homogenates with

existing antibodies. Note that a much greater level of overall protein loading was required to visualize the human α and β subunits compared to mouse.

Sodium channel β subunit localization

After our examination of channel protein expression, we next wished to examine the localization of sodium channel β subunits in cryosections generated from control or MS NAWM and NAGM as well as MS lesion. Immunofluorescent imaging of sodium channel β subunits in MS tissue has not been previously reported.

In addition to the Western blot results for anti-β2 signal in *Scn2b* null brain, shown above, as well as our previously published Western blot showing the specificity of anti-β1 in *Scn1b* wildtype vs. null brain (Chen et al., 2007), we demonstrated the specificity of the anti-β1 and anti-β2 antibodies for immunofluorescence using *Scn1b* and *Scn2b* null optic nerve, respectively (**Figure 3.4**). Insets in each panel show individual nodes of Ranvier to clearly demonstrate the presence or absence of β subunit expression in the nodal gap. As *Scn3b* and *Scn4b* null animals are not available, similar studies could not be performed for anti-β3 and anti-β4; however, Western blot experiments in β subunit transfected vs. non-transfected HEK cells support the specificity of these antisera (Wong et al., 2005).

We attempted to perform immunostaining of human brain cryosections to examine the localization of $Na_v1.1$ in addition to the protein expression levels shown above. However, all of the commercially $Na_v1.1$ antibodies tested yielded inconsistent or non-specific results despite several modifications to the immunolabeling protocol (data not shown). To demonstrate that our protocol for immunofluorescence worked in human brain sections, in spite of the inconclusive results for anti-$Na_v1.1$, we performed dual immunolabeling in NAWM and NAGM sections with anti-pan-sodium channel antibody to mark nodes of Ranvier and anti-Caspr to mark paranodal regions of myelinated axons (**Figure 3.5**). As expected, sodium channel α subunits cluster at nodes of Ranvier in both NAGM (**Figure 3.5, A-C**) and NAWM (**Figure 3.5, D-F**). Thus, our immunolabeling protocol was appropriate for visualization of sodium channel α subunits in human brain. It is possible that the antigen to which these anti-$Na_v1.1$ antibodies were raised is accessible when the $Na_v1.1$ polypeptide is denatured for SDS-PAGE Western blotting, but that in its native form in human brain the epitope is not accessible to the antibody. Other laboratories in the field have obtained similar results with sodium channel antibodies (Dr. B. Trapp and Dr. S. Waxman, personal communication).

Sodium channel β1 localization in control and MS brain

We examined expression of the sodium channel β1 subunit in control and MS brain sections (**Figure 3.6**). As expected (Chen et al., 2004), we observed expression of β1 in a subset of nodes of Ranvier in control brain in both white and grey matter, indicated as anti-β1 labeling in the node surrounded by anti-Caspr labeling in the paranodal regions (shown in insets in **Figure 3.6C** and **Figure 3.6I**). We also observed anti-β1 immunoreactivity in glial cells in control NAGM sections (**Figure 3.6, A-C**). β1 immunoreactivity was reported previously in MS brain tissue (Aronica et al., 2003). Consistent with this, we observed glial expression of β1 in NAGM from MS brain, with β1 expressed diffusely along the slender glial processes (**Figure 3.6, D-F**). In control NAWM sections, glial expression of β1 was observed at high levels along glial processes as well as at nodes of Ranvier (**Figure 3.6, G-I**). NAWM regions of MS brain also displayed glial β1 immunoreactivity (**Figure 3.6, J-L**). Finally, in sections from MS brain containing a demyelinated lesion, β1 expression adopted a more diffuse pattern of expression which appeared coincident with staining of anti-acetylated α-tubulin along axons (**Figure 3.6, M-O**). These data suggest that expression of β1 in demyelinated regions follows the diffuse localization of sodium channels along axons, observed in previous studies in MS lesions (Craner et al., 2003a; Craner et al., 2004a; Craner et al., 2004b; Coman et al., 2006; Herrero-Herranz et al., 2008), as well as being expressed in glia.

Sodium channel β2 localization in control and MS brain

We performed immunohistochemical experiments to examine the expression of β2 subunits in both MS and control brain (**Figure 3.7**). Our previous Western blotting experiments did not demonstrate significant changes in β2 protein expression when comparing these samples (see **Figure 3.1C**, **Figure 3.2B** and **Figure 3.3B**). However, we were interested to determine whether changes in β2 localization might occur in MS vs. control sections. Control NAGM showed strong expression of β2 in cells located irregularly throughout the section which morphologically resembled stellate astrocytes (**Figure 3.7, A-C**). Glial expression of β2 was again observed in MS NAGM sections (**Figure 3.7, D-F**). Anti-β2 signal was also detected in diffuse patterns in addition to the glial cell-specific expression in MS NAGM. In control NAWM sections, the numbers of glial cells expressing β2 decreased as compared to control NAGM and β2 expression appeared to be restricted to small punctate regions on axons throughout the section that were likely nodes of Ranvier, consistent with our previous reports in mouse brain (Chen et al., 2002; O'Malley et al., 2009) (**Figure 3.7, G-I**, also see inset in **Figure 3.7G**). This pattern was similar in MS NAWM regions (**Figure 3.7, J-L**). However, in these sections β2 was also observed in short, irregular process-like regions of expression that did not coincide with axonal labeling with anti-acetylated α-tubulin and may have represented glial processes. Finally, in sections containing a demyelinated lesion, β2 was observed to be expressed in extended segments that were co-labeled with anti-acetylated α-tubulin. These regions likely indicated demyelinated axons,

consistent with previously observed sodium channel α subunit localization (Craner et al., 2003a; Craner et al., 2004b; Coman et al., 2006; Herrero-Herranz et al., 2007). We also observed segments of anti-β2 labeling that were not α-tubulin-positive, resembling glial processes (**Figure 3.7, M-O**).

In summary, in normal tissue β1 and β2 subunits are expressed at nodes of Ranvier along myelinated axons and in glia, likely astrocytes. In MS tissue, β1 and β2 subunits are expressed in glia and along demyelinated axons.

Sodium channel β3 localization in control and MS brain

The localization of β3 subunits in human brain appears to be very different from that of β1 or β2, although a caveat is our lack of a *Scn3b* null mouse in which to test the specificity of the antibody for immunofluorescence. **Figure 3.8** shows immunofluorescent detection of β3 localization in MS and control brain sections. Detection of β3 was performed concurrently with an antibody against glial fibrillary acidic protein (GFAP), to label astrocytes, or alternately with an antibody against acetylated α-tubulin, to identify axons. Control NAGM displayed intense β3 immunostaining in nuclei, coincident with DAPI staining (**Figure 3.8, A-C**). β3 signal was not detected in other regions within these cells nor in astrocytes. In MS NAGM, β3 expression was again high in nuclei. β3 was also detected in processes in a subset of glial cells in these NAGM sections (**Figure 3.8, D-F**). In control NAWM, similar to control NAGM, β3 was observed only in nuclei and was

not detected in axons (**Figure 3.8, G-I**). In NAWM from MS brain, β3 expression was detected at high levels in nuclei and, similarly to MS NAGM, in the processes of a subset of glial cells (**Figure 3.8, J-L**). Finally, in regions of MS white matter sections containing a lesion, in addition to high levels of nuclear expression, β3 is expressed in processes of glial cells within the demyelinated lesion (**Figure 3.8, M-O**). In order to aid in the identification of these anti-β3-positive glial cells, we performed double immunolabeling with anti-β3 and anti-GFAP (**Figure 3.8, P-Q**). We concluded that these β3-positive glial cells were GFAP-positive astrocytes. In contrast, we demonstrated using double labeling that GFAP-positive astrocytes in control NAWM and control NAGM sections did not express β3 (higher magnification of merged image from **Figure 3.8, D-F** presented in **Figure 3.8P**). These results suggest that astrocytes in NAGM from MS patients may be activated, compared to control patients, and that this process involves β3 expression.

Sodium channel β4 localization in control and MS brain

In our final set of experiments we performed immunostaining of control and MS brain sections using anti-β4 antibody with double labeling for the axonal marker acetylated α-tubulin (**Figure 3.9**). Similar to β3, a potential caveat in these experiments is the non-availability of a *Scn4b* null mouse to test antibody specificity. In control NAGM, β4 expression was observed in small punctate regions throughout the section (**Figure 3.9, A-C**). It is possible that these puncta represent β4 expression at nodes of Ranvier, although the size of the puncta

appear to be large compared to the size of nodal sodium channel clusters observed in previous sections. Nodal expression of β4 has not been well-examined, and future experiments should use markers such as Caspr to delineate the nodal region in order to investigate this question in greater detail. Unexpectedly, β4 expression was also observed in irregular regions of intense staining (**Figure 3.9, A-C**). These regions were non-uniform in appearance and were typically broad and long in dimensions. We hypothesized that these regions might be elements of the brain vasculature. Other immunostained sections supported this notion when β4 expression was seen clearly in cross-sectioned blood vessels and/or capillaries (**Figure 3.9, P-Q**). The striated pattern of labeling suggests that β4 is expressed within the vascular smooth muscle. Expression of other β subunits in vasculature was not observed and was a pattern unique to the β4 subunit. In MS NAGM, β4 exhibited the same vascular pattern of expression with other small punctate staining throughout the section (**Figure 3.9, D-F**). Control NAWM (**Figure 3.9, G-I**) and MS NAWM (**Figure 3.9, J-L**) displayed a pattern of β4 expression which was also at high levels within the vasculature as well as exhibiting small regions of punctate subunit expression in all regions of the section. In tissue obtained from sections containing a demyelinated lesion, β4 expression was again observed in the vasculature (**Figure 3.9, M-O**). This region also showed a general increase in regions of linear, extended β4 signal which was not coincident with axonal acetylated α-tubulin and may represent capillary labeling.

DISCUSSION

In this study we have presented evidence for the expression of $Na_v1.1$ and β2 sodium channel subunit polypeptides in NAGM and NAWM in both control and MS brain as well as in MS lesion. In addition, we demonstrated the localization of the sodium channel β1, β2, β3 and β4 subunits in these regions of control and MS brain. Precise localization of specific sodium channel gene products to certain subcellular subdomains is critical for the maintenance of normal excitability. During pathology, alterations in channel expression can represent either adaptive changes to allow for recovery from injury, or changes occurring as downstream effects of insult which are themselves elements of pathology.

We previously demonstrated that *Scn2b* null mice have increased expression of $Na_v1.1$ polypeptides in whole brain homogenates in the EAE mouse model of MS (O'Malley et al., 2009). Both *Scn2b* null and wildtype mice exhibited aberrant expression of $Na_v1.1$ in a subset of CNS nodes of Ranvier and along demyelinated axons following the induction of EAE. Thus, even though increases in $Na_v1.1$ protein expression levels were detected biochemically only in *Scn2b* null mice, both wildtype and null genotypes displayed changes in $Na_v1.1$ localization in disease, implicating $Na_v1.1$ as an interesting new candidate for demyelinating channelopathies. In the present study, we examined the expression of $Na_v1.1$ protein by Western blot in NAGM, NAWM and lesioned human brain. In NAGM, $Na_v1.1$ may be expressed at higher levels in MS

samples compared to controls. We propose that increased channel expression may be an early indicator of pathology in these "normal appearing" regions of gray matter obtained from MS patients.

We examined the specific localization of sodium channel β subunits in MS versus control brain. In addition to the expected localization at nodes of Ranvier, anti-β1 exhibited strong labeling of glial cells in both disease and control patients. This pattern of expression was observed in both NAGM and NAWM. In demyelinated lesions, β1 was also observed along axons coincident with acetylated α-tubulin, consistent with previously reported labeling for sodium channel α subunits along demyelinated axons in MS. The glial cells in which β1 was expressed displayed astrocytic morphology. This is consistent with previous studies demonstrating upregulation of β1 protein in diseases which include reactive gliosis, including MS and amyotrophic lateral sclerosis (Aronica et al., 2003) as well as expression of *Scn1b* mRNA in cultured astrocytes (Oh and Waxman, 1994). These data suggest that β1 subunit expression in astrocytes in disease may be a pattern repeated throughout a variety of neurodegenerative diseases. A caveat to this is that we observed glial β1 expression in control tissue as well as in diseased tissue. Further study of β1 protein expression levels as well as the prevalence and specific distribution of these β1-expressing astrocytes in normal versus diseased brain is needed to determine specific changes in the disease state.

In the investigation of β2 localization in brain, glial expression was again observed in NAGM from control and MS brain. MS NAGM displayed slight increases in β2 immunofluorescence compared with controls. Our Western blot experiments did not show changes in β2 expression in NAGM between control and MS brain. However, due to the small contribution that astrocytes expressing β2 would make to brain homogenates, we are not able to make conclusions about changes in astrocytic β2 protein expression in human brain. In control and MS NAWM, anti-β2 labeling displayed an axonal pattern, with β2 expression restricted primarily to clusters at putative nodes of Ranvier. Interestingly, in MS NAWM anti-β2 signal was also frequently detected in short non-axonal processes, suggesting that β2 expression in glia in diseased NAWM may be increased over controls. Finally, β2 expression in demyelinated lesions was observed coincident with axonal staining, similar to β1 in this region. These data suggest, as expected, that sodium channel α, β1 and β2 subunits are diffusely distributed as a heterotrimeric complex along demyelinated axons in MS.

Our results showing immunolocalization of β3 supports the hypothesis that β subunit expression in glial cells, specifically astrocytes, may play a role in MS disease pathology or progression. Control brain sections displayed anti-β3 labeling only in nuclei, which must be investigated further to determine its specificity. The anti-β3 antibody used in this study was raised against a C-terminal peptide from mouse β3 (sequence IPSENKENSVVPVEE) and shares 14/15 residue identity with the human β3 sequence (Wong et al., 2005).

In MS brain, anti-β3 labeling was consistently observed in a subset of GFAP-positive astrocytes. This was observed as well in lesioned brain. Unlike β1, β3 does not participate in *trans* homophilic cell-cell adhesion (McEwen et al., 2009). β1, but not β3, is expressed in cancer cells where it modulates cell adhesion and migration (Chioni et al., 2009). In contrast, *Scn3b*, unlike *Scn1b*, is up-regulated in response to DNA damage and mediates a p53-dependent apoptotic pathway (Adachi et al., 2004). Thus, these two VGSC β subunits may play very different physiological and pathophysiological roles *in vivo*, specifically, in reactive astrocytes in MS.

Finally, we examined control and MS brain to determine the pattern of β4 localization. No differences were observed between diseased and non-diseased tissue. Interestingly, in contrast to the other β subunits, β4 expression was only weakly detected in neurons and instead was detected at high levels in the brain vasculature in all sections examined. This is in contrast to previous labeling of rat brain tissue with another anti-β4 antibody which demonstrated immunopositive brain neurons (Yu, 2003). Both this antibody and our antibody appear to be specific using β4-transfected fibroblasts. The antibody used in this study was raised against the C-terminal region of β4 (sequence GLPGSKAEEKPPTKV, which is identical with human β4 in 14/15 amino acids (Wong et al., 2005)), whereas the antibody used in the study by Yu et al. was raised against an N-

terminal sequence spanning amino acid residues 51-67 (Yu et al., 2003). Further investigations must be performed in the future comparing multiple anti-β4 antibodies and eventually testing *Scn4b* null mice.

Our observations in this study have provided new evidence demonstrating the expression of sodium channel β subunits in astrocytes in both normal and MS brain. In addition, we provide novel results opening the possibility of β4 subunit expression in brain vasculature. Our immunofluorescence results support the hypothesis derived from previous mouse and rat data that sodium channels are expressed during the early stages of oligodendrocyte precursor cell (OPC) development but are not expressed in mature, myelinating oligodendrocytes (OLs) (Sontheimer et al., 1989; Karadottir et al., 2008). In cultured OPCs, we observed expression of β subunits at the A2B5-positive and A007-positive stages of differentiation (**Chapter 4**). In contrast, in adult human tissue, shown in this chapter, β subunits were observed in astrocytes but were not detected in mature OLs or in the myelin sheath. OPCs have been shown to express sodium currents in during the early A2B5-positive stage, however, this current decreases to undetectable levels at later stages of differentiation (Sontheimer et al., 1989; Karadottir et al., 2008). These results are consistent with data presented in this chapter showing the lack of sodium channel β subunit immunoreactivity in the myelin sheath and in surrounding OL cell bodies in adult human brain sections. In contrast, we did observe expression of β subunits in GFAP-positive astrocytes in both control and diseased adult human brain. Astrocytes express multiple

forms of ionic current, including voltage-gated sodium current (Barres et al., 1990a; Sontheimer, 1994; Barres, 2008) and make contact with the neuronal axolemma at nodes of Ranvier (Butt et al., 1999). Expression of β subunits in adult astrocytes is thus consistent with their known functions in channel modulation and cell adhesion. In conclusion, sodium channel β subunits are expressed in both neurons and glia in the CNS and their cellular localization changes in demyelinating disease. In addition, sodium channel β subunit expression in glia may be regulated by both development and pathophysiology.

EXPERIMENTAL METHODS

Sample preparation: Fresh-frozen brain specimens from 10 female control and 9 female MS patients were obtained from the Human Brain and Spinal Fluid Resource Centre, VA West Los Angeles Healthcare Centre, Los Angeles, CA 90073 which is sponsored by NINDS/NIMH, National Multiple Sclerosis Society, and Department of Veterans Affairs. Control patients had not been diagnosed with any neurological disease. Details of each specimen obtained, including patient age at death, patient diagnosis, and time post-mortem before tissue autopsy are provided in **Table 1**. Blocks provided were classified as NAGM or NAWM (for control), or plaque, adjacent NAWM, and nearest NAGM (for MS brain). Blocks of brain were stored at -80°C until use. For immunofluorescence,

blocks were removed directly onto a cryostat without fixation or cryopreservation. 10-20 μm cryosections were generated and stored at -20°C until used for immunostaining. For Western blotting, membrane preparations were obtained as previously described (Isom et al., 1995a; O'Malley et al., 2009).

Immunofluorescent staining and microscopy: 10-20 μm brain sections were fixed for no longer than 10 min with 1% paraformaldehyde, washed 3 times in 0.05 M phosphate buffer (PB), and blocked for a minimum of 1 h in PBTGS (0.1M PB, 0.3% Triton X-100, 10% normal goat serum). Sections were incubated at RT overnight in primary antibody diluted in PBTGS, followed by incubation for 2 h in goat anti-mouse or anti-rabbit secondary antibody as appropriate, coupled to either Alexa 488 (green) or Alexa 594 (red) (Molecular Probes, Carlsbad, CA) and diluted in PBTGS. Sections were washed three times with 0.1 M PB after each antibody step. Sections were air-dried and coverslipped using GelMount anti-fade mounting medium (Biomeda, Foster City, CA). Digital images were collected using an Olympus FluoView 500 confocal microscope with FluoView software located in the Department of Pharmacology, University of Michigan.

Western blot: Western blots were performed with brain membrane preparations as described previously (Malhotra et al., 2000b; Malhotra et al., 2004; O'Malley et al., 2009) and as modified below to detect Na^+ channel α and β subunit polypeptides. Briefly, samples were solubilized in SDS-PAGE sample buffer

containing 1% SDS and 500 mM β-mercaptoethanol, heated for 5-10 min at 85°C, and separated on a 4-15% acrylamide SDS-PAGE gradient gel (Bio-Rad, Hercules, CA) for detection. Proteins were transferred to nitrocellulose and blocked for a minimum of 15 minutes with block solution (0.5% non-fat dry milk and 0.1% bovine serum albumin in 1x TBS-T). The membrane was then probed with specific primary antibodies against Na^+ channel α or β subunits followed by secondary anti-mouse or anti-rabbit antibodies as appropriate conjugated to horseradish peroxidase. The membrane was washed three times in 1x TBS-T following each antibody step. All blocking, washing, and antibody incubation steps were performed using the SNAP i.d. Western blot system (Millipore, Billerica, MA). Proteins were visualized using the West Dura or West Femto enhanced chemiluminescence detection system (Pierce, Rockford, IL). Some sections of the membrane were stripped with ReBlot Plus Antibody Stripping Solution (Chemicon, Temecula, CA) according to manufacturer's instructions, washed 2 times in Western block solution, and subsequently re-incubated with a different primary antibody against α-tubulin as a loading control or against a second Na^+ channel α subunit, then protein detection was completed as described above. For quantification of Western blots, densitometric analysis of bands was performed using NIH ImageJ software. Band density was normalized to α-tubulin signal for comparison.

Antibodies: Primary antibodies for Western blotting and immunocytochemistry were used as follows: rabbit anti-β1 (1:300, Western blotting or 1:250,

immunofluorescence, obtained from Dr. N. Nukina (Wong et al., 2005)), rabbit anti-β2 (1:500, Western blotting or 1:250, immunofluorescence, obtained from Dr. N. Nukina (Wong et al., 2005)), rabbit anti-β3 (1:500, Western blotting or 1:500, immunofluorescence, obtained from Dr. N. Nukina (Wong et al., 2005)), rabbit anti-β4 (1:500, Western blotting or 1:500, obtained from Dr. N. Nukina (Wong et al., 2005)), mouse anti-$Na_v1.1$ (1:250, NeuroMab, Davis, CA), mouse anti-$Na_v1.2$ (1:250, NeuroMab, Davis, CA), mouse anti-$Na_v1.6$ (1:250, NeuroMab, Davis, CA or 1:250, Sigma-Aldrich), mouse or rabbit anti-pan-Na^+ channel (1:250, Sigma-Aldrich), and mouse anti-α-tubulin (1:5000, Cedarlane Laboratories, Hornby, ON), anti-Caspr (rabbit, 1:500, a gift from Dr. E. Peles), mouse anti-GFAP (1:500, Molecular Probes) and mouse anti-acetylated α-tubulin (1:1000, Sigma-Aldrich).

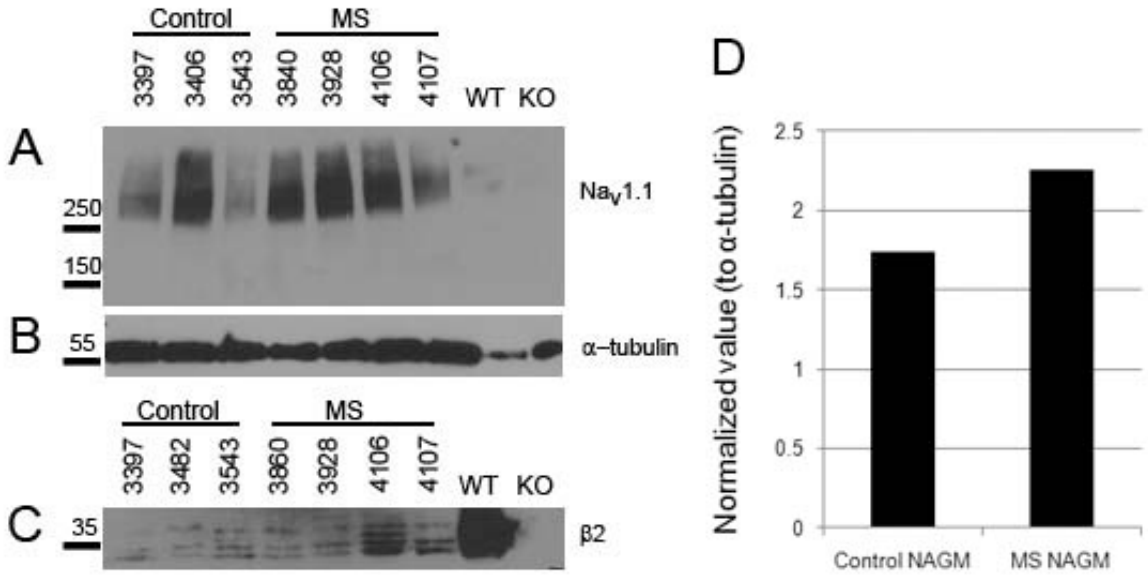

Figure 3.1: Expression of $Na_v1.1$ and β2 in NAGM.

Western blots of brain homogenate from NAGM obtained from MS and control brains were probed with antibodies against $Na_v1.1$ or β2. The membrane probed for $Na_v1.1$ was stripped and reprobed with anti α-tubulin (as a loading control).

(A) Anti-$Na_v1.1$. (B) Anti-α-tubulin. (C) Anti-β2. (D) Quantification of anti-$Na_v1.1$ immunoreactive bands in panel A.

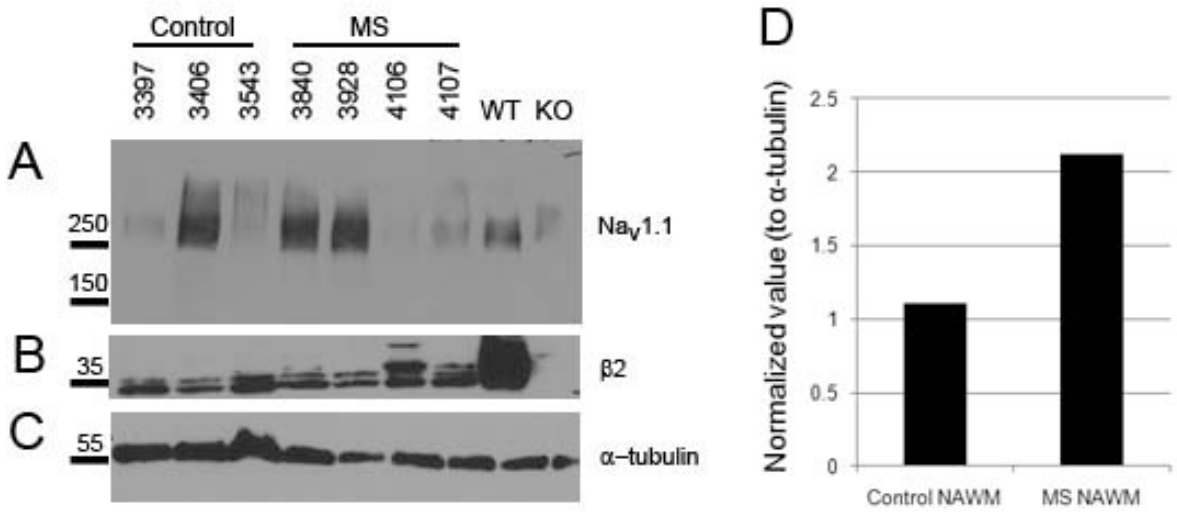

<u>Figure 3.2</u>: Expression of $Na_v1.1$ and β2 in NAWM.

Western blots of brain homogenate from NAWM obtained from MS and control brains were probed with antibodies against $Na_v1.1$ or β2. Blots were then stripped and reprobed with anti α-tubulin (as a loading control).

(A) Anti-$Na_v1.1$. (B) Anti-β2. (C) Anti-α-tubulin. (D) Quantification of anti-$Na_v1.1$ immunoreactive bands in panel A.

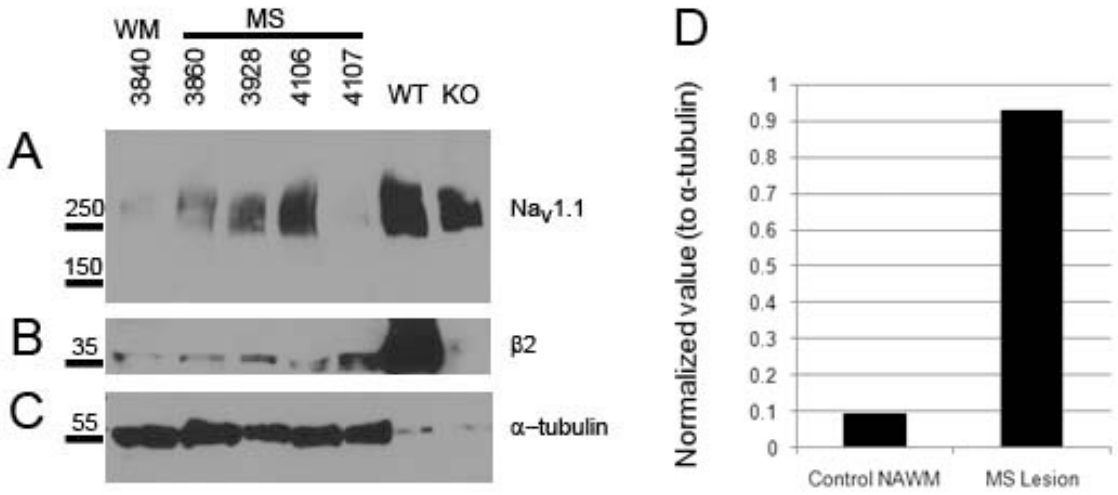

Figure 3.3: Expression of Na$_v$1.1 and β2 in MS lesion.

Western blots of brain homogenate from white matter brain blocks containing lesions were probed with antibodies against Na$_v$1.1 or β2. An aliquot of MS NAWM was included for purposes of comparison. Blots were then stripped and reprobed with anti α-tubulin (as a loading control).

(A) Anti-Na$_v$1.1. (B) Anti-β2. (C) Anti-α-tubulin. (D) Quantification of anti-Na$_v$1.1 immunoreactive bands in panel A.

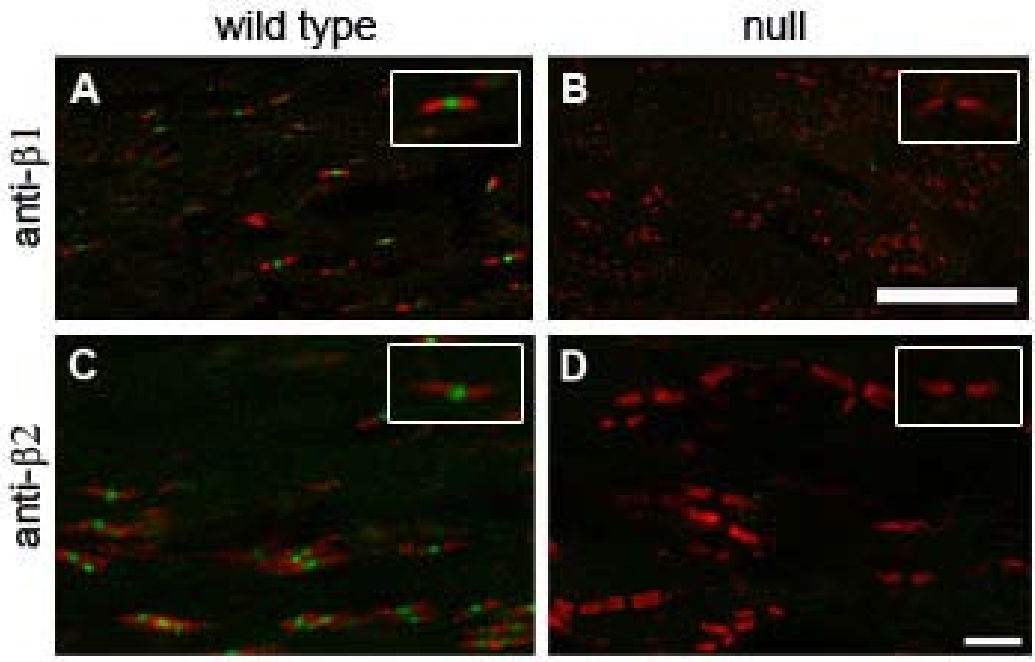

Figure 3.4: Specificity of anti-β1 and anti-β2 antibodies.

Anti-β1 and anti-β2 antibodies specifically recognize β1 and β2, respectively, in optic nerve cryosections. **A, B**: Anti-β1. Anti-β1 antibody (green) detects β1 protein at nodes of Ranvier in wildtype optic nerve (**A**) while optic nerve from *Scn1b* null mice (**B**) shows an absence of β1 immunoreactivity. Paranodes are marked by anti-Caspr. Scale bar = 20 μm. **C, D**: Anti-β2. Anti-β2 antibody (green) shows specific expression of β2 protein at nodes of Ranvier in wildtype optic nerve (**C**), while nodes of Ranvier in optic nerve from *Scn2b* null mice (**D**) are devoid of β2 immunoreactivity. Paranodes are marked by anti-Caspr (red). Scale bar = 10 μm.

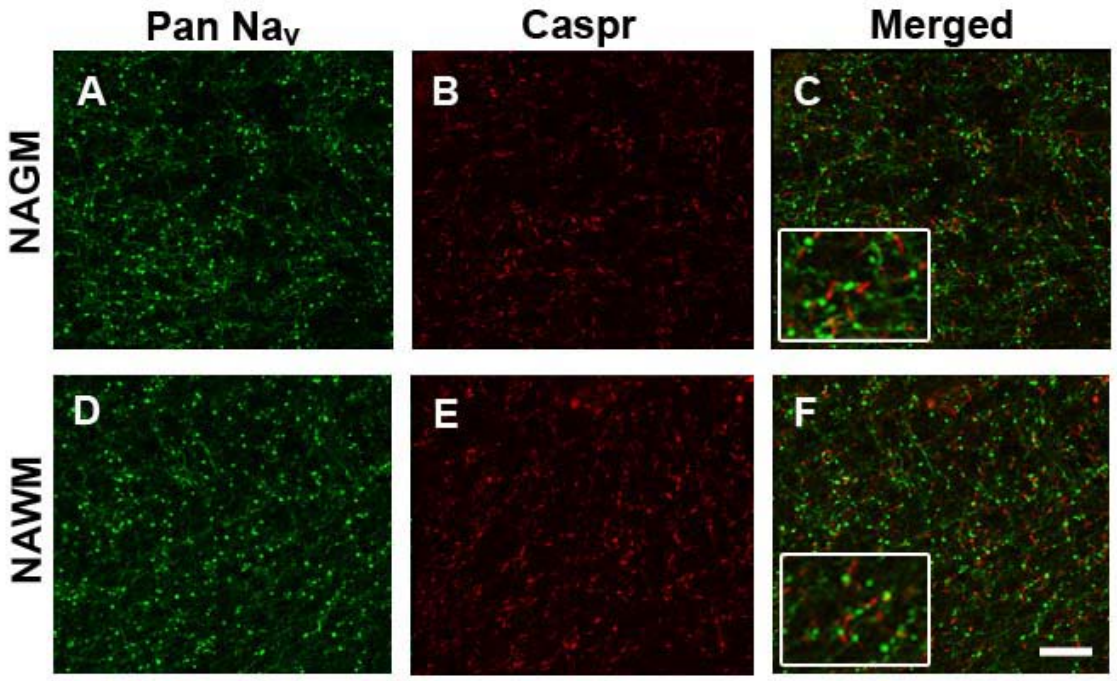

<u>Figure 3.5</u>: Expression of sodium channel α subunits at nodes of Ranvier in control human brain.

A-C: Sodium channels are expressed at nodes of Ranvier in NAGM. (**A**) anti-pan-sodium channel, (**B**) anti-Caspr, (**C**) merged. **D-F**: Sodium channels are expressed at nodes of Ranvier in NAWM. (**D**) anti-pan-sodium channel, (**E**) anti-Caspr, (**F**) merged. Scale bar = 20 μm.

Figure 3.6: β1 expression in control and MS brain.

β1 is expressed in glial cells in both control and MS brain as well as along axons in demyelinated lesions in MS brain. **A-C**: Control NAGM. (**A**): anti-β1, (**B**) anti-Caspr, (**C**) merged. Inset shows a single node of Ranvier displaying β1 immunoreactivity. **D-F**: MS NAGM. (**D**): anti-β1, (**E**) anti-Caspr, (**F**) merged. **G-I**: control NAWM. (**G**): anti-β1, (**H**) anti-Caspr, (**I**) merged. Inset shows a single node of Ranvier displaying β1 immunoreactivity. **J-L**: MS NAWM. (**J**): anti-β1, (**K**): anti-Caspr, (**L**): merged. **M-O**: MS lesion. (**M**): anti-β1, (**N**): anti- acetylated α-tubulin, (**O**): merged.

Scale bar, panels M-O = 50μm. Scale bar, all other panels = 100 μm.

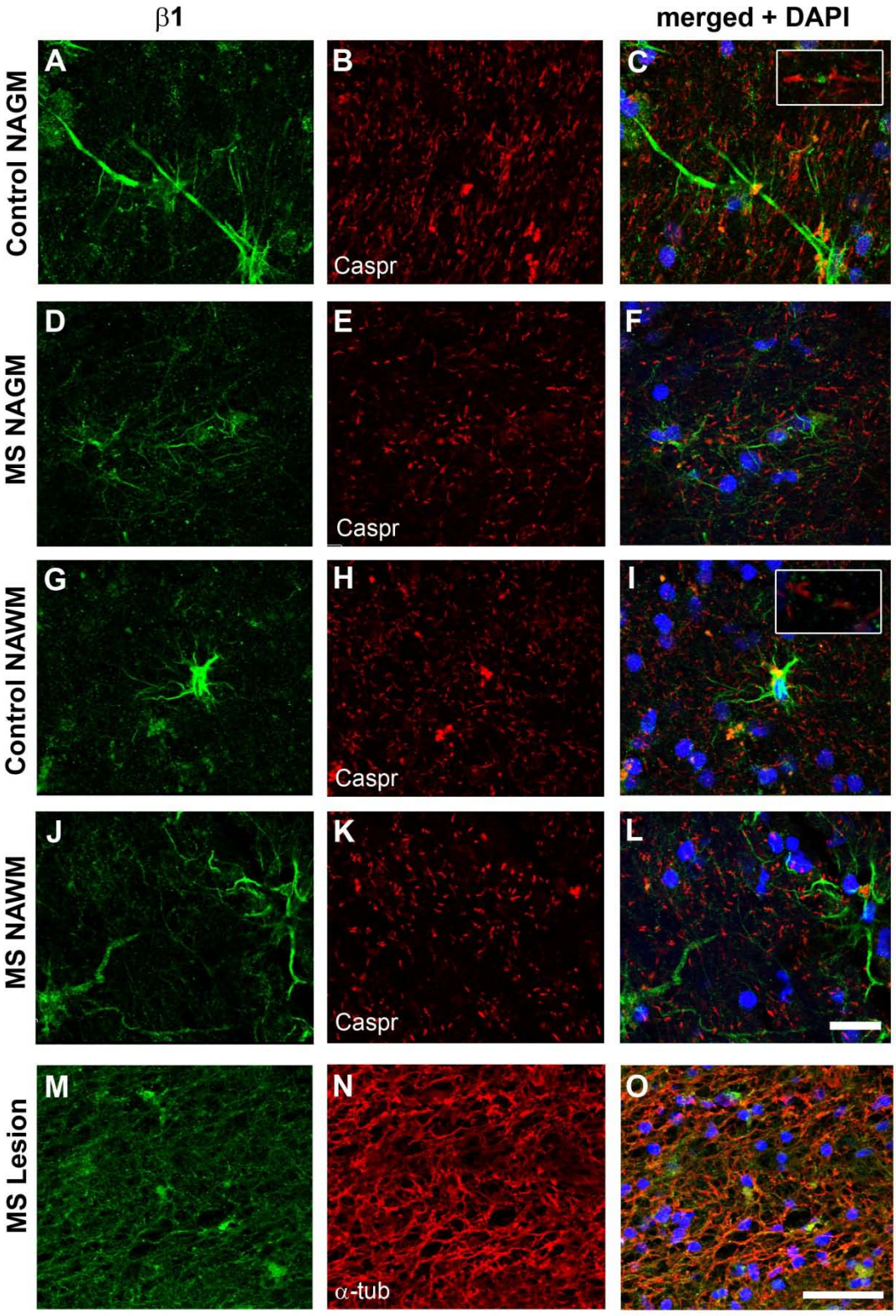
β1
merged + DAPI
Control NAGM
MS NAGM
Control NAWM
MS NAWM
MS Lesion
A
B
C
D
E
F
G
H
I
J
K
L
M
N
O
Caspr
Caspr
Caspr
Caspr
α-tub

Figure 3.7: β2 expression in control and MS brain.

β2 is expressed in glial cells in both control and MS brain. **A-C**: Control NAGM. (**A**): anti-β2, (**B**) anti-Caspr, (**C**) merged. **D-F**: MS NAGM. (**D**): anti-β2, (**E**) anti-Caspr, (**F**) merged. **G-I**: Control NAWM. (**G**): anti-β2, (**H**) anti- acetylated α-tubulin, (**I**) merged. **J-L**: MS NAWM. (**J**): anti-β2, (**K**): anti-acetylated α-tubulin, (**L**): merged. **M-O**: MS lesion. (**M**): anti-β2, (**N**): anti-acetylated α-tubulin, (**O**): merged.

Scale bar = 50 μm.

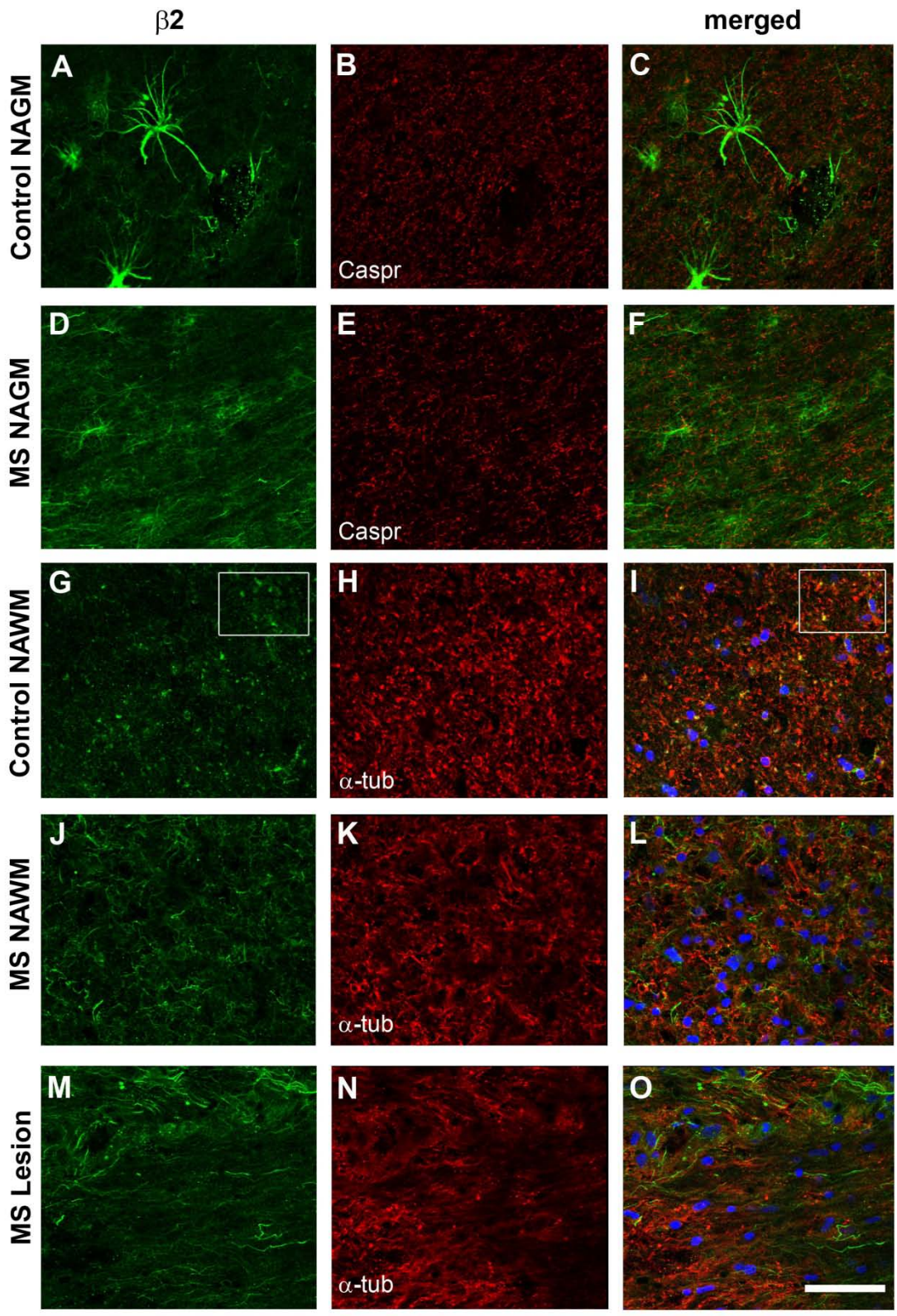
β2
merged
Control NAGM
MS NAGM
Control NAWM
MS NAWM
MS Lesion
A
B
C
D
E
F
G
H
I
J
K
L
M
N
O
Caspr
Caspr
α-tub
α-tub
α-tub

Figure 3.8: β3 expression in control and MS brain.

β3 is expressed at high levels in nuclei as well as in glial cells in MS brain but no control brain. **A-C**: Control NAGM. (**A**): anti-β3, (**B**) anti-GFAP, (**C**) merged. **D-F**: MS NAGM. (**D**): anti-β3, (**E**) anti-GFAP, (**F**) merged. **G-I**: Control NAWM. (**G**): anti-β3, (**H**) anti- acetylated α-tubulin, (**I**) merged. **J-L**: MS NAWM. (**J**): anti-β3, (**K**): anti-GFAP, (**L**): merged. **M-O**: MS lesion. (**M**): anti-β3, (**N**): anti-GFAP, (**O**): merged. **P, Q:** Specific expression of β3 in GFAP-positive cells in MS brain (**Q**) but not control brain (**P**). Anti-β3 (green), anti-GFAP (red).

Scale bar, panels A-P = 50 μm. Scale bar, panel Q = 20 μm.

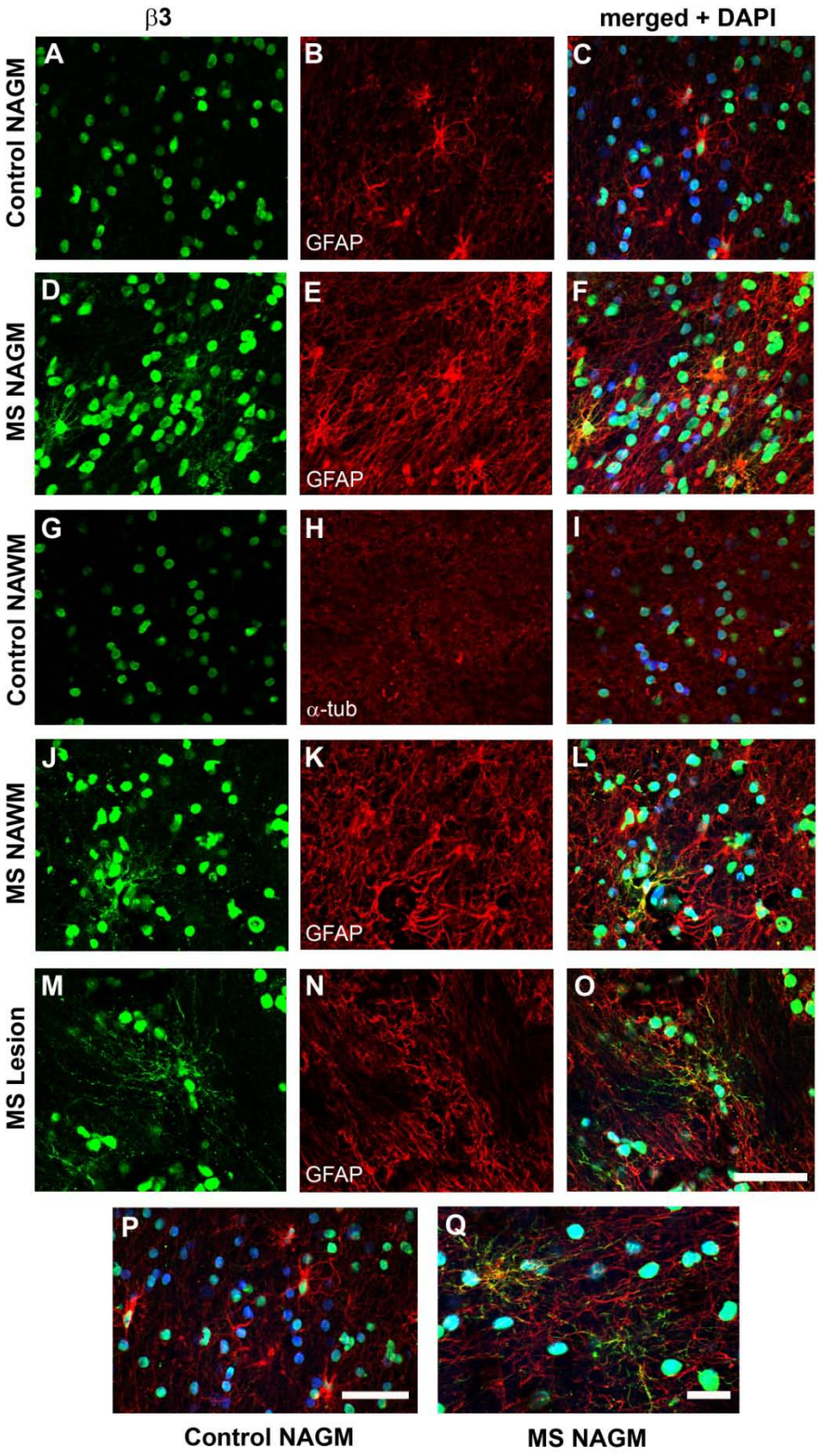
β3
merged + DAPI
Control NAGM
MS NAGM
Control NAWM
MS NAWM
MS Lesion
A
B
C
D
E
F
G
H
I
J
K
L
M
N
O
P
Q
GFAP
α-tub
Control NAGM
MS NAGM

.

Figure 3.9: β4 expression in control and MS brain.

β4 is expressed in vasculature in control and MS brain. **A-C**: Control NAGM. (**A**): anti-β4, (**B**) anti-acetylated α-tubulin, (**C**) merged. **D-F**: MS NAGM. (**D**): anti-β4, (**E**) anti-acetylated α-tubulin, (**F**) merged. **G-I**: Control NAWM. (**G**): anti-β4, (**H**) anti-acetylated α-tubulin, (**I**) merged. **J-L**: MS NAWM. (**J**): anti-β4, (**K**): anti-acetylated α-tubulin, (**L**): merged. **M-O**: MS lesion. (**M**): anti-β4, (**N**): anti-acetylated α-tubulin, (**O**): merged. P, Q: Localization of β4 to a blood vessel in cross-section. (**P**) anti-β4, (**Q**) merged with anti-acetylated α-tubulin (red).

Scale bar = 100 μm.

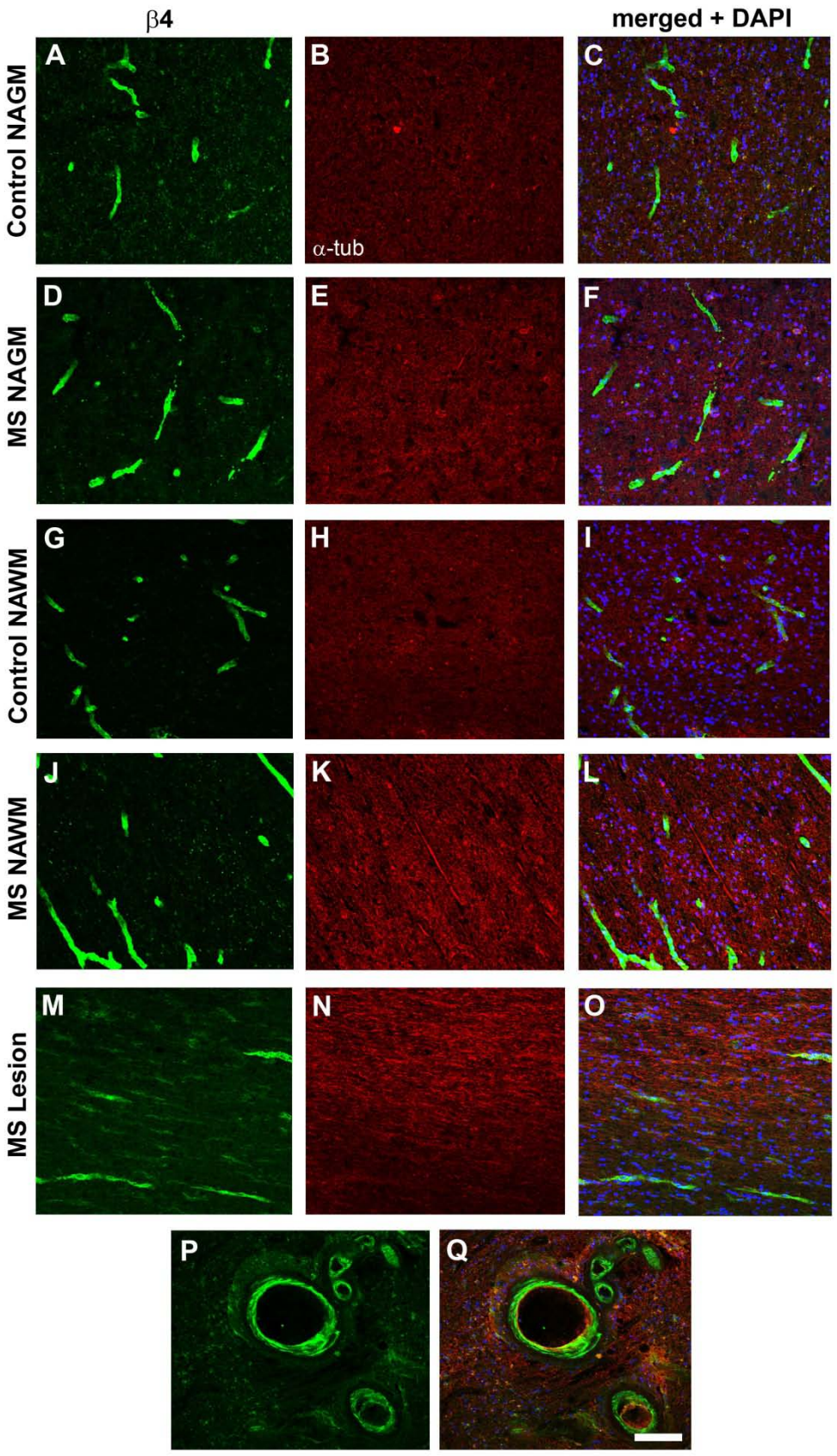
β4
merged + DAPI
Control NAGM
MS NAGM
Control NAWM
MS NAWM
MS Lesion
α-tub
A
B
C
D
E
F
G
H
I
J
K
L
M
N
O
P
Q

	Sample Number	Age	Post-mortem time (hours)	Diagnosis
Control	3175	54	21.5	Pancytopenia
	3346	91	10.0	Congestive heart failure
	3397	72	19.5	Cancer
	3406	72	20.1	Congestive heart failure
	3465	93	20.25	Von Willebrand's disease
	3482	79	14.0	Coronary artery disease
	3543	73	12.0	Chronic obstructive pulmonary disease
	3558	59	19.5	Non-Hodgkins lymphoma
	3603	74	12.0	Cancer
	3698	84	N/A	Cancer
MS	3509	74	11.25	Chronic MS
	3840	61	22.8	Active MS
	3860	81	11.8	MS
	3928	53	10.3	Chronic MS
	3954	72	40.1	MS
	4106	63	23.0	Chronic MS
	4107	52	20.6	Chronic-active MS
	4201	75	13.8	Chronic MS
	4212	50	18.9	Chronic MS

Table 3.1: Summary of human brain samples.

CHAPTER FOUR

EXPRESSION OF VOLTAGE-GATED SODIUM CHANNEL α AND β SUBUNITS IN CULTURED RAT OLIGODENDROCYTES

SUMMARY

Oligodendrocytes (OLs) are the myelinating glial cells of the central nervous system (CNS). These cells have typically been considered to be “non-excitable.” However, sodium currents were reported in isolated A2B5-positive oligodendrocyte precursor cells (OPCs) in culture (Sontheimer et al., 1989). More recent evidence has demonstrated that a sub-population of NG2-expressing progenitor cells in rat, presumably OPCs, are capable of generating tetrodotoxin (TTX)-sensitive action potentials in response to depolarizing stimuli (Karadottir et al., 2008). These action potentials are dependent on neuronal contact and have been proposed to contribute to brain development by allowing OPCs to sense electrically active axons and target these axons for myelination. In addition, it is postulated that OPCs may be able to modulate axonal conduction velocity, although the underlying mechanism is unknown. Further, OPC-generated action potentials disappeared with differentiation to mature OLs, in agreement with (Sontheimer et al., 1989), who earlier reported that sodium

currents are barely detectable in cultured OLs. These results have led researchers in the field to begin to re-think the roles of electrically excitable and non-excitable glia in brain and to consider that sodium currents may be essential for normal OPC functions.

The purpose of the present study was to investigate the expression of voltage-gated sodium channel α and β subunits in A2B5-positive OPCs and then after differentiation into more mature A007-positive cells, to gain a greater understanding of the molecular basis of the observed sodium channel current in OPCs. We performed immunofluorescent labeling of cultured rat OPCs isolated from neonatal rat brain. OPCs displayed differential expression of sodium channel α and β subunits, with changing patterns of expression as OPCs differentiated from A2B5-positive to the A007-positive pro-OL stage. β2 and β4 subunits, which share 35% homology and associate covalently with sodium channel α subunits, were expressed at low levels at both stages. Anti-β1 produced moderate labeling of A2B5-positive OPCs that increased with differentiation to the A007-positive stage. Anti-β3 displayed moderate labeling in the cellular processes and an intense nuclear signal in both A2B5- and A007-positive cells. Unexpectedly, antibodies specific to the pore-forming sodium channel α subunits $Na_v1.1$, $Na_v1.2$, and $Na_v1.6$ showed low to moderate labeling of A2B5-positive OPCs that increased in more differentiated A007-positive pro-OLs. However, in agreement with previous studies, anti-pan sodium channel antibody labeling suggested that fewer channels were functionally available at

the OPC plasma membrane in A007-positive compare to A2B5-positive cells. Taken together, these results demonstrate the expression of both sodium channel α and β subunits in cultured rat OPCs at two stages of differentiation.

INTRODUCTION

Oligodendrocytes (OLs) are the glial cells responsible for the myelination of CNS axons. Early OL precursor cells (OPCs) are highly migratory and remain mitotic, while mature OLs, capable of elaborating extensive myelin membranes to ensheathe axons, have withdrawn from the cell cycle and are no longer capable of migration (Baumann and Pham-Dinh, 2001; McTigue and Tripathi, 2008). OL development follows a stepwise process, beginning with the induction of progenitor cells in the neuroepithelium (Miller, 2002; Simons and Trajkovic, 2006; McTigue and Tripathi, 2008). These cells migrate into presumptive CNS white matter where they differentiate (Baumann and Pham-Dinh, 2001; Miller, 2002). Differentiation proceeds through morphologically distinct intermediate stages, with each stage identifiable by cell shape and specific subset of cell-surface antigens. The earliest OPCs display bipolar morphology and express the A2B5 antigen, platelet-derived growth factor α (PDGF-α), and chondroitin sulfate proteoglycan NG2 (Miller, 2002; Chittajallu et al., 2004; McTigue and Tripathi, 2008). These progenitor cells develop into a multipolar intermediate cell type

termed the pro-OL. Pro-OLs retain expression of the three progenitor antigens and begin to express the O4 antigen (Baumann and Pham-Dinh, 2001; Miller, 2002) (also detected with anti-A007 antibody (Bansal et al., 1992)). As pro-OLs differentiate into mature OLs, they downregulate PDGFRα and A2B5 (Trapp et al., 1997; Baumann and Pham-Dinh, 2001). These cells retain a multipolar morphology while starting to display a sheet-like or rarified membrane appearance similar to the myelinating OL. These mature cells retain O4 antigen expression while beginning to express the O1 galactocerebroside antigen and eventually upregulating 2', 3'-cyclic nucleotide 3'-phosphodiesterase (CNP) (Baumann and Pham-Dinh, 2001; Zhang, 2001; Miller, 2002). Expression of NG2 is downregulated at this mature stage of differentiation. As mature cells make contact with nearby axons and differentiate into myelinating OLs capable of forming compact myelin, they finally express the myelin proteins myelin basic protein (MBP), proteolipid protein (PLP), and myelin-associated glycoprotein (MAG) (Baumann and Pham-Dinh, 2001; Zhang, 2001; McTigue and Tripathi, 2008). By virtue of these progressive changes in cell surface antigens, OLs in culture can be identified using specific antibodies in conjunction with observation of morphology.

Voltage-gated sodium channels are responsible for the generation and propagation of action potentials in excitable cells. Sodium channels in brain are heterotrimers, consisting of one central, pore-forming α subunit in association with two β subunits which do not contribute to pore formation but play roles in

modulation of channel kinetics and regulation of channel cell surface expression (Catterall, 2000; Isom, 2001; Chen et al., 2002; Chen et al., 2004; Brackenbury and Isom, 2008). Sodium channel β subunits also play multiple distinct, non-conducting roles separate from their roles in channel modulation, most notably in cell-cell adhesion, cellular migration, and neuronal fasciculation (Malhotra et al., 2000a; Isom, 2002; Davis et al., 2004; McEwen and Isom, 2004; Brackenbury et al., 2008b; Brackenbury et al., 2008a).

The myelination of excitable axons by OLs is a well-established function for these cells (Baumann and Pham-Dinh, 2001; Sherman and Brophy, 2005; Simons and Trotter, 2007). Multiple groups have begun to solidify the importance of the OL beyond its role in axon ensheathment. The identity of OLs as excitable cells presents a novel and intriguing addition to our understanding of CNS function and development. OLs had been known to be capable of generating low levels of sodium current which had been proposed to play a role in functions such as the maintenance of the resting membrane potential, but until recently were believed not to fire action potentials (Williamson et al., 1997; Xie et al., 2007). Electrophysiological studies of cultured OPCs have demonstrated measurable sodium current at early developmental stages that disappeared with maturation (Sontheimer et al., 1989; Barres et al., 1990b). A2B5-positive OPCs were reported to uniformly express tetrodotoxin (TTX)-sensitive sodium currents, with O4-positive pro-OLs expressing sodium currents with similar kinetics but significantly reduced current density in a much smaller fraction of total cells.

Interestingly, with differentiation to mature OLs, sodium current was no longer detectable (Sontheimer et al., 1989). Thus, sodium channel expression in OPCs and OLs appears to be under tight developmental control. These data also suggest that sodium current may play a functional role in early stages of OPC development.

Recently, two populations of morphologically similar NG2-expressing OPCs in slices of rat cerebellum at postnatal day P7 were identified, only one of which was capable of generating action potentials in response to depolarization (Karadottir et al., 2008). Similar to the non-spiking sodium current seen previously in OPCs, these action potentials were shown to be TTX-sensitive and to inactivate during sustained depolarization, consistent with their generation by voltage-gated sodium channels. These action potential-generating cells form synaptic connections, receiving both excitatory and inhibitory input from neurons (Karadottir et al., 2008). Spiking NG2-positive cells also displayed pan-sodium channel immunostaining while non-spiking cells did not (Karadottir et al., 2008). A separate study identified a population of subcortical NG2-positive OLs which were capable of firing single TTX-sensitive action potentials while NG2-positive OPCs from white matter were not able to generate action potentials (Chittajallu et al., 2004). These studies suggest that sodium channel function in OPCs and OLs may be more complex than originally believed, opening the possibility of new roles for OPCs and OLs involving excitability. It is important to note, when considering these data, that NG2-positive cells represent a heterogeneous

population that also include multipotent progenitor cells (Mallon et al., 2002; Chittajallu et al., 2004; McTigue and Tripathi, 2008). These cells are capable of differentiation into OLs, but may also differentiate into neurons as seen in a subpopulation that express the neuronal marker doublecortin (Belachew et al., 2003; Wang and He, 2009).

Previous studies have examined sodium channel α subunit expression in OPCs and OLs by electrophysiological measurements; however, a comprehensive evaluation of sodium channel β subunit expression has not yet been undertaken. We were interested in examining the expression of sodium channel α and β subunits using immunofluorescence to determine the complement of channel subunits expressed in differentiating OPCs. Here we present evidence of differential expression of α and β subunits in cultured OPCs derived from neonatal rat brain at two stages of differentiation.

RESULTS

In this study, we employed two antibodies against OPC cell surface antigens in order to mark the stage of differentiation of cells in culture. Anti-A2B5 recognizes an antigen present on cell surface gangliosides on OPCs and identifies early bipolar cells as well as those which are beginning to adopt a multipolar morphology (Eisenbarth et al., 1979). Anti-A2B5 labeling is strong at all plasma

membranes of OPCs (for example, **Figure 4.1B**). The anti-A007 antibody can be used to identify cells at the same stage of differentiation as those marked by the O4 antigen (Bansal et al., 1992). These cells are multipolar and are more differentiated than A2B5-positive cells. Anti-A007 labels all pro-OL cell processes, but shows low or undetectable amounts of labeling at the cell body (for example, **Figure 4.1E**).

Expression of sodium channel β1 and β3 subunits in OPCs

The specificity of the anti-β1 and anti-β2 antibodies used in this study was demonstrated using *Scn1b* and *Scn2b* null tissues, respectively, in Chapter 3 of this thesis (see **Figure 3.4**). *Scn3b* and *Scn4b* null animals are not available, and so similar studies could not be performed for anti-β3 and anti-β4. However, Western blot experiments in β subunit transfected vs. non-transfected HEK cells demonstrated the specificity of the anti-β3 and anti-β4 antibodies (Wong et al., 2005).

The β1 and β3 subunits both associate non-covalently with the sodium channel pore-forming α subunit, although likely not simultaneously. We first examined expression of β1 and β3 in OPCs at two stages of differentiation.

Figure 4.1 shows expression of the sodium channel β1 subunit in both A2B5-positive and A007-positive OPCs. In A2B5-positive precursor cells, β1 is expressed uniformly throughout the cell at moderate levels, detectable in the cell body as well as the processes (**Figure 4.1A-C**). In A007-positive cells, β1 expression is upregulated as compared to A2B5-positive cells. This increase in expression of β1 can be clearly seen in comparing β1 signal in A2B5-positive OPCs and β1 signal in the multipolar, extensively branched mature pro-OLs in the same field of view (**Figure 4.1A**). These mature cells are no longer recognized by anti-A2B5 (see **Figure 4.1B**), but their morphology resembles that of the A007-positive cells (see **Figure 4.1E**). In A007-positive cells, β1 is strongly expressed at the plasma membrane of the cell body, with some detectable labeling within the soma (**Figure 4.1D-F**). It is most highly expressed in the major processes branching directly off of the cell body with slightly diminished levels in the secondary processes.

We then performed immunostaining to examine β3 expression in A2B5- and A007-positive cells. In both stages of differentiation, the expression pattern of β3 is strikingly different from that of β1. Anti-β3 shows intense nuclear labeling in all cells, coincident with DAPI staining (**Figure 4.2**). A2B5-positive precursors express β3 at low levels in processes as well as in the cell body and cytoplasm (**Figure 4.2, A-C**). A007-positive cells retain β3 expression in the cell body and processes (**Figure 4.2, D-F**). More extensively arborized processes show moderate amounts of β3 signal throughout. Nuclear labeling in both stages of

differentiation remains at the same high levels in all nuclei, sometimes complicating the imaging process for these cells due to oversaturation.

Expression of sodium channel β2 and β4 subunits in OPCs

We examined expression of β2 and β4 in differentiating OLs. The β2 and β4 channel subunits share only 35% homology, although both associate covalently with sodium channel α subunits through disulfide bonding.

Labeling of A2B5-positive OPCs with anti-β2 demonstrates low overall expression of β2, with moderate levels of expression observed in the cell body (**Figure 4.3, A-C**). In contrast to anti-β3, nuclei in these cells do not express β2. Expression of β2 in the cellular processes is at moderate levels in the proximal regions and rapidly decreases at distances further from the cell soma. In A007-positive cells, the pattern of β2 expression is similar to that in A2B5 cells, with expression of β2 highest in the cell body and decreasing progressively in the processes with increasing distance from the cell body (**Figure 4.3, D-F**). Interestingly, a number of cells appear to display perinuclear β2 staining (see **Figure 4.3D**).

We then labeled OPCs using anti-β4. Expression of β4 is barely detectable above background levels in both stages of differentiation (**Figure 4.4**). This

holds true for the cell body, nucleus and processes of all A2B5-positive cells observed (**Figure 4.4, A-C**), with β4 expression also virtually undetectable in A007-positive cells (**Figure 4.4, D-F**). Unexpectedly, β4 expression is observed strongly in non-OL lineage cells which do not express A007 (see **Figure 4.4D**). These cells have a flattened appearance, lack a centrally-positioned cell body as seen in labeled OPCs and do not extend processes consistent with those observed in either A2B5- or A007-positive OPCs.

Sodium channel α subunit expression in OPCs

Sodium current has been observed in OPCs in early stages of differentiation, including in a subpopulation of NG2-positive precursor cells in cerebellar brain slices which generate TTX-sensitive action potentials (Karadottir et al., 2008). We therefore examined the expression of the TTX-sensitive sodium channel α subunits $Na_v1.1$, $Na_v1.2$ and $Na_v1.6$ in OPCs using immunofluorescence. All three of these channels are expressed in CNS neurons.

We labeled OPCs with anti-$Na_v1.1$. $Na_v1.1$ is extensively expressed within brain, including localization at axon initial segments and select nodes of Ranvier (Westenbroek et al., 1989; Duflocq et al., 2008). Nav1.1 is expressed at nodes of Ranvier in a subpopulation of axons within the spinal cord in normal animals as well as aberrantly in optic nerve in a mouse model of demyelinating disease (Duflocq et al., 2008; O'Malley et al., 2009). $Na_v1.1$ plays a major role in normal

neuronal excitability as well as pathophysiology (Yu et al., 2006; Kalume et al., 2007; Gambardella and Marini, 2009). In A2B5-positive OPCs, $Na_v1.1$ is expressed at low levels throughout the cell without polarized subcellular localization (**Figure 4.5, A-C**). This channel expression is not unique to OPCs, however, as $Na_v1.1$ signal is also detectable in cells not expressing the A2B5 antigen (**Figure 4.5A**). As cells differentiate into A007-expressing pro-OLs, the pattern of $Na_v1.1$ expression alters slightly. The highest amount of $Na_v1.1$ signal is detected in the cell body and proximal processes, with lower levels of expression in secondary and distal processes (**Figure 4.5, D-F**).

We next examined expression of $Na_v1.2$ in A2B5- and A007-positive OPCs. In the CNS, $Na_v1.2$ is expressed along normally non-myelinated axons as well as at nodes of Ranvier in early stages of development (Boiko et al., 2001b). In A2B5-positive progenitor cells, $Na_v1.2$ is expressed at moderate levels within the cell body while immunofluorescence along the processes is low to nearly undetectable (**Figure 4.7, A-C**). $Na_v1.2$ expression in A007-positive cells is readily detectable, with strong expression in cell bodies and along some major processes with moderate expression along secondary processes (**Figure 4.7, D-F**).

$Na_v1.6$ is the channel subtype normally expressed at nodes of Ranvier along myelinated axons as well as at axon initial segments (Caldwell et al., 2000; Boiko

et al., 2001b). $Na_v1.6$ expression has also been detected in microglia that have been activated following injury (Black et al., 2008). In A2B5-positive OPCs, strong $Na_v1.6$ expression was observed within the cell body and at low but detectable levels in the processes (**Figure 4.7, A-C**). $Na_v1.6$ expression can be seen within the cytoplasm and at the plasma membrane, but is not detected in the nucleus. In A007-positive cells, $Na_v1.6$ expression is at highest levels in the cell body with expression also detectable in all processes at low to moderate levels, relative to the cell body (**Figure 4.7, D-F**).

Finally, immunostaining of cultured OPCs was performed using anti-pan-sodium channel antibody to detect all sodium channels present. Sodium channel expression was visible throughout A2B5-positive cells with strong labeling detected at the plasma membrane (**Figure 4.8, A-C**). In A007-expressing cells, channel expression was similar within all regions of the cell (**Figure 4.8, D-F**). These data confirm the expression of sodium channels in OPCs detected by the individual anti- $Na_v1.1$, -$Na_v1.2$, and -$Na_v1.6$ antibodies. Interestingly, and in contrast to the specific sodium channel antibodies tested, anti-pan-sodium channel antibody immunofluorescence displayed intense plasma membrane labeling in A2B5-positive cells (**Figure 4.8A**), but this polarized expression was not observed in A007-positive cells (**Figure 4.8D**). These results suggest that another sodium channel α subunit gene product than the ones tested may be expressed in at the plasma membrane in OPCs. These data also suggest, consistent with previous electrophysiological results, that a higher proportion of

channels are localized to the plasma membrane in early stages of differentiation where they would then be able to generate sodium current.

DISCUSSION

Voltage-gated sodium channels are key players in excitability, and have been classically considered to be required only by excitable cells such as neurons or myocytes. Sodium channels are now known to be expressed in a variety of cells historically considered to be “non-excitable” such as cancer cells (Brackenbury and Djamgoz, 2006; Brackenbury et al., 2007) and macrophages (Craner et al., 2005), as well as being important molecular components of a wide variety of pathological processes and diseases. This prompts the question: what is the functional role of sodium channels in OPCs, long considered to be non-excitable? Do sodium channels in myelinating glia have conducting as well as non-conducting functions?

In this study, we have provided evidence for the expression of multiple sodium channel α and β subunits in OPCs at two stages of development, A2B5-expressing and A007-expressing OPCs. Previous publications have demonstrated the presence of sodium current in isolated A2B5-positive OPCs, although with rare exception this current was not sufficient to fire an action potential. This sodium current was most evident in early progenitor cells and

progressively decreased as cells differentiated to more mature stages (Sontheimer et al., 1989; Barres et al., 1990b). Spiking NG2-positive precursor cells in brain slices, which are in contact with neurons and capable of firing action potentials, also appear to lose excitability as cells continue to differentiate. In agreement with (Sontheimer et al., 1989), our results demonstrate that sodium channel α subunits are expressed in both A2B5-positive and A007-positive OPCs. Further, our results with anti-pan sodium channel antibody suggest that fewer channels may be functionally expressed at the OPC plasma membrane at the more A007-positive stage compared with the immature A2B5 stage. These data are consistent with previous results showing that sodium currents decrease in cultured OPCs with differentiation from bipolar to multipolar morphology (Sontheimer et al., 1989). Because this previous study did not include immunocytochemical labeling, we cannot compare our results directly with theirs.

The specific subcellular expression of sodium channel α and β subunits in cultured OPCs during differentiation has not been examined previously. The ion-conducting α subunit has been investigated through the observation of sodium current (Sontheimer et al., 1989; Chittajallu et al., 2004; Karadottir et al., 2008), but the β subunits have not been studied carefully. One previous study examined *Scn1b* (β1) mRNA expression in cultured optic nerve astrocytes and in Schwann cells (Oh and Waxman, 1994). *Scn1b* mRNA in astrocytes was visible in process-bearing astrocytes, but not those with a fibroblast-like morphology, with expression higher in the soma as well as in the processes. In Schwann

cells, both the soma and the processes express *Scn1b* mRNA (Oh and Waxman, 1994). These observations are consistent with the observations of β1 protein localization in both cell body and processes in our immunofluorescent studies of cultured oligodendrocytes. Another group of investigators examined β1 protein expression in post-mortem brain tissue from patients suffering from diseases which exhibit gliosis, one of which was multiple sclerosis. β1 expression was shown to be increased in astrocytes in lesioned tissue in each gliosis-associated disease (Aronica et al., 2003). This same group also observed increases in β1 expression in reactive astrocytes in hippocampus in a model of epilepsy, the electrical induction of status epilepticus in rat, while resting astrocytes did not express significant levels of β1 (Gorter et al., 2002).

In this study we also show a strikingly different pattern of expression for β3 as compared to β1, with β1 expressed in A2B5-positive OPCs and at higher levels in A007-positive OPCs and β3 primarily observed in nuclei and at low to moderate levels in the cell body and processes. These subunits both exhibit a similar type I integral membrane protein topology with a single extracellular immunoglobulin loop. β1 and β3 share 57% sequence identity, but display different and often complementary tissue localization in CNS despite both being broadly expressed (Morgan 2000). β1 has been well-characterized as a cell adhesion molecule separate from its function in channel modulation (Isom, 2002; McEwen and Isom, 2004). Despite the homology between β1 and β3, however, β3 does not engage in *trans* homophilic cell adhesion (McEwen et al., 2009). It is

not capable of binding to either contactin or ankyrin G, two of the known binding partners of β1 , nor of engaging in heterophilic cell adhesion with β1 (McEwen and Isom, 2004; McEwen et al., 2009). It is possible that the different expression patterns of β1 and β3 in OPCs are predicated on their differing ability to engage in cell adhesion, a property which is well known to contribute to a variety of cellular functions such as cell migration.

The expression of β4 in non-OL lineage cells in differentiated cultures was unexpected. β4 is the most recently cloned of the sodium channel β subunits and is consequently the least well-characterized. It has been implicated in the promotion of channel opening and increased current amplitudes when co-expressed with an α subunit in heterologous systems (Aman et al., 2009). The expression pattern of β4 in this study raises several intriguing questions. These cells morphologically resemble fibroblast lineage cells. Sodium current has been observed in epithelial and epithelial-derived cells in multiple studies. TTX-resistant sodium channel current was detected in cells derived from rat and human vascular cells (Gordienko and Tsukahara, 1994; Gosling et al., 1998; Walsh et al., 1998). The channel involved in this current appears to be the cardiac voltage-gated sodium channel $Na_v1.5$ (Gordienko and Tsukahara, 1994; Walsh et al., 1998). It would be valuable to use markers of fibroblast cells, as well as markers for astrocytes, which can also take on a fibroblast morphology, to positively identify these cells.

The pathology of demyelinating and dysmyelinating diseases such as multiple sclerosis (MS) and Charcot-Marie-Tooth disease is intricately intertwined with myelin structure, formation and deterioration as well as the potential for remyelination. Understanding the biology of the myelinating glia is a critical step in our understanding of these diseases. We have shown previously that loss of the β2 subunit is neuroprotective in a mouse model of MS (O'Malley et al., 2009), where deletion of β2 leads to not only reductions in axonal loss and degeneration but also preservation of the myelin sheath. In the current study, β2 expression in cultured OPCs is at low to moderate levels, suggesting that deletion of β2 in these cells may not have a significant functional effect. This is consistent with the model we proposed previously, in which deletion of β2 in central axons, not the myelin sheath, was the critical element in the process of neuroprotection (O'Malley et al., 2009). However, the role of β2 in OPCs in vivo is worth considering. Also, the presence of ion channels in glia has been implicated in other studies of demyelinating disease, and so the other voltage-gated sodium channel subunits may play a role in pathology different from that of β2.

What might the role of glial sodium channels be in the absence of action potential firing? Two strong possibilities are cell migration and cell proliferation. OPCs, especially during progenitor stages, are highly motile and migratory (Baumann and Pham-Dinh, 2001; McTigue and Tripathi, 2008). Survival requires the ability

to make contact with the axon (Trapp et al., 1997; Barres and Raff, 1999; Gao and Miller, 2006), suggesting cell adhesive functions to have potential import. Sodium channels have previously been implicated in processes of cell proliferation (Pardo, 2004; Wu et al., 2006) and cell migration (Kim et al., 2005; Paez et al., 2008). Evidence for sodium channel α and β subunit involvement in cancer, particularly in proliferation, migration, metastasis, and invasion, supports these two processes as strong potentials for the role of channels in glia (Fraser et al., 2005; Mycielska et al., 2005; Brackenbury et al., 2007; Brackenbury et al., 2008a).

Finally, it is important to note that the properties of OPCs and OLs *in situ* and *in vitro* are likely not identical. Some A2B5-positive cells may also be bipotent progenitor cells capable of differentiating into neurons. Cultured cells thus offer a valuable tool for the investigation of protein expression and cellular function, but ultimately observations made *in vitro* must be confirmed in an appropriate physiological setting. This study thereby represents an early step in the investigation of the expression and function of sodium channel α and β subunits in myelinating glia. Further experiments making use of specific genetic models such as the *Scn1b* and *Scn2b* null mice will help to elucidate the specific importance of these channel subunits in glia.

EXPERIMENTAL METHODS

Oligodendrocyte precursor cell primary culture: Primary cultures were prepared in the Benjamins laboratory at Wayne State University, Detroit, MI. Oligodendroglial cell cultures were obtained from neonatal rat brain using the shake-off technique (McCarthy and de Vellis, 1980), as modified previously (Dyer and Benjamins, 1988). Briefly, cultures were prepared from neonatal Sprague Dawley rat brain and OPCs were separated from the astroglial layer by physically rapping flasks against the benchtop. These separated cells were then placed into plastic dishes in order to separate microglia and other cell types by differential adherence. The remaining cells, enriched in OPCs, were plated onto poly-D-lysine coated coverslips. OPCs were maintained in a 2:1 mixture of chemically defined medium (Bottenstein, 1986) containing 2% newborn calf serum with astrocyte-conditioned medium (DMEM F-12) containing 10% newborn calf serum.

Immunofluorescent staining and microscopy: Coverslips with adherent OPCs were used for immunofluorescent staining. Coverslips were fixed with 4% paraformaldehyde and stored in PBS at 4°C until used. Cells were incubated for 1 h at RT with monoclonal primary antibodies against OPC cell surface epitopes A007 or A2B5. Coverslips were washed 3 times in PBS and then incubated for 30 minutes at RT with goat anti-mouse secondary antibody coupled to Alexa 546 (red) fluorophore (Molecular Probes, Carlsbad, CA). Cells were then fixed for 10

minutes with 4% paraformaldehyde and washed in PBS before permeabilization and blocking for a minimum of 1 h in PBTGS (0.1M PB, 0.3% Triton X-100, 10% normal goat serum). Coverslips were then incubated overnight in polyclonal primary antibodies against sodium channel α or β subunits diluted in PBTGS. The following day, coverslips were incubated for 2 h in goat anti-rabbit secondary antibodies coupled to Alexa 488 (green) (Molecular Probes, Carlsbad, CA) diluted in PBTGS. Coverslips were washed three times with 0.1 M PB after each antibody step. Some coverslips were additionally incubated with DAPI and washed again with 0.1M PB. Coverslips were then air-dried briefly and mounted onto SuperFrost Plus slides using GelMount anti-fade mounting medium (Biomeda, Foster City, CA). Digital images were collected using an Olympus FluoView 500 confocal microscope with FluoView software located in the Department of Pharmacology, University of Michigan. Composite images were assembled using Adobe Photoshop CS4.

Antibodies: Primary antibodies for immunocytochemistry were as follows: mouse anti-A2B5 (dilution 1:1 or 1:5, obtained from Dr. J. Benjamins, characterized in (Eisenbarth et al., 1979)), mouse anti-A007 (1:1 or 1:5, obtained from Dr. J. Benjamins, characterized in (Bansal et al., 1992)), rabbit anti-β1 (1:500-1000, obtained from Dr. N. Nukina (Wong et al., 2005)), rabbit anti-β2 (1:500-1:1000, obtained from Dr. N. Nukina (Wong et al., 2005)), rabbit anti-β3 (1:1000, obtained from Dr. N. Nukina (Wong et al., 2005)), rabbit anti-β4 (1:1000, obtained from Dr. N. Nukina (Wong et al., 2005)), rabbit anti-$Na_v1.1$ (1:250,

Sigma-Aldrich), rabbit anti-$Na_v1.2$ (1:200, Sigma-Aldrich), rabbit anti-$Na_v1.6$ (1:200, Sigma-Aldrich), and rabbit anti-Pan-Na_v (1:200, Sigma-Aldrich).

Figure 4.1: β1 expression in OPCs.

β1 is expressed in both A2B5-positive and A007-positive OPCs. (**A-C**) β1 immunolocalization in A2B5-positive OPCs is expressed uniformly in all regions of the cell. **A**: Anti-β1, **B**: Anti-A2B5, **C**: merged. (**D-F**) β1 expression in A007-positive oligodendrocytes is detectable in all regions of the cell, with increased expression in major processes. **D**: Anti-β1, **E**: Anti-A007, **F**: merged.

Scale bar = 50 μm.

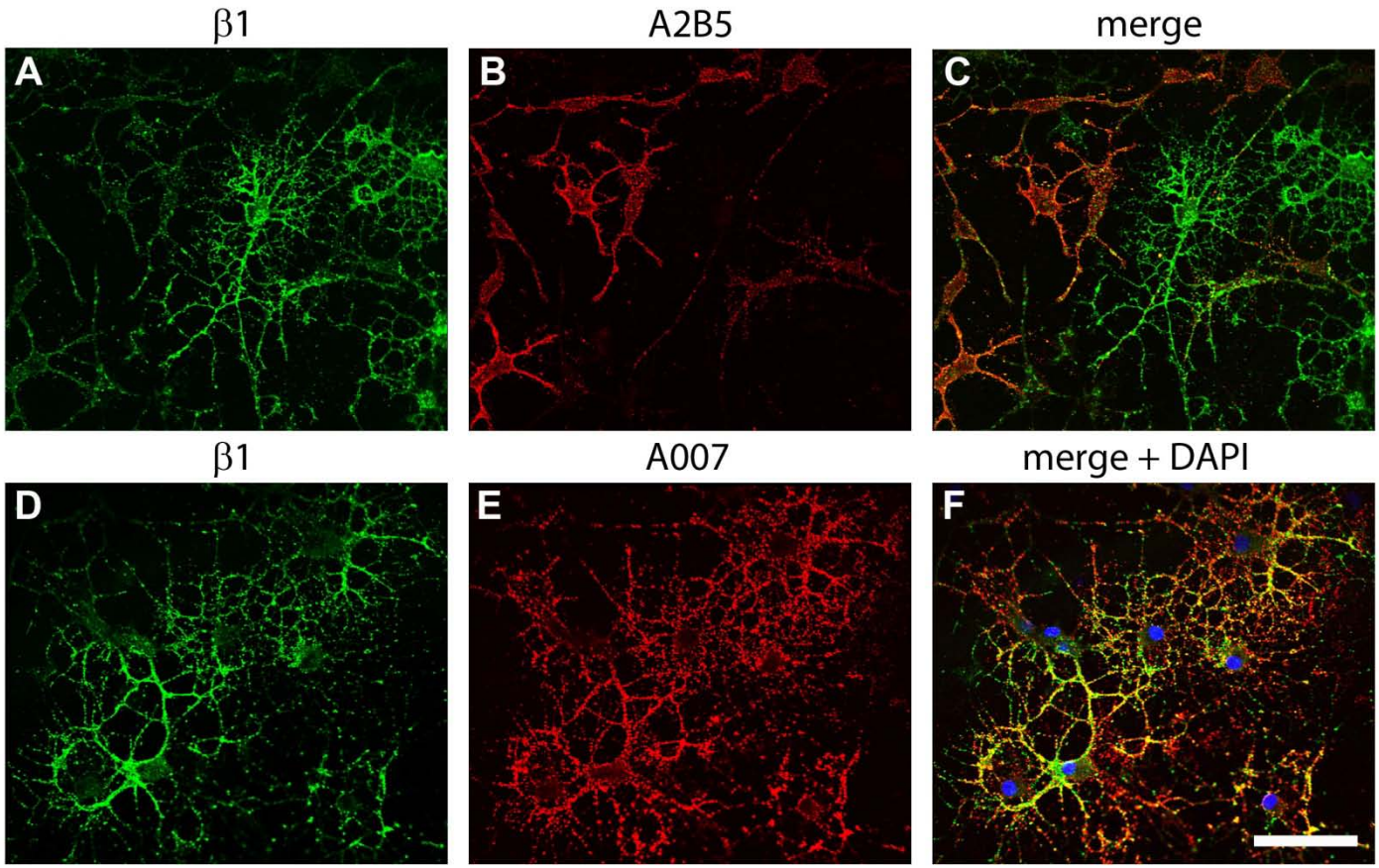
β1
A2B5
merge
A
B
C
β1
A007
merge + DAPI
D
E
F

Figure 4.2: β3 expression in OPCs.

β3 is strongly expressed in nuclei in both A2B5-positive and A007-positive OPCs as well as in cell processes. (**A-C**) β3 immunolocalization in A2B5-positive OPCs is seen at high levels in nuclei as well as in processes and the cell body. **A**: Anti-β3, **B**: Anti-A2B5, **C**: merged. (**D-F**) β3 expression in A007-positive OPCs is retained at high levels in the nucleus with moderate expression in processes. **D**: Anti-β3, **E**: Anti-A007, **F**: merged.

Scale bar = 50 μm.

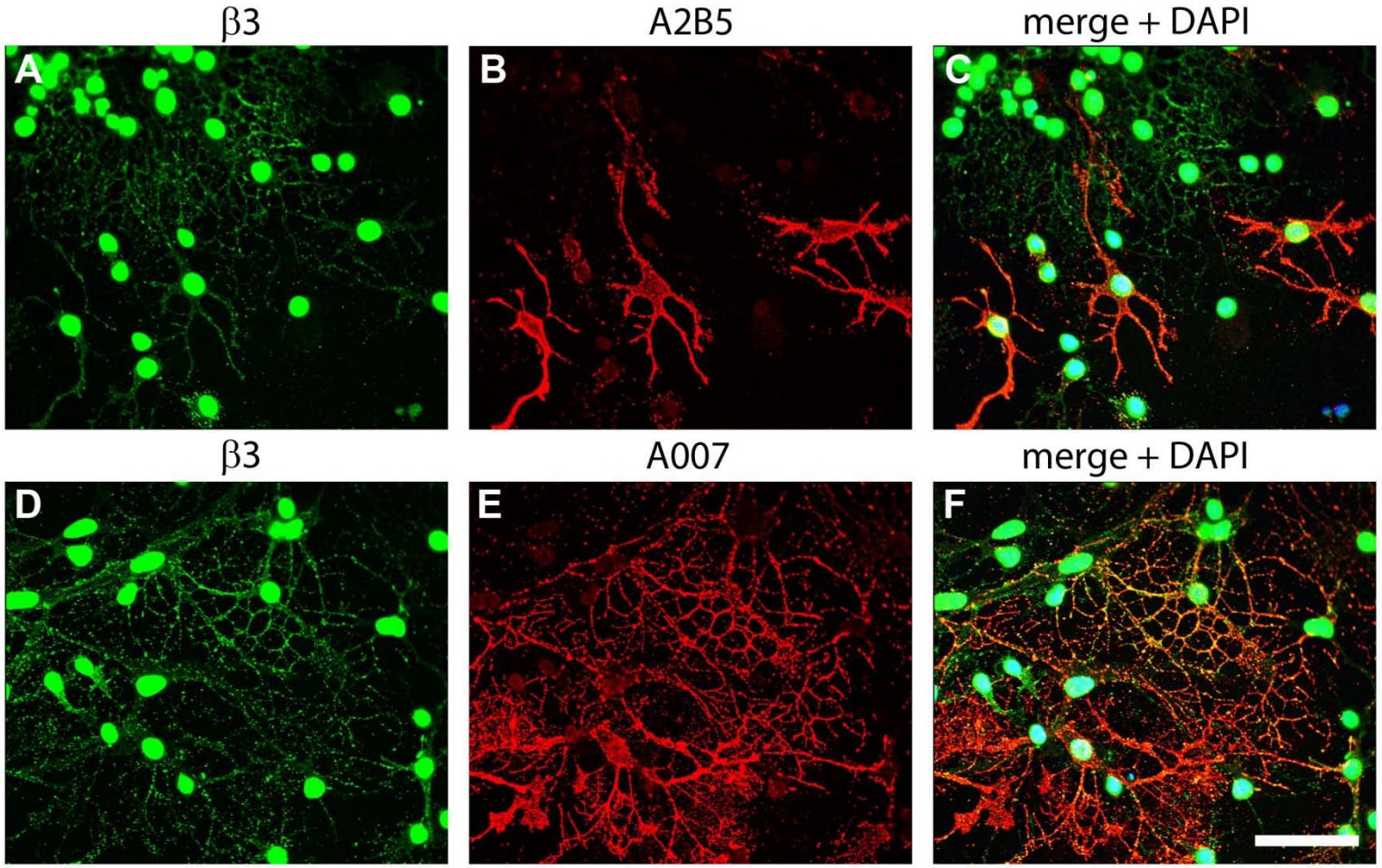
β3
A2B5
merge + DAPI
A
B
C
β3
A007
merge + DAPI
D
E
F

Figure 4.3: β2 expression in OPCs.

β2 is expressed in both A2B5- and A007-positive OPCs at low levels. (**A-C**) β2 immunolocalization in A2B5-expressing OPCs is detected primarily in the cell body and processes immediately proximal to the soma. **A**: Anti-β2, **B**: Anti-A2B5, **C**: merged. (**D-F**) β2 expression in A007-positive cells resembles the pattern of low β2 expression in A2B5-positive OPCs, with some expression of β2 in perinuclear regions. **D**: Anti-β2, **E**: Anti-A007, **F**: merged.

Scale bar = 50 μm.

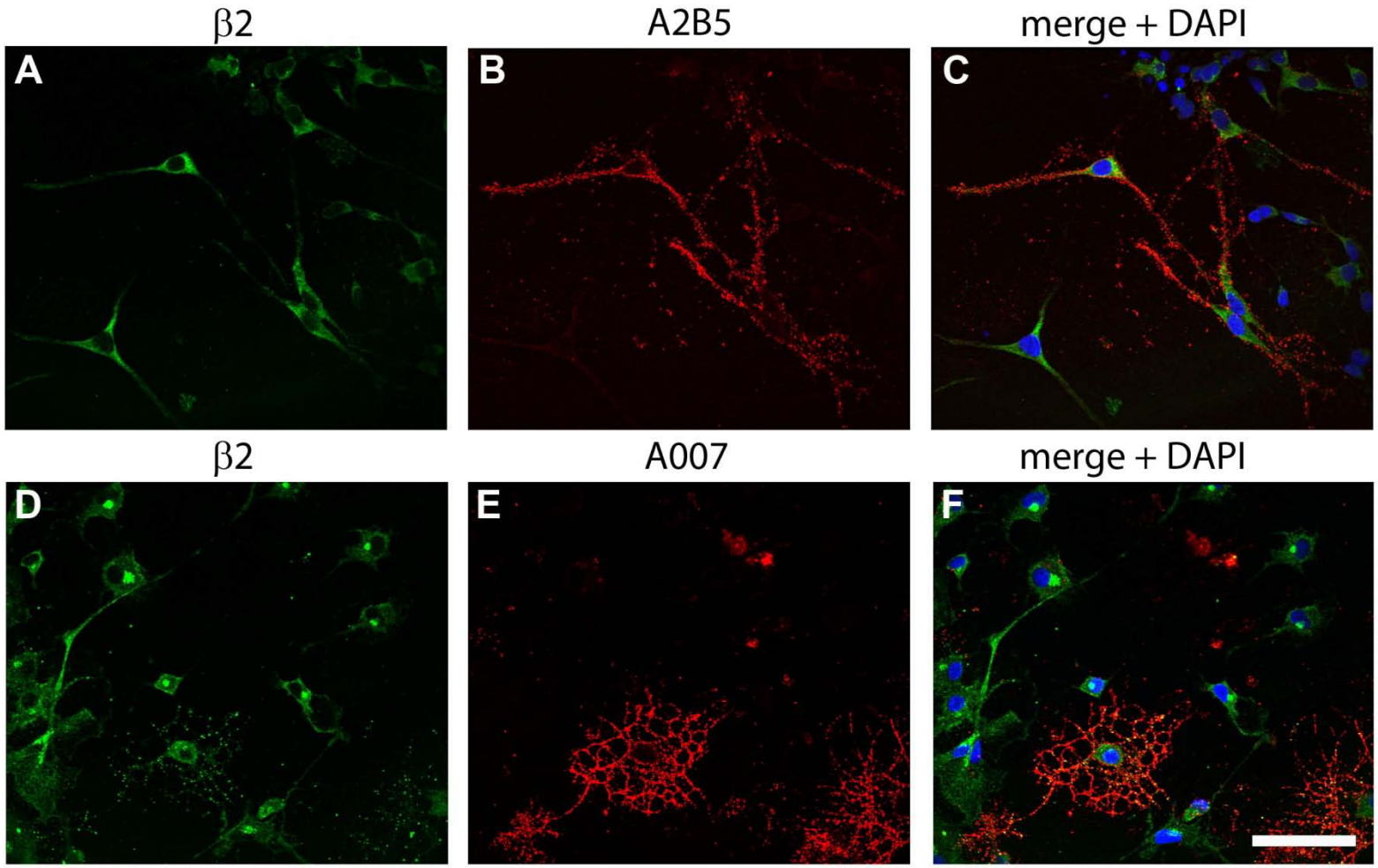
β2
A2B5
merge + DAPI
A
B
C
β2
A007
merge + DAPI
D
E
F

Figure 4.4: β4 expression in OPCs.

β4 expression is not detected in A2B5- and A007-positive OPCs but is expressed strongly in non-oligodendrocyte lineage cells. (**A-C**) β4 expression in A2B5-positive OPCs is not detected at levels significantly above background signal. **A**: Anti-β4, **B**: Anti-A2B5, **C**: merged. (**D-F**) β4 expression in A007-positive oligodendrocytes is virtually undetectable, similar to A2B5-positive OPCs. β4 is strongly expressed in non-OLs. **D**: Anti-β4, **E**: Anti-A007, **F**: merged. Scale bar = 50 μm.

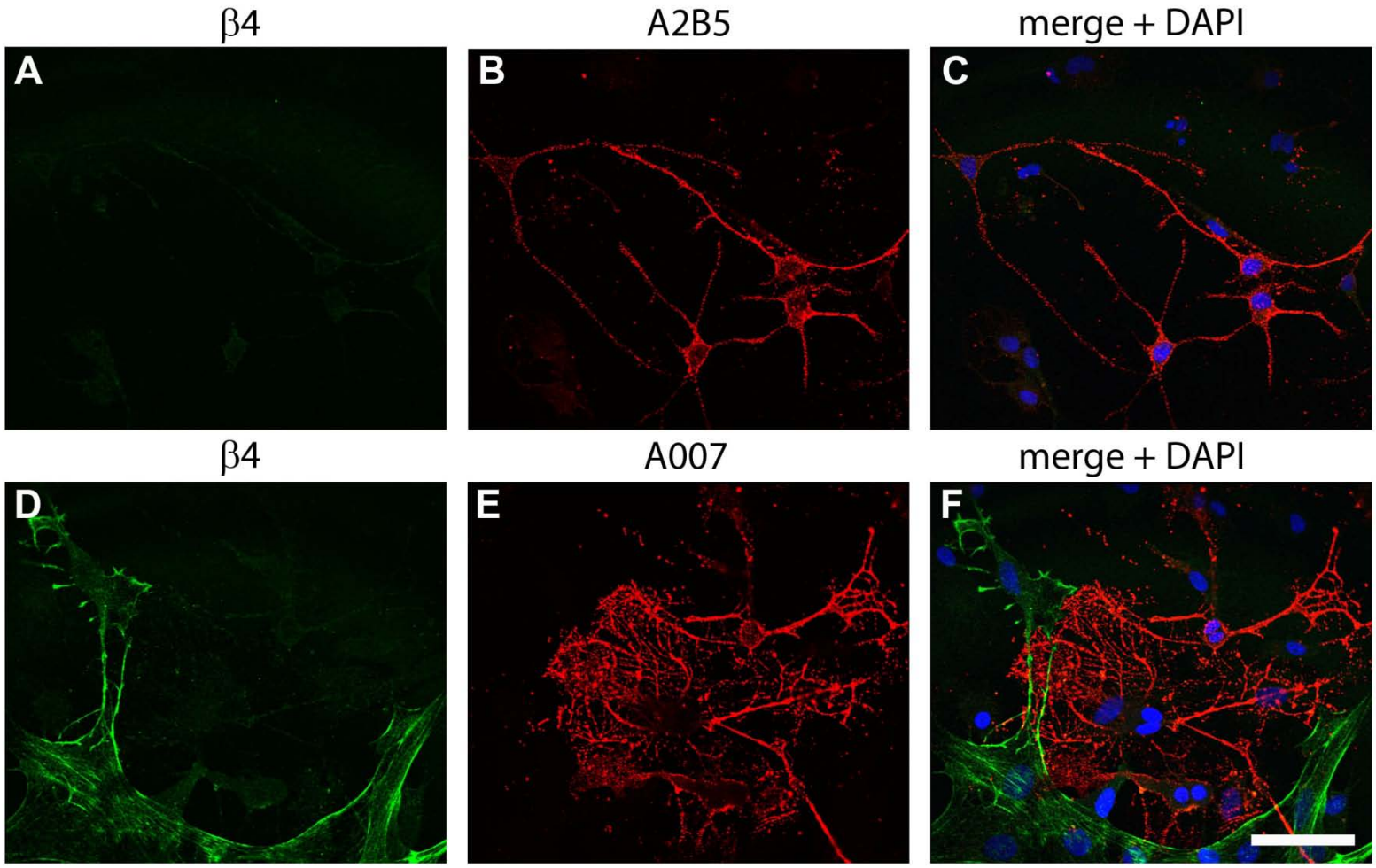
β4
A2B5
merge + DAPI
A
B
C
β4
A007
merge + DAPI
D
E
F

Figure 4.5: $Na_v1.1$ expression in OPCs.

$Na_v1.1$ is expressed in both A2B5-positive and A007-positive OPCs and displays increases of expression during differentiation. (**A-C**) $Na_v1.1$ immunolocalization in A2B5-expressing OPCs is seen at low levels in all regions of the cell. **A**: Anti-$Na_v1.1$, **B**: Anti-A2B5, **C**: merged. (**D-F**) $Na_v1.1$ expression in $A007^+$ OPCs is detectable in all regions of the cell with expression in major processes. **D**: Anti-$Na_v1.1$, **E**: Anti-A007, **F**: merged. Scale bar = 50 μm.

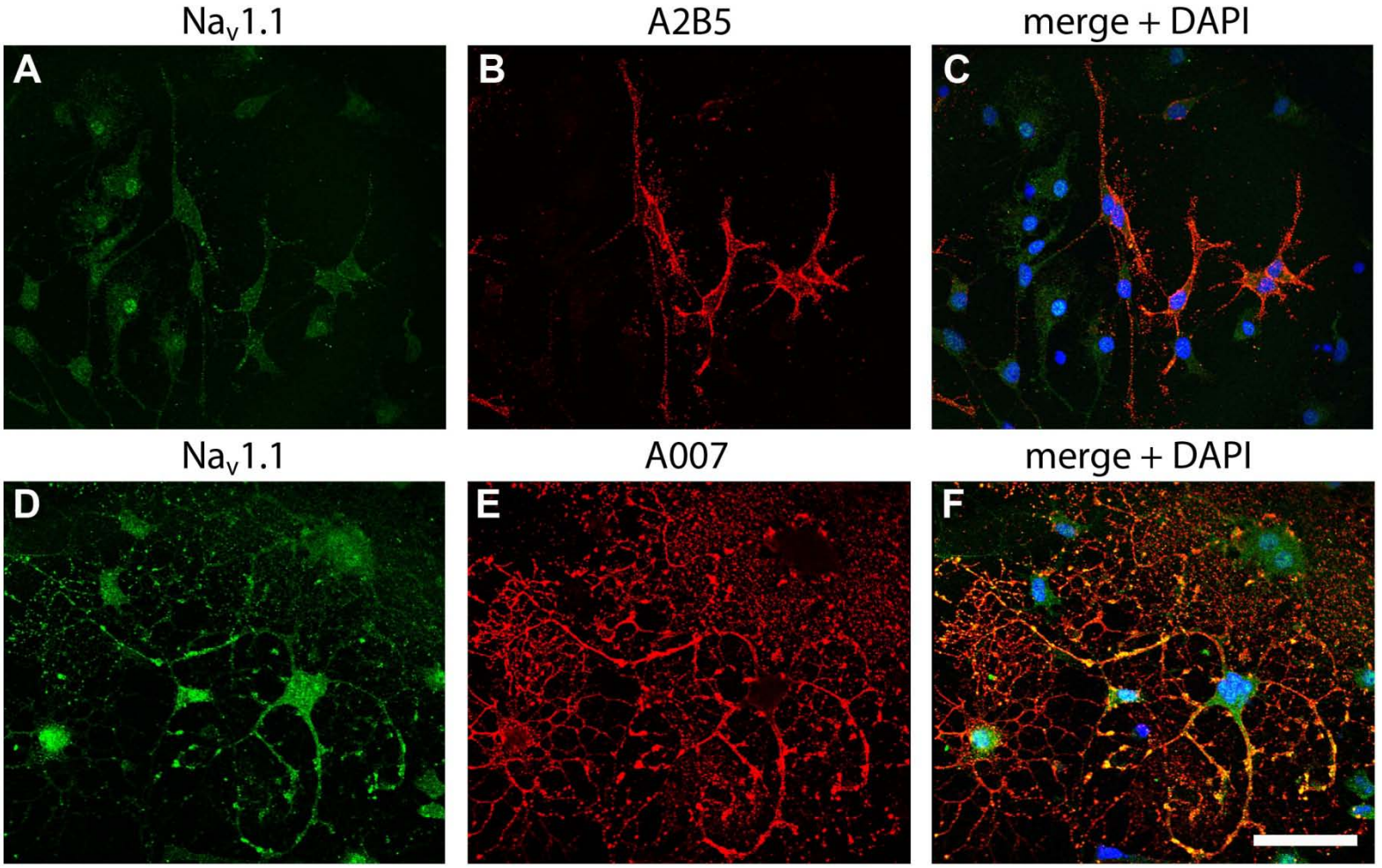
Na$_v$1.1
A2B5
merge + DAPI
A
B
C
Na$_v$1.1
A007
merge + DAPI
D
E
F

Figure 4.6: $Na_v1.2$ expression in OPCs.

$Na_v1.2$ is expressed in both A2B5- and A007-positive OPCs. (**A-C**) $Na_v1.2$ immunolocalization in A2B5-positive OPCs is seen at low levels in the cell body with low expression in processes. **A**: Anti-$Na_v1.2$, **B**: Anti-A2B5, **C**: merged. (**D-F**) $Na_v1.2$ expression in A007-positive oligodendrocytes is strong in the cell body as well as major processes. **D**: Anti-$Na_v1.2$, **E**: Anti-A007, **F**: merged.

Scale bar = 50 μm.

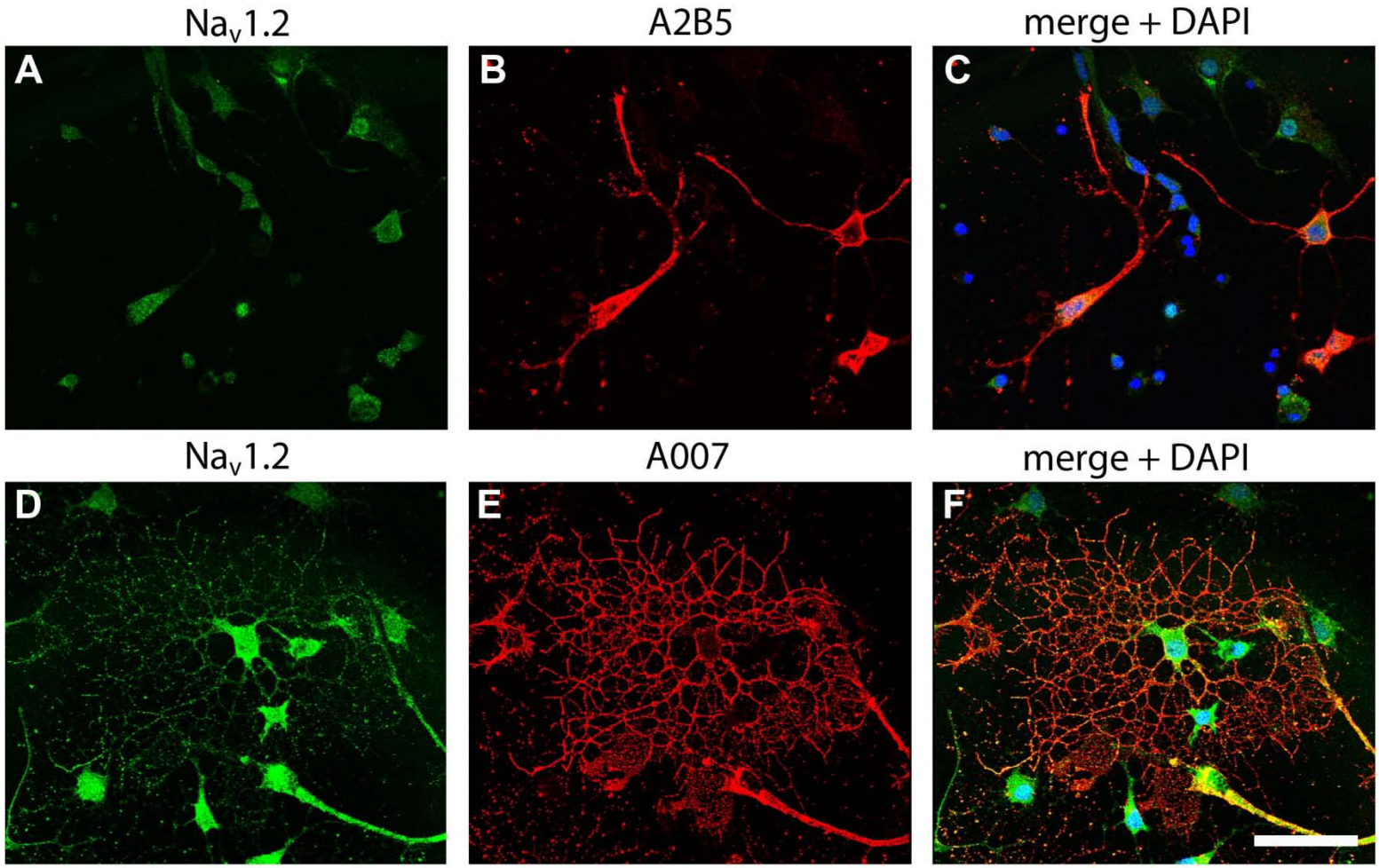
Na$_v$1.2
A2B5
merge + DAPI
A
B
C
Na$_v$1.2
A007
merge + DAPI
D
E
F

Figure 4.7: $Na_v1.6$ expression in OPCs.

$Na_v1.6$ is expressed in both A2B5-positive and A007-positive OPCs. (**A-C**) $Na_v1.6$ expression in A2B5-positive OPCs is seen in all regions of the cell, with highest levels of expression in the cell body and proximal processes. **A**: Anti-$Na_v1.6$, **B**: Anti-A2B5, **C**: merged. (**D-F**) $Na_v1.6$ expression in A007-positive cells is detectable in all regions of the cell with high levels of expression in the soma and proximal processes. **D**: Anti-$Na_v1.6$, **E**: Anti-A007, **F**: merged.

Scale bar = 50 μm.

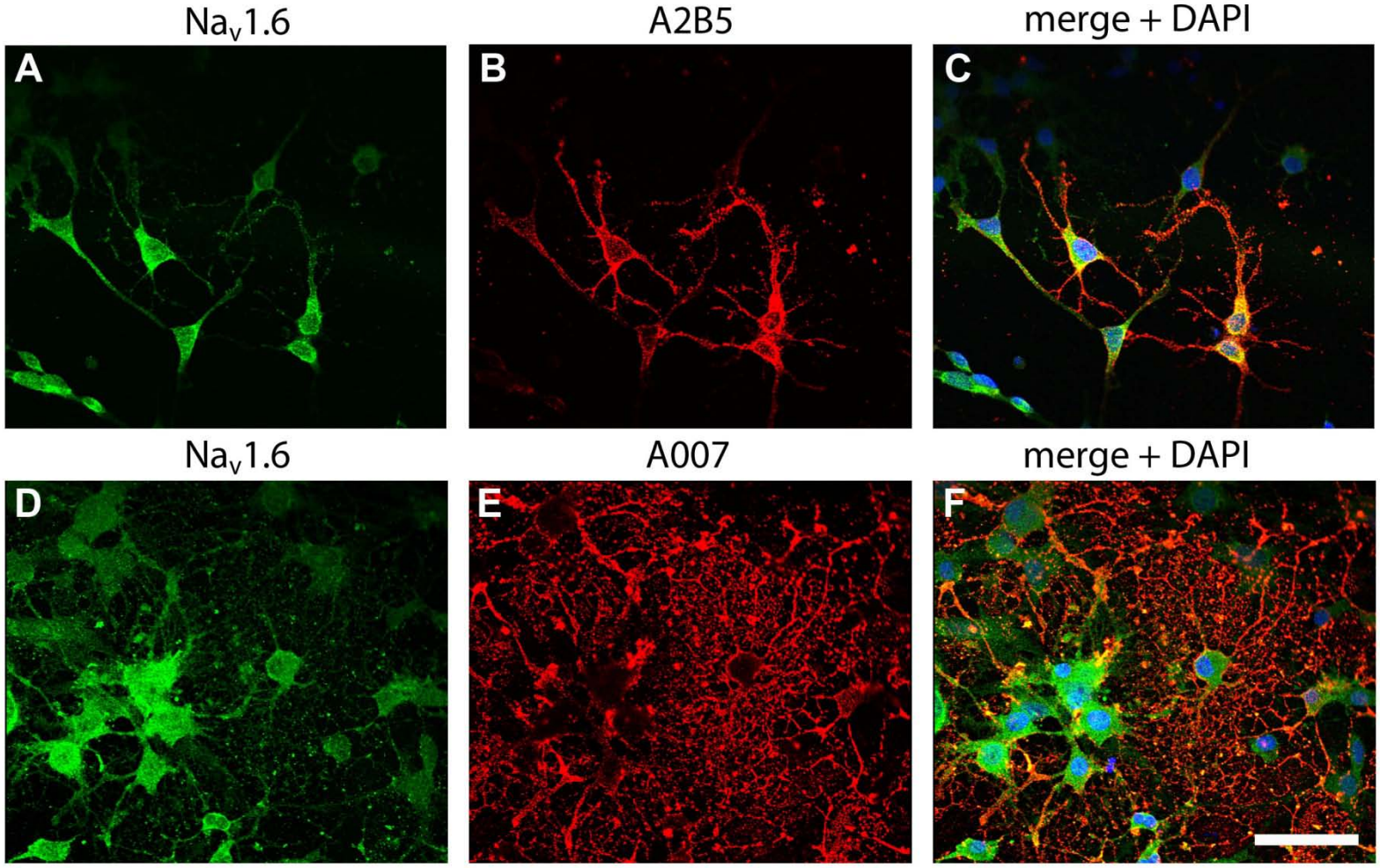
Na$_v$1.6
A2B5
merge + DAPI
A
B
C
Na$_v$1.6
A007
merge + DAPI
D
E
F

Figure 4.8: Pan-sodium channel expression in OPCs.

Sodium channels are expressed in both A2B5-positive and A007-positive OPCs as detected by the pan-sodium channel antibody. (**A-C**) Anti-pan sodium channel immunostaining in A2B5-positive OPCs is seen in all regions of the cell with high expression at the plasma membrane. **A**: Anti-pan-Na_v, **B**: Anti-A2B5, **C**: merged. (**D-F**) Sodium channel expression in $A007^+$ oligodendrocytes is detectable in all regions of the cell. **A**: Anti-pan-Na_v, **B**: Anti-A007, **C**: merged. Scale bar = 50 μm.

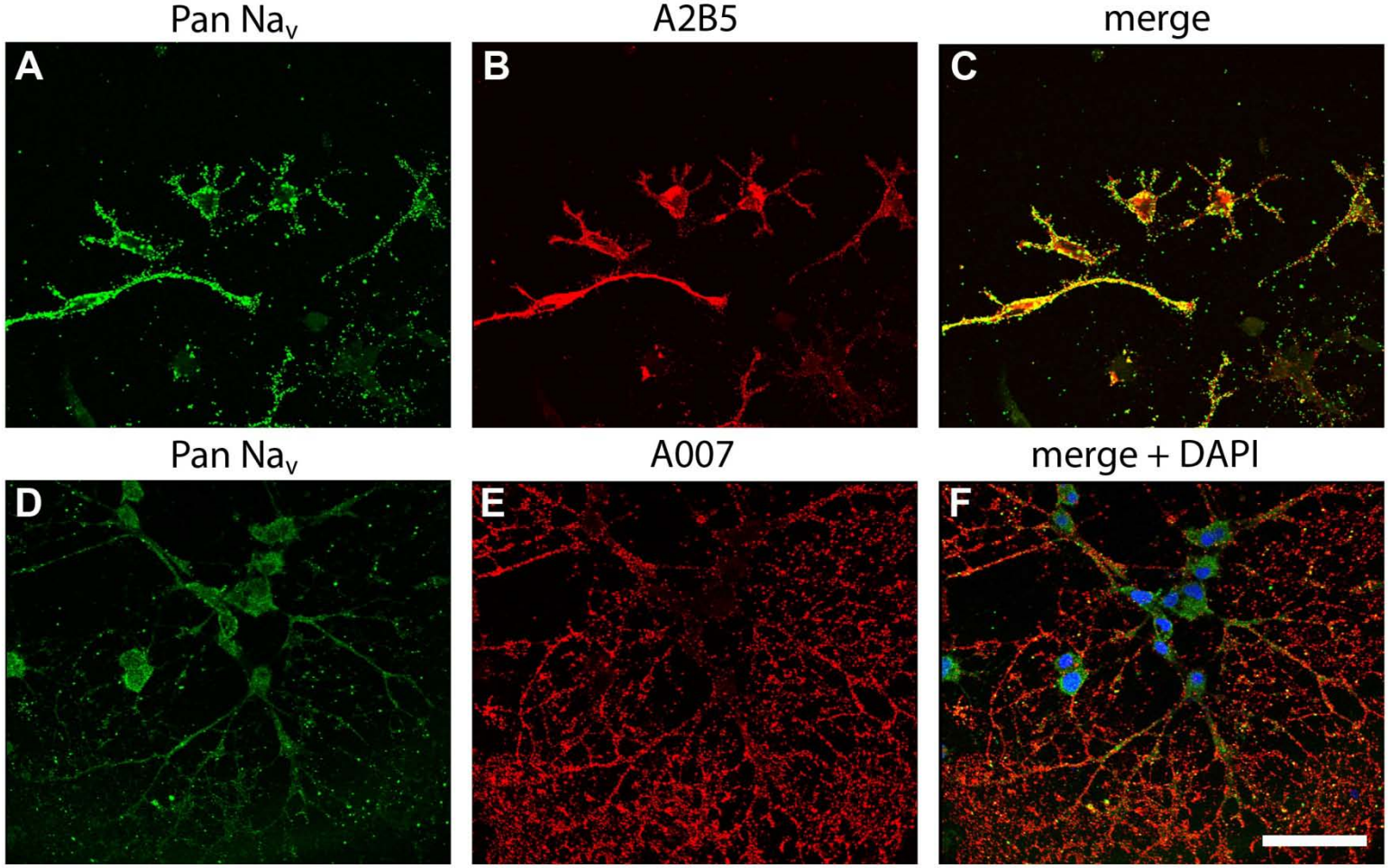
Pan Na_v
A2B5
merge
A
B
C
Pan Na_v
A007
merge + DAPI
D
E
F

CHAPTER FIVE

DISCUSSION AND CONCLUSIONS

Voltage-gated sodium channels play key roles in processes throughout the body and at all points in development. In embryonic life, channel subunits contribute to essential steps in the genesis of what will become adult tissues and systems. The β subunits engage in cell adhesive interactions and help guide nascent neurons toward their destinations, contributing to axonal pathfinding and helping axons fasciculate into the closely-knit, elegant fiber bundles that become part of the circuitry of the nervous system. Developing cerebellar granule neurons, extending newly-formed neurites as they establish orientation within and connections to their cellular environment, rely on the properties of the β1 subunit for neurite outgrowth. Sodium channel α and β subunits have been observed in excitable and non-excitable cells, suggesting unknown roles that extend beyond ion conduction. Mutations in sodium channel subunits or aberrant regulation of subunit expression can be linked directly to the development of a multitude of disorders, with novel mutations being identified on an ongoing basis. These offer a handful of examples from the panoply of scenarios in which sodium channels are of importance.

My dissertation research has focused on the role of sodium channel α and β subunits in myelinating glia as well as demyelinating disorders of the CNS. In this thesis, I have provided evidence implicating sodium channel β subunits in the pathogenesis of demyelinating disease in mice and humans. I have shown that deletion of sodium channel β2 subunits is neuroprotective in a mouse model of demyelinating disease, a process that is hypothesized to contribute to amelioration of disease symptoms through a reduction in the number of sodium channels at the plasma membrane, thereby decreasing the extent of potentially damaging downstream injury cascades. I have translated my research in this animal model into the human demyelinating disorder multiple sclerosis (MS), contributing to the growing body of published evidence implicating sodium channel subunits in this and related diseases. Finally, I have examined the expression of sodium channel α and β subunits in cultured rat oligodendrocytes in order to better understand their roles in normal glial development and function. In the present chapter, I will review my findings and reiterate their importance, propose some directions for future research in each area, and finally remark on some potential implications of my observations.

SODIUM CHANNELS IN MYELINATING GLIA

I have demonstrated the presence of voltage-gated sodium channel α and β subunits in cultured rat oligodendrocytes (OLs) at two stages of differentiation: A2B5-positive and A007-positive progenitor cells. Sodium channel β subunit expression has been studied only cursorily in myelinating CNS glial cells, and my results offer a starting point for a number of additional lines of investigation. Sodium channel α subunits have been studied in terms of their ability to generate sodium current in both cultured oligodendrocyte precursor cells (OPCs) as well as, in a subset of publications, OPCs in *in situ* in brain slices. My observations of α subunit expression in progenitor cells are consistent with and support these previously published studies in which sodium channels are expressed in progenitor cells and levels then become downregulated during differentiation.

I observed that sodium channel α subunits are expressed in OPCs at both A2B5-expressing and A007-expressing stages of differentiation, consistent with the implications of previous electrophysiological studies. Are the channels identified in my studies functional? Have they been inserted into the plasma membrane where they are able to play a role in ion conductance? These questions can be approached by using both biochemical and electrophysiological means. First, sodium current should be measured at each of these two stages of differentiation. In keeping with the literature, our prediction would be that bipolar precursor cells at the A2B5-expressing stage would generate detectable levels of

sodium current, while more differentiated A007-expressing cells would generate lower levels of sodium current and perhaps be incapable of generating enough current to fire an action potential if co-cultured with axons. Previous studies have demonstrated the presence of TTX-sensitive sodium current in OPCs, and my data have also specifically shown the expression of three TTX-sensitive channel subtypes. The properties of this TTX-sensitive current should be further examined. Do different channel subtypes make different relative contributions to current in OPCs? It could also be valuable to allow OPCs to further differentiate into mature OLs capable of elaborating myelin membranes, although at this stage normal development of these cells becomes dependent on the presence of axonal signals and support for continued survival and perhaps for proper expression of the normal complement of proteins. Detailed investigation of channel expression in mature myelinating glia in culture should be carried out in co-culture systems in order to ensure glial cell survival; it would, however, be intriguing to examine specific changes in protein expression or glial cell properties in the presence or absence of supporting neuronal cells.

Second, sodium channel subunit protein expression in OPCs should be measured via Western blotting techniques in addition to immunofluorescence. An essential caveat when considering the question of protein expression as examined through immunofluorescence is how best to compare expression in different samples or images. Strategies in which pixel intensity is measured in order to evaluate signal strength require careful controls and data acquisition to

ensure that comparisons are being made among samples which are in fact comparable. Performing Western blotting with protein lysates from A2B5- and A007-expressing cells is an important experiment to accompany immunofluorescent imaging. This can measure not just the total amount of channel protein present in cultured OLs, but complementary experiments utilizing surface biotinylation techniques would contribute to answering the question of whether channels have been inserted into the plasma membrane or if they have been retained in membranes in intracellular compartments. An alternative approach to this question is the use of ^{3}H-saxitoxin binding assays to quantify the number of sodium channels present at the plasma membrane; this technique, however, detects only TTX-sensitive channels and does not differentiate between individual subtypes.

Results from experiments investigating expression of sodium channel α subunits using the pan-sodium channel antibody as well as antibodies specific to $Na_v1.1$, $Na_v1.2$ and $Na_v1.6$ raise another interesting question. These data show low to moderate levels of expression of each specific channel subtype in A2B5-expressing progenitor cells as well as moderate or higher expression in A007-positive cells. However, experiments with the pan-sodium channel antibody showed particularly high levels of expression at the plasma membrane in the earlier, A2B5-positive stage which is not accounted for by the lack of similarly strong plasma membrane labeling detected when probing for the three specific channel subtypes. $Na_v1.1$, $Na_v1.2$ and $Na_v1.6$ were selected for these

experiments based on their importance in central nervous tissue as well as their relevance to demyelinating disorders. Is there a different channel protein which is expressed in early stages of OL differentiation? Likely candidates are $Na_v1.3$, known to be expressed during embryonic brain development, as well as $Na_v1.8$ which is also expressed within some CNS regions under pathophysiological conditions. The possibility that these channels are expressed in OPCs should be explored.

My observations of sodium channel β subunit expression in OPCs suggest that the β subunits which are of highest importance in these cells are β1 and β3, while the low to undetectable levels of β2 and β4 in OPCs imply that these subunits may not play a significant role in these precursor cells. This implication dovetails well with my data demonstrating that the loss of β2 is neuroprotective in demyelinating disease. The model we proposed for the mechanism of action of β2 based on those data implicated β2 as an important element within the axon, rather than within the myelinating glia, and the low levels of β2 detected in cultured OPCs support this model. Further examination of the connection between my observations in the EAE model and in cultured OLs will require study of β subunit expression at later stages of differentiation, when cells begin to become competent to engage in myelination. Our hypothesis is that β subunit expression is important in OPCs, potentially for cellular migration and cell-cell adhesion, but is less important, or perhaps does not play a role, in the mature, compact myelin sheath. Depending on antibody quality, immuno-electron

microscopy could be a valuable tool for the examination of β subunit expression specifically in compact versus non-compact myelin. This could potentially help to clarify the stages at which β subunit expression is important in the myelinating glia versus the myelin sheath.

β1 expression in OPCs and OLs is intriguing. β1 has been shown to play a role in cell signaling, migration and adhesion separate from its function in channel modulation. OPCs are highly motile in early stages of development, and axon ensheathment by mature myelinating OLs requires contact between the axon and glial cell before myelination can initiate. In this way, expression of β1 by OPCs in early stages of differentiation may mediate critical cell adhesive functions, ensuring that OPCs migrate to the correct location of presumptive white matter and, once there, establish correct contact with axons. This is supported by data from our *Scn1b* null mouse, in which a subset of axons display disruption of normal myelination as seen by the eversion of the terminal paranodal loop adjacent to the node of Ranvier in a subset of axons. In addition there are fewer nodes of Ranvier present, and axonal degeneration is observed. Preliminary results show that OPC-specific β1 null mice have dysmyelination and axonal degeneration. β1 is not required for the formation of compact myelin, since compact myelin is formed in both mouse models, but is likely to play a role OPC migration as well as in axo-glial communication required for the initiation of myelination. These hypotheses regarding the role of β1 in CNS glial cells and myelination offer a wide variety of potential lines of investigation.

In addition to the investigation of β1 and β3 in OPCs, my results using the anti-β4 antibody in these cultures were interesting and novel. OPCs were obtained for these experiments using the "shake-off" method, which produces cultures enriched in oligodendroglia but retains a small number of cells of non-glial lineages. I did not detect the expression of β4 in any OPCs during either observed stage of differentiation. However, I observed strong β4 expression in non-OL lineage cells. These cells have a fibroblast-like morphology and express high levels of β4 as compared to A007-expressing cells in the same fields of view. The identity of these β4-expressing cells should be determined in co-labeling experiments for β4 with markers for cells of the fibroblast lineage, as well as with markers for astrocytes.

The function of β4 has to date been primarily investigated in the context of its potential role in channel modulation. The promotion of neurite outgrowth seen as a consequence of β4 overexpression suggests that β4 may be able to function as a cell adhesion molecule (Oyama et al., 2006), but this has not been extensively studied to date. My experiments with human MS brain sections also showed high levels of β4 immunofluorescence in putative vascular cells. This offers the potential for a novel role for β4 in non-neuronal and non-glial cell types. Expression of β4 in these cells may be linked to excitability, for example, in vascular smooth muscle. However, the importance of β4 in these cells may alternately be in relation to a role in cell-cell adhesion. Important first experiments should determine the specific cell types in which β4 is expressed,

followed by experiments in heterologous systems to assay the ability of β4 to act as a cell adhesion molecule. Future research can then examine either the role of β4 in channel modulation or in cell adhesion in these tissues and cells.

SODIUM CHANNELS IN DEMYELINATING DISORDERS

I have presented evidence in this thesis for the role of sodium channel subunits in demyelinating disease, first in an animal model of disease and then in the corresponding human syndrome. Induction of *Scn2b* null mice using the MOG-EAE model of MS led to the development of a clinical course which was less severe and displayed decreased lethality as compared with the disease course in wild type controls. *Scn2b* null animals displayed decreases in axonal loss and axonal degeneration as well as numbers of demyelinated axons. These differences were not a result of changes in immune cell function or peripheral cell populations, nor of the ability of immune cells to infiltrate into the damaged CNS. Interestingly, mice lacking β2 displayed significant upregulation of $Na_v1.1$ in brain during EAE and, to a lesser extent, in spinal cord, as well as decreased expression of $Na_v1.6$. Examination of optic nerve and spinal cord sections demonstrated diffuse localization of sodium channel subtypes $Na_v1.2$ and $Na_v1.6$, consistent with multiple previously-published studies, as well as $Na_v1.1$. $Na_v1.1$ was also aberrantly localized to a subset of nodes of Ranvier in EAE.

These data implicate the β2 subunit in the pathogenesis of demyelinating disease.

Our model for the involvement of β2 is predicated on its role as a molecular chaperone in the insertion of sodium channels into the plasma membrane as well as differential properties of the channel subtypes $Na_v1.2$ and $Na_v1.6$. This model implicates β2 in pathological processes which are located specifically at the axon, not the glia. As mentioned previously, this hypothesis is supported by the data I have shown in which β2 expression in cultured OPCs is low. The relative importance of β2 during EAE on the axon or glia could be elucidated by the re-introduction of β2 into the *Scn2b* null mouse. β2 could then be expressed from cell type-specific promoters in either the neuron or the OL, and the effect on EAE pathogenesis could be observed. If the effect of β2 loss is, as we hypothesize, important at the axon, then reintroduction of β2 in the axon is predicted to produce EAE symptoms similar to those observed in wildtype animals.

A key outstanding question unanswered in the course of this thesis is the role played by $Na_v1.1$ in demyelinating disease. $Na_v1.1$ has been implicated by its altered expression and localization in β2 null mice during EAE as well as its altered expression in human MS patients compared to non-diseased individuals. What is the importance of $Na_v1.1$? One means by which this question can be investigated also makes use of the EAE model. EAE has not been induced in

$Na_v1.1$ heterozygotes. $Na_v1.1$ deletion in null mice is lethal, but heterozygotes with a single *Scn1a* allele can be maintained successfully on a hybrid 129/SvJ:C57BL/6 genetic background for analysis and breeding purposes (Yu et al., 2006). The phenotype of these animals during demyelinating disease would help to determine the role of $Na_v1.1$ in EAE pathogenesis. However, haploinsufficiency of $Na_v1.1$ might not produce a significant phenotype in this model due to compensatory mechanisms.

The proposed $Na_v1.2$ versus $Na_v1.6$ model of MS and EAE pathogenesis implies that deletion, reduction or inhibition of $Na_v1.6$ should reduce its axon damaging persistent current contribution and thus ameliorate disease symptoms. During the course of my thesis work, I obtained *Scn8a*$^{med\text{-}tg}$ heterozygote mice from the laboratory of Dr. Miriam Meisler and induced these mice with MOG-EAE in a set of preliminary experiments. We predicted that, since these mice are lacking approximately half of the normal complement of $Na_v1.6$ channels, they would resemble our *Scn2b* null mice during EAE. Contrary to expectations, the lack of a full complement of $Na_v1.6$ did not have any significant effect on disease course as compared to wildtype. These results are intriguing and suggest that factors beyond $Na_v1.2$ and $Na_v1.6$ underlie sodium channel-mediated pathogenesis. Alternatively, the 50% level of $Na_v1.6$ expression in these mice may have been sufficient for disease progression. Could this shed light on the role of $Na_v1.1$? Other *Scn8a* mutant mice display varying levels of $Na_v1.6$ expression, with selective breeding of mice carrying different alleles allowing for the generation of mice expressing as little as 12% of normal *Scn8a* protein levels without lethality

(Meisler et al., 2004). It would be worthwhile to induce other $Na_v1.6$-deficient mice with MOG-EAE to observe whether disease course or pathology are influenced by differing levels of $Na_v1.6$ expression beyond those observed in *med*$^{tg/+}$ mice. Is there a critical amount of $Na_v1.6$ which will be neuroprotective while still permitting normal conduction? This answer could have broad applicability, for example, in the development of targeted therapeutics which modulate $Na_v1.6$ levels.

After obtaining evidence regarding the role of the β2 subunit, I translated my findings into an investigation of brain tissue obtained post-mortem from human MS patients. My examination of $Na_v1.1$ expression in human brain was a result of the data obtained from *Scn2b* null mice in which increased $Na_v1.1$ expression was observed in EAE brain. I observed possible alterations in $Na_v1.1$ expression in normal-appearing grey and white matter from human patients, supporting the potential importance of this channel subtype in the pathogenesis of demyelinating disease. What is the function of $Na_v1.1$ alteration in demyelinating disease? It is possible that upregulation of $Na_v1.1$ may be an adaptive change intended to result in neuroprotection which is more apparent in the MOG-EAE mouse model. Additionally, $Na_v1.1$ may have differing functions in excitatory vs. inhibitory neurons as seen in $Na_v1.1$ heterozygotic mice (Yu et al., 2006; Catterall et al., 2008), which may be differently affected during demyelinating disease. Expression of β2 was not altered during the disease state in either human or mouse. This suggests that, while channel levels may be dynamically regulated in

pathological conditions, the total amount of β2 expression may not be critical for the ability of β2 to play a role in demyelinating disease.

My experiments provided evidence suggesting alterations in expression of $Na_v1.1$ and changes in localization of β1, β2 and β3 during MS. Another important set of experiments will be to evaluate protein expression levels of β1, β3, and β4 subunits in human MS brain samples biochemically. It is possible that expression of β3 may increase in disease, since β3 expression in astrocytes was absent in normal brain but present in MS brain. Additionally, protein expression levels of $Na_v1.2$ and $Na_v1.6$ should be assayed in the human samples. I predict that, consistent with my data obtained from the EAE model, expression of $Na_v1.2$ will be unchanged and expression of $Na_v1.6$ will be increased during MS.

I observed high levels of β subunit immunofluorescence in astrocytes in the human samples. Astrocytes cultured from spinal cord have been shown previously to express sodium channel subunit mRNA, including *Scn2a* and *Scn3a* (Black et al., 1994b), as have astrocytes from optic nerve (Barres et al., 1989). Astrogliosis is a prominent component of many MS and EAE lesions (Bjartmar et al., 2003; Bannerman et al., 2007) and GFAP levels in patients (as determined by ELISA) are increased, particularly in progressive disease forms (Norgren et al., 2004). These reactive astrocytes are thought to contribute to cytokine production and T cell activation (Bannerman et al., 2007) and are able to come into contact with neurons and neuronal synapses, form gap junctions,

and make contact with the vasculature (Hansson and Ronnback, 2003). Astrocytes contribute to the formation of the glial scar at injury sites in order to promote healing (Wang and He, 2009). In MS, many damaged regions are closely associated with GFAP-positive astrocyte processes, which may extend along the length of demyelinated regions (Black et al., 2007a).

What might be the role of β subunits in reactive astrocytes during disease or damage? My immunofluorescent studies do not indicate whether these β subunits are playing a role as channel modulators, cell adhesion molecules, or both. Astrocytes express sodium current (Bevan et al., 1987; Barres et al., 1989; Sontheimer and Waxman, 1992), opening the possibility that β subunits associate with these channels to contribute to astrocyte excitability. β subunits in astrocytes, specifically β1, could play a role in cell adhesion, helping to modulate migration or cell-cell communication. Electrophysiological examination of the sodium currents expressed by these cells, as well as immunofluorescent investigation of the channel subtypes present and coincident with β subunit expression, would be valuable.

Lastly, β4 subunits were found to be potentially expressed in the brain vasculature, potentially in the vascular smooth muscle. The precise identity of the cells in which β4 is expressed in this region is the first step to be undertaken, followed by further characterization of the potential role of β4. Are sodium

channel α subunits expressed in these locations as well, such that β4 could be present to modulate channel function? Alternately, this could help to elucidate a role for β4 in cell adhesion which has been suggested by the role of β4 in neurite outgrowth observed in previously published studies (Oyama et al., 2006).

FUTURE DIRECTIONS

The results presented in this thesis also raise a number of other interesting questions and suggest ways in which these data can be extended into novel areas of investigation. Here, I will comment on two such areas: first, the importance of remyelination, and secondly, the role of BACE1 secretase function during demyelination, specifically as it pertains to the cleavage of β2.

A critical component of functional recovery in patients is the ability to remyelinate axons which have undergone demyelination. Remyelination allows for the restoration of normal conduction and helps to protect axons from further degeneration (Dubois-Dalcq et al., 2005). Remyelinated fibers tend to have characteristics slightly different from unaffected nerves, with thinner myelin sheaths, shorter internodes and wider nodes (Patrikios et al., 2006). Remyelination in damaged CNS tissue is often carried out by Schwann cells which migrate in from the peripheral nervous system and this newly-formed myelin sheath can persist for long periods of time, up to one year or more (Black

et al., 2006a). MS patients display variability in the extent of remyelination. Older patients or those with longer disease duration show more remyelination despite the fact that remyelination can occur at any stage of the disease, even during acute stages. Interestingly, periventricular plaques, the most common location in which MS lesions are found, display less remyelination compared with lesions in deeper regions of the white matter (Patrikios et al., 2006).

Remyelination in the CNS is susceptible to failure and may not proceed completely, potentially as a result of inhibition (Franklin, 2002). What inhibits remyelination? Multiple factors have been proposed to play a role. There may be a lack of progenitor cells available to produce new myelinating glial cells, suggesting defects in migration or proliferation (Patrikios et al., 2006). Factors unique to the patient, such as age or genetic background, influence ability to remyelinate (Franklin and fFrench-Constant, 2008). Axons themselves may express factors that are non-permissive to myelination (Patrikios et al., 2006). My research has demonstrated the presence of sodium channel β subunits in myelinating glia in culture. One strategy for remyelination which is the subject of active investigation is the use of OPCs to promote the formation of new myelin segments along demyelinated axons. Could the β subunits offer a means by which migration, proliferation or adhesion of these OPCs into regions of damage be promoted? Examination of β subunits in remyelination, either in MS and EAE or in separate models of remyelination, may contribute to answering this question. Further experiments should also be performed to investigate the

expression of β subunits in populations of proliferating OPCs which are this capable of engaging in remyelination.

The role of the β-secretase BACE1 has been well-established in the deposition of β-amyloid in regions of pathology during Alzheimer's disease. BACE1 is highly expressed in brain. Along with γ-secretase, it cleaves APP to generate amyloid-β peptide (Aβ) (Willem et al., 2009). This cleavage product then accumulates in damaged Alzheimer's brain. The sodium channel β subunits are one of the few protein families identified as substrates for sequential BACE1- and γ-secretase-mediated cleavage, and this appears especially relevant for β2 and β4. Many proteins have been shown to be cleaved by either BACE1 or γ-secretase, however, few are shown to be sequentially cleaved. In cortex, β2 seems to be a preferential BACE1 substrate, with β4 cleavage not observed (Kim et al., 2007). Cleavage of β subunits by BACE1 generates a C-terminal fragment (CTF) which can be further processed by γ-secretase to release a shorter intracellular domain (ICD). BACE1-mediated cleavage of β subunits may play a role in normal cellular function. Overexpression of β4 promotes neurite outgrowth as well as production of dendritic filopodia (Oyama et al., 2006). Co-expression of β4 with BACE1 increases the extent of neurite outgrowth and decreases the numbers of filopodia formed. This effect is mediated specifically by the β4-CTF. BACE1 function has also been suggested to play a role in the modulation of neuronal membrane excitability and may have a role in neuronal function (Kim et al., 2007). This may

be a result of BACE1 cleavage of β2. In B104 rat neuroblastoma cells, BACE1 cleavage of β2 results in increased in *Scn1a*/$Na_v1.1$ mRNA and protein expression, and this effect was specifically dependent on the presence of the β2 ICD (Kim et al., 2007). In Alzheimer's disease patients, in which BACE1 levels are increased, $Na_v1.1$ expression was also increased. However, these channels were not properly localized to the plasma membrane due to cleavage of β2. It was not determined whether this improper localization of channels was due to inhibition of insertion into the plasma membrane, or increased turnover of channels (Kim et al., 2007). It has been suggested that the β2 ICD is involved in a feedback mechanism that contributes to the intracellular retention of $Na_v1.1$ (Willem et al., 2009). The effect of BACE1 cleavage products may differ between channel subtypes, as cells expressing $Na_v1.2$ did not show alterations in current density in the presence of BACE1 (Huth et al., 2009). Thus, similar to my results in *Scn2b* null mice in EAE, *Scn2b* and *Scn1a* expression appear to be linked in neurons. This will be the focus of future investigations.

Evidence has begun to emerge implicating BACE1 activity in disease and pathological processes beyond APP deposition in Alzheimer's disease. Deletion of BACE1 impairs remyelination of sciatic nerve after nerve crush injury, leading to a delay in remyelination as well as hypomyelination (Hu et al., 2008). This effect may be a result of BACE1 cleavage of the neuronal protein neuregulin-1 (NRG-1), which contributes to myelin protein expression as well as axon ensheathement. BACE1 expression can also be upregulated by cellular stress,

by cytokines released from activated microglia, and during conditions of acute hypoxia or energy deprivation (Willem et al., 2009).

BACE1 activity is reduced in the cerebrospinal fluid of MS patients, with a resultant decrease in BACE1 cleavage products (Mattsson et al., 2009). This decrease appears to be more severe in patients suffering from progressive disease as compared to relapsing-remitting disease, but this trend did not reach statistical significance. It also displays a weak correlation with disease duration and clinical disability (Mattsson et al., 2009). These data, combined with BACE1 cleavage of β2, the observations presented in this thesis regarding $Na_v1.1$ expression in MS and EAE, and the potential for BACE1 to be upregulated during hypoxia, suggest that the study of BACE1 activity during EAE in the *Scn2b* null mouse may offer valuable insights.

BIBLIOGRAPHY

Aboul-Enein F, Weiser P, Hoftberger R, Lassmann H, Bradl M (2006) Transient axonal injury in the absence of demyelination: a correlate of clinical disease in acute experimental autoimmune encephalomyelitis. Acta Neuropathol 111:539-547.

Adachi K, Toyota M, Sasaki Y, Yamashita T, Ishida S, Ohe-Toyota M, Maruyama R, Hinoda Y, Saito T, Imai K, Kudo R, Tokino T (2004) Identification of SCN3B as a novel p53-inducible proapoptotic gene. Oncogene 23:7791-7798.

Adelmann M, Wood J, Benzel I, Fiori P, Lassmann H, Matthieu JM, Gardinier MV, Dornmair K, Linington C (1995) The N-terminal domain of the myelin oligodendrocyte glycoprotein (MOG) induces acute demyelinating experimental autoimmune encephalomyelitis in the Lewis rat. J Neuroimmunol 63:17-27.

Agnew WS, Levinson SR, Brabson JS, Raftery MA (1978) Purification of the tetrodotoxin-binding component associated with the voltage-sensitive sodium channel from Electrophorus electricus electroplax membranes. Proc Natl Acad Sci U S A 75:2606-2610.

Aman TK, Grieco-Calub TM, Chen C, Rusconi R, Slat EA, Isom LL, Raman IM (2009) Regulation of persistent Na current by interactions between beta subunits of voltage-gated Na channels. J Neurosci 29:2027-2042.

Aronica E, Troost D, Rozemuller AJ, Yankaya B, Jansen GH, Isom LL, Gorter JA (2003) Expression and regulation of voltage-gated sodium channel beta1 subunit protein in human gliosis-associated pathologies. Acta Neuropathol 105:515-523.

Arroyo EJ, Xu T, Grinspan J, Lambert S, Levinson SR, Brophy PJ, Peles E, Scherer SS (2002) Genetic dysmyelination alters the molecular architecture of the nodal region. J Neurosci 22:1726-1737.

Ayers MM, Hazelwood LJ, Catmull DV, Wang D, McKormack Q, Bernard CC, Orian JM (2004) Early glial responses in murine models of multiple sclerosis. Neurochem Int 45:409-419.

Balcer LJ (2001) Clinical outcome measures for research in multiple sclerosis. J Neuroophthalmol 21:296-301.

Banasiak KJ, Burenkova O, Haddad GG (2004) Activation of voltage-sensitive sodium channels during oxygen deprivation leads to apoptotic neuronal death. Neuroscience 126:31-44.

Bannerman P, Hahn A, Soulika A, Gallo V, Pleasure D (2007) Astrogliosis in EAE spinal cord: derivation from radial glia, and relationships to oligodendroglia. Glia 55:57-64.

Bansal R, Stefansson K, Pfeiffer SE (1992) Proligodendroblast antigen (POA), a developmental antigen expressed by A007/O4-positive oligodendrocyte progenitors prior to the appearance of sulfatide and galactocerebroside. J Neurochem 58:2221-2229.

Barres BA (2008) The mystery and magic of glia: a perspective on their roles in health and disease. Neuron 60:430-440.

Barres BA, Raff MC (1999) Axonal control of oligodendrocyte development. J Cell Biol 147:1123-1128.

Barres BA, Chun LL, Corey DP (1989) Glial and neuronal forms of the voltage-dependent sodium channel: characteristics and cell-type distribution. Neuron 2:1375-1388.
Barres BA, Chun LL, Corey DP (1990a) Ion channels in vertebrate glia. Annu Rev Neurosci 13:441-474.
Barres BA, Koroshetz WJ, Swartz KJ, Chun LL, Corey DP (1990b) Ion channel expression by white matter glia: the O-2A glial progenitor cell. Neuron 4:507-524.
Baumann N, Pham-Dinh D (2001) Biology of oligodendrocyte and myelin in the mammalian central nervous system. Physiol Rev 81:871-927.
Bechtold DA, Smith KJ (2005a) Sodium-mediated axonal degeneration in inflammatory demyelinating disease. Journal of the Neurological Sciences 233:27-35.
Bechtold DA, Smith KJ (2005b) Sodium-mediated axonal degeneration in inflammatory demyelinating disease. J Neurol Sci 233:27-35.
Bechtold DA, Kapoor R, Smith KJ (2004) Axonal protection using flecainide in experimental autoimmune encephalomyelitis. Ann Neurol 55:607-616.
Bechtold DA, Yue X, Evans RM, Davies M, Gregson NA, Smith KJ (2005) Axonal protection in experimental autoimmune neuritis by the sodium channel blocking agent flecainide. Brain 128:18-28.
Bechtold DA, Miller SJ, Dawson AC, Sun Y, Kapoor R, Berry D, Smith KJ (2006) Axonal protection achieved in a model of multiple sclerosis using lamotrigine. J Neurol 253:1542-1551.
Beckh S, Noda M, Lubbert H, Numa S (1989) Differential regulation of three sodium channel messenger RNAs in the rat central nervous system during development. EMBO J 8:3611-3616.
Belachew S, Chittajallu R, Aguirre AA, Yuan X, Kirby M, Anderson S, Gallo V (2003) Postnatal NG2 proteoglycan-expressing progenitor cells are intrinsically multipotent and generate functional neurons. J Cell Biol 161:169-186.
Bernard CC, Johns TG, Slavin A, Ichikawa M, Ewing C, Liu J, Bettadapura J (1997) Myelin oligodendrocyte glycoprotein: a novel candidate autoantigen in multiple sclerosis. J Mol Med 75:77-88.
Besancon E, Guo S, Lok J, Tymianski M, Lo EH (2008) Beyond NMDA and AMPA glutamate receptors: emerging mechanisms for ionic imbalance and cell death in stroke. Trends in pharmacological sciences 29:268-275.
Bevan S, Lindsay RM, Perkins MN, Raff MC (1987) Voltage gated ionic channels in rat cultured astrocytes, reactive astrocytes and an astrocyte-oligodendrocyte progenitor cell. J Physiol (Paris) 82:327-335.
Bhat MA, Rios JC, Lu Y, Garcia-Fresco GP, Ching W, St Martin M, Li J, Einheber S, Chesler M, Rosenbluth J, Salzer JL, Bellen HJ (2001) Axon-glia interactions and the domain organization of myelinated axons requires neurexin IV/Caspr/Paranodin. Neuron 30:369-383.
Bielefeldt K, Whiteis CA, Chapleau MW, Abboud FM (1999) Nitric oxide enhances slow inactivation of voltage-dependent sodium currents in rat nodose neurons. Neuroscience letters 271:159-162.

Bishop A, Hobbs KG, Eguchi A, Jeffrey S, Smallwood L, Pennie C, Anderson J, Estevez AG (2009) Differential sensitivity of oligodendrocytes and motor neurons to reactive nitrogen species: implications for multiple sclerosis. J Neurochem 109:93-104.
Bitsch A, Schuchardt J, Bunkowski S, Kuhlmann T, Bruck W (2000) Acute axonal injury in multiple sclerosis. Correlation with demyelination and inflammation. Brain 123 (Pt 6):1174-1183.
Bjartmar C, Yin X, Trapp BD (1999) Axonal pathology in myelin disorders. J Neurocytol 28:383-395.
Bjartmar C, Wujek JR, Trapp BD (2003) Axonal loss in the pathology of MS: consequences for understanding the progressive phase of the disease. J Neurol Sci 206:165-171.
Bjartmar C, Kidd G, Mork S, Rudick R, Trapp BD (2000) Neurological disability correlates with spinal cord axonal loss and reduced N-acetyl aspartate in chronic multiple sclerosis patients. Ann Neurol 48:893-901.
Bjartmar C, Kinkel RP, Kidd G, Rudick RA, Trapp BD (2001) Axonal loss in normal-appearing white matter in a patient with acute MS. Neurology 57:1248-1252.
Black JA, Waxman SG, Smith KJ (2006a) Remyelination of dorsal column axons by endogenous Schwann cells restores the normal pattern of Nav1.6 and Kv1.2 at nodes of Ranvier. Brain 129:1319-1329.
Black JA, Liu S, Waxman SG (2008) Sodium channel activity modulates multiple functions in microglia. Glia 57:1072-1081.
Black JA, Newcombe J, Trapp BD, Waxman SG (2007a) Sodium channel expression within chronic multiple sclerosis plaques. J Neuropathol Exp Neurol 66:828-837.
Black JA, Felts P, Smith KJ, Kocsis JD, Waxman SG (1991) Distribution of sodium channels in chronically demyelinated spinal cord axons: immuno-ultrastructural localization and electrophysiological observations. Brain Res 544:59-70.
Black JA, Yokoyama S, Higashida H, Ransom BR, Waxman SG (1994a) Sodium channel mRNAs I, II and III in the CNS: cell-specific expression. Brain Res Mol Brain Res 22:275-289.
Black JA, Liu S, Hains BC, Saab CY, Waxman SG (2006b) Long-term protection of central axons with phenytoin in monophasic and chronic-relapsing EAE. Brain 129:3196-3208.
Black JA, Liu S, Carrithers M, Carrithers LM, Waxman SG (2007b) Exacerbation of experimental autoimmune encephalomyelitis after withdrawal of phenytoin and carbamazepine. Ann Neurol 62:21-33.
Black JA, Dib-Hajj S, Baker D, Newcombe J, Cuzner ML, Waxman SG (2000) Sensory neuron-specific sodium channel SNS is abnormally expressed in the brains of mice with experimental allergic encephalomyelitis and humans with multiple sclerosis. Proc Natl Acad Sci U S A 97:11598-11602.
Black JA, Yokoyama S, Waxman SG, Oh Y, Zur KB, Sontheimer H, Higashida H, Ransom BR (1994b) Sodium channel mRNAs in cultured spinal cord

astrocytes: in situ hybridization in identified cell types. Brain Res Mol Brain Res 23:235-245.
Boiko T, Van Wart A, Caldwell JH, Levinson SR, Trimmer JS, Matthews G (2003) Functional specialization of the axon initial segment by isoform-specific sodium channel targeting. J Neurosci 23:2306-2313.
Boiko T, Rasband M, Levinson S, Caldwell J, Mandel G, Trimmer J, Matthews G (2001a) Compact myelin dictates the differential targeting of two sodium channel isoforms in the same axon. Neuron 30:91-104.
Boiko T, Rasband MN, Levinson SR, Caldwell JH, Mandel G, Trimmer JS, Matthews G (2001b) Compact myelin dictates the differential targeting of two sodium channel isoforms in the same axon. Neuron 30:91-104.
Borges K, Wolswijk G, Ohlemeyer C, Kettenmann H (1995) Adult rat optic nerve oligodendrocyte progenitor cells express a distinct repertoire of voltage- and ligand-gated ion channels. J Neurosci Res 40:591-605.
Bottenstein JE (1986) Growth requirements in vitro of oligodendrocyte cell lines and neonatal rat brain oligodendrocytes. Proc Natl Acad Sci U S A 83:1955-1959.
Boyle ME, Berglund EO, Murai KK, Weber L, Peles E, Ranscht B (2001) Contactin orchestrates assembly of the septate-like junctions at the paranode in myelinated peripheral nerve. Neuron 30:385-397.
Brackenbury WJ, Djamgoz MB (2006) Activity-dependent regulation of voltage-gated Na+ channel expression in Mat-LyLu rat prostate cancer cell line. J Physiol 573:343-356.
Brackenbury WJ, Isom LL (2008) Voltage-gated Na+ channels: potential for beta subunits as therapeutic targets. Expert Opin Ther Targets 12:1191-1203.
Brackenbury WJ, Djamgoz MB, Isom LL (2008a) An emerging role for voltage-gated Na+ channels in cellular migration: regulation of central nervous system development and potentiation of invasive cancers. Neuroscientist 14:571-583.
Brackenbury WJ, Chioni AM, Diss JK, Djamgoz MB (2007) The neonatal splice variant of Nav1.5 potentiates in vitro invasive behaviour of MDA-MB-231 human breast cancer cells. Breast Cancer Res Treat 101:149-160.
Brackenbury WJ, Davis TH, Chen C, Slat EA, Detrow MJ, Dickendesher TL, Ranscht B, Isom LL (2008b) Voltage-gated Na+ channel beta1 subunit-mediated neurite outgrowth requires Fyn kinase and contributes to postnatal CNS development in vivo. J Neurosci 28:3246-3256.
Brand-Schieber E, Werner P (2004) Calcium channel blockers ameliorate disease in a mouse model of multiple sclerosis. Exp Neurol 189:5-9.
Brown DA, Sawchenko PE (2007) Time course and distribution of inflammatory and neurodegenerative events suggest structural bases for the pathogenesis of experimental autoimmune encephalomyelitis. J Comp Neurol 502:236-260.
Brysch W, Creutzfeldt OD, Luno K, Schlingensiepen R, Schlingensiepen KH (1991) Regional and temporal expression of sodium channel messenger RNAs in the rat brain during development. Exp Brain Res 86:562-567.

Burbidge SA, Dale TJ, Powell AJ, Whitaker WR, Xie XM, Romanos MA, Clare JJ (2002) Molecular cloning, distribution and functional analysis of the NA(V)1.6. Voltage-gated sodium channel from human brain. Brain Res Mol Brain Res 103:80-90.

Butt AM, Duncan A, Hornby MF, Kirvell SL, Hunter A, Levine JM, Berry M (1999) Cells expressing the NG2 antigen contact nodes of Ranvier in adult CNS white matter. Glia 26:84-91.

Cahoy JD, Emery B, Kaushal A, Foo LC, Zamanian JL, Christopherson KS, Xing Y, Lubischer JL, Krieg PA, Krupenko SA, Thompson WJ, Barres BA (2008) A transcriptome database for astrocytes, neurons, and oligodendrocytes: a new resource for understanding brain development and function. J Neurosci 28:264-278.

Calabrese M, Rocca MA, Atzori M, Mattisi I, Bernardi V, Favaretto A, Barachino L, Romualdi C, Rinaldi L, Perini P, Gallo P, Filippi M (2009) Cortical lesions in primary progressive multiple sclerosis: a 2-year longitudinal MR study. Neurology 72:1330-1336.

Caldwell JH, Schaller KL, Lasher RS, Peles E, Levinson SR (2000) Sodium channel Na(v)1.6 is localized at nodes of ranvier, dendrites, and synapses. Proc Natl Acad Sci U S A 97:5616-5620.

Carson MJ (2002) Microglia as liaisons between the immune and central nervous systems: functional implications for multiple sclerosis. Glia 40:218-231.

Catterall WA (1992) Cellular and molecular biology of voltage-gated sodium channels. Physiol Rev 72:S15-48.

Catterall WA (2000) From ionic currents to molecular mechanisms: the structure and function of voltage-gated sodium channels. Neuron 26:13-25.

Catterall WA, Goldin AL, Waxman SG (2003) International Union of Pharmacology. XXXIX. Compendium of voltage-gated ion channels: sodium channels. Pharmacol Rev 55:575-578.

Catterall WA, Goldin AL, Waxman SG (2005) International Union of Pharmacology. XLVII. Nomenclature and structure-function relationships of voltage-gated sodium channels. Pharmacol Rev 57:397-409.

Catterall WA, Dib-Hajj S, Meisler MH, Pietrobon D (2008) Inherited neuronal ion channelopathies: new windows on complex neurological diseases. J Neurosci 28:11768-11777.

Catterall WA, Cestele S, Yarov-Yarovoy V, Yu FH, Konoki K, Scheuer T (2007) Voltage-gated ion channels and gating modifier toxins. Toxicon 49:124-141.

Cestele S, Catterall WA (2000) Molecular mechanisms of neurotoxin action on voltage-gated sodium channels. Biochimie 82:883-892.

Chabas D, Baranzini SE, Mitchell D, Bernard CC, Rittling SR, Denhardt DT, Sobel RA, Lock C, Karpuj M, Pedotti R, Heller R, Oksenberg JR, Steinman L (2001) The influence of the proinflammatory cytokine, osteopontin, on autoimmune demyelinating disease. Science 294:1731-1735.

Chard D, Miller D (2009) Is multiple sclerosis a generalized disease of the central nervous system? An MRI perspective. Curr Opin Neurol 22:214-218.

Chen C, Dickendesher TL, Oyama F, Miyazaki H, Nukina N, Isom LL (2007) Floxed allele for conditional inactivation of the voltage-gated sodium channel beta1 subunit Scn1b. Genesis 45:547-553.

Chen C, Bharucha V, Chen Y, Westenbroek RE, Brown A, Malhotra JD, Jones D, Avery C, Gillespie PJ, 3rd, Kazen-Gillespie KA, Kazarinova-Noyes K, Shrager P, Saunders TL, Macdonald RL, Ransom BR, Scheuer T, Catterall WA, Isom LL (2002) Reduced sodium channel density, altered voltage dependence of inactivation, and increased susceptibility to seizures in mice lacking sodium channel beta 2-subunits. Proc Natl Acad Sci U S A 99:17072-17077.

Chen C, Westenbroek RE, Xu X, Edwards CA, Sorenson DR, Chen Y, McEwen DP, O'Malley HA, Bharucha V, Meadows LS, Knudsen GA, Vilaythong A, Noebels JL, Saunders TL, Scheuer T, Shrager P, Catterall WA, Isom LL (2004) Mice lacking sodium channel beta1 subunits display defects in neuronal excitability, sodium channel expression, and nodal architecture. J Neurosci 24:4030-4042.

Chioni AM, Brackenbury WJ, Calhoun JD, Isom LL, Djamgoz MB (2009) A novel adhesion molecule in human breast cancer cells: voltage-gated Na+ channel beta1 subunit. Int J Biochem Cell Biol 41:1216-1227.

Chittajallu R, Aguirre A, Gallo V (2004) NG2-positive cells in the mouse white and grey matter display distinct physiological properties. J Physiol 561:109-122.

Coleman M (2005) Axon degeneration mechanisms: commonality amid diversity. Nat Rev Neurosci 6:889-898.

Coman I, Aigrot MS, Seilhean D, Reynolds R, Girault JA, Zalc B, Lubetzki C (2006) Nodal, paranodal and juxtaparanodal axonal proteins during demyelination and remyelination in multiple sclerosis. Brain 129:3186-3195.

Courtney AM, Treadaway K, Remington G, Frohman E (2009) Multiple sclerosis. Med Clin North Am 93:451-476, ix-x.

Coward K, Jowett A, Plumpton C, Powell A, Birch R, Tate S, Bountra C, Anand P (2001) Sodium channel beta1 and beta2 subunits parallel SNS/PN3 alpha-subunit changes in injured human sensory neurons. Neuroreport 12:483-488.

Craner MJ, Lo AC, Black JA, Waxman SG (2003a) Abnormal sodium channel distribution in optic nerve axons in a model of inflammatory demyelination. Brain 126:1552-1561.

Craner MJ, Hains BC, Lo AC, Black JA, Waxman SG (2004a) Co-localization of sodium channel Nav1.6 and the sodium-calcium exchanger at sites of axonal injury in the spinal cord in EAE. Brain 127:294-303.

Craner MJ, Newcombe J, Black JA, Hartle C, Cuzner ML, Waxman SG (2004b) Molecular changes in neurons in multiple sclerosis: altered axonal expression of Nav1.2 and Nav1.6 sodium channels and Na+/Ca2+ exchanger. Proc Natl Acad Sci U S A 101:8168-8173.

Craner MJ, Lo AC, Black JA, Baker D, Newcombe J, Cuzner ML, Waxman SG (2003b) Annexin II/p11 is up-regulated in Purkinje cells in EAE and MS. Neuroreport 14:555-558.
Craner MJ, Damarjian TG, Liu S, Hains BC, Lo AC, Black JA, Newcombe J, Cuzner ML, Waxman SG (2005) Sodium channels contribute to microglia/macrophage activation and function in EAE and MS. Glia 49:220-229.
Crill WE (1996) Persistent sodium current in mammalian central neurons. Annu Rev Physiol 58:349-362.
Cummins TR, Dib-Hajj SD, Herzog RI, Waxman SG (2005) Nav1.6 channels generate resurgent sodium currents in spinal sensory neurons. FEBS Lett 579:2166-2170.
Dal Canto MC, Melvold RW, Kim BS, Miller SD (1995) Two models of multiple sclerosis: experimental allergic encephalomyelitis (EAE) and Theiler's murine encephalomyelitis virus (TMEV) infection. A pathological and immunological comparison. Microsc Res Tech 32:215-229.
Damarjian TG, Craner MJ, Black JA, Waxman SG (2004) Upregulation and colocalization of p75 and Nav1.8 in Purkinje neurons in experimental autoimmune encephalomyelitis. Neurosci Lett 369:186-190.
Dave JR, Lin Y, Ved HS, Koenig ML, Clapp L, Hunter J, Tortella FC (2001) RS-100642-198, a novel sodium channel blocker, provides differential neuroprotection against hypoxia/hypoglycemia, veratridine or glutamate-mediated neurotoxicity in primary cultures of rat cerebellar neurons. Neurotox Res 3:381-395.
Davis TH, Chen C, Isom LL (2004) Sodium channel beta1 subunits promote neurite outgrowth in cerebellar granule neurons. J Biol Chem 279:51424-51432.
DeLuca GC, Ebers GC, Esiri MM (2004) Axonal loss in multiple sclerosis: a pathological survey of the corticospinal and sensory tracts. Brain 127:1009-1018.
DeLuca GC, Williams K, Evangelou N, Ebers GC, Esiri MM (2006) The contribution of demyelination to axonal loss in multiple sclerosis. Brain 129:1507-1516.
Demerens C, Stankoff B, Logak M, Anglade P, Allinquant B, Couraud F, Zalc B, Lubetzki C (1996) Induction of myelination in the central nervous system by electrical activity. Proc Natl Acad Sci U S A 93:9887-9892.
Derfuss T, Parikh K, Velhin S, Braun M, Mathey E, Krumbholz M, Kumpfel T, Moldenhauer A, Rader C, Sonderegger P, Pollmann W, Tiefenthaller C, Bauer J, Lassmann H, Wekerle H, Karagogeos D, Hohlfeld R, Linington C, Meinl E (2009) Contactin-2/TAG-1-directed autoimmunity is identified in multiple sclerosis patients and mediates gray matter pathology in animals. Proc Natl Acad Sci U S A 106:8302-8307.
Devaux JJ, Scherer SS (2005) Altered ion channels in an animal model of Charcot-Marie-Tooth disease type IA. J Neurosci 25:1470-1480.

Dib-Hajj SD, Waxman SG (1995) Genes encoding the beta 1 subunit of voltage-dependent Na+ channel in rat, mouse and human contain conserved introns. FEBS Lett 377:485-488.
Dubois-Dalcq M, fFrench-Constant C, Franklin RJ (2005) Enhancing central nervous system remyelination in multiple sclerosis. Neuron 48:9-12.
Duflocq A, Le Bras B, Bullier E, Couraud F, Davenne M (2008) Nav1.1 is predominantly expressed in nodes of Ranvier and axon initial segments. Mol Cell Neurosci 39:180-192.
Dugandzija-Novakovic S, Koszowski AG, Levinson SR, Shrager P (1995) Clustering of Na+ channels and node of Ranvier formation in remyelinating axons. J Neurosci 15:492-503.
Dutta R, Trapp BD (2007) Pathogenesis of axonal and neuronal damage in multiple sclerosis. Neurology 68:S22-31; discussion S43-54.
Dutta R, McDonough J, Yin X, Peterson J, Chang A, Torres T, Gudz T, Macklin WB, Lewis DA, Fox RJ, Rudick R, Mirnics K, Trapp BD (2006) Mitochondrial dysfunction as a cause of axonal degeneration in multiple sclerosis patients. Ann Neurol 59:478-489.
Dyer CA, Benjamins JA (1988) Antibody to galactocerebroside alters organization of oligodendroglial membrane sheets in culture. J Neurosci 8:4307-4318.
Einheber S, Zanazzi G, Ching W, Scherer S, Milner TA, Peles E, Salzer JL (1997) The axonal membrane protein Caspr, a homologue of neurexin IV, is a component of the septate-like paranodal junctions that assemble during myelination. J Cell Biol 139:1495-1506.
Eisenbarth GS, Walsh FS, Nirenberg M (1979) Monoclonal antibody to a plasma membrane antigen of neurons. Proc Natl Acad Sci U S A 76:4913-4917.
Emerson MR, Gallagher RJ, Marquis JG, LeVine SM (2009) Enhancing the ability of experimental autoimmune encephalomyelitis to serve as a more rigorous model of multiple sclerosis through refinement of the experimental design. Comp Med 59:112-128.
England JD, Gamboni F, Levinson SR (1991) Increased numbers of sodium channels form along demyelinated axons. Brain Res 548:334-337.
England JD, Gamboni F, Levinson SR, Finger TE (1990) Changed distribution of sodium channels along demyelinated axons. ProcNatlAcadSciUSA 87:6777-6780.
Eubanks J, Srinivasan J, Dinulos MB, Disteche CM, Catterall WA (1997) Structure and chromosomal localization of the beta2 subunit of the human brain sodium channel. Neuroreport 8:2775-2779.
Evangelou N, Konz D, Esiri MM, Smith S, Palace J, Matthews PM (2001) Size-selective neuronal changes in the anterior optic pathways suggest a differential susceptibility to injury in multiple sclerosis. Brain 124:1813-1820.
Fein AJ, Meadows LS, Chen C, Slat EA, Isom LL (2007) Cloning and expression of a zebrafish SCN1B ortholog and identification of a species-specific splice variant. BMC Genomics 8:226.

Felts PA, Black JA, Waxman SG (1995) Expression of sodium channel alpha- and beta-subunits in the nervous system of the myelin-deficient rat. J Neurocytol 24:654-666.
Ferguson B, Matyszak MK, Esiri MM, Perry VH (1997) Axonal damage in acute multiple sclerosis lesions. Brain 120 (Pt 3):393-399.
Fern R, Ransom BR, Stys PK, Waxman SG (1993) Pharmacological protection of CNS white matter during anoxia: actions of phenytoin, carbamazepine and diazepam. The Journal of pharmacology and experimental therapeutics 266:1549-1555.
Fields RD (2008) Oligodendrocytes changing the rules: action potentials in glia and oligodendrocytes controlling action potentials. Neuroscientist 14:540-543.
Fisher E, Lee JC, Nakamura K, Rudick RA (2008) Gray matter atrophy in multiple sclerosis: a longitudinal study. Ann Neurol 64:255-265.
Fisniku LK, Chard DT, Jackson JS, Anderson VM, Altmann DR, Miszkiel KA, Thompson AJ, Miller DH (2008) Gray matter atrophy is related to long-term disability in multiple sclerosis. Ann Neurol 64:247-254.
Fok-Seang J, Miller RH (1994) Distribution and differentiation of A2B5+ glial precursors in the developing rat spinal cord. J Neurosci Res 37:219-235.
Forte M, Gold BG, Marracci G, Chaudhary P, Basso E, Johnsen D, Yu X, Fowlkes J, Bernardi P, Bourdette D (2007) Cyclophilin D inactivation protects axons in experimental autoimmune encephalomyelitis, an animal model of multiple sclerosis. Proc Natl Acad Sci U S A 104:7558-7563.
Franklin RJ (2002) Why does remyelination fail in multiple sclerosis? Nat Rev Neurosci 3:705-714.
Franklin RJ, fFrench-Constant C (2008) Remyelination in the CNS: from biology to therapy. Nat Rev Neurosci 9:839-855.
Fraser SP et al. (2005) Voltage-gated sodium channel expression and potentiation of human breast cancer metastasis. Clin Cancer Res 11:5381-5389.
Frohman EM, Filippi M, Stuve O, Waxman SG, Corboy J, Phillips JT, Lucchinetti C, Wilken J, Karandikar N, Hemmer B, Monson N, De Keyser J, Hartung H, Steinman L, Oksenberg JR, Cree BA, Hauser S, Racke MK (2005) Characterizing the mechanisms of progression in multiple sclerosis: evidence and new hypotheses for future directions. Arch Neurol 62:1345-1356.
Gallo V, Armstrong RC (2008) Myelin repair strategies: a cellular view. Curr Opin Neurol 21:278-283.
Gambardella A, Marini C (2009) Clinical spectrum of SCN1A mutations. Epilepsia 50 Suppl 5:20-23.
Ganter P, Prince C, Esiri MM (1999) Spinal cord axonal loss in multiple sclerosis: a post-mortem study. Neuropathol Appl Neurobiol 25:459-467.
Gao L, Miller RH (2006) Specification of optic nerve oligodendrocyte precursors by retinal ganglion cell axons. J Neurosci 26:7619-7628.

Garrido JJ, Fernandes F, Giraud P, Mouret I, Pasqualini E, Fache MP, Jullien F, Dargent B (2001) Identification of an axonal determinant in the C-terminus of the sodium channel Na(v)1.2. EMBO J 20:5950-5961.
Garthwaite G, Goodwin DA, Batchelor AM, Leeming K, Garthwaite J (2002) Nitric oxide toxicity in CNS white matter: an in vitro study using rat optic nerve. Neuroscience 109:145-155.
Gehrmann J, Banati RB, Cuzner ML, Kreutzberg GW, Newcombe J (1995) Amyloid precursor protein (APP) expression in multiple sclerosis lesions. Glia 15:141-151.
Gennarini G, Cibelli G, Rougon G, Mattei MG, Goridis C (1989) The mouse neuronal cell surface protein F3: a phosphatidylinositol-anchored member of the immunoglobulin superfamily related to chicken contactin. J Cell Biol 109:775-788.
Geurts JJ, Barkhof F (2008) Grey matter pathology in multiple sclerosis. Lancet Neurol 7:841-851.
Gold R, Linington C, Lassmann H (2006) Understanding pathogenesis and therapy of multiple sclerosis via animal models: 70 years of merits and culprits in experimental autoimmune encephalomyelitis research. Brain 129:1953-1971.
Gong B, Rhodes KJ, Bekele-Arcuri Z, Trimmer JS (1999) Type I and type II Na(+) channel alpha-subunit polypeptides exhibit distinct spatial and temporal patterning, and association with auxiliary subunits in rat brain. J Comp Neurol 412:342-352.
Goodin DS (2009) The causal cascade to multiple sclerosis: a model for MS pathogenesis. PLoS ONE 4:e4565.
Gordienko DV, Tsukahara H (1994) Tetrodotoxin-blockable depolarization-activated Na+ currents in a cultured endothelial cell line derived from rat interlobar arter and human umbilical vein. Pflugers Arch 428:91-93.
Gordon D, Merrick D, Auld V, Dunn R, Goldin AL, Davidson N, Catterall WA (1987) Tissue-specific expression of the RI and RII sodium channel subtypes. Proc Natl Acad Sci U S A 84:8682-8686.
Gorter JA, van Vliet EA, Lopes da Silva FH, Isom LL, Aronica E (2002) Sodium channel beta1-subunit expression is increased in reactive astrocytes in a rat model for mesial temporal lobe epilepsy. Eur J Neurosci 16:360-364.
Gosling M, Harley SL, Turner RJ, Carey N, Powell JT (1998) Human saphenous vein endothelial cells express a tetrodotoxin-resistant, voltage-gated sodium current. J Biol Chem 273:21084-21090.
Grant AO (2001) Molecular biology of sodium channels and their role in cardiac arrhythmias. Am J Med 110:296-305.
Grieco TM, Malhotra JD, Chen C, Isom LL, Raman IM (2005a) Open-channel block by the cytoplasmic tail of sodium channel β4 as a mechanism for resurgent sodium current. Neuron 45:233-244.
Grieco TM, Malhotra JD, Chen C, Isom LL, Raman IM (2005b) Open-channel block by the cytoplasmic tail of sodium channel beta4 as a mechanism for resurgent sodium current. Neuron 45:233-244.

Guy HR, Seetharamulu P (1986) Molecular model of the action potential sodium channel. Proc Natl Acad Sci U S A 83:508-512.
Hains BC, Waxman SG (2005) Neuroprotection by sodium channel blockade with phenytoin in an experimental model of glaucoma. Invest Ophthalmol Vis Sci 46:4164-4169.
Hains BC, Saab CY, Lo AC, Waxman SG (2004) Sodium channel blockade with phenytoin protects spinal cord axons, enhances axonal conduction, and improves functional motor recovery after contusion SCI. Exp Neurol 188:365-377.
Hakim P, Gurung IS, Pedersen TH, Thresher R, Brice N, Lawrence J, Grace AA, Huang CL (2008) Scn3b knockout mice exhibit abnormal ventricular electrophysiological properties. Prog Biophys Mol Biol 98:251-266.
Hammarstrom AK, Gage PW (1999) Nitric oxide increases persistent sodium current in rat hippocampal neurons. J Physiol 520 Pt 2:451-461.
Hampton DW, Anderson J, Pryce G, Irvine KA, Giovannoni G, Fawcett JW, Compston A, Franklin RJ, Baker D, Chandran S (2008) An experimental model of secondary progressive multiple sclerosis that shows regional variation in gliosis, remyelination, axonal and neuronal loss. J Neuroimmunol 201-202:200-211.
Hansson E, Ronnback L (2003) Glial neuronal signaling in the central nervous system. FASEB J 17:341-348.
Hartline DK, Colman DR (2007) Rapid conduction and the evolution of giant axons and myelinated fibers. Curr Biol 17:R29-35.
Hartmann HA, Colom LV, Sutherland ML, Noebels JL (1999) Selective localization of cardiac SCN5A sodium channels in limbic regions of rat brain. Nat Neurosci 2:593-595.
Hartshorne RP, Catterall WA (1984) The sodium channel from rat brain. Purification and subunit composition. J Biol Chem 259:1667-1675.
Hassen GW, Feliberti J, Kesner L, Stracher A, Mokhtarian F (2008) Prevention of axonal injury using calpain inhibitor in chronic progressive experimental autoimmune encephalomyelitis. Brain Res 1236:206-215.
Hemmings HC, Jr. (2004) Neuroprotection by Na+ channel blockade. J Neurosurg Anesthesiol 16:100-101.
Henderson R, Ritchie JM, Strichartz GR (1973) The binding of labelled saxitoxin to the sodium channels in nerve membranes. J Physiol 235:783-804.
Henry MA, Freking AR, Johnson LR, Levinson SR (2006) Increased sodium channel immunofluorescence at myelinated and demyelinated sites following an inflammatory and partial axotomy lesion of the rat infraorbital nerve. Pain 124:222-233.
Herrero-Herranz E, Pardo LA, Gold R, Linker RA (2008) Pattern of axonal injury in murine myelin oligodendrocyte glycoprotein induced experimental autoimmune encephalomyelitis: implications for multiple sclerosis. Neurobiol Dis 30:162-173.
Herrero-Herranz E, Pardo LA, Bunt G, Gold R, Stuhmer W, Linker RA (2007) Re-expression of a developmentally restricted potassium channel in

autoimmune demyelination: Kv1.4 is implicated in oligodendroglial proliferation. Am J Pathol 171:589-598.
Herzog RI, Cummins TR, Ghassemi F, Dib-Hajj SD, Waxman SG (2003) Distinct repriming and closed-state inactivation kinetics of Nav1.6 and Nav1.7 sodium channels in mouse spinal sensory neurons. J Physiol 551:741-750.
Hewitt KE, Stys PK, Lesiuk HJ (2001) The use-dependent sodium channel blocker mexiletine is neuroprotective against global ischemic injury. Brain Res 898:281-287.
Hobom M, Storch MK, Weissert R, Maier K, Radhakrishnan A, Kramer B, Bahr M, Diem R (2004) Mechanisms and time course of neuronal degeneration in experimental autoimmune encephalomyelitis. Brain Pathol 14:148-157.
Hodgkin AL, Huxley AF (1952) A quantitative description of membrane current and its application to conduction and excitation in nerve. J Physiol 117:500-544.
Holley JE, Gveric D, Newcombe J, Cuzner ML, Gutowski NJ (2003) Astrocyte characterization in the multiple sclerosis glial scar. Neuropathol Appl Neurobiol 29:434-444.
Howell OW, Palser A, Polito A, Melrose S, Zonta B, Scheiermann C, Vora AJ, Brophy PJ, Reynolds R (2006) Disruption of neurofascin localization reveals early changes preceding demyelination and remyelination in multiple sclerosis. Brain 129:3173-3185.
Hu X, He W, Diaconu C, Tang X, Kidd GJ, Macklin WB, Trapp BD, Yan R (2008) Genetic deletion of BACE1 in mice affects remyelination of sciatic nerves. FASEB J 22:2970-2980.
Huizinga R, Gerritsen W, Heijmans N, Amor S (2008) Axonal loss and gray matter pathology as a direct result of autoimmunity to neurofilaments. Neurobiol Dis 32:461-470.
Huth T, Schmidt-Neuenfeldt K, Rittger A, Saftig P, Reiss K, Alzheimer C (2009) Non-proteolytic effect of beta-site APP-cleaving enzyme 1 (BACE1) on sodium channel function. Neurobiol Dis 33:282-289.
Inglese M, Ge Y, Filippi M, Falini A, Grossman RI, Gonen O (2004) Indirect evidence for early widespread gray matter involvement in relapsing-remitting multiple sclerosis. Neuroimage 21:1825-1829.
Isom LL (2001) Sodium channel beta subunits: anything but auxiliary. Neuroscientist 7:42-54.
Isom LL (2002) The role of sodium channels in cell adhesion. Front Biosci 7:12-23.
Isom LL, Catterall WA (1996) Na+ channel subunits and Ig domains. Nature 383:307-308.
Isom LL, De Jongh KS, Catterall WA (1994) Auxiliary subunits of voltage-gated ion channels. Neuron 12:1183-1194.
Isom LL, Scheuer T, Brownstein AB, Ragsdale DS, Murphy BJ, Catterall WA (1995a) Functional co-expression of the beta 1 and type IIA alpha subunits of sodium channels in a mammalian cell line. J Biol Chem 270:3306-3312.

Isom LL, Scheuer T, Brownstein AB, Ragsdale DS, Murphy BJ, Catterall WA (1995b) Functional co-expression of the β1 and type IIA α subunits of sodium channels in a mammalian cell line. J Biol Chem 270:3306-3312.
Isom LL, Ragsdale DS, De Jongh KS, Westenbroek RE, Reber BF, Scheuer T, Catterall WA (1995c) Structure and function of the beta 2 subunit of brain sodium channels, a transmembrane glycoprotein with a CAM motif. Cell 83:433-442.
Isom LL, De Jongh KS, Patton DE, Reber BF, Offord J, Charbonneau H, Walsh K, Goldin AL, Catterall WA (1992) Primary structure and functional expression of the beta 1 subunit of the rat brain sodium channel. Science 256:839-842.
Jackson SJ, Lee J, Nikodemova M, Fabry Z, Duncan ID (2009) Quantification of Myelin and Axon Pathology During Relapsing Progressive Experimental Autoimmune Encephalomyelitis in the Biozzi ABH Mouse. J Neuropathol Exp Neurol 68:616-625.
Jiang Y, Ruta V, Chen J, Lee A, MacKinnon R (2003a) The principle of gating charge movement in a voltage-dependent K+ channel. Nature 423:42-48.
Jiang Y, Lee A, Chen J, Ruta V, Cadene M, Chait BT, MacKinnon R (2003b) X-ray structure of a voltage-dependent K+ channel. Nature 423:33-41.
Johnson D, Bennett ES (2006) Isoform-specific effects of the beta2 subunit on voltage-gated sodium channel gating. J Biol Chem 281:25875-25881.
Jones JM, Meisler MH, Isom LL (1996) Scn2b, a voltage-gated sodium channel beta2 gene on mouse chromosome 9. Genomics 34:258-259.
Jones MV, Nguyen TT, Deboy CA, Griffin JW, Whartenby KA, Kerr DA, Calabresi PA (2008) Behavioral and pathological outcomes in MOG 35-55 experimental autoimmune encephalomyelitis. J Neuroimmunol 199:83-93.
Kalume F, Yu FH, Westenbroek RE, Scheuer T, Catterall WA (2007) Reduced sodium current in Purkinje neurons from Nav1.1 mutant mice: implications for ataxia in severe myoclonic epilepsy in infancy. J Neurosci 27:11065-11074.
Kandel ER, Schwartz JH, Jessell TM (2000) Principles of neural science, 4th Edition. New York: McGraw-Hill, Health Professions Division.
Kaplan MR, Cho M-H, Ullian EM, Isom LL, Levinson SR, Barres BA (2001a) Differential control of clustering of the sodium channels Nav1.2 and Nav1.6 at developing CNS nodes of Ranvier. Neuron 30:105-119.
Kaplan MR, Cho MH, Ullian EM, Isom LL, Levinson SR, Barres BA (2001b) Differential control of clustering of the sodium channels Na(v)1.2 and Na(v)1.6 at developing CNS nodes of Ranvier. Neuron 30:105-119.
Kapoor R (2008) Sodium channel blockers and neuroprotection in multiple sclerosis using lamotrigine. J Neurol Sci.
Kapoor R, Davies M, Blaker PA, Hall SM, Smith KJ (2003) Blockers of sodium and calcium entry protect axons from nitric oxide-mediated degeneration. Ann Neurol 53:174-180.
Kaptanoglu E, Solaroglu I, Surucu HS, Akbiyik F, Beskonakli E (2005a) Blockade of sodium channels by phenytoin protects ultrastructure and attenuates

lipid peroxidation in experimental spinal cord injury. Acta Neurochir (Wien) 147:405-412.
Kaptanoglu E, Solaroglu I, Surucu HS, Akbiyik F, Beskonakli E (2005b) Blockade of sodium channels by phenytoin protects ultrastructure and attenuates lipid peroxidation in experimental spinal cord injury. Acta Neurochir (Wien) 147:405-412; discussion 412.
Karadottir R, Hamilton NB, Bakiri Y, Attwell D (2008) Spiking and nonspiking classes of oligodendrocyte precursor glia in CNS white matter. Nat Neurosci 11:450-456.
Kazarinova-Noyes K, Shrager P (2002) Molecular constituents of the node of Ranvier. Mol Neurobiol 26:167-182.
Kazarinova-Noyes K, Malhotra JD, McEwen DP, Mattei LN, Berglund EO, Ranscht B, Levinson SR, Schachner M, Shrager P, Isom LL, Xiao ZC (2001) Contactin associates with Na+ channels and increases their functional expression. J Neurosci 21:7517-7525.
Kazen-Gillespie KA, Ragsdale DS, D'Andrea MR, Mattei LN, Rogers KE, Isom LL (2000) Cloning, localization, and functional expression of sodium channel beta1A subunits. J Biol Chem 275:1079-1088.
Kearney JA, Buchner DA, De Haan G, Adamska M, Levin SI, Furay AR, Albin RL, Jones JM, Montal M, Stevens MJ, Sprunger LK, Meisler MH (2002) Molecular and pathological effects of a modifier gene on deficiency of the sodium channel Scn8a (Na(v)1.6). Hum Mol Genet 11:2765-2775.
Khan NA, Poisson JP (1999) 5-HT3 receptor-channels coupled with Na+ influx in human T cells: role in T cell activation. J Neuroimmunol 99:53-60.
Kim DY, Ingano LA, Carey BW, Pettingell WH, Kovacs DM (2005) Presenilin/gamma-secretase-mediated cleavage of the voltage-gated sodium channel beta2-subunit regulates cell adhesion and migration. J Biol Chem 280:23251-23261.
Kim DY, Carey BW, Wang H, Ingano LA, Binshtok AM, Wertz MH, Pettingell WH, He P, Lee VM, Woolf CJ, Kovacs DM (2007) BACE1 regulates voltage-gated sodium channels and neuronal activity. Nat Cell Biol 9:755-764.
Kolbe S, Chapman C, Nguyen T, Bajraszewski C, Johnston L, Kean M, Mitchell P, Paine M, Butzkueven H, Kilpatrick T, Egan G (2009) Optic nerve diffusion changes and atrophy jointly predict visual dysfunction after optic neuritis. Neuroimage 45:679-686.
Kole MH, Letzkus JJ, Stuart GJ (2007) Axon initial segment Kv1 channels control axonal action potential waveform and synaptic efficacy. Neuron 55:633-647.
Krafte DS, Snutch TP, Leonard JP, Davidson N, Lester HA (1988) Evidence for the involvement of more than one mRNA species in controlling the inactivation process of rat and rabbit brain Na channels expressed in Xenopus oocytes. J Neurosci 8:2859-2868.
Kuchroo VK, Anderson AC, Waldner H, Munder M, Bettelli E, Nicholson LB (2002) T cell response in experimental autoimmune encephalomyelitis (EAE): role of self and cross-reactive antigens in shaping, tuning, and

regulating the autopathogenic T cell repertoire. Annu Rev Immunol 20:101-123.
Kuerten S, Angelov DN (2008) Comparing the CNS morphology and immunobiology of different EAE models in C57BL/6 mice - a step towards understanding the complexity of multiple sclerosis. Ann Anat 190:1-15.
Kurnellas MP, Nicot A, Shull GE, Elkabes S (2005) Plasma membrane calcium ATPase deficiency causes neuronal pathology in the spinal cord: a potential mechanism for neurodegeneration in multiple sclerosis and spinal cord injury. Faseb J 19:298-300.
Kursula P (2008) Structural properties of proteins specific to the myelin sheath. Amino Acids 34:175-185.
Lai ZF, Chen YZ, Nishimura Y, Nishi K (2000) An amiloride-sensitive and voltage-dependent Na+ channel in an HLA-DR-restricted human T cell clone. J Immunol 165:83-90.
Lassmann H, Bartsch U, Montag D, Schachner M (1997) Dying-back oligodendrogliopathy: a late sequel of myelin-associated glycoprotein deficiency. Glia 19:104-110.
Lee SC, Moore GR, Golenwsky G, Raine CS (1990) Multiple sclerosis: a role for astroglia in active demyelination suggested by class II MHC expression and ultrastructural study. J Neuropathol Exp Neurol 49:122-136.
Lemaillet G, Walker B, Lambert S (2003) Identification of a conserved ankyrin-binding motif in the family of sodium channel alpha subunits. J Biol Chem 278:27333-27339.
Li HL, Galue A, Meadows L, Ragsdale DS (1999) A molecular basis for the different local anesthetic affinities of resting versus open and inactivated states of the sodium channel. Mol Pharmacol 55:134-141.
Li Z, Chapleau MW, Bates JN, Bielefeldt K, Lee HC, Abboud FM (1998) Nitric oxide as an autocrine regulator of sodium currents in baroreceptor neurons. Neuron 20:1039-1049.
Lo AC, Black JA, Waxman SG (2002) Neuroprotection of axons with phenytoin in experimental allergic encephalomyelitis. Neuroreport 13:1909-1912.
Lo AC, Saab CY, Black JA, Waxman SG (2003) Phenytoin protects spinal cord axons and preserves axonal conduction and neurological function in a model of neuroinflammation in vivo. J Neurophysiol 90:3566-3571.
Lonigro A, Devaux JJ (2009) Disruption of neurofascin and gliomedin at nodes of Ranvier precedes demyelination in experimental allergic neuritis. Brain 132:260-273.
Lopez-Santiago LF, Pertin M, Morisod X, Chen C, Hong S, Wiley J, Decosterd I, Isom LL (2006a) Sodium channel beta2 subunits regulate tetrodotoxin-sensitive sodium channels in small dorsal root ganglion neurons and modulate the response to pain. J Neurosci 26:7984-7994.
Lopez-Santiago LF, Pertin M, Morisod X, Chen C, Hong S, Wiley J, Decosterd I, Isom LL (2006b) Sodium channel β2 subunits regulate tetrodotoxin-sensitive sodium channels in small dorsal root ganglion neurons and modulate the response to pain. J Neurosci 26:7984-7994.

Lopez-Santiago LF, Meadows LS, Ernst SJ, Chen C, Malhotra JD, McEwen DP, Speelman A, Noebels JL, Maier SK, Lopatin AN, Isom LL (2007) Sodium channel Scn1b null mice exhibit prolonged QT and RR intervals. J Mol Cell Cardiol 43:636-647.

Lorincz A, Nusser Z (2008) Cell-type-dependent molecular composition of the axon initial segment. J Neurosci 28:14329-14340.

Lossin C, Rhodes TH, Desai RR, Vanoye CG, Wang D, Carniciu S, Devinsky O, George AL, Jr. (2003) Epilepsy-associated dysfunction in the voltage-gated neuronal sodium channel SCN1A. J Neurosci 23:11289-11295.

Ludwin SK (2006) The pathogenesis of multiple sclerosis: relating human pathology to experimental studies. J Neuropathol Exp Neurol 65:305-318.

Maier SK, Westenbroek RE, Schenkman KA, Feigl EO, Scheuer T, Catterall WA (2002) An unexpected role for brain-type sodium channels in coupling of cell surface depolarization to contraction in the heart. Proc Natl Acad Sci U S A 99:4073-4078.

Makita N, Sloan-Brown K, Weghuis DO, Ropers HH, George AL, Jr. (1994) Genomic organization and chromosomal assignment of the human voltage-gated Na+ channel beta 1 subunit gene (SCN1B). Genomics 23:628-634.

Malhotra JD, Kazen-Gillespie K, Hortsch M, Isom LL (2000a) Sodium channel beta subunits mediate homophilic cell adhesion and recruit ankyrin to points of cell-cell contact. J Biol Chem 275:11383-11388.

Malhotra JD, Kazen-Gillespie K, Hortsch M, Isom LL (2000b) Sodium channel β subunits mediate homophilic cell adhesion and recruit ankyrin to points of cell-cell contact. J Biol Chem 275:11383-11388.

Malhotra JD, Thyagarajan V, Chen C, Isom LL (2004) Tyrosine-phosphorylated and nonphosphorylated sodium channel beta1 subunits are differentially localized in cardiac myocytes. J Biol Chem 279:40748-40754.

Malhotra JD, Koopmann MC, Kazen-Gillespie KA, Fettman N, Hortsch M, Isom LL (2002) Structural requirements for interaction of sodium channel beta 1 subunits with ankyrin. J Biol Chem 277:26681-26688.

Mallon BS, Shick HE, Kidd GJ, Macklin WB (2002) Proteolipid promoter activity distinguishes two populations of NG2-positive cells throughout neonatal cortical development. J Neurosci 22:876-885.

Mattsson N et al. (2009) Reduced cerebrospinal fluid BACE1 activity in multiple sclerosis. Mult Scler 15:448-454.

McCarthy KD, de Vellis J (1980) Preparation of separate astroglial and oligodendroglial cell cultures from rat cerebral tissue. J Cell Biol 85:890-902.

McCormick KA, Srinivasan J, White K, Scheuer T, Catterall WA (1999) The extracellular domain of the beta1 subunit is both necessary and sufficient for beta1-like modulation of sodium channel gating. J Biol Chem 274:32638-32646.

McEwen DP, Isom LL (2004) Heterophilic interactions of sodium channel beta1 subunits with axonal and glial cell adhesion molecules. J Biol Chem 279:52744-52752.

McEwen DP, Chen C, Meadows LS, Lopez-Santiago L, Isom LL (2009) The voltage-gated Na(+) channel beta3 subunit does not mediate trans homophilic cell adhesion or associate with the cell adhesion molecule contactin. Neurosci Lett.
McLaurin JA, Yong VW (1995) Oligodendrocytes and myelin. Neurol Clin 13:23-49.
McQualter JL, Darwiche R, Ewing C, Onuki M, Kay TW, Hamilton JA, Reid HH, Bernard CC (2001) Granulocyte macrophage colony-stimulating factor: a new putative therapeutic target in multiple sclerosis. J Exp Med 194:873-882.
McTigue DM, Tripathi RB (2008) The life, death, and replacement of oligodendrocytes in the adult CNS. J Neurochem 107:1-19.
Meadows LS, Isom LL (2005) Sodium channels as macromolecular complexes: implications for inherited arrhythmia syndromes. Cardiovascular Research 67:448-458.
Meadows LS, Malhotra J, Loukas A, Thyagarajan V, Kazen-Gillespie KA, Koopman MC, Kriegler S, Isom LL, Ragsdale DS (2002) Functional and biochemical analysis of a sodium channel beta1 subunit mutation responsible for generalized epilepsy with febrile seizures plus type 1. J Neurosci 22:10699-10709.
Meisler MH, Plummer NW, Burgess DL, Buchner DA, Sprunger LK (2004) Allelic mutations of the sodium channel SCN8A reveal multiple cellular and physiological functions. Genetica 122:37-45.
Messner DJ, Feller DJ, Scheuer T, Catterall WA (1986) Functional properties of rat brain sodium channels lacking the beta 1 or beta 2 subunit. J Biol Chem 261:14882-14890.
Miescher GC, Schreyer M, MacDonald HR (1989) Production and characterization of a rat monoclonal antibody against the murine CD3 molecular complex. Immunology letters 23:113-118.
Miller RH (2002) Regulation of oligodendrocyte development in the vertebrate CNS. Prog Neurobiol 67:451-467.
Miyazaki H, Oyama F, Wong HK, Kaneko K, Sakurai T, Tamaoka A, Nukina N (2007) BACE1 modulates filopodia-like protrusions induced by sodium channel beta4 subunit. Biochem Biophys Res Commun 361:43-48.
Moll C, Mourre C, Lazdunski M, Ulrich J (1991) Increase of sodium channels in demyelinated lesions of multiple sclerosis. Brain Res 556:311-316.
Morgan K, Stevens EB, Shah B, Cox PJ, Dixon AK, Lee K, Pinnock RD, Hughes J, Richardson PJ, Mizuguchi K, Jackson AP (2000) beta 3: an additional auxiliary subunit of the voltage-sensitive sodium channel that modulates channel gating with distinct kinetics. Proc Natl Acad Sci U S A 97:2308-2313.
Mycielska ME, Palmer CP, Brackenbury WJ, Djamgoz MB (2005) Expression of Na+-dependent citrate transport in a strongly metastatic human prostate cancer PC-3M cell line: regulation by voltage-gated Na+ channel activity. J Physiol 563:393-408.

Newell EW, Stanley EF, Schlichter LC (2007) Reversed Na+/Ca2+ exchange contributes to Ca2+ influx and respiratory burst in microglia. Channels (Austin) 1:366-376.
Nicot A, Ratnakar PV, Ron Y, Chen CC, Elkabes S (2003) Regulation of gene expression in experimental autoimmune encephalomyelitis indicates early neuronal dysfunction. Brain 126:398-412.
Noda M, Ikeda T, Suzuki H, Takeshima H, Takahashi T, Kuno M, Numa S (1986) Expression of functional sodium channels from cloned cDNA. Nature 322:826-828.
Noda M, Shimizu S, Tanabe T, Takai T, Kayano T, Ikeda T, Takahashi H, Nakayama H, Kanaoka Y, Minamino N, et al. (1984) Primary structure of Electrophorus electricus sodium channel deduced from cDNA sequence. Nature 312:121-127.
Noebels JL, Marcom PK, Jalilian-Tehrani MH (1991) Sodium channel density in hypomyelinated brain increased by myelin basic protein gene deletion. Nature 352:431-434.
Norgren N, Sundstrom P, Svenningsson A, Rosengren L, Stigbrand T, Gunnarsson M (2004) Neurofilament and glial fibrillary acidic protein in multiple sclerosis. Neurology 63:1586-1590.
O'Malley HA, Shreiner AB, Chen GH, Huffnagle GB, Isom LL (2009) Loss of Na+ channel beta2 subunits is neuroprotective in a mouse model of multiple sclerosis. Mol Cell Neurosci 40:143-155.
Oh Y, Waxman SG (1994) The beta 1 subunit mRNA of the rat brain Na+ channel is expressed in glial cells. Proc Natl Acad Sci U S A 91:9985-9989.
Olechowski CJ, Truong JJ, Kerr BJ (2009) Neuropathic pain behaviours in a chronic-relapsing model of experimental autoimmune encephalomyelitis (EAE). Pain 141:156-164.
Oyama F, Miyazaki H, Sakamoto N, Becquet C, Machida Y, Kaneko K, Uchikawa C, Suzuki T, Kurosawa M, Ikeda T, Tamaoka A, Sakurai T, Nukina N (2006) Sodium channel beta4 subunit: down-regulation and possible involvement in neuritic degeneration in Huntington's disease transgenic mice. J Neurochem 98:518-529.
Paez PM, Fulton D, Colwell CS, Campagnoni AT (2008) Voltage-operated Ca(2+) and Na(+) channels in the oligodendrocyte lineage. J Neurosci Res.
Papadopoulos D, Pham-Dinh D, Reynolds R (2006) Axon loss is responsible for chronic neurological deficit following inflammatory demyelination in the rat. Exp Neurol 197:373-385.
Papazisis G, Kallaras K, Kaiki-Astara A, Pourzitaki C, Tzachanis D, Dagklis T, Kouvelas D (2008) Neuroprotection by lamotrigine in a rat model of neonatal hypoxic-ischaemic encephalopathy. The international journal of neuropsychopharmacology / official scientific journal of the Collegium Internationale Neuropsychopharmacologicum (CINP) 11:321-329.
Pardo LA (2004) Voltage-gated potassium channels in cell proliferation. Physiology (Bethesda) 19:285-292.

Patino GA, Claes LR, Lopez-Santiago LF, Slat EA, Dondeti RS, Chen C, O'Malley HA, Gray CB, Miyazaki H, Nukina N, Oyama F, De Jonghe P, Isom LL (2009) A functional null mutation of SCN1B in a patient with Dravet syndrome. J Neurosci 29:10764-10778.
Patrikios P, Stadelmann C, Kutzelnigg A, Rauschka H, Schmidbauer M, Laursen H, Sorensen PS, Bruck W, Lucchinetti C, Lassmann H (2006) Remyelination is extensive in a subset of multiple sclerosis patients. Brain 129:3165-3172.
Patton DE, Isom LL, Catterall WA, Goldin AL (1994) The adult rat brain beta 1 subunit modifies activation and inactivation gating of multiple sodium channel alpha subunits. J Biol Chem 269:17649-17655.
Peles E, Salzer JL (2000) Molecular domains of myelinated axons. Curr Opin Neurobiol 10:558-565.
Pender MP (1987) Demyelination and neurological signs in experimental allergic encephalomyelitis. J Neuroimmunol 15:11-24.
Perrot R, Berges R, Bocquet A, Eyer J (2008) Review of the multiple aspects of neurofilament functions, and their possible contribution to neurodegeneration. Mol Neurobiol 38:27-65.
Pertin M, Ji RR, Berta T, Powell AJ, Karchewski L, Tate SN, Isom LL, Woolf CJ, Gilliard N, Spahn DR, Decosterd I (2005) Upregulation of the voltage-gated sodium channel beta2 subunit in neuropathic pain models: characterization of expression in injured and non-injured primary sensory neurons. J Neurosci 25:10970-10980.
Poliak S, Peles E (2003) The local differentiation of myelinated axons at nodes of Ranvier. Nat Rev Neurosci 4:968-980.
Poliak S, Gollan L, Salomon D, Berglund EO, Ohara R, Ranscht B, Peles E (2001) Localization of Caspr2 in myelinated nerves depends on axon-glia interactions and the generation of barriers along the axon. J Neurosci 21:7568-7575.
Qin N, D'Andrea MR, Lubin ML, Shafaee N, Codd EE, Correa AM (2003) Molecular cloning and functional expression of the human sodium channel beta1B subunit, a novel splicing variant of the beta1 subunit. Eur J Biochem 270:4762-4770.
Qu Y, Curtis R, Lawson D, Gilbride K, Ge P, DiStefano PS, Silos-Santiago I, Catterall WA, Scheuer T (2001a) Differential modulation of sodium channel gating and persistent sodium currents by the beta1, beta2, and beta3 subunits. Mol Cell Neurosci 18:570-580.
Qu Y, Curtis R, Lawson D, Gilbride K, Ge P, DiStefano PS, Silos-Santiago I, Catterall WA, Scheuer T (2001b) Differential modulation of sodium channel gating and persistent sodium currents by the beta1, beta2, and beta3 subunits. Mol Cell Neurosci 18:570-580.
Quarles RH (2002) Myelin sheaths: glycoproteins involved in their formation, maintenance and degeneration. Cell Mol Life Sci 59:1851-1871.
Raman IM, Bean BP (1997) Resurgent sodium current and action potential formation in dissociated cerebellar Purkinje neurons. J Neurosci 17:4517-4526.

Ranscht B (1988) Sequence of contactin, a 130-kD glycoprotein concentrated in areas of interneuronal contact, defines a new member of the immunoglobulin supergene family in the nervous system. J Cell Biol 107:1561-1573.
Rasband MN, Kagawa T, Park EW, Ikenaka K, Trimmer JS (2003) Dysregulation of axonal sodium channel isoforms after adult-onset chronic demyelination. J Neurosci Res 73:465-470.
Rasband MN, Tayler J, Kaga Y, Yang Y, Lappe-Siefke C, Nave KA, Bansal R (2005) CNP is required for maintenance of axon-glia interactions at nodes of Ranvier in the CNS. Glia 50:86-90.
Ratcliffe CF, Westenbroek RE, Curtis R, Catterall WA (2001) Sodium channel beta1 and beta3 subunits associate with neurofascin through their extracellular immunoglobulin-like domain. J Cell Biol 154:427-434.
Ratcliffe CF, Qu Y, McCormick KA, Tibbs VC, Dixon JE, Scheuer T, Catterall WA (2000) A sodium channel signaling complex: modulation by associated receptor protein tyrosine phosphatase beta. Nat Neurosci 3:437-444.
Raval-Fernandes S, Rome LH (1998) Role of axonal components during myelination. Microsc Res Tech 41:379-392.
Renganathan M, Gelderblom M, Black JA, Waxman SG (2003) Expression of Nav1.8 sodium channels perturbs the firing patterns of cerebellar Purkinje cells. Brain Res 959:235-242.
Ritchie JM, Rang HP, Pellegrino R (1981) Sodium and potassium channels in demyelinated and remyelinated mammalian nerve. Nature 294:257-259.
Robinson AP, White TM, Mason DW (1986) Macrophage heterogeneity in the rat as delineated by two monoclonal antibodies MRC OX-41 and MRC OX-42, the latter recognizing complement receptor type 3. Immunology 57:239-247.
Roger S, Rollin J, Barascu A, Besson P, Raynal PI, Iochmann S, Lei M, Bougnoux P, Gruel Y, Le Guennec JY (2007) Voltage-gated sodium channels potentiate the invasive capacities of human non-small-cell lung cancer cell lines. Int J Biochem Cell Biol 39:774-786.
Rosenbluth J (2009) Multiple functions of the paranodal junction of myelinated nerve fibers. J Neurosci Res.
Rush AM, Dib-Hajj SD, Waxman SG (2005) Electrophysiological properties of two axonal sodium channels, Nav1.2 and Nav1.6, expressed in mouse spinal sensory neurones. J Physiol 564:803-815.
Rush AM, Dib-Hajj SD, Liu S, Cummins TR, Black JA, Waxman SG (2006) A single sodium channel mutation produces hyper- or hypoexcitability in different types of neurons. Proc Natl Acad Sci U S A 103:8245-8250.
Saab CY, Craner MJ, Kataoka Y, Waxman SG (2004) Abnormal Purkinje cell activity in vivo in experimental allergic encephalomyelitis. Exp Brain Res 158:1-8.
Sajad M, Zargan J, Chawla R, Umar S, Sadaqat M, Khan HA (2009) Hippocampal neurodegeneration in experimental autoimmune encephalomyelitis (EAE): potential role of inflammation activated myeloperoxidase. Mol Cell Biochem.

Sakurai M, Kanazawa I (1999) Positive symptoms in multiple sclerosis: their treatment with sodium channel blockers, lidocaine and mexiletine. J Neurol Sci 162:162-168.
Salzer JL (2003) Polarized domains of myelinated axons. Neuron 40:297-318.
Sareen D (2002) Neuroprotective agents in acute ischemic stroke. J Assoc Physicians India 50:250-258.
Schaller KL, Caldwell JH (2000) Developmental and regional expression of sodium channel isoform NaCh6 in the rat central nervous system. J Comp Neurol 420:84-97.
Schantz EJ (1986) Chemistry and biology of saxitoxin and related toxins. Ann N Y Acad Sci 479:15-23.
Scheinman RI, Auld VJ, Goldin AL, Davidson N, Dunn RJ, Catterall WA (1989) Developmental regulation of sodium channel expression in the rat forebrain. J Biol Chem 264:10660-10666.
Scherer SS (1999) Nodes, paranodes, and incisures: from form to function. Ann N Y Acad Sci 883:131-142.
Schmidt J, Rossie S, Catterall WA (1985) A large intracellular pool of inactive Na channel alpha subunits in developing rat brain. Proc Natl Acad Sci U S A 82:4847-4851.
Schmidt JW, Catterall WA (1986a) Biosynthesis and processing of the alpha subunit of the voltage-sensitive sodium channel in rat brain neurons. Cell 46:437-445.
Schmidt JW, Catterall WA (1986b) Biosynthesis and processing of the alpha subunit of the voltage-sensitive sodium channel in rat brain neurons. Cell 46:437-444.
Schwartz G, Fehlings MG (2001) Evaluation of the neuroprotective effects of sodium channel blockers after spinal cord injury: improved behavioral and neuroanatomical recovery with riluzole. J Neurosurg 94:245-256.
Shah BS, Gonzalez MI, Bramwell S, Pinnock RD, Lee K, Dixon AK (2001) Beta3, a novel auxiliary subunit for the voltage gated sodium channel is upregulated in sensory neurones following streptozocin induced diabetic neuropathy in rat. Neurosci Lett 309:1-4.
Shah BS, Stevens EB, Gonzalez MI, Bramwell S, Pinnock RD, Lee K, Dixon AK (2000) beta3, a novel auxiliary subunit for the voltage-gated sodium channel, is expressed preferentially in sensory neurons and is upregulated in the chronic constriction injury model of neuropathic pain. Eur J Neurosci 12:3985-3990.
Shao D, Okuse K, Djamgoz MB (2009) Protein-protein interactions involving voltage-gated sodium channels: Post-translational regulation, intracellular trafficking and functional expression. Int J Biochem Cell Biol 41:1471-1481.
Shea TB, Chan WK (2008) Regulation of neurofilament dynamics by phosphorylation. Eur J Neurosci 27:1893-1901.
Sherman DL, Brophy PJ (2005) Mechanisms of axon ensheathment and myelin growth. Nat Rev Neurosci 6:683-690.

Shindler KS, Ventura E, Dutt M, Rostami A (2008) Inflammatory demyelination induces axonal injury and retinal ganglion cell apoptosis in experimental optic neuritis. Exp Eye Res 87:208-213.
Silber E, Sharief MK (1999) Axonal degeneration in the pathogenesis of multiple sclerosis. J Neurol Sci 170:11-18.
Simons M, Trajkovic K (2006) Neuron-glia communication in the control of oligodendrocyte function and myelin biogenesis. J Cell Sci 119:4381-4389.
Simons M, Trotter J (2007) Wrapping it up: the cell biology of myelination. Curr Opin Neurobiol 17:533-540.
Slavin A, Ewing C, Liu J, Ichikawa M, Slavin J, Bernard CC (1998) Induction of a multiple sclerosis-like disease in mice with an immunodominant epitope of myelin oligodendrocyte glycoprotein. Autoimmunity 28:109-120.
Smith KJ (2007) Sodium channels and multiple sclerosis: roles in symptom production, damage and therapy. Brain pathology (Zurich, Switzerland) 17:230-242.
Smith MR, Smith RD, Plummer NW, Meisler MH, Goldin AL (1998) Functional analysis of the mouse Scn8a sodium channel. J Neurosci 18:6093-6102.
Sontheimer H (1994) Voltage-dependent ion channels in glial cells. Glia 11:156-172.
Sontheimer H, Waxman SG (1992) Ion channels in spinal cord astrocytes in vitro. II. Biophysical and pharmacological analysis of two Na+ current types. J Neurophysiol 68:1001-1011.
Sontheimer H, Trotter J, Schachner M, Kettenmann H (1989) Channel expression correlates with differentiation stage during the development of oligodendrocytes from their precursor cells in culture. Neuron 2:1135-1145.
Spampanato J, Kearney JA, de Haan G, McEwen DP, Escayg A, Aradi I, MacDonald BT, Levin SI, Soltesz I, Benna P, Montalenti E, Isom LL, Goldin AL, Meisler MH (2004) A novel epilepsy mutation in the sodium channel SCN1A identifies a cytoplasmic domain for beta subunit interaction. J Neurosci 24:10022-10034.
Srinivasan J, Schachner M, Catterall WA (1998) Interaction of voltage-gated sodium channels with the extracellular matrix molecules tenascin-C and tenascin-R. Proc Natl Acad Sci U S A 95:15753-15757.
Stys P, Ransom BR, Waxman SG (1991) Compound action potential of nerve recorded by suction electrode: theoretical and experimental analysis. Brain Res 546:18-32.
Stys PK (2004) White matter injury mechanisms. Curr Mol Med 4:113-130.
Stys PK (2005) General mechanisms of axonal damage and its prevention. J Neurol Sci 233:3-13.
Stys PK, Waxman SG, Ransom BR (1992a) Ionic mechanisms of anoxic injury in mammalian CNS white matter: role of Na+ channels and Na(+)-Ca2+ exchanger. J Neurosci 12:430-439.

Stys PK, Waxman SG, Ransom BR (1992b) Ionic mechanisms of anoxic injury in mammalian CNS white matter: Role of Na^+ channels and Na^+-Ca^{2+} exchanger. JNeurosci 12:430-439.
Tallantyre EC, Bo L, Al-Rawashdeh O, Owens T, Polman CH, Lowe J, Evangelou N (2009) Greater loss of axons in primary progressive multiple sclerosis plaques compared to secondary progressive disease. Brain 132:1190-1199.
Tani M, Glabinski AR, Tuohy VK, Stoler MH, Estes ML, Ransohoff RM (1996) In situ hybridization analysis of glial fibrillary acidic protein mRNA reveals evidence of biphasic astrocyte activation during acute experimental autoimmune encephalomyelitis. Am J Pathol 148:889-896.
Trapp BD, Stys PK (2009) Virtual hypoxia and chronic necrosis of demyelinated axons in multiple sclerosis. Lancet Neurol 8:280-291.
Trapp BD, Nishiyama A, Cheng D, Macklin W (1997) Differentiation and death of premyelinating oligodendrocytes in developing rodent brain. J Cell Biol 137:459-468.
Trapp BD, Peterson J, Ransohoff RM, Rudick R, Mork S, Bo L (1998) Axonal transection in the lesions of multiple sclerosis. N Engl J Med 338:278-285.
Tzakos AG, Troganis A, Theodorou V, Tselios T, Svarnas C, Matsoukas J, Apostolopoulos V, Gerothanassis IP (2005) Structure and function of the myelin proteins: current status and perspectives in relation to multiple sclerosis. Curr Med Chem 12:1569-1587.
Ulbricht W (2005) Sodium channel inactivation: molecular determinants and modulation. Physiol Rev 85:1271-1301.
Utzschneider DA, Thio C, Sontheimer H, Ritchie JM, Waxman SG, Kocsis JD (1993) Action potential conduction and sodium channel content in the optic nerve of the myelin-deficient rat. Proc Biol Sci 254:245-250.
Vacher H, Mohapatra DP, Trimmer JS (2008) Localization and targeting of voltage-dependent ion channels in mammalian central neurons. Physiol Rev 88:1407-1447.
van der Valk P, Amor S (2009) Preactive lesions in multiple sclerosis. Curr Opin Neurol 22:207-213.
Van Wart A, Matthews G (2006) Impaired firing and cell-specific compensation in neurons lacking nav1.6 sodium channels. J Neurosci 26:7172-7180.
Vanoye CG, Lossin C, Rhodes TH, George AL, Jr. (2006) Single-channel properties of human NaV1.1 and mechanism of channel dysfunction in SCN1A-associated epilepsy. J Gen Physiol 127:1-14.
Vega AV, Henry DL, Matthews G (2008) Reduced expression of Na(v)1.6 sodium channels and compensation by Na(v)1.2 channels in mice heterozygous for a null mutation in Scn8a. Neurosci Lett 442:69-73.
Vellinga MM, Geurts JJ, Rostrup E, Uitdehaag BM, Polman CH, Barkhof F, Vrenken H (2009) Clinical correlations of brain lesion distribution in multiple sclerosis. J Magn Reson Imaging 29:768-773.
Wallace RH, Wang DW, Singh R, Scheffer IE, George AL, Jr., Phillips HA, Saar K, Reis A, Johnson EW, Sutherland GR, Berkovic SF, Mulley JC (1998)

Febrile seizures and generalized epilepsy associated with a mutation in the Na+-channel beta1 subunit gene SCN1B. Nat Genet 19:366-370.
Walsh KB, Wolf MB, Fan J (1998) Voltage-gated sodium channels in cardiac microvascular endothelial cells. Am J Physiol 274:H506-512.
Wang A, He BP (2009) Characteristics and functions of NG2 cells in normal brain and neuropathology. Neurol Res 31:144-150.
Wang D, Ayers MM, Catmull DV, Hazelwood LJ, Bernard CC, Orian JM (2005) Astrocyte-associated axonal damage in pre-onset stages of experimental autoimmune encephalomyelitis. Glia 51:235-240.
Wang GK, Russell C, Wang SY (2003) State-dependent block of wild-type and inactivation-deficient Na+ channels by flecainide. J Gen Physiol 122:365-374.
Waxman SG (2001) Transcriptional channelopathies: an emerging class of disorders. Nat Rev Neurosci 2:652-659.
Waxman SG (2002) Sodium channels as molecular targets in multiple sclerosis. J Rehabil Res Dev 39:233-242.
Waxman SG (2005) Sodium channel blockers and axonal protection in neuroinflammatory disease. Brain 128:5-6.
Waxman SG (2006a) Axonal conduction and injury in multiple sclerosis: the role of sodium channels. Nat Rev Neurosci 7:932-941.
Waxman SG (2006b) Ions, energy and axonal injury: towards a molecular neurology of multiple sclerosis. Trends Mol Med 12:192-195.
Waxman SG (2008a) Axonal dysfunction in chronic multiple sclerosis: Meltdown in the membrane. Ann Neurol.
Waxman SG (2008b) Mechanisms of disease: sodium channels and neuroprotection in multiple sclerosis-current status. Nature clinical practice 4:159-169.
Waxman SG, Ritchie JM (1993) Molecular dissection of the myelinated axon. Ann Neurol 33:121-136.
Waxman SG, Craner MJ, Black JA (2004) Na+ channel expression along axons in multiple sclerosis and its models. Trends Pharmacol Sci 25:584-591.
Westenbroek RE, Merrick DK, Catterall WA (1989) Differential subcellular localization of the RI and RII Na+ channel subtypes in central neurons. Neuron 3:695-704.
Westenbroek RE, Noebels JL, Catterall WA (1992a) Elevated expression of type II Na+ channels in hypomyelinated axons of shiverer mouse brain. J Neurosci 12:2259-2267.
Westenbroek RE, Noebels JL, Catterall WA (1992b) Elevated expression of type II Na^+ channels in hypomyelinated axons of *shiverer* mouse brain. JNeurosci 12:2259-2267.
Whitaker WR, Clare JJ, Powell AJ, Chen YH, Faull RL, Emson PC (2000) Distribution of voltage-gated sodium channel alpha-subunit and beta-subunit mRNAs in human hippocampal formation, cortex, and cerebellum. J Comp Neurol 422:123-139.

Whitaker WR, Faull RL, Waldvogel HJ, Plumpton CJ, Emson PC, Clare JJ (2001) Comparative distribution of voltage-gated sodium channel proteins in human brain. Brain Res Mol Brain Res 88:37-53.
Willem M, Lammich S, Haass C (2009) Function, regulation and therapeutic properties of beta-secretase (BACE1). Semin Cell Dev Biol 20:175-182.
Williamson AV, Compston DA, Randall AD (1997) Analysis of the ion channel complement of the rat oligodendrocyte progenitor in a commonly studied in vitro preparation. Eur J Neurosci 9:706-720.
Wolswijk G, Balesar R (2003) Changes in the expression and localization of the paranodal protein Caspr on axons in chronic multiple sclerosis. Brain 126:1638-1649.
Wong HK, Sakurai T, Oyama F, Kaneko K, Wada K, Miyazaki H, Kurosawa M, De Strooper B, Saftig P, Nukina N (2005) beta Subunits of voltage-gated sodium channels are novel substrates of beta-site amyloid precursor protein-cleaving enzyme (BACE1) and gamma-secretase. J Biol Chem 280:23009-23017.
Wu J, Ohlsson M, Warner EA, Loo KK, Hoang TX, Voskuhl RR, Havton LA (2008) Glial reactions and degeneration of myelinated processes in spinal cord gray matter in chronic experimental autoimmune encephalomyelitis. Neuroscience 156:586-596.
Wu M, Tsirka SE (2009) Endothelial NOS-deficient mice reveal dual roles for nitric oxide during experimental autoimmune encephalomyelitis. Glia.
Wu WK, Li GR, Wong HP, Hui MK, Tai EK, Lam EK, Shin VY, Ye YN, Li P, Yang YH, Luo JC, Cho CH (2006) Involvement of Kv1.1 and Nav1.5 in proliferation of gastric epithelial cells. J Cell Physiol 207:437-444.
Wujek JR, Bjartmar C, Richer E, Ransohoff RM, Yu M, Tuohy VK, Trapp BD (2002) Axon loss in the spinal cord determines permanent neurological disability in an animal model of multiple sclerosis. J Neuropathol Exp Neurol 61:23-32.
Xiao ZC, Ragsdale DS, Malhotra JD, Mattei LN, Braun PE, Schachner M, Isom LL (1999) Tenascin-R is a functional modulator of sodium channel beta subunits. J Biol Chem 274:26511-26517.
Xie M, Lynch DT, Schools GP, Feustel PJ, Kimelberg HK, Zhou M (2007) Sodium channel currents in rat hippocampal NG2 glia: characterization and contribution to resting membrane potential. Neuroscience 150:853-862.
Xu R, Thomas EA, Gazina EV, Richards KL, Quick M, Wallace RH, Harkin LA, Heron SE, Berkovic SF, Scheffer IE, Mulley JC, Petrou S (2007) Generalized epilepsy with febrile seizures plus-associated sodium channel beta1 subunit mutations severely reduce beta subunit-mediated modulation of sodium channel function. Neuroscience 148:164-174.
Yu FH, Catterall WA (2003) Overview of the voltage-gated sodium channel family. Genome Biol 4:207.
Yu FH, Mantegazza M, Westenbroek RE, Robbins CA, Kalume F, Burton KA, Spain WJ, McKnight GS, Scheuer T, Catterall WA (2006) Reduced

sodium current in GABAergic interneurons in a mouse model of severe myoclonic epilepsy in infancy. Nat Neurosci 9:1142-1149.
Yu FH, Westenbroek RE, Silos-Santiago I, McCormick KA, Lawson D, Ge P, Ferriera H, Lilly J, DiStefano PS, Catterall WA, Scheuer T, Curtis R (2003) Sodium channel beta4, a new disulfide-linked auxiliary subunit with similarity to beta2. J Neurosci 23:7577-7585.
Zalc B (2006) The acquisition of myelin: a success story. Novartis Found Symp 276:15-21; discussion 21-15, 54-17, 275-281.
Zapryanova E, Sotnikov OS, Sergeeva SS, Deleva D, Filchev A, Sultanov B (2004) Axon reactions precede demyelination in experimental models of multiple sclerosis. Neurosci Behav Physiol 34:337-342.
Zeis T, Graumann U, Reynolds R, Schaeren-Wiemers N (2008a) Normal-appearing white matter in multiple sclerosis is in a subtle balance between inflammation and neuroprotection. Brain 131:288-303.
Zeis T, Kinter J, Herrero-Herranz E, Weissert R, Schaeren-Wiemers N (2008b) Gene expression analysis of normal appearing brain tissue in an animal model for multiple sclerosis revealed grey matter alterations, but only minor white matter changes. J Neuroimmunol 205:10-19.
Zhang SC (2001) Defining glial cells during CNS development. Nat Rev Neurosci 2:840-843.
Zhang ZN, Li Q, Liu C, Wang HB, Wang Q, Bao L (2008) The voltage-gated Na+ channel Nav1.8 contains an ER-retention/retrieval signal antagonized by the beta3 subunit. J Cell Sci 121:3243-3252.
Zivadinov R, Bakshi R (2004) Central nervous system atrophy and clinical status in multiple sclerosis. J Neuroimaging 14:27S-35S.